Azeotropic separation: playing with the ionicity of ionic liquids

Filipe Serrão Santos Oliveira

Dissertation presented to obtain the Ph.D degree in
Engineering and Technology Sciences, Chemical Engineering

Instituto de Tecnologia Química e Biológica António Xavier | Universidade Nova de Lisboa

Oeiras, July, 2015

INSTITUTO
DE TECNOLOGIA
QUÍMICA E BIOLÓGICA
ANTÓNIO XAVIER /UNL

Knowledge Creation

Title

Azeotropic separation: playing with the ionicity of ionic liquids

Dissertation presented to obtain the Ph.D degree in Engineering Sciences and Technology – Chemical Engineering

Cover Image

Design adapted from http://www.shutterstock.com/ by Filipe S. Oliveira and Liliana C. Tomé

Author

Filipe Serrão Santos Oliveira

Molecular Thermodynamics Laboratory
Separation and Extraction Technology Laboratory
Instituto de Tecnologia Química e Biológica António Xavier
Universidade Nova de Lisboa
Av. da República
Estação Agronómica Nacional
2780-157 Oeiras
Portugal

Second Edition, July 2015

Printed in Portugal

I declare that the work presented in this thesis, except where otherwise stated, is based on my own research. The work was mainly performed in the Molecular Thermodynamics Laboratory and in the Separation and Extraction Technologies Laboratory of the Instituto de Tecnologia Química e Biológica António Xavier, Universidade Nova de Lisboa, between May 2011 and May 2015, and supervised by Doctor Isabel M. Marrucho (ITQB-UNL) and Doctor Luís Paulo N. Rebelo (ITQB-UNL). Part of the results were attained during a visiting period to the Monash Ionic Liquids Group, School of Chemistry, University of Monash, Clayton, Australia.

Financial support was provided by Fundação para a Ciência e a Tecnologia through the doctoral fellowship SFRH/BD/73761/2010.

À minha família,

juntos caminhamos para cima e para a frente!

Acknowledgments

Aos meus orientadores, Dra. Isabel Marrucho e Dr. Luís Paulo Rebelo, pela oportunidade que me proporcionaram de fazer um doutoramento, assim como pela orientação científica e conhecimentos transmitidos. Em especial à Isa, pela sua orientação a todos os níveis, pela paciência e apoio ao longo destes anos, pela motivação que sempre me deu para acreditar no meu trabalho e essencialmente por me ter ajudado a crescer! tanto como cientista como pessoa. "*To you... grateful I am*"

A todas as pessoas no ITQB, extra ou intra laboratório, que me ajudaram a alcançar este objectivo. Em especial a Ana B. Pereiro pela sua ajuda na fase inicial do meu trabalho, e ao Arturo e à Esther pelo apoios nestes últimos meses de escrita... muchas gracias!

To Dr. Douglas R. MacFarlane and Dra. Maria Forsyth for welcoming me into their respective labs during my stay abroad. In addition, there are a bunch of name that I can forget, namely my great office mates Mega, Leo, Naoki and Manoj. The rest of the "Monash crew" Alison, Jenny, Derick, Gary, Rob, Bartek, Basia and specially Matt! Also to the "Deakin crew" Cristina, Tim, Matze and Rainier. To all of these people who contributed in their own way, thank you for a great stay.

À Liliana, a minha mana mais velha, é difícil pôr em palavras o quanto te estou agradecido, mas dito de uma forma simplista e directa (à Filipe portanto), os dedos de uma mão sobram para contar pessoas como tu! Aos inesquecíveis Rui e Helga, partilhar o lab com vocês foi espectacular, pelos amigos e colegas espectaculares que são. Obrigado pelos bons exemplos e conselhos (e aos pelos maus também... se é que os houve!) Ao David, melhor colega de casa era difícil! É espectacular chegar ao final do dia a casa e rir pelo dia inteiro, seja a jogar FIFA, ver vídeos estúpidos na net ou simplesmente a falar do que não interessa a ninguém. A estas 4 fantásticas pessoas, não poderia deixar de incluir o Arlindo, por nos aturar nos nossos jantares e conversas ate às tantas, mesmo depois de já estar a dormir na cadeira da cozinha ou no puf da sala!

À minha querida avozinha! A qual me alimentou e abrigou durante grande parte deste percurso, que todos os dias se preocupou em me telefonar a perguntar o que queria jantar,

e que independentemente da minha escolha me disse sempre que ia comer peixe!... pois eu nunca como peixe! Adoro-te avó!

A toda a família Batista! por terem aberto as portas das suas casas no outro lado do Mundo, a um desconhecido que vinha de Portugal. Obrigado por me fazerem sentir em família e por tudo o que me proporcionaram a troco de nada. Em vossa honra dedico também este trabalho à Janine que ficará para sempre nos nossos corações e pensamentos. Ao Pepe, Irene, Alana, Paulo, D. Isabel, e restantes membros da família, obrigada!

À minha malta de Aveiro! Aos meus bros de longa data, Diogo, Igor, Checa e Marco, entre risadas, basket, poker e noitadas ficaram muitas histórias que dariam documentos maiores que este! Ao Telmo e ao Márcio que me acompanharam desde o inicio do meu percurso académico sempre disponíveis para qualquer coisa. Ao Ferrão e ao "King" Nuno, pelas suas visitas animadas ao ITQB, foram sempre grandes garrafas de oxigénio que me ajudaram a chegar ao fim deste percurso. E um especial agradecimento também ao Malaquias, que mesmo à distância, pareceu que por vezes estávamos os dois num pub à conversa, obrigado pelo apoio!

E como a parte final é a que sabe sempre melhor... à minha família! Às minhas tias "velhas" Mila (e ao Zezito!!!), Nanda e Lé e ao dragão zangão do Manho, pelos seus pequenos (e no entanto tão grandes) mimos com que me vão presenteando.

Ao meu pai e à minha mãe, sem os quais nada disto era possível, nenhum filho alguma vez poderia pedir melhor! Sem esquecer a minha pequenita lá de casa, que salta e me abraça sempre que eu chego a casa (adoro!), fico a espera de ler o que vais escrever nos agradecimentos da tua tese pois não tenho dúvida nenhuma que não vou esperar muito mais para os ler! Luv u sis!

Obrigado a todos por me fazerem chegar aqui!

"It ain't where you from, it's where you at!"

William Michael Griffin, Jr. *aka* Rakim Allah

Members of the Jury

President

Dr. João Paulo Serejo Goulão Crespo, Vice Dean and Full Professor at Departamento de Química, Faculdade de Ciências e Tecnologia, Universidade Nova de Lisboa, Portugal.

Thesis Supervisors

Dra. Isabel Maria Delgado Jana Marrucho Ferreira, Research Coordinator at Instituto de Tecnologia Química e Biológica António Xavier, Universidade Nova de Lisboa, Portugal (supervisor).

Dr. Luís Paulo da Silva Nieto Marques Rebelo, Full Professor at Instituto de Tecnologia Química e Biológica António Xavier, Universidade Nova de Lisboa, Portugal (co-supervisior).

Thesis Examiners

Dr. Manuel Luís Nunes da Ponte, Full Professor at Departamento de Química, Faculdade de Ciências e Tecnologia, Universidade Nova de Lisboa, Portugal

Dra. Mara Guadalupe Freire Martins, Research Coordinator at Centro de Materiais Cerâmicos e Compósitos (CICECO), Departamento de Química, Universidade de Aveiro, Portugal.

Dra. Maria Eugénia Rebelo de Almeida Macedo, Associate Professor with Aggregation at Departamento de Engenharia Química, Faculdade de Engenharia, Universidade do Porto, Portugal.

Dr. Eurico José da Silva Cabrita, Assistant Professor at Departamento de Química, Faculdade de Ciências e Tecnologia, Universidade Nova de Lisboa, Portugal

Contents

Azeotropic separation: playing with the ionicity of ionic liquids

Abstract

In modern chemical industry, the separation of solvent mixtures into their pure compounds is mandatory not only to prevent their accumulation, but also for that their reusability may assure a sustainable overall process. However, the presence of azeotropes or close boiling point mixtures constitute one of the most challenging tasks in industrial processes in the separation of solvent mixtures, since their separation by simple distillation is basically impossible. The processes designed for the efficient separation of azeotropic mixtures usually require the use of a separation agent.

Separation agents can range from an organic solvent, to an inorganic salt (IS), or even combinations of both. More recently, ionic liquids (ILs), deep eutectic solvents (DES) and hyperbranched polymers have also been successfully tested. ISs are known for their high separation efficiencies, due to their ionic character, and ILs for their liquid state and negligible vapour pressures. So, the next natural step is to combine the advantages of both these classes of compounds.

This thesis explores the separation of azeotropic mixtures using a combination of an IL and an IS as separation agent. The work presented herein starts by studying different IL-IS mixtures in terms of their physical and chemical properties, which allowed the determination of their ionicity or ionic character (Chapter 2 and 3). Afterwards, the studied IL-IS mixtures are tested in the separation of one specific azeotropic mixture, n-heptane + ethanol that will serve as test model (proof-of-concept) for the application of IL-IS mixtures as separation agents for breaking azeotropes (Chapter 4 and 5). In addition, deep eutectic solvents (DES), viewed as greener analogues of ILs, are also tested as potential azeotrope breakers (Chapter 6).

The obtained results enable the establishment of relationships between the thermophysical properties of IL-IS mixtures and their ionicity, and about the chemical structures of the ILs and ISs required to produce mixtures with increased ionicity. Furthermore, the work presented in this thesis shows that IL-IS mixtures can surpass neat ILs as efficient separation agents, allowing the establishment of a link between ionicity and extraction efficiency in the separation of azeotropic mixtures.

Resumo

Actualmente, a separação de misturas de solventes é um processo crucial para qualquer indústria química, não só para evitar a acumulação dos mesmo mas também porque a reutilização de solventes purificados pode assegurar a sustentabilidade global de processos. No entanto, muitos dos compostos encontrados nas misturas de solventes industriais apresentam pontos azeotrópicos ou apresentam pontos de ebulição muito próximos entre si, dificultando a separação destas misturas, uma vez que os processos de destilação convencionais não são capazes de as separarem. Assim, novos processos foram desenvolvidos para a separação destas misturas "especiais", onde a adição de um agente de separação é necessário.

Os agentes de separação mais comuns são solventes orgânicos, sais inorgânicos (SIs) ou combinações entre ambos. Recentemente, líquidos iónicos (LIs), solventes eutécticos e polímeros hiper-ramificados também tem sido testados a nível laboratorial. Os SIs, devido ao seu carácter iónico, são extremamente eficazes na separação de misturas azeotrópicas, enquanto que os LIs têm sido testados pelo facto se serem líquidos e não apresentarem pressão de vapor à pressão atmosférica. Assim, a combinação das vantagens oferecidas por ambos estes compostos, SIs e LIs, apresenta-se como uma estratégia natural a seguir.

Nesta tese, estudou-se a separação de misturas azeotrópicas utilizando um mistura de um LI com um SI como agente de separação. Inicialmente, as propriedades físicas e químicas de diferentes misturas de LIs com SIs são estudadas, e posteriormente foram efectuados estudos sobre a sua ionicidade (Capítulos 2 e 3). De forma a estabelecer uma ligação entre a ionicidade (carácter iónico) das misturas de LI-SI e a sua eficiência na separação de misturas azeotrópicas, as misturas de LI-SI com maior potencial foram testadas na separação de misturas de n-heptano e etanol (Capítulos 4 e 5). Esta mistura azeotrópica é usada como modelo, de forma a mostrar o potencial da aplicação de combinações de LIs e SIs como agentes de separação. Além disso, foram também testados solventes eutécticos, vistos como análogos mais verdes dos LIs, como potenciais agentes de separação para a mesma mistura azeotrópica (Capítulo 6).

Os resultados obtidos nesta tese permitem estabelecer relações entre as propriedades termofísicas das misturas de LI-SI e sua ionicidade, assim como sobre as estruturas químicas dos LIs e SIs necessárias para produzir misturas com maior ionicidade. Adicionalmente, o trabalho apresentado nesta tese mostra ainda que as misturas de LI-SI podem ultrapassar a performance dos LIs puros como agentes de separação, permitindo o estabelecimento de uma ponte entre a ionicidade e a eficiência de separação na separação de misturas azeotrópicas.

Publications

Thesis publications (6)

Filipe S. Oliveira, Eurico J. Cabrita, Smilja Todorovic, Carlos E. S. Bernardes, José N. Canongia Lopes, Jennifer L. Hodgson, Douglas R. Macfarlane, Luís P. N. Rebelo and Isabel M. Marrucho, Mixtures of the 1-ethyl-3-methylimidazolium acetate ionic liquid with different inorganic salts: insights into their interactions, *manuscript in preparation,* 2015.

Filipe S. Oliveira, Ralf Dohrn, Luís P. N. Rebelo and Isabel M. Marrucho, Improving the separation of n-heptane + ethanol azeotropic mixtures combining ionic liquid 1-ethyl-3-methylimidazolium acetate with different inorganic salts, *manuscript in preparation,* 2015.

Filipe S. Oliveira, Ana B. Pereiro, João M. M. Araújo, Luís P. N. Rebelo and Isabel M. Marrucho, Designing high ionicity ionic liquids based on 1-ethyl-3-methylimidazolium ethyl sulfate for effective azeotrope breaking, *submitted to J. Chem. Thermodyn.,* 2015.

Filipe S. Oliveira, Luís P. N. Rebelo and Isabel M. Marrucho, Influence of different inorganic salts on the ionicity and thermophysical properties of 1-ethyl-3-methylimidazolium acetate ionic liquid, *J. Chem. Eng. Data* (2015), **60**, 781-789.

Filipe S. Oliveira, Ana B. Pereiro, João M. M. Araújo, Carlos E. S. Bernardes, José N. Canongia Lopes, Smilja Todorovic, Gabriel Feio, Pedro L. Almeida, Luís P. N. Rebelo and Isabel M. Marrucho, High ionicity ionic liquids (HIILs): comparing the effect of ethylsulfonate and ethylsulfate anions, *Phys. Chem. Chem Phys.* (2013), **15**, 18138-18147.

Filipe S. Oliveira, Ana B. Pereiro, Luís P. N. Rebelo and Isabel M. Marrucho, Deep eutectic solvents as extraction media for azeotropic mixtures, *Green Chem.* (2013), **15**, 1326-1330.

Other publications (5)

Pedro D. A. Bastos, **Filipe S. Oliveira**, Luís P. N. Rebelo, Ana B. Pereiro and Isabel M. Marrucho, Separation of azeotropic mixtures using high ionicity ionic liquids based on 1-ethyl-3-methylimidazolium thiocyanate*, Fluid Phase Equilibr.* (2015), **389**, 48-54.

Catarina Florindo, **Filipe S. Oliveira**, Luís P. N. Rebelo, Ana M. Fernandes and Isabel M. Marrucho, Insights into the synthesis and properties of deep eutectic solvents based on cholinium chloride and carboxylic acids, *ACS Sustain. Chem. Eng.* (2014), **2**, 2416-2425.

Filipa Alves, **Filipe S. Oliveira**, Bernd Schröder, Carla Matos and Isabel M. Marrucho, Synthesis, characterization and liposome partition of a novel tetracycline derivative using the ionic liquids framework, *J. Pharm. Sci.* (2013), **102**, 1504-1512.

Ana B. Pereiro, João M. M. Araújo, **Filipe S. Oliveira**, José M. S. S. Esperança, José N. Canongia Lopes, Isabel M. Marrucho and Luís P. N. Rebelo, Solubility of inorganic salts in pure ionic liquids, *J. Chem. Thermodyn.* (2012), **55**, 29-36.

Ana B. Pereiro, João M. M. Araújo, **Filipe S. Oliveira**, Carlos E. S. Bernardes, José M. S. S. Esperança, José N. Canongia Lopes, Isabel M. Marrucho and Luís P. N. Rebelo, Inorganic salts in purely ionic liquid media: the development of high ionicity ionic liquids (HIILs), *Chem. Commun.* (2012), **48**, 3656-3658.

Thesis Layout

Chapter 1 | Introduction

A brief overview of the state-of-art and general concepts are presented, along with the motivation and objectives of this thesis.

Chapter 2 | Ionicity in -SO_x based Ionic Liquids: comparing the effect of ethyl sulfonate and ethyl sulfate anions

A comparison study between two mixtures of an ionic liquid and an inorganic salts is made in terms of their thermophysical properties and ionicity. The effects of the different ionic liquids' anion and of the addition of inorganic salt are assessed.

Chapter 3 | Ionicity in the 1-ethyl-3-methylimidazolium acetate Ionic Liquid: comparing the effect of different Inorganic Salts

The origin of ionicity in mixtures of 1-ethyl-3-methylimidazolium acetate and several ammonium and sodium-based inorganic salts is studied. The thermophysical properties are measured and spectroscopic and simulations techniques provide meaningful insights at the molecular level.

Chapter 4 | Combining one Ionic Liquid with different amounts of one Inorganic Salt for the separation of ethanol from n-heptane

Mixtures of the 1-ethyl-3-methylimidazolium ethyl sulfate ionic liquid with different amounts of ammonium thiocyanate are tested as extraction solvents in the liquid-liquid extraction of the azeotropic mixture of n-heptane + ethanol.

Chapter 5 | Combining one Ionic Liquid with different Inorganic Salts for the separation of ethanol from n-heptane

The ionic liquid 1-ethyl-3-methylimidazolium acetate is combined with three different ammonium-based inorganic salts, and used for the extraction of ethanol from n-heptane by liquid-liquid extraction.

Chapter 6 | Using deep eutectic solvents for the separation of ethanol from n-heptane

Ethanol is separated from n-heptane using deep eutectic solvents, based on cholinium chloride and alcohols or acids, as extraction solvents in liquid-liquid extraction processes.

Chapter 7 | Concluding Remarks and Outlook

The main achievements and conclusions are highlighted herein. Possible challenges and perspectives for future research are also presented.

Chapter 1

Introduction

Section 5 contains parts of the following publications:

Ana B. Pereiro, João M. M. Araújo, **Filipe S. Oliveira**, José M. S. S. Esperança, José N. Canongia Lopes, Isabel M. Marrucho and Luís P. N. Rebelo, Solubility of inorganic salts in pure ionic liquids, *J. Chem. Thermodyn.* (2012), **55**, 29-36.

Ana B. Pereiro, João M. M. Araújo, **Filipe S. Oliveira**, Carlos E. S. Bernardes, José M. S. S. Esperança, José N. Canongia Lopes, Isabel M. Marrucho and Luís P. N. Rebelo, Inorganic salts in purely ionic liquid media: the development of high ionicity ionic liquids (HIILs), *Chem. Commun.* (2012), **48**, 3656-3658.

1. General context

Since early civilizations, different separation processes have been developed and used in the whole world. They allow us to produce some of the most common products that we use today, such as the salt that we use in our kitchens, the fuel that we put in our cars, the coffee we drink after lunch or even the casual beer we drink after work.

Nowadays, separation processes are essential in the modern industrial economy, since any industrial production of chemicals requires numerous purification steps, the reuse of solvents and the disposal of by-products and / or unreacted raw materials. Each separation process is based on a specific principle. Evaporation, condensation and distillation all involve a liquid and a gas phase, while the solvent extraction involves two liquid phases. Crystallization, drying and leaching involve a liquid and a solid phase. Sorption processes can involve gas, liquid or solid phases. All of these processes, have as ground principles the mass transport and the equilibrium of phases.[1]

The separation of a homogeneous liquid mixture into its compounds is an important step in many industrial processes, where distillation is without doubt one of the most important processes used. Indeed, it is estimated that only in USA, there are approximately 40 000 of distillation columns working, which are accountable for nearly 7 % of the total energy consumed in the country. The distillation is therefore the dominating separation process, due to its high efficiency, accounting for more applications than all the others techniques. However, it is known that distillation processes are the most costly in terms of energy, accounting for more than 95 % of the total energy used in separations, in industries worldwide.[1, 2]

The employment of efficient separation techniques in the petrochemical, chemistry and pharmaceutical industries is of utmost importance not only for the development of products but also in the recovery / reuse of solvents or other secondary compounds, allowing the reduction of environmental problems and, at the same time, leading to economic advantages.

2. Azeotropic mixtures

In many areas of industry, the recovery and reuse of organic solvents is generally practiced because of increased solvent costs and potential solvent shortages, but mainly because their disposal often results in violation of air, water or land-pollution regulations. Therefore, the separation of solvent mixtures into their pure compounds is mandatory, preventing their accumulation, allowing their reuse and assuring the sustainability of the overall process. Nevertheless, in some cases, the presence of azeotropic or close boiling point mixtures poses difficulties in their recycling, which in turn can lead to the accumulation of hazardous solvent mixtures.

Azeotropic mixtures are non-ideal mixtures that do not follow the Raoult law. The Raoult's law states that in an ideal mixture of two liquids, A and B, the vapour pressure of each one of the compounds (p_i) is related to its own molar fraction (x_i) and to the vapour pressure of the pure compound (p_i^*) as shown by equation 1:

$$p_i = x_i \times p_i^* \quad (1)$$

If this mixture is heated until the boiling temperature is reached, the compositions of the liquid and gas phases in equilibrium will be different, since the gas phase will have higher content of the more volatile compound (Figure 1a).[3]

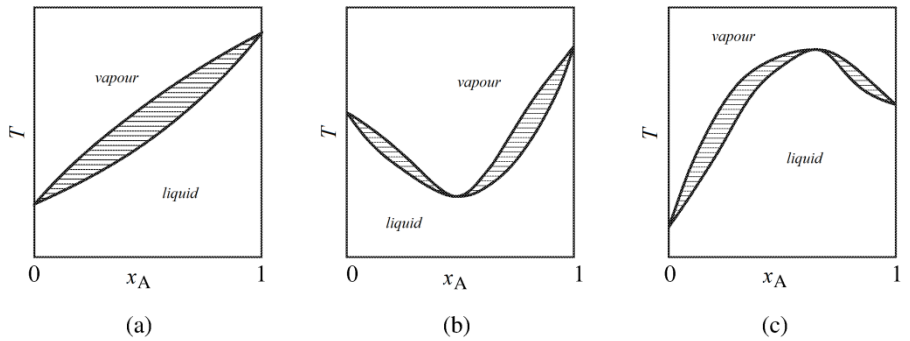

Figure 1 | Temperature - composition phase diagram of a mixture of two liquids A and B that present: a) ideal behaviour, b) positive deviation from the Raoult's law (minimum-boiling azeotrope) and c) negative

deviation from the Raoult's law (maximum-boiling azeotrope).

In the case of azeotropic mixtures, the establishment of interactions between the molecules of liquid A and the molecules of liquid B, will lead to the formation of an azeotropic point, causing a deviation from the Raoult's law.

If the deviation is positive then the interactions between A and B molecules are unfavourable, meaning that the attraction between identical molecules (A-A and B-B) is stronger than between different molecules (A-B) and hence the (*T, x*) phase diagrams show a minimum, indicating that the mixture is destabilized relative to the ideal solution (Figure 1b). On the other hand, a negative deviation means that the interactions between the A and B molecules are favourable, i.e., the attraction between different molecules (A-B) is the strongest, causing a maximum in the (*T*, *x*) phase diagram of the mixture (Figure 1c).[3]

In the azeotropic point, the compositions of both phases of the mixture, liquid and gas, are equal, allowing the mixture to boil at a constant temperature, making it impossible to separate by a simple distillation. Because of this fact, azeotropes are sometimes mistaken for single components. Nonetheless, in the case of azeotropes the variation of pressure changes not only the boiling temperature but also the composition of the mixture, and this easily distinguishes it from a pure component.

Besides being classified by the positive or negative deviation from the Raoult's law, azeotropes can also be divided into two groups: homoazeotropes or heteroazotropes. If in the equilibrium temperature the liquid mixture is homogeneous, the azeotrope is classified as a homoazeotrope. However, if in the equilibrium the vapour phase coexists with the liquid phases, then we are in the presence of a heteroazeotrope. Heteroazeotropes usually result from mixtures of liquid with very small solubility in each other, such as water with benzene or water with dichloromethane.[4]

The most famous example of a homoazeotropic mixture is that formed by ethanol and water. At atmospheric pressure this mixture will boil at a temperature of 78.2 ºC and the composition obtained in both liquid and gas phases will be 96 wt% of ethanol and 4 wt% of water. This example represents also positive azeotropy, meaning that it is a minimum-boiling azeotrope. Indeed, more than 90 % of the know azeotropes display the same

behaviour, where 80 % of these are homoazeotropic. Common examples of negative azeotropy are mixtures of chloroform + acetone or nitric acid + water.

In this thesis, the homoazeotrope of n-heptane + ethanol is studied. The azeotropic point for this mixture happens at a composition of 48 wt% (0.3325 in mole fraction) of ethanol and 52 wt% (0.6675 in mole fraction) of n-heptane and it boils at 72 ºC, thus presenting a minimum in the phase diagram.[5] This azeotropic mixture is formed in the production of oxygenated additives for gasoline[6] and its separation gains industrial relevance because of the importance of ethanol as an attractive alternative fuel, since it can be used both as a fuel and as a gasoline oxygenated additive.

3. Separation technologies

Since azeotropic mixtures are impossible to separate by simple distillation, other techniques that allow the breaking of the azeotropic point, and hence the separation of the compounds in the mixture, have been developed. The separation of these mixtures requires the disruption of the chemical interactions between the compounds and alteration of the phase equilibrium. This effect can be obtained by pressure variation or by the introduction of another compound in the mixture, a separation agent, which promotes the separation of the components in the azeotropic mixture.[7, 8]

The most used technique is enhanced distillation that covers three different types of distillation, namely the azeotropic distillation, the extractive distillation and the pressure swing distillation. Other techniques rely on the use of membranes for the separation, such as pervaporation or membrane distillation. In addition, liquid-liquid extraction has also emerged since this technique can be viewed as a more economical and environmentally beneficial option.[7, 8]

3.1. Extractive distillation

Extractive distillation is the most used technique in the industry for the separation of azeotropic or close boiling point mixtures, due to its efficiency and versatility, especially in the petrochemical industry. This technique is commonly used in the separation of mixtures of hydrocarbons with close boiling point, such as n-butane (C_4H_{10}), n-pentane (C_5H_{12}) and n-hexane (C_6H_{14}) among others; and azeotropic mixtures of alcohol + water, acetic acid + water, acetone + methanol, methanol + methyl acetate, ethanol + ethyl acetate and acetone + ethyl ether to name a few examples.[9]

In order for this technique to be efficient in the separation of azeotropic or close boiling point mixtures, it requires the addition of a separation agent to the mixture. This separating agent, also known as entrainer, interacts with the compounds of the mixture and alters their relative volatility allowing their total separation.

The feasibility of an entrainer can be assessed by the determination of two parameters, the relative volatility (α) and the selectivity (S). The first parameter can be calculated from the vapour + liquid equilibria data as shown in the following equation:

$$\alpha_{ij} = \frac{\left(y_i / x_i\right)}{\left(y_j / x_j\right)} = \frac{\gamma_i p_i^*}{\gamma_j p_j^*} \tag{2}$$

where x is mole fraction in the liquid phase, y is mole fraction in the vapour phase and γ is the activity coefficient. The selectivity of the entrainer is calculated by the change in the γ_i / γ_j ratio, since the ratio of p_i^* / p_j^* is constant for small temperature changes.[9]

In azeotropic mixtures, α is equal to the unity and in close boiling point mixtures it is also very close to 1. Therefore, the most promising entrainers should have the highest relative volatility possible, as well as a high boiling point difference from the components to be separated, to facilitate its separation from the distillation products. Other parameters such as, corrosion, prices, sources, etc. should also be taken into consideration.[1, 9]

In extractive distillation the entrainer doesn't need to be vaporized and remains with

one of the components at the bottom of the distillation column, while the other is obtained pure at the top. For the separation of the entrainer from the remaining component a simple distillation is commonly used. In addition, this technique is known for its high efficiency and for the vast range of entrainers that can be used, from solid to liquid. On the downside, it requires high pressures or high temperatures and, thus, a tremendous amount of energy to obtain one fluid-phase system.[9]

3.2. Azeotropic distillation

The azeotropic distillation follows the same basic principles that of the extractive distillation, requiring two distillation columns for the separation, where the first serves as the main column for the separation while the second one is for the recovery of the entrainer. The main difference between the azeotropic and the extractive distillation is that the former requires the vaporization of all compounds, including the entrainer. Therefore, in this technique the energy consumption is much higher and the range of entrainers that can be used in smaller than in the extractive distillation.[7, 8]

The majority of the entrainers used in azeotropic distillation are highly volatile when compared to the components of the azeotropic mixture, which allows the formers to evaporate first, along with the lightest component of the mixture, to the top of the first column, leaving the heavier compound to be recovered at the bottom of the column. Afterwards, the entrainer and the lightest compound are fed to the second column where they are separated by a simple distillation.

Due to the amount of energy required and the restrictions on the entrainers' selection, the azeotropic distillation is usually disfavoured over the extractive distillation. Nevertheless, because the entrainer comes out of the top in the first column, this technique produces products with higher degree of purity.[7]

Common examples of azeotropic mixtures separated by azeotropic distillation are ethanol or isopropanol + water, formic acid + water and cyclohexane + benzene among others.[7]

3.3. Liquid-liquid extraction

Liquid-liquid extraction (LLE) processes are known to be less energy demanding than any of the other processes used in the separation of azeotropic mixtures. This technique can be used at room temperature because it is based on the principle of the immiscibility between the different compounds present in the mixture, thus requiring the addition of a separation agent. In LLE processes, the separation agent (extraction solvent) interacts preferentially with one of the compounds of the azeotropic mixture, dissolving it and thus promoting a separation of phases, with one phase being composed by the most immiscible compound (diluent or inert) in the extraction solvent, the raffinate, and the other by the more miscible compound (solute) plus the extraction solvent, the extract.[8]

Two crucial parameters widely used in the assessment of an extraction solvent performance are the distribution coefficient, β and the selectivity, S, which are defined as follows:

$$\beta_j = \frac{x_j^{II}}{x_j^{I}} \tag{3}$$

$$S = \frac{x_i^{I}}{x_i^{II}} \times \beta_j \tag{4}$$

where x_i^{I} and x_j^{I} are the mole fractions of the inert and the solute in the upper phase, respectively, and x_i^{II} and x_j^{II} are the mole fractions of the inert and the solute in the lower phase. The distribution coefficient is related to the solute-carrying capacity of the extraction solvent and it determines the amount of solvent required for the extraction process. The selectivity is related to the efficiency of the extraction solvent, indicating the ease of extraction of a solute from a diluent (inert). The ideal extraction solvent should have both high values of distribution coefficient and selectivity, since high selectivity values usually lead to fewer stages in the process and lesser amounts of inert residual in the extract, while

high distribution coefficient values correspond to a lower solvent flow rate, a smaller-diameter column and lower operating costs.[8]

Although LLE processes have the advantage of being low energy consumption process, they are usually a less efficient process than extractive or azeotropic distillation. Nevertheless, LLE is commonly used when distillation is impractical or too costly and becomes more suitable than the later when the relative volatility of the mixture falls between 1 and 1.2.[10] The most well-known examples of the feasibility of LLE for the separation of azeotropic mixture are in mixtures of aromatic + aliphatic hydrocarbons for the range of 20 to 65 wt% of aromatic content,[11] water + 2-butanone,[10] and alcohols + aliphatic hydrocarbons, such as ethanol + n-heptane.[8]

3.4. Other processes

As mentioned before, the separation of azeotropic mixtures can also be accomplished even without the introduction of a separation agent to the mixture. This is the case when pressure swing distillation (PSD) processes are used. This technique takes advantage of the changes in the relative volatility of the liquids by changing the pressure of the mixture. For instance, when the operating pressure is increased, the azeotropic point shifts to lower composition values of the light component, promoting an increase in the relative volatility of the azeotropic mixture. This change in the azeotrope point is sufficient to allow the separation of the mixture without the need for a separating agent.[7]

PSD processes take advantage over other processes, such as azeotropic or extractive distillation and liquid-liquid extraction, since they do not require an additional chemical compound to separate azeotropic mixtures. In addition, Hamad and Dunn[12] showed that by using a PSD process in the separation of the azeotropic mixture of tetrahydrofuran (THF) + water, the energy requirements of the plant could be reduced by more than 60%, when global energy optimization strategies were applied.[12]

Nevertheless, there are far more disadvantages to PSD processes than advantages, including higher complexity of the operation (requires more sophisticated automation and

more complex process control) and the lack of literature data on the phase behaviour of azeotropic mixtures at different pressures (experimental studies tend to be limited to atmospheric conditions), which limits the application of PSD processes in industry.[7]

Another example of processes that do not require the addition of separation agent for the separation of azeotropic mixtures, are processes that use membrane technology, although the membrane itself could also be viewed as a separation agent. Membrane processes are regarded as "clean technology" since they are low energy demanding processes and do not use additional chemicals (extraction solvent or entrainer), but their main advantage is that the selectivity is independent of the vapour-liquid equilibria of the mixture. They are usually applied in the separation of alcohols + water, ketones + esters and aromatic + aliphatic azeotropic mixtures.[7] However, membrane processes' suffer some drawbacks such as low permeate flux, increased processing costs, they are generally limited to moderate volumes (high prices for membrane modules for large capacities) and they have little flexibility to variations in the feed composition.[13]

4. Separation agents

In order to successfully separate azeotropic mixtures there two main factors that have to be considered. The first is the selection of the separation process and the second is the selection of the separation agent. Assuming that the separation process is determined, the most difficult task is to select a feasible separation agent that can assure an efficient and cost-effective separation of the mixture. Indeed, the choice of the separation agent is crucial for the design of a economical viable process. The selection of a the separation agent should always be adjusted to the of azeotropic mixture to be separated, taking into account some key characteristics such as, solubility of the separation agent on the components of the azeotropic mixture, efficiency and recover / regeneration capability, price and handling.

Up to date, only two kinds of separation agents are used at the industrial level: the common volatile organic solvents and inorganic salts or combinations of both. Nevertheless, in the last decade other compounds such as ionic liquids, hyperbranched polymers and

even deep eutectic solvents have been tested at laboratorial level as potential separation agents for the separation of azeotropic mixtures.

4.1. Organic solvents

Organic solvents are the most widely separation agents used in industry for azeotropic mixtures. These compounds can be used in any type of azeotropic or extractive distillation processes as well as in liquid-liquid extraction. They are usually cheap, since most are produced from abundant commodities, such as oil. In addition, the fact that they are liquid poses minimal problems with dissolution, reuse and transport. Nevertheless, organic solvents usually have a very high solvent ratio, i.e., large quantity of solvent to feed mass ratio, which leads to higher energy consumption, adding to the fact that they are volatile and thus pose additional health and environment concerns.

Common examples of organic solvents are polar compounds such as sulfolane, *N*-methylpyrrolidone (NMP), *N*-formylmorpholine (NFM), ethylene glycols and propylene carbonate that are used in the separation of aromatic hydrocarbons like benzene, toluene, ethylbenzene and xylenes from C_4 - C_{10} aliphatic hydrocarbons.[11, 14] *N*,*N*-dimethylformamide (DMF) or acetonitrile (ACN) are used in the separation of C_4 hydrocarbons and ethylene glycol and DMF in the separation of water + alcohols.[9, 13]

4.2. Inorganic salts

Inorganic salts (ISs) are known to be the most efficient separation agents for the azeotropic mixtures and in cases where their solubility is not a problem, they present major advantages over organic solvents. Since they are composed entirely by ions, ISs present a much higher ionic character (the Coulombic forces are much stronger) that allows for much large effects than organic solvents on the azeotropic mixture, leading to higher efficiency on the separation. In addition, comparing with organic solvents, smaller amount of ISs are required for the separation of an azeotropic mixture, resulting in higher production capacity

and lower energy consumption. Moreover, since ISs are not volatile their recovery can be performed by either full or partial drying, rather than by the subsequent distillation as in the case of organic solvents.[13] However, when the solubility of the IS becomes an issue their disadvantages clearly exceed their advantages, limiting their application in industry. Adding to this fact, there are also problems associated with their reuse, storage, transport and in some cases even corrosion of the equipment due to extended exposure to the IS.[7]

These type of separation agents are mostly used in extraction distillation processes (they cannot be used in azeotropic distillation) and for the separation of water from alcohols. Using a 70 / 30 mixture of potassium and sodium acetate, a process known as HIAG (Holz Industrie Acetien Geselleschaft), licensed by DEGUSSA and based on patents registered by Adolph Gorhan, separates water from ethanol, producing ethanol with a purity above 99.8 %.[15] Other ISs such as, calcium chloride, sodium chloride, aluminium chloride, potassium nitrate, copper (II) nitrate, among others have also proven to be effective in the separation of water + ethanol azeotrope mixture.[13] In Japan, the Ishikawajima-Harima Heavy industries (IHI) company developed a process for the production of isopropanol from aqueous solutions using calcium chloride as the separation agent.[13]

4.3. Ionic liquids

Ionic liquids (ILs) have been one of the most studied classes of solvents in last decades. In a simplistic way, it was conventionally accepted that an IL was a salt that presented a melting point bellow a temperature of 100 ºC.[16] Even though ILs can be regarded as a combination of two ions, a cation (usually organic) and a anion (organic or inorganic), they are more than simple liquid salts (Figure 2). Indeed, they present unique characteristics that give them advantages over volatile organic solvents in some applications. The asymmetry and charge dispersion between their cation and anion allow them to be liquid at room temperatures, and the fact that they are constituted by ions permits the adjustment of their physical / chemical properties by a careful selection of ions.[16-18]

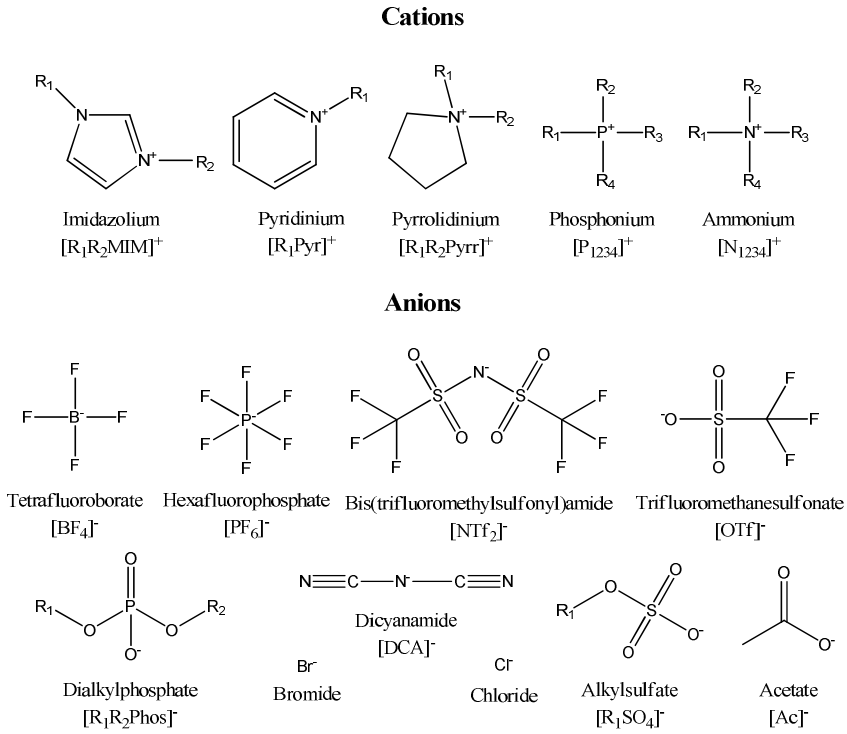

Figure 2 | Cations and anions commonly use in ionic liquids.

Better known as "designer solvents", due to the multiple possible combinations between cations and anions that can be made, ILs exhibit excellent solvent qualities for many types of compounds (polar and non-polar), and generally present high thermal stability, high ionic conductivity and a large liquid temperature range. However, their most attractive feature is their negligible vapour pressures, i.e., they do not evaporate at ambient conditions,[19] which made ILs to be considered as valid potential substitutes of many volatile organic solvents in a wide range of areas such as physical chemistry, electrochemistry, engineering, material sciences, analytics, solvents and catalysts and even biological uses.[20]

Among all of these foreseeable applications for ILs, there has been considerable interest in their use in separation processes, namely in the separation of azeotropic mixtures. Since ILs present negligible vapour pressure, it allows the extracted product to be separated from the IL by low-pressure distillation (potential for energy savings), with the recovery of the IL for reuse. Therefore, the replacement of conventional organic solvents by

ILs in extraction processes is seen as a promising field of investigation.[21]

Recently, Pereiro et al.[8] reviewed processes where ILs were used as separation agents. So far, ILs have been tested in three different processes of separation of azeotropic mixtures: extractive distillation, liquid-liquid extraction and processes using supported liquid membranes. From these processes the first two are those that have been receiving most research attention.

Most of the research in extractive distillation processes, dealing with ILs as entrainers, has been focused on the separation of azeotropic mixtures of THF + water or alcohols + water. In terms of the ILs tested, the most used are those based on the imidazolium cation, where the 1-ethyl-3-methylimidazolium trifluoromethanesulfonate ([C_2MIM][OTf]) and the 1-butyl-3-methylimidazolium chloride ([C_4MIM]Cl) have been the most studied. Nevertheless, the ILs containing chloride and acetate anions have shown the best results.[8] In what concerns liquid-liquid extraction, ILs based on imidazolium and pyridinium cations combined with cyano (-C≡N) based groups have shown higher distribution coefficient and selectivity values than the commonly used organic solvents in the separation of aromatic and aliphatic hydrocarbons, such as toluene or benzene and n-hexane or n-heptane.[11] In addition, imidazolium-based ILs combined with alkyl sulfate anions have also shown great potential in the separation of alcohols from aliphatic hydrocarbons, specifically in the separation of ethanol from n-hexane or n-heptane.[8]

Regarding the industrial application of ILs in the separation of azeotropic mixtures, Meindersma and de Haan[22] used ASPEN Plus 12.1 to simulate the liquid-liquid extraction of toluene + n-heptane azeotropic mixture with the IL 4-methyl-*N*-butylpyridinium tetrafluoroborate ([C_1C_4pyr][BF_4]). Comparing the performance of this IL with that of sulfolane as the extraction solvent, the results show that the investment costs of the process could be decreased in 35 % when the IL was used. However, the application of ILs in the industry is yet to come since the synthesis of ILs usually requires long periods of time and high costs. Moreover, most of the reported ILs still do not provide sufficiently higher values of distribution coefficients or selectivities than those achieved by organic solvents in order to justify their use,[11] adding to the fact that most ILs are moisture sensitivity.[23]

4.4. Other separation agents

Seiler et al.[24, 25] were the first authors to suggest the use of hyperbranched polymers (HyPols) as separation agents for the separation of azeotropic mixtures. These authors studied the liquid-liquid separation of THF + water mixtures using a HyPol of polyester and the separation of ethanol + water mixtures using a HyPol of polyglycerol by means of an extractive distillation process. Their experimental and simulated results lead to the conclusion that cost savings compared to conventional separation processes could be achieved. However, further studies regarding the use of HyPols in the separation of azeotropic mixtures are in need in order to enable a clearer conclusion.

Another class of solvents that has also been attracting increasing interest in recent years is the deep eutectic solvents' (DESs). A typical DES comprises a combination of a hydrogen bond acceptor (HBA), usually a quaternary ammonium or phosphonium salt, with a hydrogen bond donor (HBD) or a complexing agent (CA). The mixture of these two constituents at a certain molar ratio produces a liquid mixture that has a melting point lower than that of the individual constituents (thus, the term eutectic).[26] So far, these compounds have been tested in the separation of alcohols or aromatics from aliphatic hydrocarbons azeotropic mixtures, where Kareem et al.[27-29] and Rodriguez et al.[30] reported performances of the DESs that were comparable with or even superior to conventional organic solvents and ILs.

4.5. Combination of separation agents

In an attempt to improve the efficiency of the chemicals used as separations agents in the separation of azeotropic mixtures, the combinations of different types of separation agents has also been tested.

Lei et al.[13] were the first authors to combine organic solvents with ISs, in order to take advantage of the liquid status of the organic solvents and the high separation ability of the ISs. These authors studied the separation of systems containing polar compounds, such as ethanol + water and isopropanol + water mixtures, using combinations of ethylene glycol +

$CaCl_2$ and K[OH], respectively as entrainers in extractive distillation processes. The results obtained showed that the addition of IS to the ethylene glycol increased the amount of alcohol in the vapour phase and thus the efficiency of the separation. In addition, these authors also tested the separation of C_4 compounds mixtures with DMF, where salts like Na[SCN] and K[SCN] prove to be the best additives by improving the relative volatilities of C_4 to some extent.

Unfortunately, many ISs are corrosive to the equipment and can easily decompose at high temperatures. Also, the amount of IS added to the organic solvents is often small due to solubility issues, making the benefit of adding ISs limited. Another problem is the volatility of the organic solvents, which inevitably poses additional concerns with the recovery of the mixture, since IS are not volatile. Nevertheless, some of these problems might be overcome with the combination of ILs with ISs. Due to the negligible vapour pressures of the ILs, the recovery of a IL-IS mixture becomes simpler than a mixture of organic solvent with an IS. Moreover, ILs are also liquid in a wide range of temperatures and the fact that they are composed by ions allows for a tuning between the IL and the IS, making it possible to solubilise higher amounts of IS in an IL than in an organic solvent. In addition, recent studies show that ILs have an inhibitory effect on the corrosion behaviour of metal in aggressive media.[31-34] Therefore, combining ILs with ISs is more advantageous than combining organic solvent with ISs.

Recently, Lei et al.[35] attempted the separation of water + ethanol mixtures by extractive distillation, using mixtures of IL-IS as entrainers. In this study the 1-ethyl-3-methylimidazolium acetate ([C_2MIM][Ac]) IL was combined with 10 different ISs, namely, K[Ac], Na[Ac], KCl, NaCl, K[HCO_3], Na[HCO_3], K[NO_3], Na[NO_3], K[SCN] and Na[SCN]. The amount of IS was always fixed at a mass fraction of 5 wt%, and the experimental results showed that in all cases the mixture of IL-IS yielded better results than the neat IL, with the K[Ac] showing the most promising results.

Up to date, no other studies regarding the use of IL-IS mixtures for the separation of azeotropic mixture have been found. Nevertheless, in order to use IL-IS mixtures as separation agents is mandatory to previously study the solubility of the IS in the IL, as well as the impact of the former in the physical and chemical properties of the IL.

5. Ionicity

In many cases, the designing of the perfect task-specific IL just by adjusting the cation or the anion can be quite difficult, hence in the last years studies of involving mixtures of ILs with other ILs[36, 37] and also with ISs[38-42] started to appear in the literature. So far, most of the literature studies that merge ILs with simple ISs have been focused on the development of systems for batteries, where ILs based on the bis(trifluoromethylsulfonyl)imide anion ($[NTf_2]^-$) have been deeply investigated.[41-45]

The earliest studies regarding IL-IS mixtures were performed by Wilkes et al.[46, 47] and focused on the physical properties, solid-liquid equilibria and X-ray analysis of chloroaluminate-based ILs with distinct ISs. Rosol et al.[42] published the first studies addressing the solubility behaviour of lithium salts in four imidazolium-based ILs with distinct anions and its effect on viscosity and ionic conductivity. Lui et al.[46] studied the mixing of 1–ethyl–4–(methoxycarbonyl)pyridinium iodide (Kosower's salt) in six different ILs, and because these mixtures were composed of similar ions, particularly in terms of their relative sizes, ideal behaviour was observed. AlNashef et al.[39] studied the solubility of different commercial sodium salts for their potential use in the production of sodium metal by electrochemical processes in ILs. In a more recent work, Pereiro et al.[47] tested the solubility of different ISs that cover a substantial part of the Hofmeister series, both in terms of the cation and the anion, in a wide variety of ILs as shown in Figures 3 and 4.

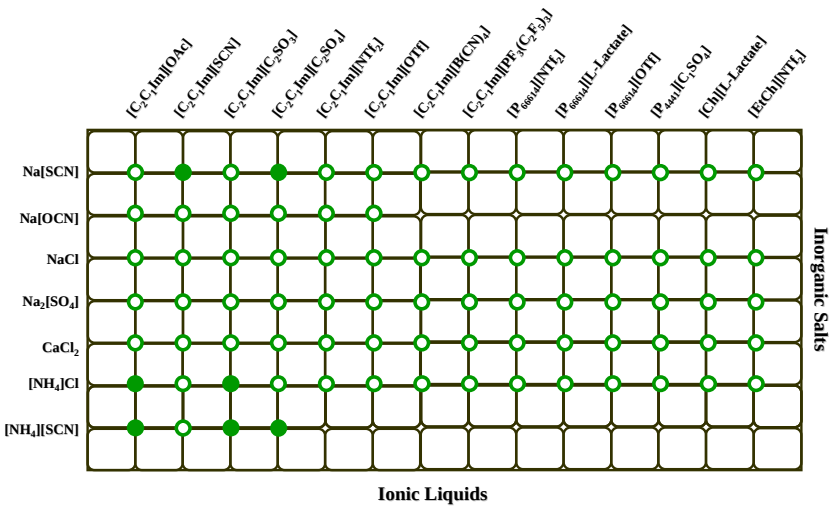

Figure 3 | Matrix of the IL-IS binary mixtures studied. The symbols ○ and ● represent the solubility tests performed using a visual detection method and using a spectroscopic method, respectively.

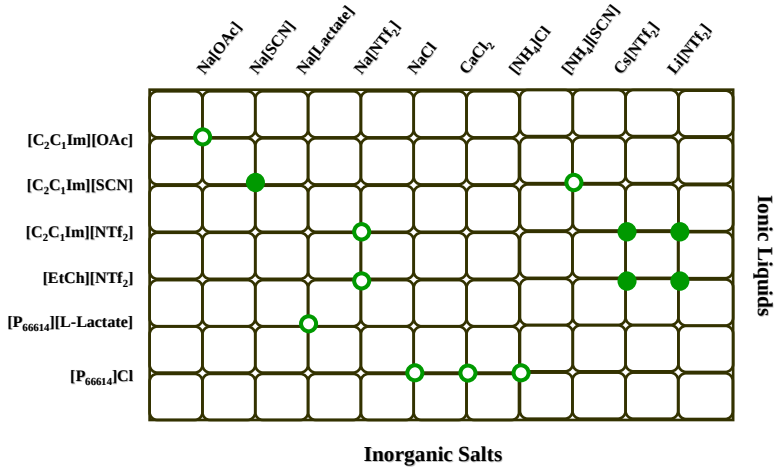

Figure 4 | Matrix of the IL-IS binary mixtures presenting common ions studied. The symbols ○ and ● represent the solubility tests performed using a visual detection method and using a spectroscopic method, respectively.

The results obtained showed that the solubility behaviour is largely dependent on the cation / anion of both the IL and the IS present in the mixture. In general, binary mixtures containing ammonium thiocyanate ([NH_4][SCN]) yielded higher solubilities. On the other

hand, ISs with divalent atom ($Na_2[SO_4]$ and $CaCl_2$) exhibit lower solubilities in the IL. In addition, a comparison between the cations $[C_2MIM]^+$ and trihexyltetradecylphosphonium ($[P_{66614}]^+$) cations demonstrated that a larger alkyl chains hindered the solubility of ISs in the IL. Regarding the binary systems which contained common ions, those with the $[NTf_2]^-$ anion yielded the highest solubilities. The IL-IS systems where high solubilities of IS were obtained are depicted in Table 1, showing that the ISs with ions such as $[NH_4]^+$, $[NTf_2]^-$, and $[SCN]^-$, that are classified according to the Hofmeister series as weakly hydrated ions, yield higher solubilities in different ILs.

Table 1 | Solubility of ISs (2) in ILs (1) at 298.15 K and atmospheric pressure.

Binary mixture	Solubility	
	Molar fraction of ISs	Mass fraction of ISs
$[C_2MIM][C_2SO_4]$ (1) + $[NH_4][SCN]$ (2)	0.6479 ± 0.0036	0.3722 ± 0.0037
$[C_2MIM][C_2SO_3]$ (1) + $[NH_4][SCN]$ (2)	0.4137 ± 0.0046	0.1960 ± 0.0030
$[C_2MIM][Ac]$ (1) + $[NH_4][SCN]$ (2)	0.4035 ± 0.0046	0.2322 ± 0.0034
$[C_2MIM][C_2SO_4]$ (1) + Na[SCN] (2)	0.2371 ± 0.0038	0.0964 ± 0.0018
$[C_2MIM][SCN]$ (1) + Na[SCN] (2)	0.2462 ± 0.0015	0.1353 ± 0.0009
$[C_2MIM][C_2SO_3]$ (1) + $[NH_4]Cl$ (2)	0.2529 ± 0.0031	0.0760 ± 0.0012
$[C_2MIM][Ac]$ (1) + $[NH_4]Cl$ (2)	0.3755 ± 0.0016	0.1590 ± 0.0009
$[C_2MIM][NTf_2]$ (1) + $Li[NTf_2]$ (2)	0.4331 ± 0.0036	0.3592 ± 0.0033
$[EtCh][NTf_2]$ (1) + $Li[NTf_2]$ (2)	0.5603 ± 0.0027	0.4787 ± 0.0028
$[C_2MIM][NTf_2]$ (1) + $Cs[NTf_2]$ (2)	0.2999 ± 0.0034	0.3114 ± 0.0035
$[EtCh][NTf_2]$ (1) + $Cs[NTf_2]$ (2)	0.3223 ± 0.0044	0.3302 ± 0.0045

These results of the solubility of ISs in ILs opened the doors to more insightful studies on the interactions of ISs with ILs, namely in terms of the effect caused by the IS on the structure and properties of the IL. Much of the current research on ILs evaluates the effect of increasing the dispersive contributions by lengthening the alkyl side chains present in the ions and on the effect of increasing other specific van der Waals interactions. However, since ILs are composed by discrete ions, the Coulombic interactions play an important role in the definition of the some thermophysical properties. In this line of thought, Pereiro et al.[48] studied the increase in the Coulombic character of ILs through the solubilisation of ISs in

their media. In this work, two IL-IS binary systems were considered, the 1-ethyl-3-methylimidazolium ethyl sulfate ([C_2MIM][C_2SO_4]) + [NH_4][SCN] and the [C_2MIM][Ac] + [NH_4][SCN]. The thermophysical properties of these two systems were thoroughly studied and NMR data and MD calculations were also obtained in order to gain a better understanding of the interactions between the IL and the IS. The results showed that by solubilising the IS into the IL media, modifications on the IL's initial structure were promoted and the Coulombic character of the ILs could be increased, which lead to the increase of the ionicity of the system leading to the formation of ILs with higher ionicity.

The subject of ionicity in ILs has been extensively discussed by Watanabe[49, 50] and MacFarlane[51] and co-authors, among others. The quantitative estimation of the ILs' ionicity is of great significance for the characterization of these fluids, since it provides a way to study their structure, namely concerning the formation of aggregates or clusters between the IL's ions. The ionicity of ILs has been interpreted as a ratio between the effective concentration of charged species and the total concentration of species (charged and neutral) in the IL, measuring the dissociativity or degree of correlative motion of ions.[50, 52]

There are two main methods to estimate the ionicity of ILs. The first is based on the Walden Plot approach, where plots of the logarithm of the molar conductivity against the logarithm of the fluidity are drawn. In these plots, the ideal Walden line is given by a straight line with a unitary slope, drawn with data of an aqueous solution of KCl, which is usually taken to be representative of the ideal electrolyte, since the ions are known to be fully dissociated. The quantitative determination of the ionicity of the IL is given by the distance of the IL's data to the ideal Walden line. However, this method has been criticized due to the use of KCl solutions of arbitrary compositions as a reference, since Schreiner et al.[53] observed that the slopes of Walden plots for KCl solutions do not represent the unity. In addition, the use of the Walden plot as a quantitative method for the ionicity has also been questioned in the case of a weak electrolyte, where the degree of dissociation is determined by the pK_a.[54] Nevertheless, from a qualitative point of view, the deviation from the ideal Walden line (ΔW) is still a versatile tool to access the ionicity of ILs.

Following the Walden Plot approach, Xu et al.[55] proposed the classification of ILs in "good ILs" or "poor ILs" according to their proximity to ideal behaviour, i.e. fully dissociated

ions, with the majority of the neat ILs tested in literature falling in the "good ILs" region.

Also based on the Walden plot approach, Ueno et al.[56] proposed another method for the calculation of the ionicity. In this method, the ionicity is defined as the ratio between the molar conductivity, calculated from the ionic conductivity measured by the electrochemical impedance method (Λ_{imp}), and the ideal molar conductivity (Λ_{ideal}), which is assumed to be equal to the fluidity (in Poise^{-1}) taken from the ideal Walden line.

The second and most consensual method used for the quantitative determination of the ionicity uses the ratio between the Λ_{imp}, that accounts for the migration of charged species in an electric field, and the molar conductivity calculated from the ion self-diffusion coefficients (Λ_{NMR}), that accounts for the migration of all species in the media (charged and neutral, ions and aggregates).[50] The value of Λ_{NMR} is determined by the Nernst-Einstein (NE) equation as follows:

$$\Lambda_{NMR} = \frac{F^2}{R \cdot T}\left(D^+ + D^-\right) \tag{5}$$

where R and F are the gas and Faraday constants, respectively, T is the temperature and $D^{+/-}$ are the ion self-diffusion coefficients of the IL obtained from the NMR. However, in the case of binary systems such as IL-IS mixtures, the mole fractions (x) of the IL and the IS should be included, as follows:

$$\Lambda_{NMR} = \frac{F^2}{R \cdot T}\left(x_{IL}D_{IL}^+ + x_{IL}D_{IL}^- + x_{IS}D_{IS}^+ + x_{IS}D_{IS}^-\right) \tag{6}$$

A comparison between the two methods used in the determination of the ionicity (ΔW and the Λ_{imp} / Λ_{NMR} ratio) has already been made for neat aprotic ILs,[49, 56] protic ILs[57] and glyme-Li salt equimolar mixtures[56] and a rough consistency was observed. In addition, other studies on the ionicity of neat ILs[50, 58, 59] and aqueous solutions of ILs,[60] where Walden plots were drawn and the ionicity calculated from the Λ_{imp} / Λ_{NMR} ratio, have also corroborated the consistency of the results obtained from both methods. However, in a study concerning IL-

IS systems, Hayamizu et al.[61] doped ILs *N*-methyl-*N*-propyl-pyrrolidinium (P_{13}) [NTf_2] and [FSA] with a fixed concentration of [Li][NTf_2] and [FSA], respectively, and obtained different trends for the ionicity when the two methods described above were used. Using the Walden plot, the authors verified that the trend in the ΔW was [P_{13}][NTf_2] > [P_{13}][NTf_2] + [Li][NTf_2] > [P_{13}][FSA] + [Li][FSA] > [P_{13}][FSA], with the latter neat IL displaying the highest ionicity, whereas when the ionicity was calculated by the Λ_{imp} / Λ_{NMR} ratio, both IL-IS mixtures yielded higher ionicities than the neat ILs according to the following trend: [P_{13}][FSA] + [Li][FSA] > [P_{13}][NTf_2] + [Li][NTf_2] > [P_{13}][FSA] > [P_{13}][NTf_2]. In this study the authors do not explore any further these results. However, these different trends clearly indicate that the determination of the ionicity in IL-IS mixtures is not as simple as in neat ILs and additional studies are needed.

Recently, Holloczki et al.[62] showed that the charge transfer between the ions in neat ILs can also affect the determination of the ionicity, since the neutralization of the mobile species in the media occurs not only due to the formation of ion pairs but also as a result of the charge transfer. Indeed, their data suggested that both phenomena are significant factors that could explain the lower than expected conductivities obtained by NMR (Λ_{NMR}). Moreover, these authors also performed a series of MD simulations on a single probe ion pair of NaCl in the IL [C_4MIM]Br, where they artificially varied the charges of the IS ions. The results showed that by increasing the charge on the IS's ions both the Na-Cl and the IL-IS interactions become stronger and the association of the ion pair is favoured, while a decrease of the charge leads to an IL that behaves more like a molecular liquid than a salt, showing higher fluidity.

6. Objectives

The work developed in this thesis exploits the separation of azeotropic mixtures by LLE processes using IL-IS mixtures as extraction solvents. The main objective is to improve the efficiency of ILs as azeotrope breakers by the increasing their ionicity through the addition of ISs. For this reason, different IL-IS mixtures are explored and their ionicity is

evaluated and understood. The ionicity of the IL-IS mixtures is used as a tool to access, explain and reason out the efficiency of the former mixtures as extraction solvents in the separation of azeotropic mixtures.

The work presented in this thesis explores three different combinations of ILs and ISs, namely one IL with several ISs, different ILs with one IS and one IL with different concentrations of the same IS. Studies of the impact of the addition of the IS on the IL properties, namely density, viscosity and conductivity, are presented and the ionicity of each mixture is calculated and compared with that of other IL-IS mixtures. Molecular insights on these systems are provided by the use of molecular dynamics and NMR in order to better understand the ionicity of the studied mixture. Finally, the studied IL-IS mixtures are tested in the separation of one specific azeotropic mixture, n-heptane + ethanol that will serve as test model (proof-of-concept) for the application of IL-IS mixtures as extraction solvents for breaking azeotropes. These two tasks, the IL-IS ionicity evaluation and their use in the separation of azeotropic mixtures, enable to address the underlying scientific question of this work, the existence of a link between ionicity and extraction efficiency of an azeotropic mixtures, described by the selectivity and distribution coefficient.

7. Thesis outline

The research developed during the time of my PhD project is presented in this article-based thesis constituted by seven chapters. The present chapter introduced the main topics discussed as well as the thesis' objectives. The subsequent chapters (2 to 6) are entirely based on published (or submitted) scientific articles which are not put together by their chronological order of publication, but rather to give the reader a perspective of the evolution of the fields studied in this thesis, starting by the combination of ILs and ISs, exploring and understanding their properties, and ending with their application as separation agents for azeotropic mixtures. Moreover, each article-based chapter includes a brief and objective review of the state of the art for that particular work, presents and discusses the results and draws conclusions. General lists of figures, tables and abbreviations or symbols

are not presented in this thesis since in each individual article-based chapter the aforementioned contents are carefully identified.

Chapter 2 focus on the study of IL-IS mixtures where the same IS is added to two different but yet similar ILs. The thermophysical properties and ionicity of the IL-IS mixture of 1-ethyl-3-methylimidazolium ethyl sulfonate with ammonium thiocyanate were studied, and then compared to those of the IL-IS mixtures with the 1-ethyl-3-methylimidazolium ethyl sulfate IL, previously measured and published by our laboratory. For a better understanding of the interactions that occur at the molecular level, spectroscopic (NMR and Raman) and Molecular Dynamic studies are also presented. The effects caused by the addition of the IS and the different chemical structures of the IL's anions, are discussed based on the changes observed on the ionicity and the thermophysical properties of the IL.

In Chapter 3, a study on IL-IS mixtures with the same IL and six different ISs is presented. This chapter is divided in two parts, where the Part I describes the effect of the different ISs used on the thermophysical properties and ionicity of the IL, while Part II shows some insights into the interactions of the same IL-IS mixtures. In Part I, the work presented considers IL-IS mixtures of the IL 1-ethyl-3-methylimidazolium acetate with four ammonium-based ISs (acetate, chloride, ethyl sulfonate and thiocyanate) and two sodium-based ISs (acetate and thiocyanate). The density, viscosity, conductivity and refractive index of these IL-IS mixtures were studied and the effect of the different cations and anions of the ISs on the aforementioned properties, as well as on the ionicity, of the IL is discussed. Part II focuses on the interactions established in the IL-IS mixtures. NMR and Raman spectroscopy were used to screen for changes in the molecular environment of the ions in the mixtures as compared to their pure state. Molecular Dynamics and *ab initio* simulations where also used for the screening of aggregates between the IL and the IS ions. The formation of preferential interactions between the different ions in the mixture is discussed as well as different methods for the calculation of the ionicity of the IL-IS mixtures.

After acquiring some insights into the behaviour of IL-IS mixtures at both macrospcopic and molecular level, the use of these solvents in the separation of azeotropic mixtures was evaluated. Therefore, in the next two chapters, Chapter 4 and 5, the use of IL-IS mixtures as potential separation agents for azeotropic mixtures by liquid-liquid extraction process is

described. The main goal of the studies presented in these two chapters, was to improve the efficiency of the IL as a separation agent of azeotropic mixtures and, at the same time, correlate the ionicity of the IL-IS mixture with the extraction efficiency. Therefore, in Chapter 4, IL-IS mixtures of $[C_2MIM][C_2SO_4]$ with ammonium thiocyanate were tested for the liquid-liquid separation of n-heptane + ethanol mixtures. Three different concentration of the IS were used in the mixtures and their impact on the distribution coefficient and selectivity values of the systems is discussed, along with a comparison of the IL-IS mixtures with the neat IL. In the next study, presented in Chapter 5, $[C_2MIM][Ac]$ was used in the studied IL-IS mixtures and the three ISs, ammonium acetate, chloride and thiocyanate, at a fixed concentration were used. The effects caused by different anions of the IS in the efficiency of the extraction of ethanol from n-heptane are discussed.

Although the main focus of this thesis is on the study of the ionicity of IL-IS mixtures and their application on the separation of azeotropic mixtures, and taking into account that DES can be understood as ILs by the formation of a new anion through the establishment of hydrogen bonds between the IL´s anion and the hydrogen bond donor, Chapter 6 describes the possible application of deep eutectic solvents as separation agents for the breaking of azeotropic mixtures. In this work, three different deep eutectic solvents were tested for the extraction of ethanol from n-heptane + ethanol azeotropic mixtures. The deep eutectic solvents used were all based on choline chloride and were combined with different HBD such as glycerol, ethylene glycol and levulinic acid. A comparison between the results obtained and those found in literature for neat ILs, as well as the impact of the different HBD on the distribution coefficient and selectivity values is discussed.

Finally, in Chapter 7, the key results presented in the different chapters are summarized, and the main conclusions are withdrawn and discussed in an integrated way. Possible challenges and future work are also discussed.

8. References

1. E. G. de Azevedo and A. M. Alves, eds., *Engenharia de processos de separação*, IST Press, 2009.

2. T. P. Ognisty, Analyze distillation columns with thermodynamics, *Chem. Eng. Prog.*, 1995, **91**, 40-46.

3. P. W. Atkins, *Physical Chemistry 6th ed.*, Oxford University Press, 1998.

4. J. Gmehling, J. Menke, J. Krafczyk and K. Fischer, eds., *Azeotropic Data Part I and Part II*, VCH-Publishers, Weinheim, New York, 1994.

5. L. H. Horsley, Azeotropic data II, *Adv. Chem. Ser.*, 1962, **35**.

6. A. Pucci, Phase equilibria of alkanol/alkane mixtures in new oil and gas process development, *Pure Appl. Chem.*, 1989, **61**, 1363-1372.

7. T. Mahdi, A. Ahmad, M. M. Nasef and A. Ripin, State-of-the-art technologies for separation of azeotropic mixtures, *Sep. Purif. Rev.*, 2015, **44**, 308-330.

8. A. B. Pereiro, J. M. M. Araújo, J. M. S. S. Esperança, I. M. Marrucho and L. P. N. Rebelo, Ionic liquids in separations of azeotropic systems - A review, *J. Chem. Thermodyn.*, 2012, **46**, 2-28.

9. Z. Lei, C. Li and B. Chen, Extractive distillation: A review, *Sep. Purif. Rev.*, 2003, **32**, 121-213.

10. L. A. Robbins and R. W. Cusack, *Liquid-liquid extraction operations and equipment*, in *Perry's chemical engineers' handbook, 7th ed.*, eds. R. H. Perry, D. W. Green and J. O. Maloney, McGraw-Hill, New York, 1999.

11. G. W. Meindersma, A. R. Hansmeier and A. B. de Haan, Ionic liquids for aromatics extraction. Present status and future outlook, *Ind. Eng. Chem. Res.*, 2010, **49**, 7530-7540.

12. A. Hamad and R. F. Dunn, Energy optimization of pressure-swing azeotropic distillation systems, *Ind. Eng. Chem. Res.*, 2002, **41**, 6082-6093.

13. Z. Lei, B. Chen and Z. Ding, *Special distillation processes, 1st ed.*, Elsevier B. V., 2005.

14. S. H. Ali, H. M. S. Lababidi, S. Q. Merchant and M. A. Fahim, Extraction of aromatics from naphtha reformate using propylene carbonate, *Fluid Phase Equilib.*, 2003,

214, 25-38.

15. W. F. Furter, Production of fuel-grade ethanol by extractive distillation employing the salt effect, *Sep. Purif. Rev.*, 1993, **22**, 1-21.

16. D. R. MacFarlane and K. R. Seddon, Ionic liquids - Progress on the fundamental issues, *Aust. J. Chem.*, 2007, **60**, 3-5.

17. L. P. N. Rebelo, J. N. C. Lopes, J. M. S. S. Esperança, H. J. R. Guedes, J. Lachwa, V. Najdanovic-Visak and Z. P. Visak, Accounting for the unique, doubly dual nature of ionic liquids from a molecular thermodynamic, and modeling standpoint, *Acc. Chem. Res.*, 2007, **40**, 1114-1121.

18. R. D. Rogers and K. R. Seddon, Ionic liquids - Solvents of the future?, *Science*, 2003, **302**, 792-793.

19. M. J. Earle, J. M. S. S. Esperança, M. A. Gilea, J. N. C. Lopes, L. P. N. Rebelo, J. W. Magee, K. R. Seddon and J. A. Widegren, The distillation and volatility of ionic liquids, *Nature*, 2006, **439**, 831-834.

20. N. V. Plechkova and K. R. Seddon, Applications of ionic liquids in the chemical industry, *Chem. Soc. Rev.*, 2008, **37**, 123-150.

21. K. N. Marsh, A. Deev, A. C.-T. Wu, E. Tran and A. Klamt, Room temperature ionic liquids as replacements for conventional solvents - A review, *Korean J. Chem. Eng.*, 2002, **19**, 357-362.

22. G. W. Meindersma and A. B. de Haan, Conceptual process design for aromatic/aliphatic separation with ionic liquids, *Chem. Eng. Res. Des.*, 2008, **86**, 745-752.

23. M. J. Earle and K. R. Seddon, Ionic liquids. Green solvents for the future, *Pure Appl. Chem.*, 2000, **72**, 1391-1398.

24. M. Seiler, Hyperbranched polymers: Phase behavior and new applications in the field of chemical engineering, *Fluid Phase Equilib.*, 2006, **241**, 155-174.

25. M. Seiler, C. Jork, A. Kavarnou, W. Arlt and R. Hirsch, Separation of azeotropic mixtures using hyperbranched polymers or ionic liquids, *AIChE J.*, 2004, **50**, 2439-2454.

26. A. P. Abbott, D. Boothby, G. Capper, D. L. Davies and R. K. Rasheed, Deep eutectic solvents formed between choline chloride and carboxylic acids: Versatile alternatives to ionic liquids, *J. Am. Chem. Soc.*, 2004, **126**, 9142-9147.

27. M. A. Kareem, F. S. Mjalli, M. A. Hashim and I. M. AlNashef, Liquid–liquid equilibria for the ternary system (phosphonium based deep eutectic solvent–benzene–hexane) at different temperatures: A new solvent introduced, *Fluid Phase Equilib.*, 2012, **314**, 52-59.

28. M. A. Kareem, F. S. Mjalli, M. A. Hashim, M. K. O. Hadj-Kali, F. S. G. Bagh and I. M. Alnashef, Phase equilibria of toluene/heptane with tetrabutylphosphonium bromide based deep eutectic solvents for the potential use in the separation of aromatics from naphtha, *Fluid Phase Equilib.*, 2012, **333**, 47-54.

29. M. A. Kareem, F. S. Mjalli, M. A. Hashim, M. K. O. Hadj-Kali, F. S. G. Bagh and I. M. Alnashef, Phase equilibria of toluene/heptane with deep eutectic solvents based on ethyltriphenylphosphonium iodide for the potential use in the separation of aromatics from naphtha, *J. Chem. Thermodyn.*, 2013, **65**, 138-149.

30. N. R. Rodriguez, B. S. Molina and M. C. Kroon, Aliphatic + ethanol separation via liquid–liquid extraction using low transition temperature mixtures as extracting agents, *Fluid Phase Equilib.*, 2015, **394**, 71-82.

31. X. Zhou, H. Yang and F. Wang, [BMIM][BF_4] ionic liquids as effective inhibitor for carbon steel in alkaline chloride solution, *Electrochim. Acta*, 2011, **56**, 4268-4275.

32. Q. B. Zhang and Y. X. Hua, Corrosion inhibition of mild steel by alkylimidazolium ionic liquids in hydrochloric acid, *Electrochim. Acta*, 2009, **54**, 1881-1887.

33. Q. B. Zhang and Y. X. Hua, Corrosion inhibition of aluminum in hydrochloric acid solution by alkylimidazolium ionic liquids, *Mater. Chem. Phys.*, 2010, **119**, 57-64.

34. L. C. Murulana, A. K. Singh, S. K. Shukla, M. M. Kabanda and E. E. Ebenso, Experimental and quantum chemical studies of some bis(trifluoromethylsulfonyl)imide imidazolium-based ionic liquids as corrosion inhibitors for mild steel in hydrochloric acid solution, *Ind. Eng. Chem. Res.*, 2012, **51**, 13282-13299.

35. Z. Lei, X. Xi, C. Dai, J. Zhu and B. Chen, Extractive distillation with the mixture of ionic liquid and solid inorganic salt as entrainers, *AIChE J.*, 2014, **60**, 2994-3004.

36. H. Niedermeyer, J. P. Hallett, I. J. Villar-Garcia, P. A. Hunt and T. Welton, Mixtures of ionic liquids, *Chem. Soc. Rev.*, 2012, **41**, 7780-7802.

37. G. Chatel, J. F. B. Pereira, V. Debbeti, H. Wang and R. D. Rogers, Mixing ionic liquids - "simple mixtures" or "double salts"?, *Green Chem.*, 2014, **16**, 2051-2083.

38. A. Abebe, S. Admassie, I. J. Villar-Garcia and Y. Chebude, 4,4-Bipyridinium ionic liquids exhibiting excellent solubility for metal salts: Potential solvents for electrodeposition, *Inorg. Chem. Commun.*, 2013, **29**, 210-212.

39. I. M. AlNashef, *Solubility and electrical conductivity of common sodium salts in selected ionic liquids*, in *Fundamental of Chemical Engineering, Pts 1-3*, eds. Z. Cao, L. Sun, X. Q. Cao and Y. H. He, 2011, vol. 233-235, pp. 2760-2764.

40. C. Chiappe, M. Malvaldi, B. Melai, S. Fantini, U. Bardi and S. Caporali, An unusual common ion effect promotes dissolution of metal salts in room-temperature ionic liquids: A strategy to obtain ionic liquids having organic-inorganic mixed cations, *Green Chem.*, 2010, **12**, 77-80.

41. J.-C. Lassègues, J. Grondin, C. Aupetit and P. Johansson, Spectroscopic identification of the lithium ion transporting species in LiTFSI-doped ionic liquids, *J. Phys. Chem. A*, 2009, **113**, 305-314.

42. Z. P. Rosol, N. J. German and S. M. Gross, Solubility, ionic conductivity and viscosity of lithium salts in room temperature ionic liquids, *Green Chem.*, 2009, **11**, 1453-1457.

43. B. Garcia, S. Lavallee, G. Perron, C. Michot and M. Armand, Room temperature molten salts as lithium battery electrolyte, *Electrochim. Acta*, 2004, **49**, 4583-4588.

44. S. F. Lux, M. Schmuck, G. B. Appetecchi, S. Passerini, M. Winter and A. Balducci, Lithium insertion in graphite from ternary ionic liquid-lithium salt electrolytes: II. Evaluation of specific capacity and cycling efficiency and stability at room temperature, *J. Power Sources*, 2009, **192**, 606-611.

45. M. J. Monteiro, F. F. C. Bazito, L. J. A. Siqueira, M. C. C. Ribeiro and R. M. Torresi, Transport coefficients, Raman spectroscopy, and computer simulation of lithium salt solutions in an ionic liquid, *J. Phys. Chem. B*, 2008, **112**, 2102-2109.

46. M. Y. Lui, L. Crowhurst, J. P. Hallett, P. A. Hunt, H. Niedermeyer and T. Welton, Salts dissolved in salts: Ionic liquid mixtures, *Chem. Sci.*, 2011, **2**, 1491-1496.

47. A. B. Pereiro, J. M. M. Araújo, F. S. Oliveira, J. M. S. S. Esperança, J. N. C. Lopes, I. M. Marrucho and L. P. N. Rebelo, Solubility of inorganic salts in pure ionic liquids, *J. Chem. Thermodyn.*, 2012, **55**, 29-36.

48. A. B. Pereiro, J. M. M. Araújo, F. S. Oliveira, C. E. S. Bernardes, J. M. S. S. Esperança, J. N. C. Lopes, I. M. Marrucho and L. P. N. Rebelo, Inorganic salts in purely ionic liquid media: The development of high ionicity ionic liquids (HIILs), *Chem. Commun.*, 2012, **48**, 3656-3658.

49. H. Tokuda, S. Tsuzuki, M. Susan, K. Hayamizu and M. Watanabe, How ionic are room-temperature ionic liquids? An indicator of the physicochemical properties, *J. Phys. Chem. B*, 2006, **110**, 19593-19600.

50. K. Ueno, H. Tokuda and M. Watanabe, Ionicity in ionic liquids: Correlation with ionic structure and physicochemical properties, *Phys. Chem. Chem. Phys.*, 2010, **12**, 1649-1658.

51. D. R. MacFarlane, M. Forsyth, E. I. Izgorodina, A. P. Abbott, G. Annat and K. Fraser, On the concept of ionicity in ionic liquids, *Phys. Chem. Chem. Phys.*, 2009, **11**, 4962-4967.

52. C. Zhang, K. Ueno, A. Yamazaki, K. Yoshida, H. Moon, T. Mandai, Y. Umebayashi, K. Dokko and M. Watanabe, Chelate effects in glyme/lithium bis(trifluoromethanesulfonyl)amide solvate ionic liquids. I. Stability of solvate cations and correlation with electrolyte properties, *J. Phys. Chem. B*, 2014, **118**, 5144-5153.

53. C. Schreiner, S. Zugmann, R. Hartl and H. J. Gores, Fractional walden rule for ionic liquids: Examples from recent measurements and a critique of the so-called ideal KCl line for the walden plot, *J. Chem. Eng. Data*, 2010, **55**, 1784-1788.

54. K. R. Harris, Relations between the fractional Stokes-Einstein and Nernst-Einstein equations and velocity correlation coefficients in ionic liquids and molten salts, *J. Phys. Chem. B*, 2010, **114**, 9572-9577.

55. W. Xu, E. I. Cooper and C. A. Angell, Ionic liquids: Ion mobilities, glass temperatures, and fragilities, *J. Phys. Chem. B*, 2003, **107**, 6170-6178.

56. K. Ueno, K. Yoshida, M. Tsuchiya, N. Tachikawa, K. Dokko and M. Watanabe, Glyme–lithium salt equimolar molten mixtures: Concentrated solutions or solvate ionic liquids?, *J. Phys. Chem. B*, 2012, **116**, 11323-11331.

57. M. S. Miran, H. Kinoshita, T. Yasuda, M. A. B. H. Susan and M. Watanabe, Physicochemical properties determined by ΔpK_a for protic ionic liquids based on an organic

super-strong base with various Bronsted acids, *Phys. Chem. Chem. Phys.*, 2012, **14**, 5178-5186.

58. K. Hayamizu, S. Tsuzuki and S. Seki, Transport and electrochemical properties of three quaternary ammonium ionic liquids and lithium salts doping effects studied by NMR spectroscopy, *J. Chem. Eng. Data*, 2014, **59**, 1944-1954.

59. B. E. M. Tsamba, S. Sarraute, M. Traikia and P. Husson, Transport properties and ionic association in pure imidazolium-based ionic liquids as a function of temperature, *J. Chem. Eng. Data*, 2014, **59**, 1747-1754.

60. J. M. Andanson, M. Traikia and P. Husson, Ionic association and interactions in aqueous methylsulfate alkyl-imidazolium-based ionic liquids, *J. Chem. Thermodyn.*, 2014, **77**, 214-221.

61. K. Hayamizu, S. Tsuzuki, S. Seki, K. Fujii, M. Suenaga and Y. Umebayashi, Studies on the translational and rotational motions of ionic liquids composed of N-methyl-N-propyl-pyrrolidinium (P-13) cation and bis(trifluoromethanesulfonyl)amide and bis(fluorosulfonyl)amide anions and their binary systems including lithium salts, *J. Chem. Phys.*, 2010, **133**, 1945051-19450513.

62. O. Holloczki, F. Malberg, T. Welton and B. Kirchner, On the origin of ionicity in ionic liquids. Ion pairing versus charge transfer, *Phys. Chem. Chem. Phys.*, 2014, **16**, 16880-16890.

Chapter 2

Ionicity in -SO_x based ILs: comparing the effect of ethyl sulfonate and ethyl sulfate anions.

Adapted from: **Filipe S. Oliveira**, Ana B. Pereiro, João M. M. Araújo, Carlos E. S. Bernardes, José N. Canongia Lopes, Smilja Todorovic, Gabriel Feio, Pedro L. Almeida, Luís P. N. Rebelo and Isabel M. Marrucho, High ionicity ionic liquids (HIILs): comparing the effect of ethylsulfonate and ethylsulfate anions, *Phys. Chem. Chem Phys.* (2013), **15**, 18138-18147.

The sample preparation for all the experiments presented herein was performed by the author. The author was also involved in all the experiments, as well as on the discussion and interpretation of the data and preparation of the manuscript. Raman Spectroscopy and Molecular Dynamics sections, were performed by Smilja Todorovic, and Carlos E. S. Bernardes and José N. Canongia Lopes, respectively. The NMR experiments were carried out in collaboration with Gabriel Feio and Pedro L. Almeida.

1. Abstract

In this work, a comparison between the thermophysical properties of two binary systems containing ionic liquid + inorganic salt, is presented. The effect of ammonium thiocyanate salt on the ionicity of two similar ionic liquids, 1-ethyl-3-methylimidazolium ethyl sulfonate and ethyl sulfate, is deconstructed in terms of the related thermophysical properties, namely density, viscosity and ionic conductivity in the temperature range 298.15 K – 323.15 K. In addition, spectroscopic (NMR and Raman) and Molecular Dynamic studies were conducted in order to understand, at a molecular level, the interactions that occur in these system. The obtained results reveal that although the two anions of the ionic liquid exhibit similar chemical structures, the presence of one additional oxygen in the ethyl sulfate anion has a major impact on interactions and thus on the thermophysical properties of the studied systems.

2. Introduction

In the last couple of years, several authors have debated the concept of the ionicity of ionic liquids (ILs), and showed that a quantitative description of the ionicity can be a useful indicator of the thermodynamic and thermophysical behaviour of ionic liquids.[1, 2]

The ionicity of an IL or the degree of dissociation / association of an IL is related to its ionic nature, which is controlled by the magnitude and balance of the interactive forces. Due to the complex nature of these solvents, several interactions are present in ILs, such as Coulombic, van der Waals, hydrogen-bonding and π-π interactions, with Coulombic being the predominant. Although ideally ILs consist of discrete ions, in reality they form aggregates or clusters to some extent. The formation of aggregates has obviously strong impact on some ILs properties such as viscosity, conductivity, and diffusion coefficients. However, other IL's properties, as vapour pressure and hydrogen acceptor or donor character, can also be linked to ionicity.[3] Thus, the evaluation of the ionicity of ILs has become an interesting and important parameter for their characterization.[2, 4]

Several studies on the ionicity of pure ILs have already been conducted.[2-9] Based on the classical Walden rule [3, 10], which relates the ionic conductivity to the fluidity, the ionicity of ILs can be assessed. Most of the ILs studied so far showed a behaviour close to the ideal, where the ion-ion interactions are absent and the ions are fully dissociated and have equal mobility. The former ILs were classified as "good ILs", while the others that present a behaviour very distant from the ideal were regarded as "poor ILs".[3, 11]

In our previous work,[12] we showed that the Coulombic character of the IL can be incremented through the solubilisation of simple inorganic salts (ISs) in their milieu, thus increasing the ionicity of ILs at very low cost, while the liquid state status is still preserved.

Most of the literature studies that merge ILs with simple ISs focus on the development of systems for batteries, where ILs based on bistriflamide anion have been deeply investigated.[13-17] For example, Lui et al.[18] show results on mixing 1–ethyl–4–(methoxycarbonyl)pyridinium iodide (Kosower's salt) in six different ILs, but these mixtures are composed of similar ions, particularly in terms of relative sizes, and thus ideal behaviour is observed. Umebayashi et al.[19, 20] studied the solvation structure of the lithium ion (from lithium bis(trifluoromethylsulfonyl)amide salt, [Li][NTf_2]) in three different ILs, two imidazolium-based (1-ethyl-3-methylimidazolium bis(trifluoromethylsulfonyl)amide and 1-butyl-3-methylimidazolium bis(trifluoromethylsulfonyl)amide) and one pyrrolidinium-based (N-butyl-N-methylpyrrolidinium bis(trifluoromethylsulfonyl)amide) by Raman spectroscopy, Density Functional Theory and ab initio calculations. In the Raman spectra, these authors observed that the intensity of strong band at 744 cm^{-1}, attributed to the free [NTf_2]$^-$ anion in the bulk, decreases with the increasing concentration of lithium salt. Simultaneously, a new band at 750 cm^{-1} appeared with the increase in salt content, which is attributed to the binding of [NTf_2]$^-$ anions to the lithium cation. In addition, using ab initio calculations it was possible to show that the lithium cation coordinated with the four oxygen atoms of the bidentate [NTf_2]$^-$ anion. Another important observation is that the IL cation played a key role in the stabilization of the complex formed by the lithium cation and the [NTf_2]$^-$ anions. Zhou et al.[21] used crystallography and Raman studies to show that lithium cations serve as crosslinkers between the anions, forming aggregates and eventually new networks of ions which results in a dramatic decrease in the ionic conductivity. Hayamizu et al.[9] studied the

diffusion behaviour of 1-ethyl-3-methylimidazolium bis(trifluoromethylsulfonyl)amide and 1-ethyl-3-methylimidazolium bis(fluorosulfonyl)amide and their corresponding binary systems with lithium salts. The results showed that in spite of the extremely small lithium radius (0.06 nm), the lithium diffusion coefficients were the smallest of all ions, which clearly confirms that lithium cations are engaged in the formation of complexes.

The present work is a continuation of our previous study[12] where the effect of the addition of ISs on the ionicity of ILs is explored. Two ionic liquids, 1-ethyl-3-methylimidazoilum ethyl sulfonate ($[C_2MIM][C_2SO_3]$) and 1-ethyl-3-methylimidazoilum ethyl sulfate ($[C_2MIM][C_2SO_4]$), which (slightly) differ in the nature of their constituting anions (ethyl sulfate has an extra oxygen atom), were selected for comparison. Deive et al.[22] conducted a study on phase equilibria of haloalkanes dissolved in the same two ILs. The results showed that the haloalkanes studied are more soluble in $[C_2MIM][C_2SO_3]$ than in $[C_2MIM][C_2SO_4]$. This fact was attributed to the extra oxygen atom in the $[C_2MIM][C_2SO_4]$, which causes shifts in the charge distribution of the anion especially at the first carbon atom of the alkyl side chain. Furthermore, the presence of the oxygen atom between the charged $–SO_3$ group and the nonpolar alkyl side chain, allows the ethyl sulfate anion to exhibit a larger polar moiety and to form more extensive polar networks.[23]

The aim of the present work is to establish a comparison between the ionicity of the binary system 1-ethyl-3-methylimidazoilum ethyl sulfonate + ammonium thiocyanate, evaluated in this work, with a similar binary system, the 1-ethyl-3-methylimidazoilum ethyl sulfate + ammonium thiocyanate, measured in a previous work.12 The ionicity of these systems will be deconstructed into the related thermophysical properties, such as density, viscosity and ionic conductivity in the temperature range 298.15 K – 323.15 K. Refractive index and thermal stability measurements have also been carried out as a function of the IS content. NMR spectroscopy was used for the determination of the diffusion coefficients and to identify preferential interactions between both cations and anions. Raman spectroscopy was employed to monitor the molecular environment of the thiocyanate anion in the two binary systems. MD studies were used to provide further insights at molecular level in order to corroborate the experimental data.

In generally, this work contributes to the understanding of interactions at the molecular

level that govern macroscopic characteristics of the IL-IS systems so that a rational design of IL-IS systems can be proposed.

3. Experimental Section

3.1. Materials

The ionic liquid 1-ethyl-3-methylimidazolium ethyl sulfonate ($[C_2MIM][C_2SO_3]$) was prepared according to a previously described procedure.[24, 25] The inorganic salt, ammonium thiocyanate ($[NH_4][SCN]$) ($\geq$ 0.99 mass fraction purity) was supplied by Sigma-Aldrich. To reduce the water and other volatile substances content, vacuum (ca. 10^{-1} Pa) and moderate temperature (ca. 323.15 K) were always applied to both the IL and the IS for more than 48 hours prior to their use. After drying, the IL purity was checked by ^1H and ^{13}C NMR. The ^1H spectra confirmed purity levels higher or around 99%. Karl Fischer coulometric titration (Metrohm 831 KF Coulometer) was used to determine the final water mass fraction of the ionic liquid, which contained less than 150 ppm of water.

3.2. IL + IS mixtures

The binary mixtures of $[C_2MIM][C_2SO_3]$ + $[NH_4][SCN]$ were prepared in the range between 0 and 0.3 in IS mole fraction, taking into account the solubility limits determined on our previous work.[26] The samples were prepared in an inert-atmosphere glove box, since the IL is moisture sensitive, using an analytical high-precision balance with an uncertainty of $\pm$ 10^{-5} g by weighing known masses of the each component into stoppered flasks. Good mixing was assured by magnetic stirring. For each sample, triplicates of the physical properties were measured to ensure accuracy. In Figure 1 the structures and numbering of the $[C_2MIM][C_2SO_3]$, $[C_2MIM][C_2SO_4]$ and $[NH_4][SCN]$ are presented.

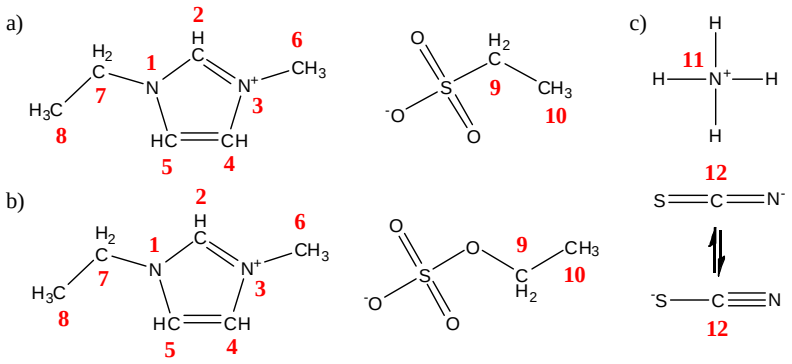

Figure 1 | Structure and numbering of the two ionic liquids compared in this work, a) $[C_2MIM][C_2SO_3]$ and b) $[C_2MIM][C_2SO_4]$, and the inorganic salt c) $[NH_4][SCN]$.

3.3. Viscosity and density measurements

Measurements of viscosity and density were performed in the temperature range between 298.15 and 323.15 K at atmospheric pressure, using an automated SVM 3000 Anton Paar rotational Stabinger viscometer-densimeter. The temperature uncertainty is ± 0.02 K. Further details on the equipment can be found elsewhere.[27] Triplicates of the IL and each IL-IS mixture were measured and the reported results is the average value. The uncertainty of the dynamic viscosity and density measurements is ± 1.3 % and ± 0.01 %, respectively.

3.4. Ionic conductivity measurements

Ionic conductivities were performed using a CDM210 Radiometer Analytical conductivimeter in the temperature range between 298.15 and 323.15 K. Measurements were performed in a glass cell containing a magnetic stirrer and temperature regulated by a water jacket connected to a bath controlled to ± 0.01 K. The temperature in the cell was measured using a platinum resistance thermometer coupled to a Keithley 199 System DMM/Scanner. The thermometer was calibrated with high–accuracy mercury thermometers

(0.01 K). Further details on the equipment can be found elsewhere.[12]

Previous to the measurements, the conductivimeter was calibrated at each temperature with certified 0.01 D KCl standard solution supplied by Radiometer Analytical. For determination of the ionic conductivity, approx. 1.5 mL of the sample was added to the thermostatic cell, closed with screw caps and vigorously stirred. Each single measurement was performed as quickly as possible to minimize undesired effects (such as self–heating of the samples, ionization in the electrodes, etc)[28, 29] that might modify the measured conductivity values.

Each conductivity value was determined at least three times to ensure its reproducibility within 1 % in absolute value.

3.5. Refractive index and thermal stability measurements

The experimental methods used for the refractive index and thermal stability measurements are described in the supporting information (SI), at the end of this chapter. The data obtained for the refractive index, molar volume, molar refraction and free molar volume for the neat $[C_2MIM][C_2SO_3]$ and $[C_2MIM][C_2SO_4]$ and their binary mixtures are depicted in Tables S1 and S2, respectively, in the SI. The thermal decomposition temperatures for the binary systems $[C_2MIM][C_2SO_3]$ or $[C_2MIM][C_2SO_4]$ + $[NH_4][SCN]$ are depicted in Table S3 in the SI.

3.6. NMR spectroscopy

NMR spectroscopy was used for two different studies in this work. In the first the changes in the ^1H and ^{13}C chemical shifts of $[C_2MIM][C_2SO_3]$ with increasing $[NH_4][SCN]$ concentration was evaluated, while in the second the diffusivity of the IL-IS systems was determined.

For the first study, the experiments were carried out on a Bruker AVANCE 400 spectrometer operated at room temperature with 16 scans for ^1H NMR and 500 scans for

^{13}C NMR. The samples were prepared gravimetrically using an analytical high–precision balance with an uncertainty of ± 10^{-5} g, by adding different amounts of $[NH_4][SCN]$ into solutions of 1:1 in mass fraction of ionic liquid and deuterated dimethyl sulfoxide (DMSO–d_6). Upon complete dissolution, the samples were transferred to 5 mm NMR tubes containing the same amount of DMSO–d_6. All spectra were obtained using DMSO–d_6, for field–frequency lock and NMR internal reference. As reported in previous studies,[30, 31] the addition of DMSO–d_6 as a co–solvent has no impact on the chemical shifts trends obtained upon IS or IL addition. For the measurements of the self-diffusion coefficients of the samples, a Bruker AVANCE 300 wide board spectrometer, with a Diff30 diffusion probe with a gradient amplifier of high power (60 A and 1500 $G \cdot cm^{-1}$) was used. The ^1H diffusion coefficients were measured using the Pulsed Gradient Stimulated Echo (PGSTE) method operating at a frequency of 300.14 MHz and at 298.15 K. The gradient pulse duration (δ) was typically of 2.5 ms, the diffusion time (Δ) of 50 ms and the maximum gradient value of 400 $G \cdot cm^{-1}$.

3.7. Raman spectroscopy

Raman spectra of the $[C_2MIM][C_2SO_4]$ + $[NH_4][SCN]$ mixtures were measured in sealed vials in backscattering geometry using Raman spectrometer (Jobin Yvon U1000), coupled to a confocal microscope equipped with 1200 1/mm grating and a liquid nitrogen cooled CCD detector. The 413 nm line from a Kr^+-laser (Coherent Innova 302) was used as excitation source. For each sample four spectra were recorded with 3 mW laser power and 60s accumulation time at RT. In order to avoid strong background fluorescence, Raman spectra of the $[C_2MIM][C_2SO_3]$ + $[NH_4][SCN]$ mixtures were measured with 1064 nm excitation (Nd-YAG cw laser) using RFS 100/S (Bruker Optics, Ettlinger, Germany) Fourier-transform Raman spectrometer. Laser power was set to 400 mW and 100 scans were recorded for each sample at room temperature.

3.8. Molecular dynamics simulations

Molecular Dynamics simulations on selected IL-IS mixtures were used to interpret the experimental data at a molecular scale. All simulation runs were performed using the DL_POLY package version 2.20.[32] The force field developed by Canongia Lopes and co-workers[23, 33] was selected to describe the inter- and intra-molecular interactions in the $[C_2MIM][C_2SO_3]$ and $[C_2MIM][C_2SO_4]$ ILs. In the case of $[NH_4][SCN]$, a previously developed parameterization for the behaviour of this IS in IL media was used.[12]

The simulation boxes, with a total number of 200 ions, were prepared by random distribution of the IL and IS ions to yield $[NH_4][SCN]$ mole fractions of 0.0, 0.1 and 0.3. In the case of $[C_2MIM][C_2SO_4]$ plus $[NH_4][SCN]$ mixtures, an equimolar fraction was also considered. Cutoff distances of 1.4 nm were used in all simulations and the Ewald summation technique (k-values set to 6 and α = 0.199 Å) were applied to account for long-range Coulomb interactions beyond the cutoff.

All simulations were performed under the isothermal-isobaric (*N*-*p*-*T*) ensemble. The equilibration period, composed of short and consecutive 0.5 ns simulation runs, was performed by using the following temperature/pressure sequence: (i) p = 5.0 MPa, T = 1000 K; (ii) p = 0.1 MPa, T = 1000 K; (iii) p = 0.5 MPa, T = 298 K; and (iv) p = 0.1 MPa, T = 298 K. After this sequence, the density of the liquid reached an approximately constant value, indicating that an equilibrium state has been obtained. Finally, a production stage of 8 ns was performed at 298.15 K and 0.1 MPa.

All subsequent structural studies, radial distribution functions and aggregation analysis, were calculated taking the positions of: the imidazolium ring centroid (IL cation); the sulfur atoms in the IL anions, the nitrogen atom in the ammonium cation; and the carbon atom in the thiocyanate anion.

Aggregation analyses between different ion pairs ($[C_2MIM]^+$ / $[C_2SO_3]^-$, $[C_2MIM]^+$ / $[SCN]^-$, $[NH_4]^+$ / $[C_2SO_3]^-$ and $[NH_4]^+$ / $[SCN]^-$) were performed by using the previously reported methodology.[34] In brief, this type of study consists of the determination of a neighbours list between different ion pairs, by using a limit connection distance (d), defined as the first solvation shell between the ions. This distance was estimated for each pair from

the corresponding radial distribution functions (Figure 8). The selected distances where: $d_{C2MIM+/C2SO3-}$ = 7.0 Å; $d_{C2MIM+/SCN-}$ = 7.0 Å; $d_{NH4+/SCN-}$ = 4.7 Å; $d_{NH4+/C2SO3-}$ = 4.5 Å.

Finally, the neighbour list is converted into an aggregate list, by assuming that two cations (or anions) can only belong to the same aggregate if both are connected by the same anion (or cation), thus establishing an ionic network. All statistical analyses where performed as previously described.[34]

4. Results and discussion

4.1. Ionicity

Based upon the Walden rule, the Walden Plot establishes a relationship between the molar conductivity and the fluidity of the solution. It has already been proved that the Walden Plot is a suitable tool to measure the ionicity of pure ILs[1, 2] and also mixtures of IL and simple ISs.[12] In Figure S1 (SI) the Walden Plot for the system $[C_2MIM][C_2SO_3]$ + $[NH_4][SCN]$ is depicted. The increasing concentration of IS corresponds to a behaviour closer to the "ideal" Walden line (ideal electrolyte, an 1 M aqueous KCl solution[2] at 298.15 K), leading to an increase in ionicity.

A simple way to measure the ionicity of the system is to quantify the deviation from the ideal electrolyte by measuring the vertical distance to the "ideal" Walden line (ΔW).[11] Figure 2 illustrates the deviations from the Walden ideality relation measured at a fixed value of log η^{-1} = 0, against the molar concentration of $[NH_4][SCN]$. Both systems, $[C_2MIM][C_2SO_3]$ + $[NH_4][SCN]$ and $[C_2MIM][C_2SO_4]$ + $[NH_4][SCN]$[12] are plotted for comparison. Despite the fact that both systems show increased ionicity with the increase in IS content, the system with the ethyl sulfonate-based IL displays a lower ionicity in all IS concentration range.

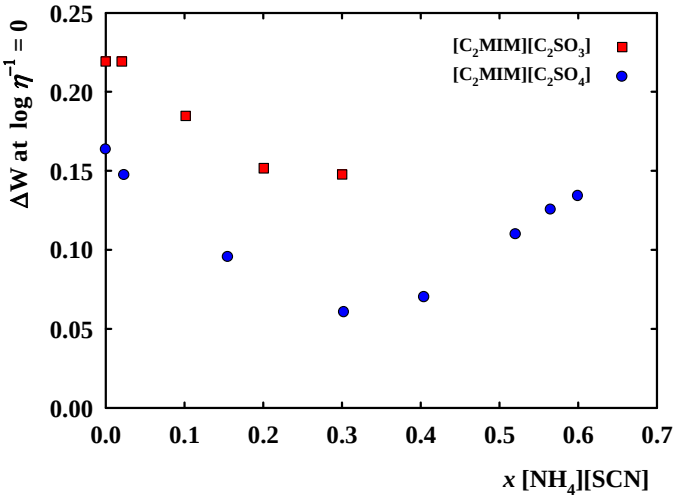

Figure 2 | Deviations from the "ideal" Walden behaviour for the binary systems $[C_2MIM][C_2SO_3]$ + $[NH_4][SCN]$ and $[C_2MIM][C_2SO_4]$ + $[NH_4][SCN]$[12] plotted against the inorganic salt molar concentration.

4.2. Viscosity and density

Figure 3 shows the temperature dependence of the viscosity for the pure ILs, $[C_2MIM][C_2SO_4]$ and $[C_2MIM][C_2SO_3]$, and their binary mixtures with $[NH_4][SCN]$ at a fixed concentration of 0.3 in mole fraction of salt. It is interesting to note that, at 298.15 K, the viscosity of $[C_2MIM][C_2SO_3]$ IL is twice that of $[C_2MIM][C_2SO_4]$. Upon the addition of IS, the viscosity of all samples increases. However, the addition of salt has a higher effect (at least 15%) on the viscosity of the ethyl sulfate-based than on ethyl sulfonate-based IL since the ratio of the viscosity of the $[C_2MIM][C_2SO_4]$ binary mixture and that of the pure IL is above 2 for all temperatures, while for $[C_2MIM][C_2SO_3]$ this value is systematically smaller. Another peculiar observation is that the binary mixture $[C_2MIM][C_2SO_4]$ + $[NH_4][SCN]$ and the neat $[C_2MIM][C_2SO_3]$ have similar viscosities.

The densities of the binary system were measured only to compare the behaviour of the two systems on the Walden Plot. A discussion about the effect of the IS addition on the IL can be found in SI. Figure S2 compares the temperature dependence of the density for

the two binary systems.

Table S1 in SI presents the experimental data for the viscosity and density of the $[C_2MIM][C_2SO_3]$ + $[NH_4][SCN]$ binary system.

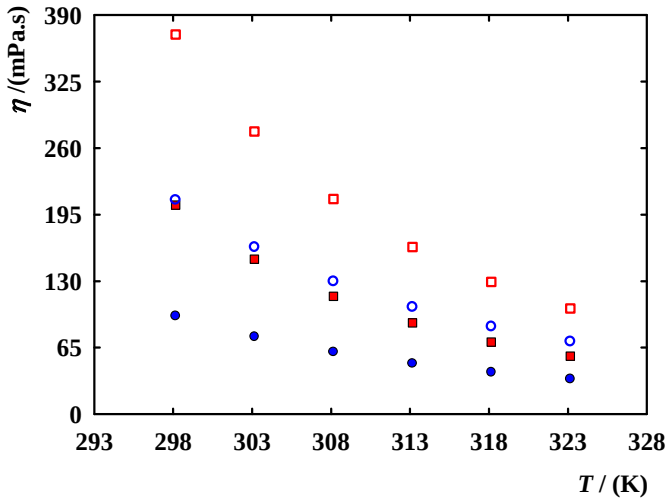

Figure 3 | Viscosity as a function of temperature for $[C_2MIM][C_2SO_4]$ (blue filled circle),[12] $[C_2MIM][C_2SO_4]$ + *x*$[NH_4][SCN]$=0.3 (blue empty circle),[12] $[C_2MIM][C_2SO_3]$ (red filled square) and $[C_2MIM][C_2SO_3]$ + *x*$[NH_4][SCN]$=0.3 (red empty square).

4.3. Ionic conductivity

The temperature dependence of the ionic conductivity for the pure ILs, $[C_2MIM][C_2SO_4]$ and $[C_2MIM][C_2SO_3]$, and their binary mixtures with $[NH_4][SCN]$ at a concentration of 0.3 in mole fraction of IS is presented in Figure 4. The ionic conductivity of pure $[C_2MIM][C_2SO_4]$ is approximately twice that of pure $[C_2MIM][C_2SO_3]$, in the whole temperature range. As expected, due to the formation of aggregates, the addition of IS decreases the ionic conductivity of the neat IL in both cases. However, the decrease observed in the ionic conductivity is less pronounced than the decrease in the viscosity (the average ratio between the neat ILs' conductivity and their binary mixture is 1.30 and 1.16 for the $[C_2MIM][C_2SO_4]$ and $[C_2MIM][C_2SO_3]$, respectively). Nevertheless, these results are consistent with those obtained for viscosity, since $[C_2MIM][C_2SO_3]$ presents higher viscosity

than $[C_2MIM][C_2SO_4]$. Identically to the trend in viscosity, the effect of the addition of $[NH_4][SCN]$ has a higher effect on the conductivity of $[C_2MIM][C_2SO_4]$ than of $[C_2MIM][C_2SO_3]$. Table S1 in SI presents the experimental data for ionic conductivity of $[C_2MIM][C_2SO_3]$ + $[NH_4][SCN]$ binary system.

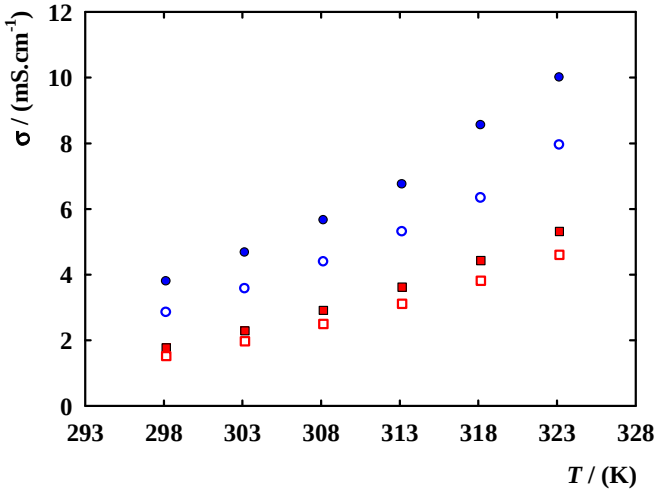

Figure 4 | Ionic conductivity as a function of temperature for $[C_2MIM][C_2SO_4]$ (blue filled circle),[12] $[C_2MIM][C_2SO_4]$ + *x*$[NH_4][SCN]$=0.3 (blue empty circle),[12] $[C_2MIM][C_2SO_3]$ (red filled square) and $[C_2MIM][C_2SO_3]$ + *x*$[NH_4][SCN]$=0.3 (red empty square).

4.4. NMR studies

To understand the interactions in the $[C_2MIM][C_2SO_3]$ + $[NH_4][SCN]$ binary system at the molecular level, the effect of the addition of $[NH_4][SCN]$ on the chemical shifts of the pure IL has been investigated using ^1H and ^{13}C NMR. In this way, the sites of the imidazolium ring participating in the ionic liquid – inorganic salt interactions, as well as the sites of ethyl sulfonate anion involved in the interactions with the inorganic salt can be identified.

Table S4 in SI shows the ^1H and ^{13}C NMR deviations for the $[C_2MIM][C_2SO_3]$ + $[NH_4][SCN]$ binary system for the concentration range between 0 and 0.4 mole fraction of salt. Figure 5 shows the relative changes of the chemical shifts for $[C_2MIM][C_2SO_3]$ ^1H NMR

spectrum with increasing inorganic salt concentration. The results for the $[C_2MIM][C_2SO_4]$ + $[NH_4][SCN]$ binary system[12] were also represented for comparison. It can be clearly seen that the deviations for the $[C_2MIM][C_2SO_3]$ system are much more pronounced than for the $[C_2MIM][C_2SO_4]$. Nevertheless, both systems reveal similar trends of the chemical shift differences for the all protons. For instance, the protons H2, H4 and H5 of the imidazolium ring, which are the most acidic ones, present upfield shifts, while the proton H9 of the anion is the only one that undergoes a downfield shift for both ILs. For the other protons, negligible changes with increasing IS concentration were observed. However, the aromatic protons (H2, H4 and H5) of the IL $[C_2MIM][C_2SO_3]$ are more affected by the increasing salt concentration since their upfield shifts are higher (Figure 5a) than the shifts observed in the other protons of the IL including the aromatic protons of the $[C_2MIM][C_2SO_4]$ (Figure 5b).

Brüssel et al.,[35, 36] used ab initio MD calculations to study the binary mixture of $[C_2MIM][SCN]$ and $[C_2MIM]Cl$. In their work, these authors showed that while in the neat ILs the main anion–cation interaction takes place through the most acidic proton of the imidazolium ring (H2), this observation does not hold for the mixture. Upon the addition of a stronger hydrogen bond acceptor (Cl^-), the thiocyanate ion starts to interact more favourably with the aromatic protons H4 and H5 than with H2, indicating that the different anions are competing for the available interaction sites. In this way, the chloride anion is replacing the thiocyanate anion at the most acidic position (H2). These results support our findings that upon the addition of $[NH_4][SCN]$, the IS ions start to compete with the IL ions, for the best interaction sites. Since $[NH_4]^+$ is a stronger hydrogen bond donor than $[C_2MIM]^+$ and $[C_2SO_4]^-$ / $[C_2SO_3]^-$ are stronger acceptors than $[SCN]^-$, the affinity between the IL's anion and the IS's cation allows the $[NH_4]^+$ to draw the IL's anion away from the $[C_2MIM]^+$ ring protons, resulting in the upfield shifts observed in the H2, H4 and H5.

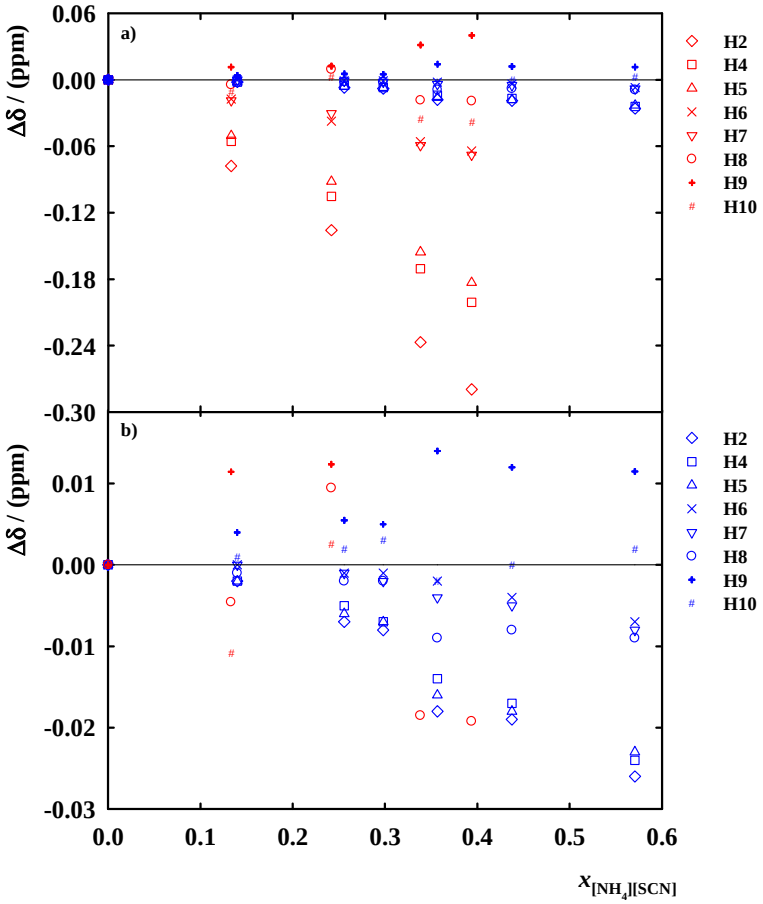

Figure 5 | Trend of the chemical shift difference of protons in ^{1}H NMR of $[C_2MIM][C_2SO_3]$ (red) and $[C_2MIM][C_2SO_4]$[12] (blue) with increasing $[NH_4][SCN]$ concentration ($\Delta\delta = \delta - \delta neat$) (b is an enlarged image of a).

The effect of $[NH_4][SCN]$ concentration on the ^{13}C NMR spectrum of both ILs is summarized in Figure S5 in the SI. Although the data obtained from the ^{13}C NMR spectra can only be viewed as qualitative, it is interesting to see that even though the deviations in the ^{1}H spectra of both ILs are similar, the ^{13}C spectra reveal significant differences. For instance, in the system containing $[C_2MIM][C_2SO_3]$ only the C6 and C7 carbons present downfield shifts, while in the $[C_2MIM][C_2SO_4]$ system, the C9 also presents a downfield shift, with higher deviations than the former carbons. This means that in the latter the anion,

$[C_2SO_4]^-$, interacts more favourably with the IS ($[NH_4]^+$) than in the $[C_2MIM][C_2SO_3]$ system. Furthermore, in both cases the C12 (corresponding to the $[SCN]^-$ anion) was the carbon that presented the highest downfield shift at higher concentrations of salt. This interpretation is further supported by Raman results (*vide* infra), which indicate that, unlike in the case of $[C_2MIM][C_2SO_4]$ + $[NH_4][SCN]$ mixtures, the $[SCN]^-$ anions are always ´engaged´ in interaction with $[C_2MIM][C_2SO_3]$, which is explained by the downfield shifts in the C6, C7 and C12 ($[C_2MIM]^+$ / $[SCN]^-$ interaction). On the other hand, in the $[C_2MIM][C_2SO_4]$ system, two populations of $[SCN]^-$ anions, one establishing similar interactions to those present in $[C_2MIM][C_2SO_3]$, and the other establishing weaker (or no) interactions, can be identified.

The intense deviations in aromatic protons as well as the upfield shift of C9 in the $[C_2MIM][C_2SO_4]$, can be attributed to the extra oxygen atom in the anion, that allows it to establish more favourable interactions with the $[NH_4][SCN]$ resulting in an higher solubilization capacity of this inorganic salt, as indicated by the solubility limits of the two systems.[26]

Tsuzuki et al.[37] used ab initio calculations to compare interactions between binary mixtures of $[Li][NTf_2]$ salt with *N*,*N*-diethyl-*N*-methyl-*N*-(2-methoxyethyl)ammonium bis(trifluoromethylsulfonyl)amide and 1-ethyl-3-methylimidazolium bis(trifluoromethylsulfonyl)amide ILs. They concluded that the interactions between the ammonium cation and the $[Li][NTf_2]$ complex are attractive when the lithium atom has close contact with the oxygen atom of the ammonium cation, while in the case of the imidazolium-based IL the interactions are always repulsive. A similar behaviour could occur in the case of the ammonium thiocyanate salt and the two ILs reported in this work, where the extra oxygen in the ethyl sulfate-based IL could play a key role in the different trends of the physical properties of both systems (*vide* supra).

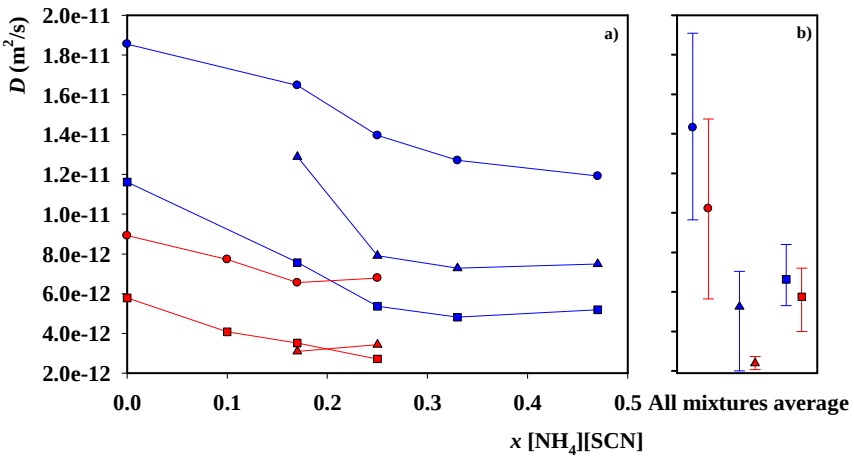

Figure 6 | a) Concentration dependence of the self-diffusion coefficients of the ions that compose the different IL+IS systems under discussion: blue symbols = sulfate-based systems; red symbols = sulfonate-based systems; ○ = $[C_2MIM]^+$ ions; □ = ($[C_2SO_4]^-$ or $[C_2SO_3]^-$) ions; Δ = $[NH_4]^+$ ions. The results were calculated from experimental (^{1}H NMR) data, the lines are guide to the eyes. b) Average values of the self-diffusion coefficients of the same ions contained in different (IL+IS) mixtures in the $0.0>x_{IS}>0.3$ mole fraction range, calculated from average squared displacement data obtained by Molecular Dynamics simulation. The simulation data were re-scaled in order to yield the same range of diffusion coefficient values obtained experimentally. In other words, panel b should be viewed only as a way to gage the self-diffusion of the different ions relative to each other.

In Figure 6a, the diffusion coefficients of the binary systems IL-IS are depicted as a function of the $[NH_4][SCN]$ content. The results show that the diffusion coefficients of the $[C_2MIM][C_2SO_4]$ binary system are larger than those of $[C_2MIM][C_2SO_3]$. These results are in agreement with the other properties measured, since $[C_2MIM][C_2SO_4]$ system shows lower viscosity and higher conductivity and free molar volume than $[C_2MIM][C_2SO_3]$. The diffusion coefficients follow the same order in both systems $D_{[C2MIM]^+} > D_{[NH4]^+} > D_{[SO4]^-}$ / $D_{[SO3]^-}$ Although $[C_2MIM]^+$ is the largest ion in both systems, it is also the one with the highest D ($D_{[SCN]-}$ could not be measured by ^{1}H NMR). This behaviour was also found in other systems with mixtures of IL-IS,[6, 38-40] where usually the IL's cation presents the highest self-diffusion coefficients. This (contra-intuitive) behaviour of D, $D_{[C2MIM]^+} > D_{[NH4]^+}$, is related with the interactions established between the $[NH_4]^+$ and the IL's anion, which is also reflected in the changes in the chemical shifts. In addition, the D_{cation} / D_{anion} can be used to assess the

degree of ion pairing, where the unity is interpreted as a diagnostic of complete ion pairing and small deviations from unity are interpreted as intermediate ion pairing.[41] From the results depicted in Figure 6a it can be seen that upon the addition of $[NH_4][SCN]$ the self diffusion coefficients decrease, with the D_{anion} showing a more pronounced decrease. Furthermore, the D_{cation} / D_{anion} ratio is lower than the $D_{[NH4]^+}$ / D_{anion} ratio in both systems, which can be seen by the proximity of the D_{anion} and $D_{[NH4]^+}$ values. These results confirm that a higher degree of ion pairing occurs between the $[NH_4]^+$ and the IL's anion, as indicated by the formation of aggregates in the MD studies (*vide* infra).

4.5. Raman studies

In the next step we probed molecular environment of the thiocyanate anions in $[NH_4][SCN]$ + IL binary mixtures employing Raman spectroscopy. We monitored frequency (ν_{SCN}) and band width ($\Delta\nu$) of this intense mode in the $[C_2MIM][C_2SO_3]$ and $[C_2MIM][C_2SO_4]$ systems upon increasing amounts of $[NH_4][SCN]$. The full-range Raman spectra of the neat ILs are depicted in Figure S6 in the SI. The frequency of the (S)C≡N stretching mode, found at ~ 2060 cm^{-1}, falls into region of the Raman spectra free from contributions of the ions of the pure ILs.

For a relatively small amount of $[SCN]^-$ (0.1 mole fraction of $[NH_4][SCN]$), the broad $[SCN]^-$ band is centred at 2055 cm^{-1} in $[NH_4][SCN]$ + $[C_2MIM][C_2SO_3]$, and at 2056 cm^{-1} in $[NH_4][SCN]$ + $[C_2MIM][C_2SO_4]$ mixtures, indicating comparable and heterogeneous environments of this anion in the two ILs. Except for a moderate broadening, ($\Delta\nu$ increases from 20 cm^{-1} for 0.1 mole fraction of $[NH_4][SCN]$ to 21.2 cm^{-1} for 0.25 mole fraction), which reveals further raise of heterogeneity, no other spectral changes take place as the amount of $[NH_4][SCN]$ increases in $[C_2MIM][C_2SO_3]$, Figure 7, inset. The situation is different for the $[SCN]^-$ in $[C_2MIM][C_2SO_4]$ system, Figure 7. An additional population characterized by ν_{SCN} at 2065 cm^{-1} clearly emerges in this system upon increasing amount of $[NH_4][SCN]$. The frequency of the new species indicates a presence of ´unengaged´ or loosely interacting $[SCN]^-$ moieties, as the respective ν_{SCN} stretching mode appears upshifted. At 0.53 mole

fraction, the second population becomes clearly predominant (Figure 7, trace c). It is noteworthy that the higher solubility of $[NH_4][SCN]$ in $[C_2MIM][C_2SO_4]$ allows for probing mixtures with higher IS : IL ratios, which are not accessible for $[C_2MIM][C_2SO_3]$. Nevertheless, even for relatively small but comparable amounts of $[NH_4][SCN]$, 0.25 mole fraction, the presence of a shoulder at 2065 cm^{-1} becomes evident in the spectrum of $[SCN]^-$ + $[C_2MIM][C_2SO_4]$ (Figure S7, upper traces). Furthermore, the band broadening is observed upon increasing of the $[NH_4][SCN]$ in both populations ($\Delta\nu$ increases from 22 cm^{-1} to 28 cm^{-1} for ν_{2056}, and from 16 cm^{-1} to 20 cm^{-1} for ν_{2065}, as the $[NH_4][SCN]$ mole fraction changes from 0.1 to 0.53). This is indicative of an increased heterogeneity of the $[SCN]^-$ molecular environment within each population.

Taken together, Raman data reveal that the interactions between $[SCN]^-$ anion and the two studied IL are indeed distinct. Other experimental and theoretical approaches (MD, *vide* infra) point to IL anion : $[NH_4]^+$ interaction as determinant in these systems. The higher flexibility and the higher free molar volume (Figure S3) of the $[C_2SO_4]^-$ anion, as compared to that of the $[C_2SO_3]^-$, implies its higher capacity to accommodate $[NH_4]^+$ that would furthermore allow the $[SCN]^-$ anion to form more than one population in $[C_2MIM][C_2SO_4]$. The ´unengaged´ $[SCN]^-$ population present in this IL shows an upshifted C≡N stretching band, close to that of $[NH_4][SCN]$ crystals, ($\nu_{SCN(crystal)}$ = 2063 cm^{-1}).[42] Increasing amount of this $[SCN]^-$ population, however, does not contribute significantly to the ionic conductivity (Figure 4), indicating a more complex interplay of ionic species in the sulfate-based IL. On the other hand, the measured ionic conductivity of the $[C_2MIM][C_2SO_3]$ in the presence / absence of $[NH_4][SCN]$ is in full accordance with Raman data, showing extremely small differences between pure IL and IL-IS mixtures.

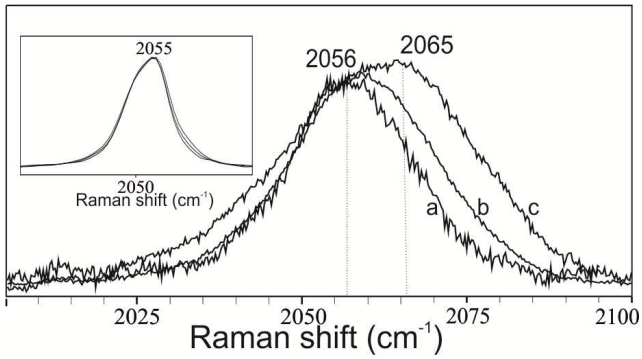

Figure 7 | Raman spectra of $[SCN]^-$ in $[C_2MIM][C_2SO_4]$ + $[NH_4][SCN]$ binary mixtures, for *x*$[NH_4][SCN]$: a) 0.17; b) 0.33 and c) 0.53. Inset: Raman spectra of $[C_2MIM][C_2SO_3]$ + $[NH_4][SCN]$ binary mixtures for *x*$[NH_4][SCN]$: 0.1, 0.17 and 0.25. Spectral intensities were normalized to 1 for clearer comparison. The experimental conditions are stated in Materials and Methods (and in Figure S7 in the SI).

4.6. Molecular Dynamics simulations

The structural analysis of the two pure ILs and their mixtures with increasing concentrations of the IS was also accomplished using MD simulation results.

Figure 8 shows selected radial distribution functions (RDFs) between relevant pairs of atoms/centres belonging to the IL ions that compose the different systems. The inset of the figure shows the characteristic fingerprint of each IL: local electro-neutrality conditions impose phase opposition behaviour between the RDFs of unlike-charged pairs (red and blue lines) and the RDFs of ions with the same charge (green line). The inset also shows that in terms of structure, the two pure ILs (sulfonate- and sulfate-based) are very similar to each other: the first peak distances corresponding to the (sulfate or sulfonate anion) S-O···H (imidazolium ring) interactions are almost identical; the slightly larger size of sulfate anion is only noticeable in the slightly shifted and less intense second peak corresponding to such interactions. This figure also shows the same unlike-charged RDFs, comparing the pure ILs with mixtures containing 30% (mole fraction) of the IS. It must be stressed out that due to the smaller size of the IS ions, a 0.3 mole fraction of IS corresponds to much smaller (lower than 0.1) volume fractions. Interestingly the position of the first peaks remain almost unchanged, albeit less intense, due to the loss of some of the cation-anion interactions,

whereas the second peaks show important shifts towards smaller distances. Such shifts are more pronounced in the case of the sulfate-based IL, with the peak exhibiting a more complex shape (shoulder). In other words, it seems that the extra bridge oxygen of the sulfate anion not only increases the size of the anion relative to its sulfonate counterpart, but also confers it a more flexible way to interact with the cations. The more structured second peak indicates that the contraction of the ionic mixture structure is caused by the introduction of the much smaller ammonium cations,[12] which are better accommodated in the sulfate-based than in the sulfonate-based system. This fact might explain the enhanced solubility of the IS in the former IL.

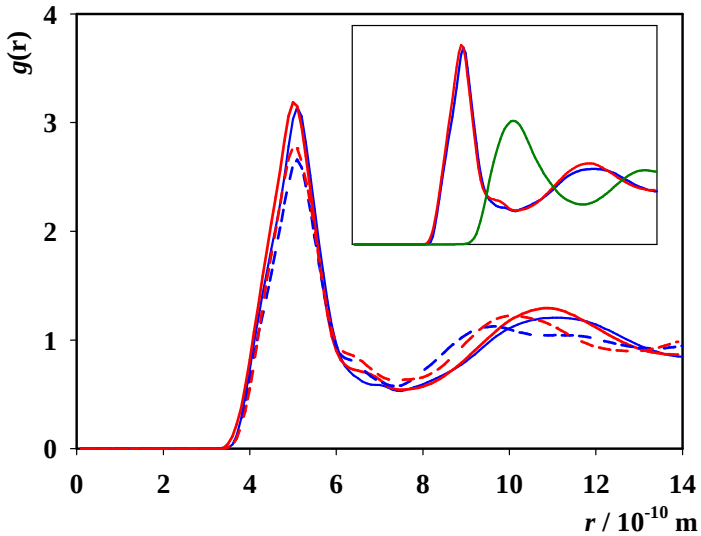

Figure 8 | Selected radial distribution functions (RDFs) between pairs of atoms/centres belonging to the ionic liquid ions that compose the (IL+IS) systems: blue curves = RDF(imidazolium centroid, sulfate sulphur atom) in pure $[C_2MIM][C_2SO_4]$;[12] red curves = RDF(imidazolium centroid, sulfonate sulphur atom) in pure $[C_2MIM][C_2SO_3]$; dashed blue curve = RDF(imidazolium centroid, sulfate sulphur atom) in the ($[C_2MIM][C_2SO_4]$ + $[NH_4][SCN]$) mixture with x_{IS} = 0.3;[12] dashed red curve = RDF(imidazolium centroid, sulfonate sulphur atom) in the ($[C_2MIM][C_2SO_3]$ + $[NH_4][SCN]$) mixture with x_{IS} = 0.3; green curve (inset)= RDF(sulfate sulphur atom, sulfate sulphur atom) in pure $[C_2MIM][C_2SO_4]$.[12] The inset scale is the same as that of the larger figure.

Figure 9 (a to f) shows the aggregation analysis results. Panels a to c show the probability of formation of aggregates of a given size composed exclusively of $[C_2MIM]^+$ and

$[SCN]^-$ ions in sulfonate- or sulfate-based IL mixtures with 0.1, 0.3 and 0.5 mole fraction of $[NH_4][SCN]$. The other three panels show similar results for aggregates composed exclusively of $[NH_4]^+$ and ($[C_2SO_3]^-$ or $[C_2SO_4]^-$) ions. When the mole fraction of IS is just 0.1, panels a and d seem to indicate that IL-IS aggregates are easier to form in the sulfonate-based ILs (red lines shifted to the right of the blue ones). This is logical if we assume that at these small concentration the IS ions are diluted in a continuous network of IL ions. The limiting step for the formation of an IL-IS aggregate, either $[C_2MIM]^+$ plus $[SCN]^-$, or $[NH_4]^+$ plus ($[C_2SO_3]^-$ or $[C_2SO_4]^-$), is the proximity of two similar IS ions. That probability is slightly higher in the sulfonate-based IL due to its smaller molar volume. In terms of the IS ions, the formation of IL-IS aggregates is also easier for the bulkier $[SCN]^-$ anion (panel a, larger aggregates) than for the smaller $[NH_4]^+$ cation (panel d, smaller aggregates).

Changes start to occur in the 0.3 concentration range. In this case the mole, and thus the volume fraction of the IS anions is large enough to form large aggregates containing almost all the ions in the simulation box (panel b). In the case of the smaller ammonium cation, its volume fraction is still not sufficient to form such extended aggregates (panel e). One also sees that the sulfate-based systems are now better at forming larger aggregates than their sulfonate counterparts. This means that the flexibility of the sulfate anion conferred by its extra oxygen atom overcomes the issue of larger ion size that is noticeable at more diluted (0.1 mole fraction) concentrations. Finally at equimolar concentrations of IL and IS (panels c and f, only for the case of the sulfate-based IL), the IL-IS aggregates encompass all ions present in the system in the case of $[C_2MIM]^+$ plus $[SCN]^-$ aggregates (panel c) or a fair proportion of those in the case of $[NH_4]^+$ plus $[C_2SO_4]^-$ aggregates (panel f). The large difference between the solubility of $[NH_4][SCN]$ in the two ILs can be interpreted as a result of the better ability of the sulfate-based IL to accommodate extended IL-IS aggregates in the midst of its polar network. Such ability is a consequence of the more flexible nature of the ethyl sulfate anion relative to its sulfonate-based counterpart.

Moreover, the simulation results can also yield the self-diffusion coefficients of each type of ion present in the mixture. These were calculated from the corresponding mean square displacements of each ion obtained in the 8 ns simulation runs and compared with experimental results obtained via NMR analysis in Figure 6. It must be stressed out at this

point that the force-field used to model the IL-IS systems (a non-polarizable, systematic force field for ionic liquids) is not particularly suited to estimate transport properties such as viscosity or mass diffusivity. Previous results have shown that very long simulation results are always required in the case of highly viscous ionic liquid systems and that in most cases viscosity is still overestimated (and mass diffusivity under-estimated) by more than one order of magnitude. Many different schemes have been attempted to overcome this issue, namely charge-transfer or charge-reduction schemes that aim to dampen the (excessive) role of the electrostatic interactions or the inclusion of polarization in the models that try to mimic the response of the electronic distribution in the ions when subjected to different electric fields caused by the surrounding ions. Unfortunately such methods lie outside the scope of the present work. Nevertheless, the current approach provides a qualitative indication about the relative magnitude of the self-diffusion coefficients of the different ions present in the mixture and such relation can be helpful in the interpretation of the experimental results.

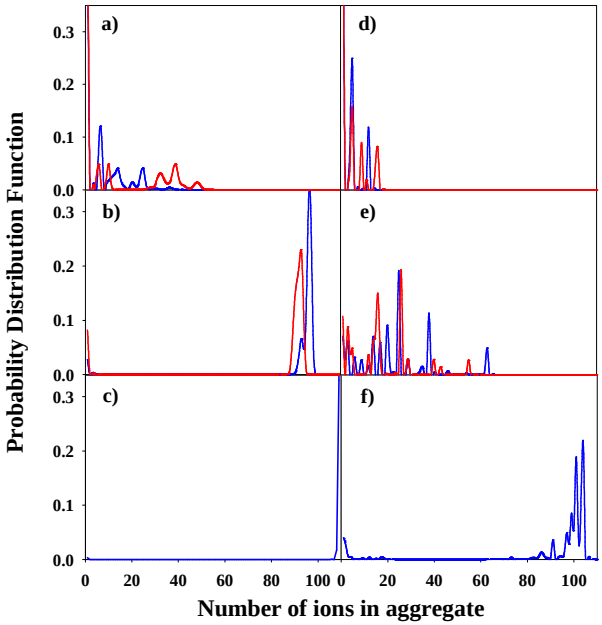

Figure 9 | Distribution functions showing the probability of finding an aggregate of a given size composed exclusively of: (a-c) $[C_2MIM]^+$ and $[SCN]^-$ ions in sulfate-based (blue lines) or sulfonate-based (red lines)

mixtures; (d-f) $[NH_4]^+$ and ($[C_2SO_4]^-$ or $[C_2SO_3]^-$) ions in sulfate-based (blue lines) or sulfonate-based (red lines) mixtures. The different mole fractions of salt, 0.1, 0.3 and 0.5, are illustrated in panels a) / d), b) / e) and c) / f), respectively.

Figure 6 shows that the relative magnitude of the self-diffusion coefficients obtained in the NMR experiments and in the simulations is the same, with the 1-ethyl-3-methylimidazolium ion cation exhibiting larger self-diffusion coefficient values than those of the ammonium, ethyl sulfate or ethyl sulfonate ions. This apparently unusual state of affairs — the 1-ethyl-3-methylimidazolium cation is much larger than the ammonium cation and should exhibit a lower mobility — can be explained by the higher charge dispersion (and less intense electrostatic interactions) in the organic cation. Simulation results also indicate that the self-diffusion of the thiocyanate anion is even higher than that of the imidazolium cation: in this case the charge delocalization across the molecular ion (between the nitrogen and sulphur atoms of $[SCN]^-$) is combined with its relatively small size. Unfortunately, these findings could not be confirmed by ^1H NMR due to the absence of hydrogen atoms in the $[SCN]^-$ structure.

Overall the simulation results support the idea that the fluidity and electrical conductivity of the IL-IS mixtures should decrease as the concentration of the IS is increased, as shown in Walden plots of Figure S1, due to the formation of ionic aggregates composed of more localized charged species (the ammonium cations). However, the ionic conductivity does not decrease as much as expected (the ionicity even increases) due to the concomitant introduction of relatively mobile species such as the thiocyanate anion.

5. Conclusions

In the present work, a comparison between the binary IL-IS systems $[C_2MIM][C_2SO_3]$ + $[NH_4][SCN]$ and $[C_2MIM][C_2SO_4]$ + $[NH_4][SCN]$ was made in order to study the effect of the nature of the IL's anion on the density, refractive index, thermal stability, viscosity and ionic conductivity.

The obtained data showed that upon the addition of ammonium thiocyanate, both

systems display the same type of behaviour and an increase in the ionicity of both these systems was observed. Nevertheless, since the neat IL $[C_2MIM][C_2SO_3]$ is much more viscous and has also a smaller ionic conductivity than the $[C_2MIM][C_2SO_4]$, it shows lower ionicity. The addition of $[NH_4][SCN]$ seems to have higher impact on the $[C_2MIM][C_2SO_4]$ system properties than on those of $[C_2MIM][C_2SO_3]$.

The NMR and Raman studies showed that the sulfate-based IL is capable of establishing stronger interactions with the $[NH_4][SCN]$ than the sulfonate-based one. The results reveal that the extra oxygen in the sulfate-based IL plays a key role in the structuring of the complexes between the IL and the IS (namely between the $[C_2SO_4]^-$ anion and the $[NH_4]^+$ cation). This becomes evident by the differences observed between the two ILs in the self-diffusion coefficients, the ^{13}C chemical shifts and the Raman spectra.

In addition, the experimental data are fully corroborated by Molecular Dynamic studies, which reveal that upon the addition of IS, the sulfate-based IL forms more aggregates than the sulfonate-based IL. The ability of the sulfate-based IL to accommodate extended IL-IS aggregates in its polar network, results from the flexibility of the sulfate anion conferred by its extra oxygen atom. The formation of aggregates between the $[C_2SO_4]^-$ anion and the $[NH_4]^+$ cation allows the other ions to become more free, which results in the increase in ionicity of the system.

6. Acknowledgements

Filipe S. Oliveira, Ana B. Pereiro and João M. M. Araújo gratefully acknowledge the financial support of FCT/MCTES (Portugal) through the PhD fellowship SFRH/BD/73761/2010 and the Post-Doc grants SFRH/BPD/84433/2012 and SFRH/BPD/65981/2009, respectively. Isabel M. Marrucho gratefully acknowledges FCT/MCTES (Portugal) for a contract under Programa Ciência 2007.

The NMR spectrometers are part of the National NMR Network and were purchased in the framework of the National Program for Scientific Re-equipment, contract REDE/1517/RMN/2005, with funds from POCI 2010 (FEDER) and FCT/MCTES.

The authors also acknowledge Fundação para a Ciência e Tecnologia for the financial support through the projects PTDC/EQU-FTT/116015/2009, Pest-C/CTM/LA0025/2011 (to the Associated Laboratory I3N-CENIMAT) and the Portuguese Nuclear Magnetic Resonance Network (PTNMR) (to the NMR equipment of CENIMAT).

7. Supplementary Information

7.1. Experimental section

7.1.1. Refractive index measurements

The refractive indexes were measured in the temperature range between 298.15 and 323.15 K at the sodium D-line using a Carl Zeiss Abbé refractometer with a precision of ± 5 × 10^{-5}. The temperature in the refractometer cell was controlled using an external thermostatic bath and measured with the refractometer thermometer (± 0.05 K accuracy). Samples were directly introduced in the cell (prism assembly) using a syringe.

At least three independent measurements were taken for each sample at each temperature to assure the effectiveness of the measurement. The absolute uncertainty of the refractive index is ± 0.00005.

7.1.2. Thermal stability measurements

Thermogravimetric analyses (TGA) were carried out using a TA instrument Model TGA Q50. Nitrogen was used as the sample gas for the TGA measurements at a flow rate of 60 mL·min^{-1}. All samples were recorded in aluminium pans within a nitrogen atmosphere. Samples were heated to 873.15 K at a rate of 10 K·min^{-1} until complete thermal degradation was achieved. Universal Analysis, version 4.4A software, was used to determine the onset temperatures (T_{onset}) corresponding to the temperature at which the baseline slope changed during heating. The relative uncertainty of the temperature is ± 0.50 %. At least three independent measurements were taken for each sample to ensure the accuracy of the

measurement.

7.2. Results and discussion

7.2.1. Ionicity

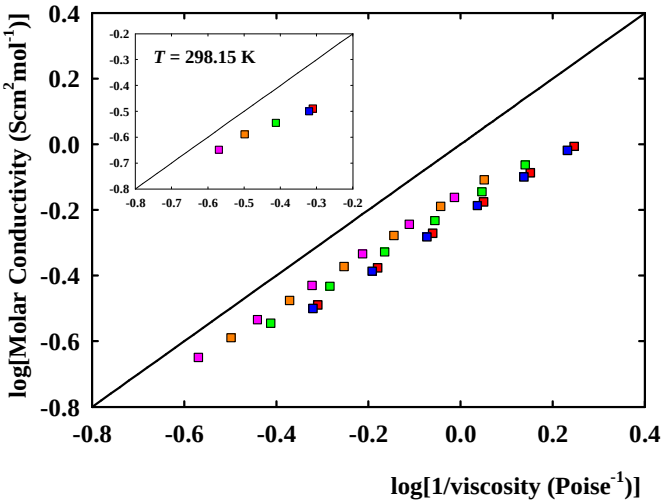

Figure S1 | Walden plot for the binary system $[C_2MIM][C_2SO_3]$ + $[NH_4][SCN]$ as a function of the inorganic salt concentration: red square $x_{[NH4][SCN]}$=0, blue square $x_{[NH4][SCN]}$=0.02, green square $x_{[NH4][SCN]}$=0.10, orange square $x_{[NH4][SCN]}$=0.20, pink square $x_{[NH4][SCN]}$=0.30. The inset figure shows the behaviour of the binary system at 298.15 K.

7.1.2. Density

The density values measured for the $[C_2MIM][C_2SO_3]$ + $[NH_4][SCN]$ system at temperatures between 293.15 and 323.15 K and at atmospheric pressure are listed in Table S1. Figure S2 illustrates the temperature dependence of the density for this mixture at a concentration of 0.3 in mole fraction of $[NH_4][SCN]$ and compares it with the pure IL, $[C_2MIM][C_2SO_3]$. Also, results for the pure $[C_2MIM][C_2SO_4]$ IL and its binary mixture $[C_2MIM][C_2SO_4]$ + $[NH_4][SCN]$ (also at a IS's mole fraction of 0.3 $[NH_4][SCN]$) are plotted.[12]

The IS's mole fraction of 0.3 was chosen for comparison of the two ILs. The density of pure $[C_2MIM][C_2SO_4]$ is higher than the pure $[C_2MIM][C_2SO_3]$ and for both binary mixtures the density is lower than the neat ILs. This behaviour is different from that found for other binary mixtures of IL-IS where the addition of salt increased the density of the mixture. The 1-ethyl-3-methylimidazolium acetate + ammonium thiocyanate system in our previous work[12] as well as the mixtures of 1-ethyl-3-methylimidazolium bis(fluorosulfonyl)amide and 1-ethyl-3-methylimidazolium bis(trifluoromethylsulfonyl)amide with their respective lithium salts[43] are examples of increased density with the addition of inorganic salt. Lassègues et al.[14] and Monteiro et al.[16] also reported density data of mixtures of different ILs based on alkyl-substituted imidazolium cations and bis(trifluoromethylsulfonyl)amide anions, with the lithium bis(trifluoromethylsulfonyl)amide salt, where the density of the mixture was higher than the neat IL. Moreover, the effect of the addition of $[NH_4][SCN]$ is more pronounced in the density of the $[C_2MIM][C_2SO_4]$ than the $[C_2MIM][C_2SO_3]$. This finding is corroborated by Raman data, which indicate a formation of ´unengaged´ SCN only in the former IL.

Table S1 | Density, ρ, dynamic viscosity, η, ionic conductivity, σ, refractive index, n_D, molar volume, V_m, molar refraction, R_m, and free molar volume, f_m, for the binary system $[C_2MIM][C_2SO_3]$ (1) + $[NH_4][SCN]$ (2) at several temperatures.

x_2	ρ (g·cm^{-3})	η (mPa·s)	σ (mS·cm^{-1})	n_D	V_m	R_m	f_m
				T = 298.15 K			
0	1.2037	204.35	1.770	1.49181	183.013	53.078	129.935
0.0206	1.2035	209.26	1.751	1.49181	180.576	52.371	128.205
0.1016	1.2025	258.52	1.668	1.49482	171.005	49.853	121.152
0.2007	1.2004	315.24	1.615	1.49816	159.407	46.739	112.669
0.3002	1.1973	371.13	1.518	1.50184	147.839	43.618	104.221
				T = 303.15 K			
0	1.2004	151.41	2.290	1.48947	183.516	53.008	130.508
0.0206	1.2002	155.49	2.267	1.48947	181.067	52.301	128.766
0.1016	1.1993	192.11	2.155	1.49314	171.466	49.844	121.623
0.2007	1.1972	235.08	2.090	1.49615	159.833	46.703	113.130
0.3002	1.1941	276.11	1.970	1.50051	148.231	43.635	104.596
				T = 308.15 K			
0	1.1971	114.96	2.912	1.48846	184.012	53.058	130.954
0.0206	1.1970	118.33	2.876	1.48879	181.556	52.381	129.176
0.1016	1.1961	146.23	2.734	1.49248	171.920	49.919	122.002
0.2007	1.1941	179.27	2.645	1.49482	160.248	46.717	113.531
0.3002	1.1910	210.28	2.499	1.49917	148.617	43.649	104.968
				T = 313.15 K			

0	1.1939	89.18	3.619	1.48779	184.510	53.140	131.370
0.0206	1.1938	91.97	3.572	1.48846	182.043	52.491	129.553
0.1016	1.1930	113.64	3.396	1.49080	172.377	49.906	122.470
0.2007	1.1910	139.49	3.286	1.49448	160.661	46.810	113.851
0.3002	1.1880	163.36	3.112	1.49750	148.992	43.635	105.357
				T = 318.15 K			
0	1.1907	70.52	4.425	1.48545	185.011	53.066	131.945
0.0206	1.1906	72.85	4.362	1.48645	182.532	52.447	130.085
0.1016	1.1899	89.94	4.145	1.48980	172.826	49.949	122.876
0.2007	1.1880	110.48	4.016	1.49314	161.076	46.824	114.252
0.3002	1.1851	129.19	3.816	1.49716	149.365	43.719	105.646
				T = 323.15 K			
0	1.1875	56.73	5.315	1.48478	185.510	53.147	132.363
0.0206	1.1874	58.68	5.240	1.48511	183.019	52.464	130.555
0.1016	1.1868	72.38	4.992	1.48913	173.277	50.021	123.256
0.2007	1.1850	88.92	4.827	1.49248	161.483	46.888	114.595
0.3002	1.1824	103.20	4.600	1.49649	149.706	43.769	105.938

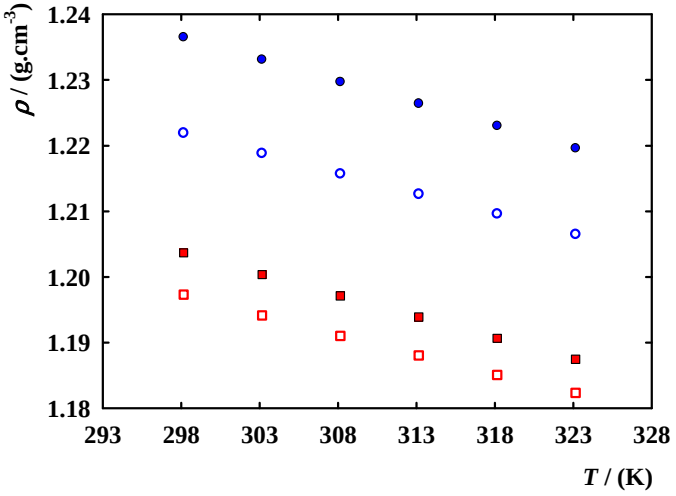

Figure S2 | Density as a function of temperature for $[C_2MIM][C_2SO_4]$ (blue filled circle),[12] $[C_2MIM][C_2SO_4]$ + $x_{[NH4][SCN]}$=0.3 (blue empty circle),[12] $[C_2MIM][C_2SO_3]$ (red filled square) and $[C_2MIM][C_2SO_3]$ + $x_{[NH4][SCN]}$=0.3 (red empty square).

7.1.3. Refractive index

The refractive indexes for the system $[C_2MIM][C_2SO_3]$ + $[NH_4][SCN]$ are shown in Table S1, for the concentration range between 0 and 0.3 mole fraction of salt. For the

system $[C_2MIM][C_2SO_4]$ + $[NH_4][SCN]$, the refractive indexes along with the molar volume, molar refraction, and free molar volume values are depicted in Table S2 for the all concentration range of salt. In both systems, the addition of salt increased the refractive index of the mixture, and within the studied concentration range of $[NH_4][SCN]$, it decreased linearly with increasing temperature.

The Lorentz–Lorenz equation (1) can be used to calculate the molar refraction or molar polarizability, R_m, which can be related both to density, ρ, and refractive index, n_D.[44]

$$R_m = \left(\frac{n_D^2 - 1}{n_D^2 + 2} \right) \times V_m \quad (1)$$

where V_m is the molar volume. The molar refraction is considered as a measure of the hard-core volume of one molecule and it can be used to calculate the molar free volume, f_m, of a solution,[45] by:

$$f_m = \left(V_m - R_m \right) \quad (2)$$

The values for the calculated molar refractions (from equation 1) and molar free volumes (from equation 2) of all the studied samples are listed in Tables S1 and S2 together with the molar volume calculated from density values. Figure S3 illustrates the molar free volumes for the neat ILs, $[C_2MIM][C_2SO_4]$ and $[C_2MIM][C_2SO_3]$, and their binary mixtures with $[NH_4][SCN]$ at a concentration of 0.3 in mole fraction of salt. It can be observed that the molar free volumes decrease with $[NH_4][SCN]$ concentration and increase as the temperature increases. In addition, the $[C_2MIM][C_2SO_4]$ IL shows higher molar free volume in the whole range of temperature, which means that it has more space available to accommodate $[NH_4][SCN]$ than $[C_2MIM][C_2SO_3]$. This is at least part of the answer for the higher solubility limit of the inorganic salts in $[C_2MIM][C_2SO_4]$ than in $[C_2MIM][C_2SO_3]$.

The analysis of the molar free volumes can be related with the solubility of different species in the mixtures of IL and ISs, especially low molecular weight solutes that are

gaseous at normal conditions. However, the mechanisms of solvation of some of these species, for example CO_2[46, 47] are controlled by the interactions and only to a minor extent by molar free volume effect.[48] Therefore, refractive data can be useful to evaluate the importance of the dispersive molecular interactions and the size of the apolar domains (dominated by dispersive molecular interactions) in the pure ILs or mixtures with ILs.[45]

Table S2 | Refractive index, n_D, molar volume, V_m, molar refraction, R_m, and free molar volume, f_m, for the binary system $[C_2MIM][C_2SO_4]$ (1) + $[NH_4][SCN]$ (2) at several temperatures.

x_2	n_D	V_m	R_m	f_m
		T = 298.15 K		
0	1.47875	191.096	54.165	136.931
0.0235	1.47976	188.128	53.420	134.708
0.1553	1.48477	171.827	49.226	122.601
0.3025	1.48980	153.727	44.430	109.297
0.4042	1.49582	141.042	41.189	99.853
0.5205	1.50385	126.110	37.333	88.778
0.5650	1.50987	120.233	35.952	84.281
0.5997	1.51389	115.649	34.811	80.838
		T = 303.15 K		
0	1.47775	191.623	54.218	137.405
0.0235	1.47875	188.647	53.471	135.176
0.1553	1.48277	172.289	49.185	123.104
0.3025	1.48879	154.118	44.464	109.653
0.4042	1.49381	141.402	41.152	100.251
0.5205	1.50284	126.434	37.365	89.069
0.5650	1.50887	120.541	35.984	84.557
0.5997	1.51188	115.965	34.791	81.174
		T = 308.15 K		
0	1.47674	192.153	54.269	137.883
0.0235	1.47775	189.169	53.523	135.645
0.1553	1.48177	172.739	49.226	123.513
0.3025	1.48779	154.511	44.500	110.011
0.4042	1.49181	141.765	41.115	100.649
0.5205	1.50184	126.759	37.398	89.361
0.5650	1.50686	120.850	35.956	84.894
0.5997	1.51088	116.253	34.820	81.433
		T = 313.15 K		
0	1.47474	192.670	54.220	138.450
0.0235	1.47574	189.678	53.474	136.204
0.1553	1.48076	173.192	49.267	123.926
0.3025	1.48678	154.906	44.535	110.371
0.4042	1.49080	142.117	41.145	100.972
0.5205	1.50083	127.075	37.427	89.647
0.5650	1.50586	121.152	35.986	85.166
0.5997	1.50886	116.543	34.790	81.753
		T = 318.15 K		
0	1.47373	193.205	54.271	138.934

0.0235	1.47474	190.190	53.522	136.668
0.1553	1.47875	173.647	49.220	124.428
0.3025	1.48578	155.290	44.567	110.723
0.4042	1.48980	142.471	41.176	101.295
0.5205	1.49883	127.382	37.391	89.991
0.5650	1.50485	121.455	36.015	85.440
0.5997	1.50787	116.834	34.820	82.014
T = 323.15 K				
0	1.47273	193.744	54.324	139.420
0.0235	1.47373	190.705	53.569	137.136
0.1553	1.47675	174.105	49.173	124.932
0.3025	1.48478	155.689	44.603	111.085
0.4042	1.48879	142.827	41.207	101.620
0.5205	1.49783	127.701	37.421	90.280
0.5650	1.50385	121.759	36.045	85.714
0.5997	1.50686	117.127	34.848	82.279

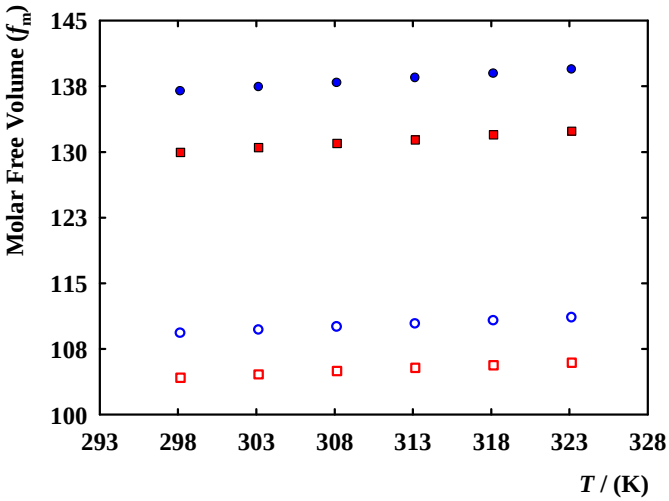

Figure S3 | Molar Free Volume as a function of temperature for [C_2MIM][C_2SO_4] (blue filled circle), [C_2MIM][C_2SO_4] + $x_{[NH4][SCN]}$=0.3 (blue empty circle), [C_2MIM][C_2SO_3] (red filled square) and [C_2MIM][C_2SO_3] + $x_{[NH4][SCN]}$=0.3 (red empty square).

7.1.4. Thermogravimetric analysis

The thermal decomposition temperatures as a function of IS concentration are listed in Table S3 and the onset temperature versus [NH_4][SCN] concentration is plotted in Figure S4. The results for the binary mixtures indicate that the thermal decomposition temperatures

decrease when the IS concentration increases. However, a deviation from this behaviour is observed for the binary mixture $[C_2MIM][C_2SO_4]$ + $[NH_4][SCN]$ in the onset temperatures at x $[NH_4][SCN]$ > 0.35. From this point, the onset temperatures stabilize with the addition of inorganic salt.

Table S3 | Thermal decomposition temperatures for the binary system $[C_2MIM][C_2SO_3]$ or $[C_2MIM][C_2SO_4]$ (1) + $[NH_4][SCN]$ (2).

$[C_2MIM][C_2SO_3]$		$[C_2MIM][C_2SO_4]$	
x_2	T_{onset} (K)	x_2	T_{onset} (K)
0	626.20	0	621.29
0.0206	623.75	0.0235	620.93
0.1016	621.72	0.1553	605.10
0.2007	611.98	0.3025	573.80
0.3002	565.54	0.4042	529.17
1	462.97	0.5205	518.05
–	–	0.5650	517.84
–	–	0.5997	525.33
–	–	1	462.97

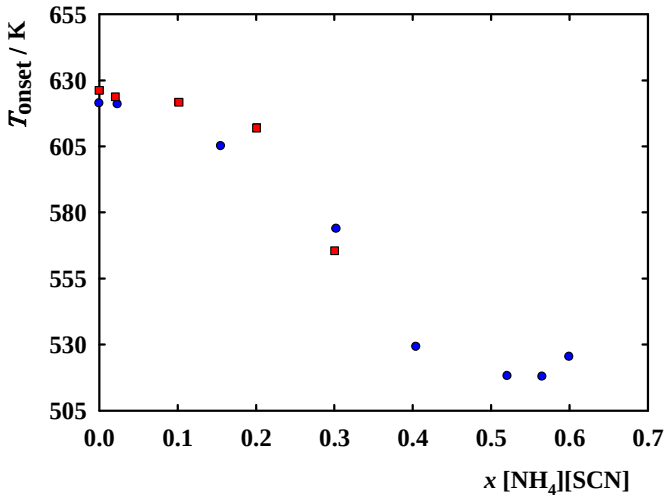

Figure S4 | The onset temperature, T_{onset}, as a function of $[NH_4][SCN]$ concentration in the solubility range for the binary systems $[C_2MIM][C_2SO_4]$ (blue filled circle) or $[C_2MIM][C_2SO_3]$ (red filled square) + $[NH_4][SCN]$.

7.1.5. NMR studies

Table S4 | ^{1}H NMR and ^{13}C NMR chemical shifts (ppm) of [C_2MIM][C_2SO_3] and the effect of [NH_4][SCN] concentration upon the chemical shifts in DMSO–d_6 at 298.15 K.

Position	Mole fraction of [NH_4][SCN]									
	0	0.1332	0.2418	0.3384	0.3939	0	0.1332	0.2418	0.3384	0.3939
	^{1}H NMR					^{13}C NMR				
2	9.397	9.319	9.261	9.160	9.117	136.639	136.553	136.444	136.368	136.322
4	7.951	7.895	7.846	7.780	7.750	123.463	123.432	123.445	123.413	123.399
5	7.843	7.793	7.751	7.687	7.660	121.939	121.896	121.893	121.855	121.837
6	3.916	3.899	3.879	3.860	3.852	35.425	35.453	35.526	35.545	35.565
7	4.245	4.226	4.214	4.185	4.177	43.934	43.983	44.037	44.079	44.104
8	1.383	1.378	1.392	1.364	1.364	15.061	15.027	15.050	15.023	15.018
9	2.473	2.484	2.485	2.504	2.513	45.188	45.168	45.159	45.146	45.143
10	1.064	1.053	1.066	1.028	1.026	9.727	9.626	9.651	9.553	9.529
12	–	–	–	–	–	–	129.953	130.003	130.193	130.274

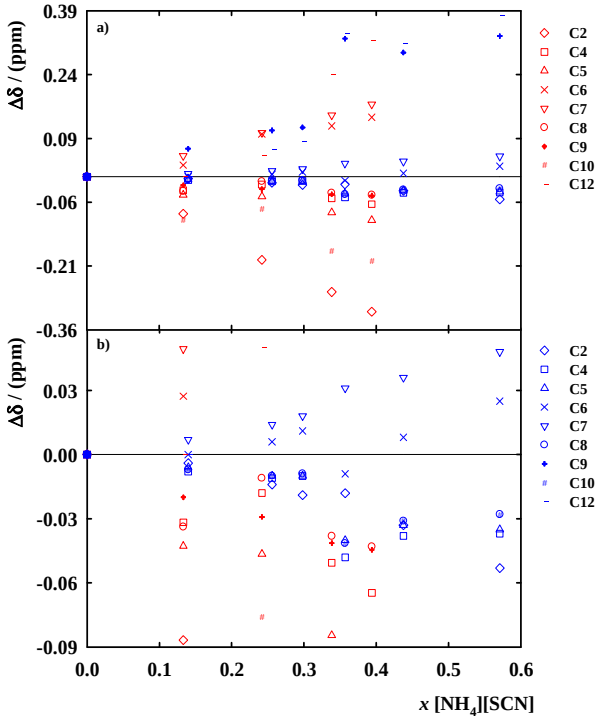

Figure S5 | Trend of the chemical shift difference of carbons in ^{13}C NMR of [C_2MIM][C_2SO_3] (red) and [C_2MIM][C_2SO_4][12] (blue) with increasing [NH_4][SCN] concentration ($\Delta\delta = \delta - \delta_{neat}$) (b is an enlarged image of a).

7.1.6. Raman studies

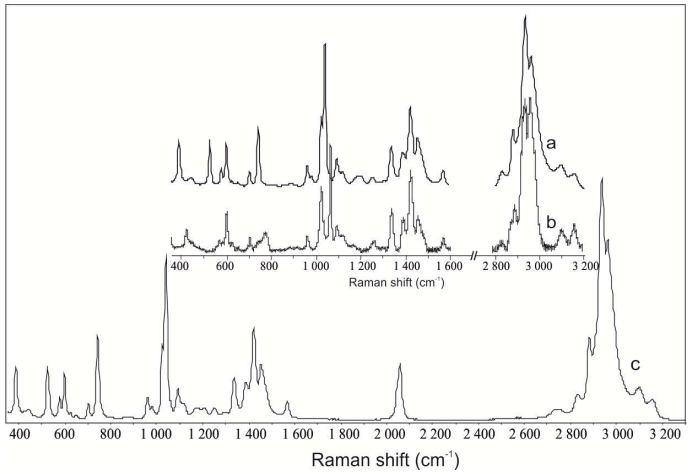

Figure S6 | Raman spectra of a) $[C_2MIM][C_2SO_3]$, b) $[C_2MIM][C_2SO_4]$ and c) $[C_2MIM][C_2SO_3]$ + $[NH_4][SCN]$ ($x_{[NH4][SCN]}$ = 0.17). a) and c) were measured with 400 mW laser power and 1064 nm excitation; b) was recorded with 3 mW laser power, 60s accumulation time, and 413 nm excitation. Spectral intensities are normalized for clearer comparison.

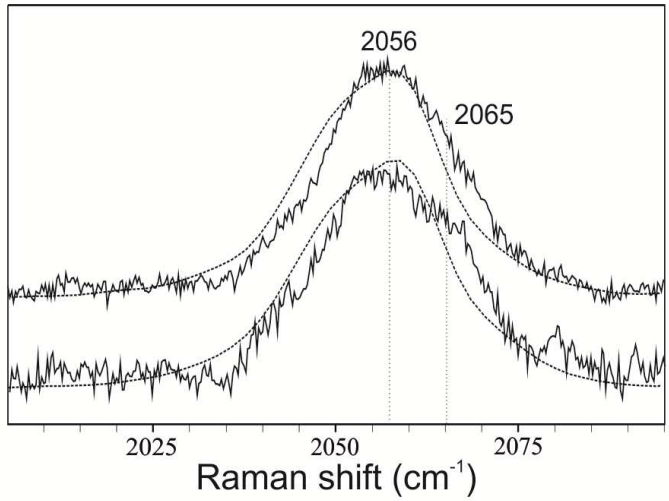

Figure S7 | Raman spectra of $[C_2MIM][C_2SO_4]$ + $[NH_4][SCN]$ (solid lines) and $[C_2MIM][C_2SO_3]$ + $[NH_4][SCN]$ (dotted lines) binary mixtures, for $x_{[NH4][SCN]}$ = 0.17 (upper traces) and for $x_{[NH4][SCN]}$ = 0.25 (lower traces). Spectra of $[C_2MIM][C_2SO_4]$ +$[NH_4][SCN]$ were recorded with 3 mW laser power, 60s accumulation time, and 413 nm excitation. Spectra of the $[C_2MIM][C_2SO_3]$ + $[NH_4][SCN]$ mixtures were measured with 400 mW laser power and 1064 nm excitation. Spectral intensities were normalized to 1 for clearer comparison.

8. References

1. D. R. MacFarlane, M. Forsyth, E. I. Izgorodina, A. P. Abbott, G. Annat and K. Fraser, On the concept of ionicity in ionic liquids, *Phys. Chem. Chem. Phys.*, 2009, **11**, 4962-4967.

2. K. Ueno, H. Tokuda and M. Watanabe, Ionicity in ionic liquids: Correlation with ionic structure and physicochemical properties, *Phys. Chem. Chem. Phys.*, 2010, **12**, 1649-1658.

3. W. Xu, E. I. Cooper and C. A. Angell, Ionic liquids: Ion mobilities, glass temperatures, and fragilities, *J. Phys. Chem. B*, 2003, **107**, 6170-6178.

4. H. Tokuda, S. Tsuzuki, M. Susan, K. Hayamizu and M. Watanabe, How ionic are room-temperature ionic liquids? An indicator of the physicochemical properties, *J. Phys. Chem. B*, 2006, **110**, 19593-19600.

5. J. Stoimenovski, E. I. Izgorodina and D. R. MacFarlane, Ionicity and proton transfer in protic ionic liquids, *Phys. Chem. Chem. Phys.*, 2010, **12**, 10341-10347.

6. K. Hayamizu, Y. Aihara, H. Nakagawa, T. Nukuda and W. S. Price, Ionic conduction and ion diffusion in binary room-temperature ionic liquids composed of emim BF_4 and $LiBF_4$, *J. Phys. Chem. B*, 2004, **108**, 19527-19532.

7. H. Shobukawa, H. Tokuda, S. Tabata and M. Watanabe, Preparation and transport properties of novel lithium ionic liquids, *Electrochim. Acta*, 2004, **50**, 305-309.

8. M. Kunze, M. Montanino, G. B. Appetecchi, S. Jeong, M. Schoenhoff, M. Winter and S. Passerini, Melting behavior and ionic conductivity in hydrophobic ionic liquids, *J. Phys. Chem. A*, 2010, **114**, 1776-1782.

9. K. Hayamizu, S. Tsuzuki, S. Seki and Y. Umebayashi, Nuclear magnetic resonance studies on the rotational and translational motions of ionic liquids composed of 1-ethyl-3-methylimidazolium cation and bis(trifluoromethanesulfonyl)amide and bis(fluorosulfonyl)amide anions and their binary systems including lithium salts, *J. Chem. Phys.*, 2011, **135**, 0845051-08450511.

10. C. Schreiner, S. Zugmann, R. Hartl and H. J. Gores, Fractional walden rule for ionic liquids: Examples from recent measurements and a critique of the so-called ideal KCl line

for the walden plot, *J. Chem. Eng. Data*, 2010, **55**, 1784-1788.

11. M. Yoshizawa, W. Xu and C. A. Angell, Ionic liquids by proton transfer: Vapor pressure, conductivity, and the relevance of Delta pK_a from aqueous solutions, *J. Am. Chem. Soc.*, 2003, **125**, 15411-15419.

12. A. B. Pereiro, J. M. M. Araújo, F. S. Oliveira, C. E. S. Bernardes, J. M. S. S. Esperança, J. N. C. Lopes, I. M. Marrucho and L. P. N. Rebelo, Inorganic salts in purely ionic liquid media: The development of high ionicity ionic liquids (HIILs), *Chem. Commun.*, 2012, **48**, 3656-3658.

13. B. Garcia, S. Lavallee, G. Perron, C. Michot and M. Armand, Room temperature molten salts as lithium battery electrolyte, *Electrochim. Acta*, 2004, **49**, 4583-4588.

14. J.-C. Lassègues, J. Grondin, C. Aupetit and P. Johansson, Spectroscopic identification of the lithium ion transporting species in LiTFSI-doped ionic liquids, *J. Phys. Chem. A*, 2009, **113**, 305-314.

15. S. F. Lux, M. Schmuck, G. B. Appetecchi, S. Passerini, M. Winter and A. Balducci, Lithium insertion in graphite from ternary ionic liquid-lithium salt electrolytes: II. Evaluation of specific capacity and cycling efficiency and stability at room temperature, *J. Power Sources*, 2009, **192**, 606-611.

16. M. J. Monteiro, F. F. C. Bazito, L. J. A. Siqueira, M. C. C. Ribeiro and R. M. Torresi, Transport coefficients, Raman spectroscopy, and computer simulation of lithium salt solutions in an ionic liquid, *J. Phys. Chem. B*, 2008, **112**, 2102-2109.

17. Z. P. Rosol, N. J. German and S. M. Gross, Solubility, ionic conductivity and viscosity of lithium salts in room temperature ionic liquids, *Green Chem.*, 2009, **11**, 1453-1457.

18. M. Y. Lui, L. Crowhurst, J. P. Hallett, P. A. Hunt, H. Niedermeyer and T. Welton, Salts dissolved in salts: Ionic liquid mixtures, *Chem. Sci.*, 2011, **2**, 1491-1496.

19. Y. Umebayashi, T. Mitsugi, S. Fukuda, T. Fujimori, K. Fujii, R. Kanzaki, M. Takeuchi and S.-I. Ishiguro, Lithium ion solvation in room-temperature ionic liquids involving bis(trifluoromethanesulfonyl)imide anion studied by Raman spectroscopy and DFT calculations, *J. Phys. Chem. B*, 2007, **111**, 13028-13032.

20. Y. Umebayashi, S. Mori, K. Fujii, S. Tsuzuki, S. Seki, K. Hayamizu and S.-i.

Ishiguro, Raman spectroscopic studies and Ab Initio calculations on conformational isomerism of 1-butyl-3-methylimidazolium bis-(trifluoromethanesulfonyl)amide solvated to a lithium ion in ionic liquids: Effects of the second solvation sphere of the lithium ion, *J. Phys. Chem. B*, 2010, **114**, 6513-6521.

21. Q. Zhou, P. D. Boyle, L. Malpezzi, A. Mele, J.-H. Shin, S. Passerini and W. A. Henderson, Phase behavior of ionic liquid-LiX mixtures: Pyrrolidinium cations and $TFSI^-$ anions - linking structure to transport properties, *Chem. Mater.*, 2011, **23**, 4331-4337.

22. F. J. Deive, A. Rodríguez, A. B. Pereiro, K. Shimizu, P. A. S. Forte, C. C. Romão, J. N. C. Lopes, J. M. S. S. Esperança and L. P. N. Rebelo, Phase equilibria of haloalkanes dissolved in ethylsulfate- or ethylsulfonate-based ionic liquids, *J. Phys. Chem. B*, 2010, **114**, 7329-7337.

23. J. N. C. Lopes, A. A. H. Pádua and K. Shimizu, Molecular force field for ionic liquids IV: Trialkylimidazolium and alkoxycarbonyl-imidazolium cations; alkylsulfonate and alkylsulfate anions, *J. Phys. Chem. B*, 2008, **112**, 5039-5046.

24. M. Blesic, M. Swadzba-Kwasny, T. Belhocine, H. Q. N. Gunaratne, J. N. C. Lopes, M. F. C. Gomes, A. A. H. Pádua, K. R. Seddon and L. P. N. Rebelo, 1-Alkyl-3-methylimidazolium alkanesulfonate ionic liquids, C_nH_{2n+1}mim $C_kH_{2k+1}SO_3$: Synthesis and physicochemical properties, *Phys. Chem. Chem. Phys.*, 2009, **11**, 8939-8948.

25. M. Blesic, M. Swadzba-Kwasny, J. D. Holbrey, J. N. C. Lopes, K. R. Seddon and L. P. N. Rebelo, New catanionic surfactants based on 1-alkyl-3-methylimidazolium alkylsulfonates, C_nH_{2n+1}mim $C_mH_{2m+1}SO_3$: Mesomorphism and aggregation, *Phys. Chem. Chem. Phys.*, 2009, **11**, 4260-4268.

26. A. B. Pereiro, J. M. M. Araújo, F. S. Oliveira, J. M. S. S. Esperança, J. N. C. Lopes, I. M. Marrucho and L. P. N. Rebelo, Solubility of inorganic salts in pure ionic liquids, *J. Chem. Thermodyn.*, 2012, **55**, 29-36.

27. M. Tariq, P. J. Carvalho, J. A. P. Coutinho, I. M. Marrucho, J. N. C. Lopes and L. P. N. Rebelo, Viscosity of (C_2-C_{14}) 1-alkyl-3-methylimidazolium bis(trifluoromethylsulfonyl)amide ionic liquids in an extended temperature range, *Fluid Phase Equilib.*, 2011, **301**, 22-32.

28. J. Hamelin, T. K. Bose and J. Thoen, Dielectric-constant and the electric-

conductivity near the consolute point of the critical binary-liquid mixture Nitroethane 3-Methylpentane, *Physical Review A*, 1990, **42**, 4735-4742.

29. O. Klug and B. A. Lopatin, eds., *New developments in conductimetric and oscillometric analysis*, Elsevier Science Publisher, Amesterdam, 1988.

30. D. A. Fort, R. P. Swatloski, P. Moyna, R. D. Rogers and G. Moyna, Use of ionic liquids in the study of fruit ripening by high-resolution C-13 NMR spectroscopy: 'green' solvents meet green bananas, *Chem. Commun.*, 2006, **7**, 714-716.

31. J. S. Moulthrop, R. P. Swatloski, G. Moyna and R. D. Rogers, High-resolution C-13 NMR studies of cellulose and cellulose oligomers in ionic liquid solutions, *Chem. Commun.*, 2005, **12**, 1557-1559.

32. W. Smith and T. R. Forester, The Council for The Central Laboratory of Research Councils; Daresbury Laboratory, Warrington, 2006.

33. J. N. C. Lopes, J. Deschamps and A. A. H. Pádua, Modeling ionic liquids using a systematic all-atom force field, *J. Phys. Chem. B*, 2004, **108**, 2038-2047.

34. C. E. S. Bernardes, M. E. Minas da Piedade and J. N. C. Lopes, The structure of aqueous solutions of a hydrophilic ionic liquid: The full concentration range of 1-ethyl-3-methylinnidazolium ethylsulfate and water, *J. Phys. Chem. B*, 2011, **115**, 2067-2074.

35. M. Brüssel, M. Brehm, A. S. Pensado, F. Malberg, M. Ramzan, A. Stark and B. Kirchner, On the ideality of binary mixtures of ionic liquids, *Phys. Chem. Chem. Phys.*, 2012, **14**, 13204-13215.

36. M. Brüssel, M. Brehm, T. Voigt and B. Kirchner, Ab initio molecular dynamics simulations of a binary system of ionic liquids, *Phys. Chem. Chem. Phys.*, 2011, **13**, 13617-13620.

37. S. Tsuzuki, K. Hayamizu, S. Seki, Y. Ohno, Y. Kobayashi and H. Miyashiro, Quaternary ammonium room-temperature ionic liquid including an oxygen atom in side chain/lithium salt binary electrolytes: Ab initio molecular orbital calculations of interactions between ions, *J. Phys. Chem. B*, 2008, **112**, 9914-9920.

38. K. Hayamizu, S. Tsuzuki, S. Seki, Y. Ohno, H. Miyashiro and Y. Kobayashi, Quaternary ammonium room-temperature ionic liquid including an oxygen atom in side chain/lithium salt binary electrolytes: Ionic conductivity and H-1, Li-7, and F-19 NMR studies

on diffusion coefficients and local motions, *J. Phys. Chem. B*, 2008, **112**, 1189-1197.

39. I. Nicotera, C. Oliviero, W. A. Henderson, G. B. Appetecchi and S. Passerini, NMR investigation of ionic liquid-LiX mixtures: Pyrrolidinium cations and $TFSI^-$ anions, *J. Phys. Chem. B*, 2005, **109**, 22814-22819.

40. K. Hayamizu, S. Tsuzuki, S. Seki, K. Fujii, M. Suenaga and Y. Umebayashi, Studies on the translational and rotational motions of ionic liquids composed of N-methyl-N-propyl-pyrrolidinium (P-13) cation and bis(trifluoromethanesulfonyl)amide and bis(fluorosulfonyl)amide anions and their binary systems including lithium salts, *J. Chem. Phys.*, 2010, **133**, 1945051-19450513.

41. P. S. Pregosin, Ion pairing using PGSE diffusion methods, *Prog. Nucl. Magn. Reson. Spectrosc.*, 2006, **49**, 261-288.

42. G. D. Tewari, D. P. Khandelwal and H. D. Bist, Raman-scattering study of phase-transitions in NH_4SCN, *J. Chem. Phys.*, 1985, **82**, 5624-5632.

43. S. Tsuzuki, K. Hayamizu and S. Seki, Origin of the low-viscosity of emim $(FSO_2)_2N$ ionic liquid and its lithium salt mixture: Experimental and theoretical study of self-diffusion coefficients, conductivities, and intermolecular interactions, *J. Phys. Chem. B*, 2010, **114**, 16329-16336.

44. M. R. Moldover, *IUPAC experimental thermodynamics Vol. VI: Measurement of the thermodynamic properties of single phases*, in *Vol. VI: Measurement of the Thermodynamic Properties of Single Phases*, eds. A. R. H. Goodwin, K. N. Marsh and W. A. Wakeham, Elsevier, 2003, pp. 435–451.

45. M. Tariq, P. A. S. Forte, M. F. C. Gomes, J. N. C. Lopes and L. P. N. Rebelo, Densities and refractive indices of imidazolium- and phosphonium-based ionic liquids: Effect of temperature, alkyl chain length, and anion, *J. Chem. Thermodyn.*, 2009, **41**, 790-798.

46. C. Cadena, J. L. Anthony, J. K. Shah, T. I. Morrow, J. F. Brennecke and E. J. Maginn, Why is CO_2 so soluble in imidazolium-based ionic liquids?, *J. Am. Chem. Soc.*, 2004, **126**, 5300-5308.

47. J. Deschamps, M. F. C. Gomes and A. A. H. Pádua, Molecular simulation study of interactions of carbon dioxide and water with ionic liquids, *ChemPhysChem*, 2004, **5**, 1049-1052.

48. M. F. C. Gomes and A. A. H. Pádua, Gas-liquid interactions in solution, *Pure Appl. Chem.*, 2005, **77**, 653-665.

Chapter 3

Ionicity in the 1-ethyl-3-methylimidazolium acetate IL: comparing the effect of different ISs.

Part I: Thermophysical properties of the different IL-IS mixtures

Part II: Interactions between the IL and the different ISs

Chapter 3

Part I: Thermophysical properties of the different IL-IS mixtures.

Adapted from: **Filipe S. Oliveira**, Luís P. N. Rebelo and Isabel M. Marrucho, Influence of different inorganic salts on the ionicity and thermophysical properties of 1-ethyl-3-methylimidazolium acetate ionic liquid, *J. Chem. Eng. Data* (2015), **60**, 781-789

The author was involved in all the experiments, as well as on the discussion, interpretation and preparation of the manuscript.

1. Abstract

In this work, we studied the effects caused by the addition of different inorganic salts, on the ionicity of the IL 1-ethyl-3-methylimidazolium acetate. The solubility of different inorganic salts, based on the ammonium and the sodium cations, in this IL was experimentally determined at room temperature. Thermophysical properties, such as viscosity, density, conductivity and refractive indexes, of the 1-ethyl-3-methylimidazolium acetate + inorganic salt mixtures were measured in different concentrations of inorganic salt and the ionicity of the systems was calculated. The results showed that when ammonium-based salts are used, the ionicity of the IL can be increased, while when sodium-based salts are used, the opposite behaviour was found.

2. Introduction

Over the last years, the field of ionic liquids (ILs) has expanded immensely due to their unique properties such as negligible vapour pressure, wide liquid range, highly specific and tunable solvent ability,[1, 2] that allowed their introduction in a wide range of industrial applications.[3] Since ILs are compounds composed entirely of ions, it is possible to tune their thermophysical properties simply by the choice of their cation or anion, which resulted on they being labelled as "designer solvents". Nevertheless, designing the perfect task-specific IL just by adjusting the cation or the anion can be quite difficult and therefore studies of mixtures of ILs with other ILs[4] and also with inorganic salts (ISs)[5-9] started to appear in the literature.

Recently, our group reported the solubility of common ISs in a wide range of different ILs.[10] The results showed that among the ILs tested, the 1-ethyl-3-methylimidazolium acetate was capable of dissolving a wider range of ISs in significant concentrations. Indeed, this IL is one of the most studied ILs and recognized by its great solvent properties, proving to be capable of dissolving lignocellulosic materials,[11-14] proteins and enzymes,[15, 16] and also of having a high performance in capturing CO_2.[17-19] In our previous work,[20] we also used 1-

ethyl-3-methylimidazolium acetate along with 1-ethyl-3-methylimidazolium ethyl sulfate, and studied the effects of the addition of ammonium thiocyanate on the thermophysical properties of these two ILs. NMR and MD calculations showed that by solubilising this salt into the IL media, modifications on the IL's initial structure were promoted and the Coulombic character of the ILs could be increased, which lead to the increase of the ionicity of the system.

The subject of ionicity in ILs has been extensively discussed by Watanabe[21, 22] and MacFarlane[23] and co-authors, among others. The quantitative estimation of the ILs' ionicity is of great significance for the characterization of these fluids, since it provides a way to study their structure, namely concerning the formation of aggregates or clusters between the IL's ions. Different methods have been proposed for the estimation of ionicity. The two most commonly used are: i) the Walden Plot approach, that is based on the Walden Rule and relates the molar conductivity of an ionically conducting liquid to its viscosity, and ii) the ratio between the measured molar conductivity (Λ_{imp}) and the molar conductivity calculated from ionic self-diffusion coefficients using the simple form of the Nernst-Einstein equation (Λ_{NMR}). Following the Walden Plot approach, Xu et al.[24] proposed the classification of ILs in "good ILs" or "poor ILs" according to their proximity to ideal behaviour, i.e. fully dissociated ions.

So far, the majority of the pure ILs tested in literature fall in the "good ILs" region, and the most studied ILs have been the bis(trifluoromethylsulfonyl)imide-based. Despite the fact that the ionicity concept has not been widely explored, the majority of authors lean on this definition to explore ILs application in several fields where this property is relevant, namely electrochemistry. For example, Watanabe's group published a collection of three papers[25-27] where they demonstrate that the ratio Λ_{imp} / Λ_{NMR} is a useful parameter to characterize ILs, since it is linked to various physicochemical and structural properties. This group recently reported on ionicity of mixtures of lithium salts and glymes to evaluate the possibility of developing lithium solvate ILs as lithium-conducting electrolytes.[28]

Bulut et al.[29] determined the viscosities and conductivities as a function of temperature for a series of bis(trifluoromethylsulfonyl)imide-based ILs using different imidazolium, pyrrolidinium and piperidinium cations. In that work, the authors showed that an increase in

the alkyl chain length of the cation leads to a lower ionicity, and that this effect was dominant over the addition of -CH_2 groups to the ring of the cation. Chiappe et al.[30] studied the transport properties of several pyrazolium-based ILs combined with bis(trifluoromethylsulfonyl)imide and dicyanamide anions, and compared them to their imidazolium counterparts. Using the Walden plot and Kamlet−Taft solvatochromic parameters, these authors observed that the ion association was increased when dicyanamide-based ILs were used instead of bis(trifluoromethylsulfonyl)imide-based ILs, and imidazolium-based instead of pyrazolium-based ILs. Regarding the study of the ionicity of IL-IS systems, Wu et al.[31] studied mixtures of 1-methyl-3-pentylimidazolium bis(trifluoromethylsulfonyl)imide and lithium bis(trifluoromethylsulfonyl)imide at various concentrations for the development of lithium-conducting electrolytes, while Hayamizu et al.[32] studied the ion conduction and diffusion in mixtures of 1-ethyl-3-methylimidazolium tetrafluoroborate with its lithium counterpart.

As a continuation of our previous studies,[20, 33] in this work we explore the influence of the addition of several inorganic salts in the thermophysical properties of the IL 1-ethyl-3-methylimidazolium acetate. The final goal of this work is to increase the ionicity of ILs through the addition of ISs. For this purpose, four salts with the ammonium cation and different anions (acetate, chloride, ethyl sulfonate and thiocyanate) and two other salts with the sodium cation, sodium acetate and sodium thiocyanate, were used.

3. Experimental Section

3.1. Materials

The following six ISs were used in this work: ammonium acetate ([NH_4][Ac]), ammonium chloride ([NH_4]Cl), ammonium thiocyanate ([NH_4][SCN]), ammonium ethyl sulfonate ([NH_4][C_2SO_3]), sodium acetate (Na[Ac]) and sodium thiocyanate (Na[SCN]). Sodium acetate, ammonium acetate, chloride and thiocyanate were all provided by Sigma-Aldrich with a purity content superior to 99.0 %, 98.0 %, 99.5 % and 99.0 %, respectively. Sodium thiocyanate was provided by Fluka with a purity content superior to 98.0 %.

Ammonium ethyl sulfonate was synthesized from the reaction between ethane sulfonic acid solution (70 wt% in water, purchased from Sigma-Aldrich) and ammonium hydroxyde solution (30 % NH_3 basis, purchased from Sigma-Aldrich). Both starting reagents were further diluted in water and then mixed in equimolar concentrations under vigorous stirring with a magnetic stirrer. The resulting solution was then dried under high vacuum in order to obtain a solid white powder (ammonium ethyl sulfonate). The powder has then analyzed by NMR and Mass Spectroscopy (spectra in the supporting information, SI) to confirm the purity of the compound.

The ILIL 1-ethyl-3-methylimidazolium acetate ([C_2MIM][Ac]) was purchased from Iolitec with a mass fraction purity of ≥ 95 %. To reduce the water and other volatile substances contents, vacuum (10^{-1} Pa) and moderate temperature (no more than 318.15 K) were always applied to the IL for at least 5 days prior to their use. After drying, the IL purity was checked by ^{1}H and ^{13}C NMR. Karl Fischer coulometric titration (Metrohm 831 KF Coulometer) was used to determine the final water mass fraction of the IL, which contained around 4000 ppm of water.

3.2. Solubility determination

The binary mixtures of [C_2MIM][Ac] + IS were prepared in the range of 0 to 0.45 in IS mole fraction. The solubility of [NH_4]Cl and [NH_4][SCN] in [C_2MIM][Ac] was experimentally determined in our previous work.[10] For the remaining systems, the solubility of the ISs in [C_2MIM][Ac] was accomplished by consecutive addition of very small amounts (≈ 0.01 g) of IS to the IL until a precipitate was observed. The samples were prepared in an inert-atmosphere glove box, since [C_2MIM][Ac] is very moisture sensitive, using an analytical high-precision balance with an uncertainty of ± 10^{-5} g by weighing known masses of the each component into stoppered flasks. Good mixing was assured by magnetic stirring. In order to ensure the accuracy of the physical properties, each sample was measured in triplicates.

3.3. Viscosity and density measurements

The measurements of density and viscosity were performed in the temperature range between 298.15 and 323.15 K at atmospheric pressure, using an automated SVM 3000 Anton Paar rotational Stabinger viscometer-densimeter. The uncertainty for the temperature, viscosity and density is ± 0.02 K, ± 0.35 % and ± 0.0005 $g \cdot cm^{-3}$, respectively. Further details on the equipment can be found elsewhere.[34] The results presented are the average value of three replicas measured for the IL and each IL-IS mixture, where the highest relative standard deviation registered for the dynamic viscosity and density measurements was ± 3.01 % and ± 0.03 %, respectively.

3.4. Ionic conductivity measurements

The measurements of ionic conductivities were performed using a CDM210 Radiometer Analytical conductivimeter in the temperature range between 298.15 and 323.15 K. The apparatus used for the measurements can be found elsewhere.[20] For the calibration of the equipment for each temperature, a certified 0.01 D KCl standard solution supplied by Radiometer Analytical was used. Each conductivity value was determined at least three times to ensure its reproducibility within 1 % in absolute value.

3.5. Refractive index measurements

The measurements of refractive indexes were performed using an automated Anton Paar Refractometer Abbemat 500 in the temperature range between 298.15 and 323.15 K and at atmospheric pressure. The absolute uncertainty of the equipment is ± 0.00005. The refractive index of each sample was determined in triplicate and the results presented are the respective average value with a relative standard deviation lower than 0.004 %.

4. Results and discussion

4.1. Solubility

The range of concentrations used for the preparation of the IL-IS mixtures depends greatly of the choice of ions of the salt, as shown in our previous work.[10] For the salts $[NH_4][SCN]$ and $[NH_4]Cl$, the solubility in $[C_2MIM][Ac]$ is 0.4035 and 0.3755 in salt mole fraction (x_{IS}), respectively. However, for the study of these IL-IS systems' thermophysical properties, only mixtures up to a concentration of 0.34 (in x_{IS}) were prepared to ensure that no salt precipitation occurred. For the remaining salts the maximum concentration used was greatly affected both by the cation and the anion of the IS. For the salts containing the acetate anion it was possible to prepare mixtures up to a x_{IS} of 0.16 for Na[Ac] and 0.45 for the $[NH_4][Ac]$. For the $[NH_4][C_2SO_3]$, the mixtures were prepared up to a x_{IS} of 0.17 and for Na[SCN], which is the less soluble salt, only mixture was prepared with a concentration of 0.05 in mole fraction of salt. It can be concluded that the ammonium-based ISs have a much higher solubility in $[C_2MIM][Ac]$ than the sodium-based, probably due to the affinity of the IS's ammonium cation for the IL's acetate anion.

4.2. Density

The experimental density data for all the studied $[C_2MIM][Ac]$ + IS systems are depicted in Figure 1 and reported in Tables S1-S5, in the SI. The results show that in all systems the density increased upon the addition of IS and decreased with temperature. Other IL-IS systems found in literature exhibited the same behaviour with increasing IS concentration. Tsuzuki et al.[35] observed an increase of density in mixtures of 1-ethyl-3-methylimidazolium bis(fluorosulfonyl)imide and 1-ethyl-3-methylimidazolium bis(trifluoromethylsulfonyl)imide with their respective lithium salts, while Lassègues et al.[8] and Monteiro et al.[36] reported increases in the density data for mixtures of different ILs based on alkyl-substituted imidazolium cations and bis(trifluoromethylsulfonyl)imide anions, upon the addition of lithium bis(trifluoromethylsulfonyl)imide salt. Wu et al.[31] studied the

transport properties and density of mixtures of 1-methyl-3-pentylimidazolium bis(trifluoromethylsulfonyl)imide with lithium bis(trifluoromethylsulfonyl)imide, and also observed increases in the density of the IL with the increase in IS concentration.

A clear comparison between the systems is difficult because of the different solubilities of each salt in the IL. In Figure 1a, a comparison is drawn between the densities of the systems containing different ammonium-based salts, where it can be seen that the IS's anions can affect the density in different ways. In the systems containing chloride and ethyl sulfonate anions, the increase in the density is much more pronounced than for those containing acetate or thiocyanate anions, where after a x_{IS} of 0.20 the density reaches an almost constant value. For pure ILs, the variations of density can be linked to the molecular weight of the ions, where a decrease in the density can be correlated with the decrease in the anion's molecular weight.[25, 37-39] However, in our systems such a correlation cannot be established since there are two other ions in the mixture and hence their interactions change the coordination and packing of the system.

In Figure 1b, the effect of the IS's cation is shown. It can be observed that sodium-based salts lead to denser mixtures in comparison to their ammonium counterparts. Yet, due to the low solubility of the sodium ISs, no conclusions can be drawn regarding the behaviour of the system with the increase in IS concentration. Nevertheless, at a x_{IS} of 0.05 a comparison between all the studied system can be made, where the density of the system is affected by the IS in the following order: Na[SCN] > $[NH_4][C_2SO_3]$ > Na[Ac] > $[NH_4]$Cl > $[NH_4]$[SCN] > $[NH_4]$[Ac], where the latter is the salt where the density of the IL increases the least.

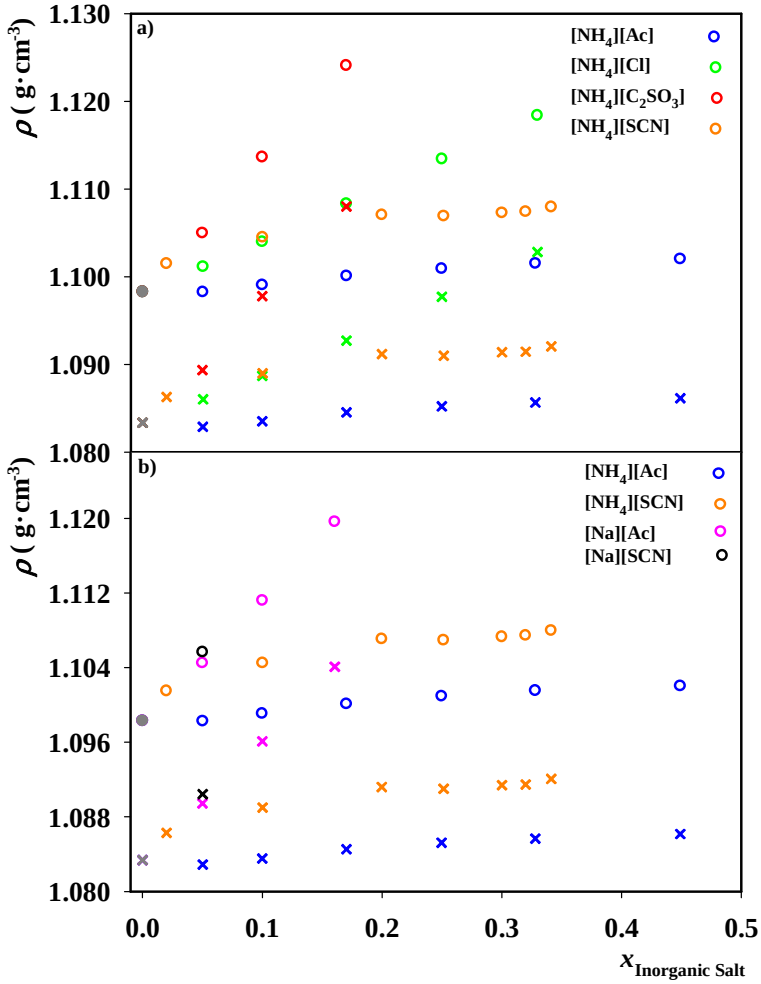

Figure 1 | Density as a function of the IS mole fraction for the systems [C2MIM][Ac] + IS. a) Comparison between systems with the same IS cation; b) Comparison between the systems with common IS anion. The system [C2MIM][Ac] + [NH4][SCN] is taken from literature.[20] The different symbols represent the temperatures 298.15 K (○) and 323.15 K (×), whereas the grey symbols represent the neat IL.

The molar volumes for all [C2MIM][Ac] + IS systems were calculated from the density data and are depicted in Figure 2 and presented on Tables S1-S5 in the SI. As expected, the molar volume of the mixtures decreases upon the addition of IS to the IL (in all systems the density increases) and increases with temperature. The molar volumes decrease in the following order: [NH4][C2SO3] > [NH4][Ac] > [NH4][SCN] > Na[Ac] > Na[SCN] > [NH4]Cl.

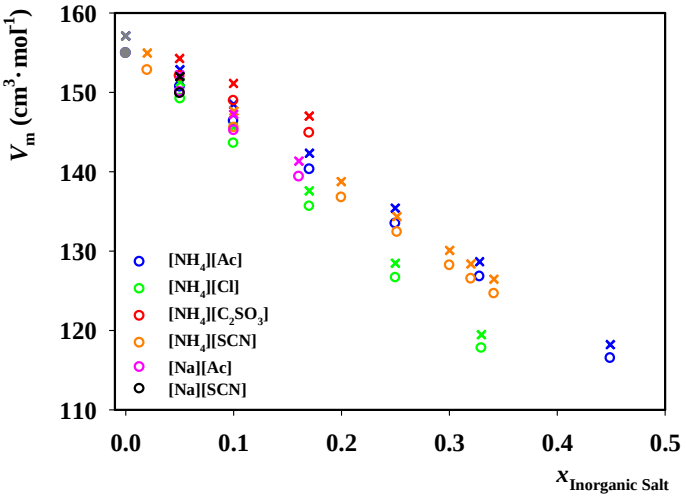

Figure 2 | Molar volume as a function of the IS mole fraction for the [C2MIM][Ac] + IS systems. The different symbols represent the temperatures 298.15 K (○) and 323.15 K (×), whereas the grey symbols represent the neat IL.

4.3. Refractive index

The determination of the refractive indexes, which are usually used as a measure of the electronic polarizability of a molecule, are important in the characterization of these systems, since they can yield useful information on the forces between molecules. In Figure 3, the refractive indexes for all IL-IS systems are depicted. Two different types of behaviours can be observed: i) the refractive index increases with the addition of ISs containing $[SCN]^-$ and Cl^- anions, and ii) the refractive index decreases upon the addition of any other IS tested. In addition, for all systems, the refractive index decreases with increasing temperature.

As observed for pure ILs,[37, 38] the refractive index is strongly dependent of the type of the anion present. The results obtained for the [C2MIM][Ac] + IS systems are in agreement with the behaviour observed in pure ILs, where the change of anion (of the IS in this case) has a stronger effect than the cation on the refractive index of the mixture.

Usually the increase of the refractive index is associated to an increase in the

polarizability, which implies that the compound is capable of enjoying particularly strong dispersion forces, allowing a better solubility for other species. The data obtained showed that the addition of ISs containing $[SCN]^-$ and Cl^- anions, increased the polarizability of the pure IL, leading to stronger dispersion forces in these systems. Although the other ISs used, present anions, such as acetate and ethyl sulfonate, which possess more electronegative atoms, like oxygen, the higher electronegativity of these atoms can limit the distortion of the electron cloud, restraining their polarizability and hence resulting in lower refractive indexes.[40]

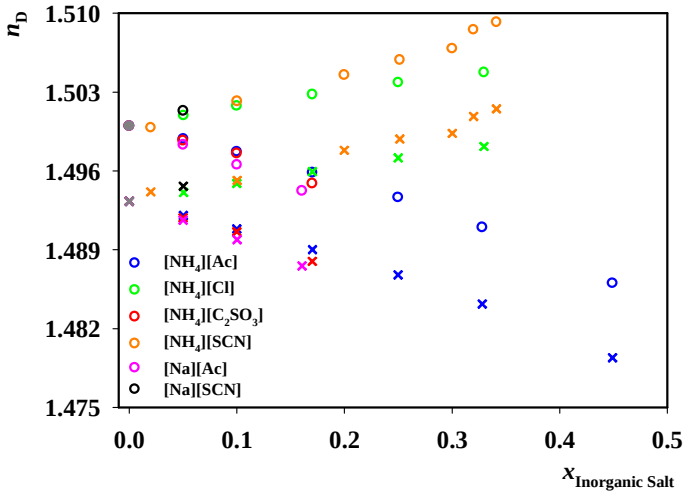

Figure 3 | Refractive index as a function of the IS mole fraction for the systems $[C_2MIM][Ac]$ + IS. The system $[C_2MIM][Ac]$ + $[NH_4][SCN]$ is taken from literature.[20] The different symbols represent the temperatures 298.15 K (○) and 323.15 K (×), whereas the grey symbols represent the neat IL.

Making use of the refractive index, n_D, and the density data (used for the calculation of the molar volume, V_m), it is possible to calculate the molar refraction, R_m, of the binary $[C_2MIM][Ac]$ + IS mixtures using the Lorenz-Lorenz equation[41] as shown in equation 1:

$$R_m = \left(\frac{n_D^2 - 1}{n_D^2 + 2} \right) \times V_m \qquad (1)$$

The molar refraction is considered as a measure of the hard-core volume of one molecule and it can be used to calculate the molar free volume, f_m, of a solution by the following equation:

$$f_m = \left(V_m - R_m\right) \tag{2}$$

Tables S1-S6 in the SI present the experimental data for the refractive indexes, molar refractions and molar free volumes. Figure 4 presents the molar free volumes for the studied systems. The molar free volumes decrease with the addition of IS and increase with the temperature. In addition, the results show the same trend observed for the molar volumes, where the addition of a IS with smaller volume leads to higher packing efficiency and hence to a lower molar free volume. The molar free volumes follow the order: $[NH_4]Cl$ < Na[SCN] < Na[Ac] < $[NH_4][SCN]$ < $[NH_4][Ac]$ < $[NH_4][C_2SO_3]$.

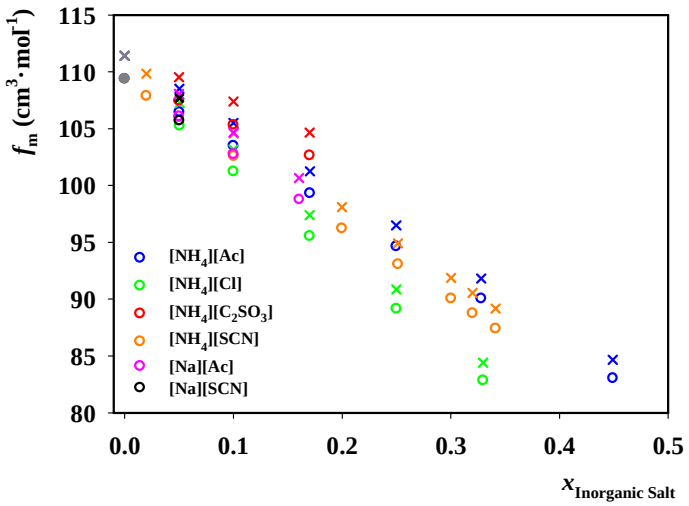

Figure 4 | Molar free volume as a function of the IS mole fraction for the systems $[C_2MIM][Ac]$ + IS. The system $[C_2MIM][Ac]$ + $[NH_4][SCN]$ is taken from literature.[20] The different symbols represent the temperatures 298.15 K (○) and 323.15 K (×), whereas the grey symbols represent the neat IL.

4.4. Viscosity

The viscosity is one of the properties required for the assessment of the ionicity of ILs, since it accounts for the flow of the molecules and therefore has direct influence on the mass transport phenomena.

In Figure 5, the data obtained for the viscosity of the studied systems are presented. The results showed that in all systems, the viscosity of the IL increases upon the addition of IS and decreases with increasing temperature. These results are consistent with those obtained for other IL-IS systems found in literature.[9, 33] The viscosity increase follows the trend $[NH_4][SCN] < Na[SCN] < [NH_4][Ac] < Na[Ac] < [NH_4][C_2SO_3] < [NH_4]Cl$, showing that the salts that contain thiocyanate are those that affect the least the viscosity of the system. In the case of the $[NH_4][SCN]$ containing system, for IS concentrations higher than 0.20, the viscosity seems to stabilize at a value of ≈ 1.5 times the viscosity of the pure IL. Regarding the two sodium-based salts, for the Na[SCN] containing system, no clear conclusion can be attained due to the low solubility of this salt in $[C_2MIM][Ac]$, while for the Na[Ac] containing system the viscosity increases upon the addition of small amounts of IS. Again, due to the lower solubility of this salt no clear tendency can be established. For the remaining systems, the viscosity is greatly affected by the increase of IS concentration. For instance, the largest increments were obtained for the $[NH_4]Cl$ system, recording increases of 3, 6, and 13 times the viscosity of the pure IL, for the 0.17, 0.25 and 0.33 concentrations of IS, respectively.

These tendencies were expected since ILs bearing -CN groups are known to be less viscous than others,[42] while those containing the Cl^- anion and oxygen atoms ($[NH_4][Ac]$, Na[Ac] and $[NH_4][C_2SO_3]$) can highly increase the viscosity of the IL, due to the establishment of hydrogen bonds.

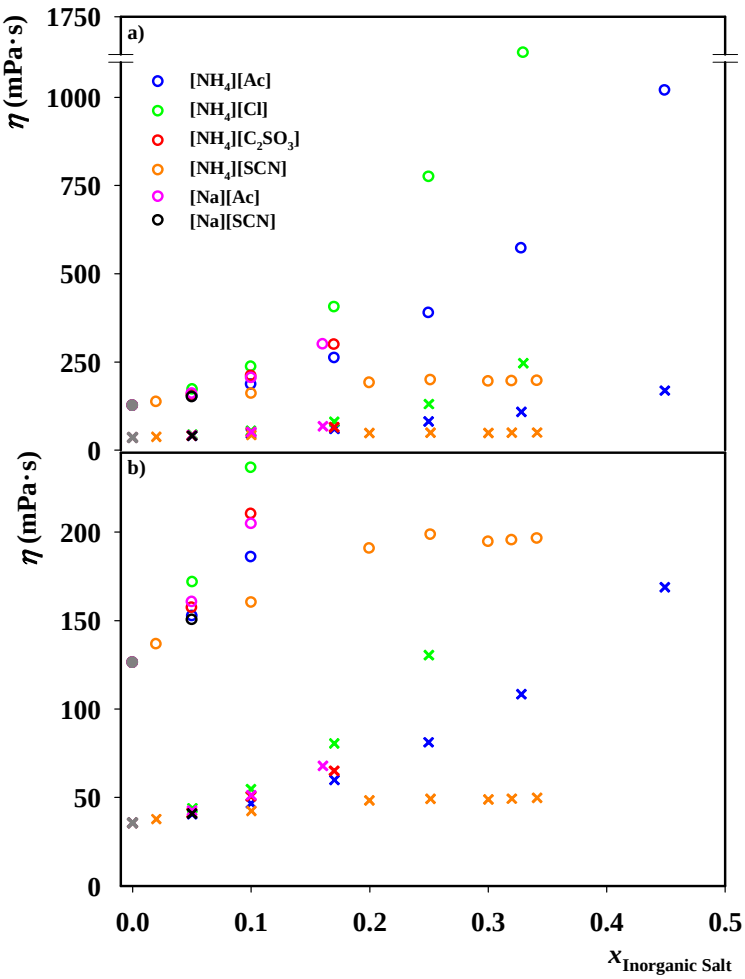

Figure 5 | Viscosity as a function of the IS mole fraction for the systems [C_2MIM][Ac] + IS [b) is an enlargement of a)]. The system [C_2MIM][Ac] + [NH_4][SCN] is taken from literature.[20] The different symbols represent the temperatures 298.15 K (○) and 323.15 K (×), whereas the grey symbols represent the neat IL.

The activation energy, Ea, can be calculated based on the viscosity dependence with temperature using Arrhenius equation, shown in equation 3:

$$Ln(\eta) = Ln(\eta_\infty) + \frac{E_a}{RT} \qquad (3)$$

where E_a is the activation energy, η the viscosity, η_∞ the viscosity at infinite temperature, R the universal gas constant and T the temperature.

Figure 6 depicts the activation energy for the systems studied, while Tables S1-S6 in the SI present the experimental data for the viscosity and Table S7 the experimental data for the activation energies. It can be seen that the activation energy increases proportionally to the increase in salt concentration, with the exception of the $[NH_4][SCN]$, which is a direct consequence of the viscosity behaviour discussed before. Since the activation energy is directly related to the flow of ions past to each other, it was expected that $[NH_4]Cl$ presented the highest E_a and $[NH_4][SCN]$ the lowest, as verified in Figure 6. It is also interesting to observe that the E_a of the $[NH_4][SCN]$ containing system follows the same behaviour found for the viscosity of this system, where a constant value was reached for IS concentrations higher than 0.20.

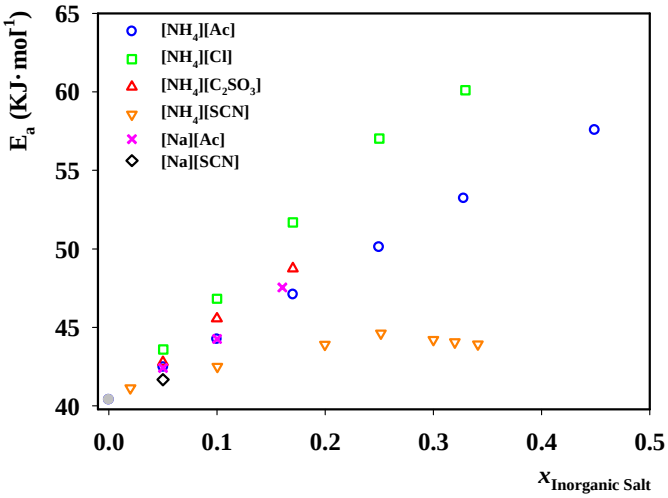

Figure 6 | Activation energy as a function of the IS mole fraction for the $[C_2MIM][Ac]$ + IS systems. The grey symbol represents the neat IL.

4.5. Ionic conductivity

The ionic conductivity is associated with the movement of ions in a media and therefore a property directly related with the ionicity. The influence of the IS content on the ionic conductivity of the IL is illustrated in Figure 7 and the experimental data is presented on Tables S1-S5 in the SI. Again two different types of behaviours can be observed: i) an increase in the concentration of the IS leads to the decrease of the ionic conductivity of the mixture, according to the IS trend $[NH_4][Ac] < [NH_4][C_2SO_3] < Na[SCN] < [NH_4]Cl < Na[Ac]$. These ionic conductivity data are in agreement with the viscosity results since the increase in the viscosity decreases the fluidity of the system and consequently the movement of ions diminishes, leading to lower ionic conductivities. Nonetheless, the decrease in the ionic conductivity is not as large as the increase in the viscosity. ii) in the system $[C_2MIM][Ac] + [NH_4][SCN]$ the ionic conductivity increases upon the addition of IS, until a constant value is reached near the solubility limit. Nevertheless, the increments in the ionic conductivity of the system are small, ranging from 1 to 1.25 times the ionic conductivity of the pure IL, in the whole concentration range. This phenomena is related with the presence of anion thiocyanate in the IS, since it is known that the present of anions with -CN groups can generate highly fluid and conductive ILs.[42] Furthermore, as shown in the viscosity section, this system exhibits the smallest decrease in fluidity which could explain the small increase in the conductivity registered.

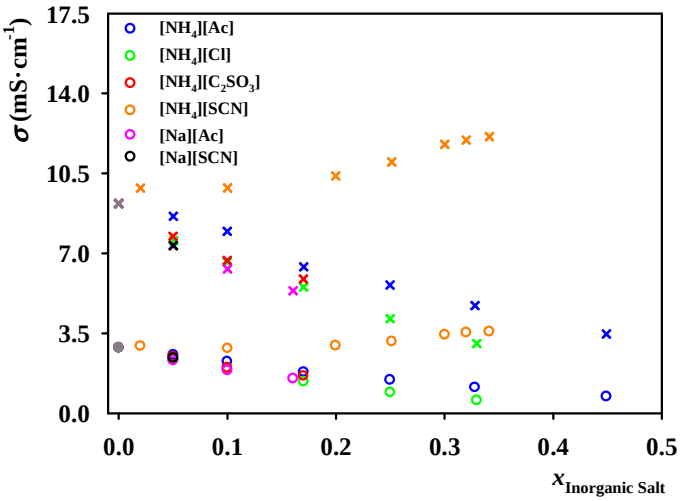

Figure 7 | Ionic conductivity as a function of the IS mole fraction, for the [C_2MIM][Ac] + IS systems. The [C_2MIM][Ac] + [NH_4][SCN] system is taken from literature.[20] The different symbols represent the temperatures 298.15 K (○) and 323.15 K (×), whereas the grey symbols represent the neat IL.

4.6. Ionicity

The ionicity of an IL is related to its ionic nature and measures the degree to which it can be considered to be composed entirely by ions or by neutral ion-pairs (large aggregates). It is known that ILs can form aggregates or clusters to some extent even though, ideally, they should consist of non-associated ions.

Based on the Walden rule, a linear relationship between the molar conductivity and the viscosity (fluidity) can be obtain, as shown in equation 4:

$$\Lambda \cdot \eta = k \tag{4}$$

where Λ is the molar conductivity, η is the viscosity and k a temperature dependent constant. By plotting the log Λ vs. log η^{-1}, the Walden Plot is obtained, where a straight line that passes through the origin with a slope equal to 1 represents the ideal electrolyte

behaviour, also known as the "ideal" Walden line. This line was drawn from data of a 1 M KCl aqueous solution where the inorganic salt is known to be fully dissociated, with the ions having equal mobility. The Walden Plot has been proved to be a convenient and versatile tool to measure the ionicity of ILs.[22, 23] However, the use of the KCl aqueous solution as the reference in the Walden plot is debatable[43] and as MacFarlane et al.[23] showed, disregarding the hydrodynamic radii of different ions has an impact on the Walden Plot, since it affects the molar conductivity as well as the viscosity of ILs, and thus what might be considered as "ideal" or "associated" behaviour. Therefore, the Walden plot should be adjusted taking into account the radius of the ions involved in each system. The role of ion size can be inferred from the Stokes-Einstein equation for each ion as shown in equation 5:

$$D_i = \frac{k_B \cdot T}{6\pi \cdot \eta \cdot r_i} \tag{5}$$

where D_i is the diffusion coefficient, k_B is the Boltzmann's constant, T the temperature and r_i the radius of the ion. To adjust the Walden Plot, it is necessary to correlate the Stokes-Einstein equation with the Nernst-Einstein equation, given by equation 6:

$$\Lambda = \frac{N_A \cdot e^2}{k_B \cdot T}\left(D^+ + D^-\right) \tag{6}$$

where N_A is the Avogadro's number, e is the electronic charge and D^+ and D^- are the diffusion coefficients for the cation and anion, respectively. Since in the systems under study there are 4 ions involved, the adjusted Walden Plot must take in consideration the molar ratios of the IL + IS mixture, as shown in equation 7:

$$\Lambda = C \cdot \eta^{-1}\left(x_{IL} \cdot \frac{1}{r_{IL}^+} + x_{IL} \cdot \frac{1}{r_{IL}^-} + x_{IS} \cdot \frac{1}{r_{IS}^+} + x_{IS} \cdot \frac{1}{r_{IS}^-} \right) \tag{7}$$

where C is a constant, and r^+ and r^- are the radius of cation and anion, respectively. For the calculation of the radius of each ion the following equation was used:

$$V^{theory} = \frac{4}{3}\pi \cdot r_{ion}^3 \quad (8)$$

where V^{theory} is the molecular volume of the ion calculated by Ab Initio calculations. The molecular volumes were computed using the M06-2X/aug-cc-pVDZ level of theory. Table S8 in the SI depicts the theoretical molecular volumes and ionic radius of each ion.

In Figure 8, the [C_2MIM][Ac] + IS systems studied in this work are represented in the adjusted Walden Plot. The solid line in Figure 8 represents the ideal Walden line and the proximity to this line indicates higher ionicity. The results show that all the systems studied are very close to the ideal Walden line, meaning that they all fall on the "good ILs" region.[24] In all systems, for each concentration, the Walden plot shows a linear behaviour with the temperature, and as the temperature increases the values deviate from the ideal line (the slope is smaller than the unit), a behaviour that is observed for protic ILs.[44]

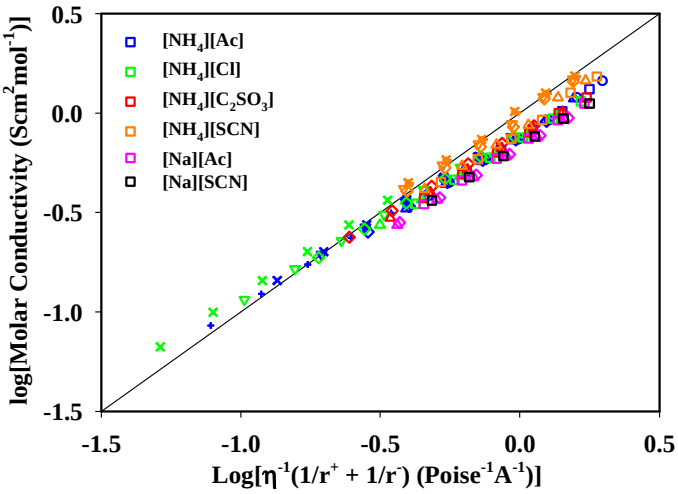

Figure 8 | Adjusted Walden Plot for the [C_2MIM][Ac] + IS systems. The [C_2MIM][Ac] + [NH_4][SCN] system is taken from literature.[20] The different symbols represent each concentration in the range of temperatures

298.15 – 323.15 K. (○) x_{IS} = 0, (□) 0.02< x_{IS} < 0.05, (Δ) x_{IS} = 0.10, (◊) 0.15< x_{IS} < 0.20, (∇) x_{IS} = 0.25, (-) x_{IS} = 0.30, (×) 0.32< x_{IS} < 0.33, (+) x_{IS} > 0.33.

By measuring the vertical distance to the ideal Walden line (Δ*W*), the ionicity of each system can be inferred.[45] Figure 9 illustrates the deviations from the adjusted Walden plot, measured at a fixed value of log η^{-1} = 0, against the concentration of IS for the binary mixtures studied. The results show that for all the systems with ammonium-based ISs, the ionicity of the mixture increases with the increasing concentration of IS, since the deviation to the ideal Walden line becomes smaller. On the other hand, when a sodium-based IS is added to the IL, the deviations become higher, meaning the ionicity decreases with the addition of these ISs. Nevertheless, for some systems, this method allows only an estimative of the ionicity since the deviation to the ideal Walden line is calculated at a given fluidity. For instance, in the case of the systems [C_2MIM][Ac] + [NH_4][Ac] and [C_2MIM][Ac] + [NH_4]Cl, the log(fluidity) = 0 is out of the range of the experimental results for higher ISs concentrations, and thus a extrapolation of the results is needed for the determination of the Δ*W*.

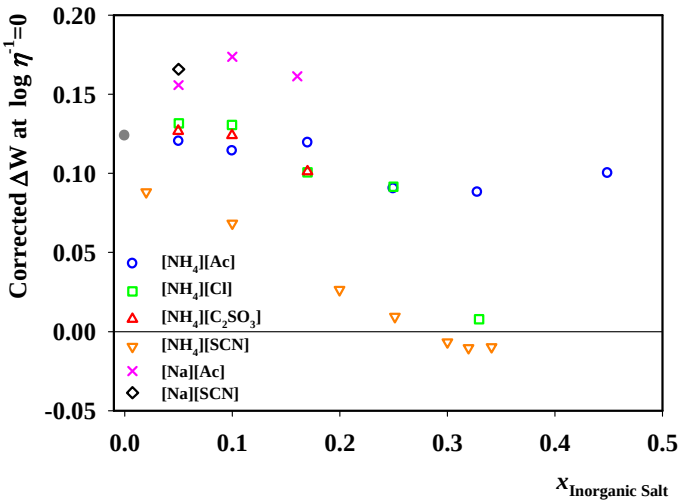

Figure 9 | Deviations from the Adjusted Walden Plot for the [C_2MIM][Ac] + IS systems. The [C_2MIM][Ac] + [NH_4][SCN] system is taken from literature.[20] The grey symbol represents the neat IL.

Following the Walden plot method for the determination of the ionicity, Ueno et al.[28] calculated the ionicity through the (Λ_{imp} / Λ_{ideal}) ratio, where the Λ_{imp} is the molar conductivity, usually measured by the impedance method, and Λ_{ideal} is assumed to be the ideal molar conductivity at a given fluidity in the ideal Walden line, i.e., the absolute value of the Λ_{ideal} ($S \cdot cm^2 \cdot mol^{-1}$) is equal to that of the fluidity (P^{-1}).

Table 1 displays the results obtained for both methods of calculating the ionicity. Although these two methods cannot be quantitatively compared, from a qualitative point, they both produce the same conclusions. When using the ΔW, the values decrease when ammonium-based salts are used (higher ionicity) and increase for the sodium-based ones (lower ionicity). For the (Λ_{imp} / Λ_{ideal}) ratio, the opposite behaviour is observed, since an increase in this ratio means proximity to the unity and hence ideality, leading to higher ionicity, which is obtained for the ammonium-based ISs but not for the sodium-based ones. These results can be explained based on the viscosity and ionic conductivity changes upon the addition of the respective IS. In the systems containing ammonium-based salts, the decrease in ionic conductivity is always much smaller than the increase in viscosity, meaning that the movement of ions is still possible despite the lower fluidity of the system. On the other hand, for the systems with sodium-based salts, the increase in the viscosity is of the same order of magnitude as the decrease in the ionic conductivity, which means that the decrease in the fluidity of these systems effectively impacts the movement ions in a stronger way than in the systems with ammonium-based salts. Furthermore, in our previous work,[33] where the ionicity of the binary systems 1-ethyl-3-methylimidazolium ethyl sulfonate and ethyl sulfate + ammonium thiocyanate was studied, we found that one of the reasons for the increase in the ionicity of these systems was the formation of aggregates between the IL's anion and the $[NH_4]^+$ cation, that allowed the other ions to become more free. From the results obtained in the present work, it can be concluded that the presence of the $[NH_4]^+$ cation is crucial for occurrence of stronger interactions between the IS and the IL and the formation of aggregates.

The two systems that displayed higher ionicity are the $[C_2MIM][Ac]$ + $[NH_4][SCN]$ and the $[C_2MIM][Ac]$ + $[NH_4]Cl$. In the first one, the increase in the ionicity was expected since this system was the only one where an increase in the ionic conductivity was observed and

simultaneously the increase in the viscosity was the lowest of all the systems studied. In the case of the system with $[NH_4]Cl$, even though it exhibits the largest increase in viscosity, the ratio between the increase in viscosity and the decrease in the ionic conductivity was much lower than for the other two ammonium salts, $[NH_4][Ac]$ and $[NH_4][C_2SO_3]$.

Table 1 | Ionicity for the binary systems $[C_2MIM][Ac]$ (1) + Salt (2) calculated through different methods: $\Lambda_{imp}/\Lambda_{ideal}$, at 323.15 K; and deviations from the ideal Walden line (at log(fluidity) = 0).

Salt	x_2	$\Lambda_{imp}/\Lambda_{ideal}$	ΔW
	0	0.5154	0.1238
$[NH_4][Ac]$	0.0503	0.5331	0.1204
	0.0999	0.5517	0.1143
	0.1703	0.5464	0.1195
	0.2498	0.6178	0.0905
	0.3280	0.6573	0.0881
	0.4491	0.6924	0.1002
$[NH_4]Cl$	0.0505	0.5027	0.1316
	0.0999	0.5268	0.1305
	0.1702	0.6127	0.1007
	0.2500	0.6944	0.0916
	0.3297	0.8990	0.0078
$[NH_4][C_2SO_3]$	0.0500	0.4936	0.1268
	0.0999	0.5119	0.1241
	0.1701	0.5628	0.1011
$[NH_4][SCN]$	0.0200	0.5770	0.0881
	0.1002	0.6183	0.0684
	0.1998	0.6977	0.0264
	0.2514	0.7282	0.0094
	0.3001	0.7489	-0.0068
	0.3199	0.7576	-0.0104
	0.3413	0.7625	-0.0098
Na[Ac]	0.0501	0.4762	0.1558
	0.1001	0.4777	0.1737
	0.1605	0.4851	0.1614
Na[SCN]	0.0502	0.4563	0.1658

5. Conclusions

In the present work, the thermophysical properties of the several binary systems of $[C_2MIM][Ac]$ + IS were determined. Six different ISs were used, four ammonium-based and two sodium-based, in order to compare the effects of using different IS cations and anions, on the density, refractive index, viscosity, ionic conductivity and ionicity of the IL.

The obtained data showed that the addition of ammonium-based ISs increased the

ionicity of the system, whereas the addition of sodium-based ISs had the opposite effect. The results showed that in all systems the viscosity increased and the ionic conductivity decreased upon the addition of IS, with the exception of the system [C_2MIM][Ac] + [NH_4][SCN]. The effect of addition of IS on the ionicity can be well described by the ratio between the variation of viscosity and variation of conductivity. To increase the ionicity of a system, it is essential to increase its ionic conductivity and decrease its viscosity. In addition, the presence of an ammonium cation instead of a sodium cation in the IS is of utmost importance in the establishment of stronger interactions between the IL and the IS, and therefore in the increase of the ionicity of the IL.

6. Acknowledgements

Filipe S. Oliveira gratefully acknowledges the financial support of FCT/MCTES (Portugal) through the PhD fellowship SFRH/BD/73761/2010 and Isabel M. Marrucho for a contract under FCT Investigator 2012 Program. The authors also acknowledge the Fundação para a Ciência e Tecnologia (FCT) for the financial support through the projects PTDC/EQU-FTT/116015/2009 and PTDC/EQU-FTT/1686/2012. The authors acknowledge Jennifer L. Hodgson and Douglas R. MacFarlane for the help in the ab initio calculations as well as the generous allocations of computing time from the Monash Campus Cluster at the *e*Research Centre of Monash University, Australia. The NMR spectrometers are part of The National NMR Facility (RECI/BBB-BQB/0230/2012), supported by Fundação para a Ciência e a Tecnologia (FCT).

7. Supplementary Information

7.1. Characterization of [NH₄][C₂SO₃]

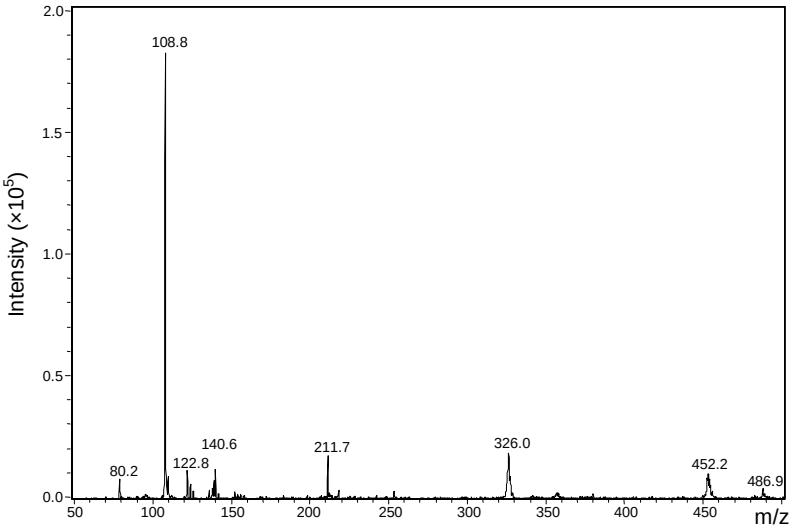

Figure S1 | Mass spectrum of ammonium ethyl sulfonate ([NH_4][C_2SO_3]) acquired in negative mode by API-ION TRAP.

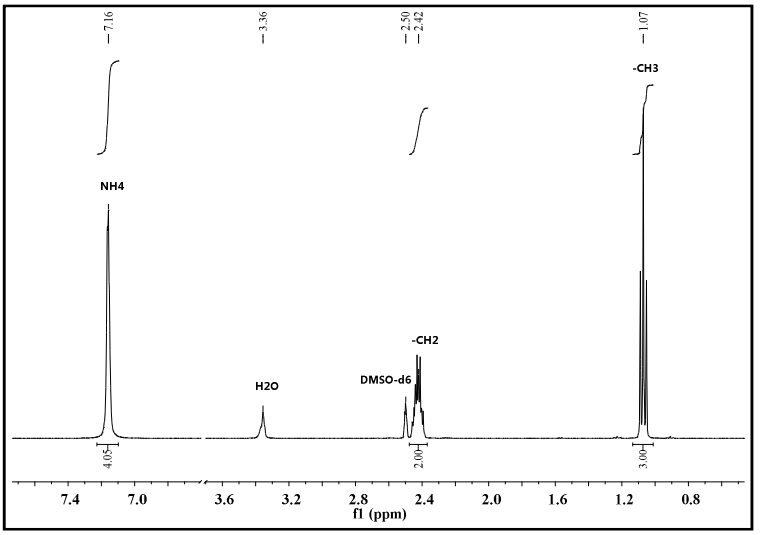

Figure S2 | ^{1}H NMR spectrum of ammonium ethyl sulfonate ([NH_4][C_2SO_3]) acquired in deuterated dimethyl sulfoxide (DMSO-d_6).

7.2. Supporting tables

Table S1 | Density, ρ, dynamic viscosity, η, ionic conductivity, σ, refractive index, n_D, molar volume, V_m, molar refraction, R_m, and free molar volume, f_m, for the binary system $[C_2MIM][Ac]$ (1) + $[NH_4][Ac]$ (2) at several temperatures.

x_2	ρ (g·cm^{-3})	η (mPa·s)	σ (mS·cm^{-1})	n_D	V_m (cm^{-3}·mol^{-1})	R_m (cm^{-3}·mol^{-1})	f_m (cm^{-3}·mol^{-1})
				T = 298.15 K			
0	1.0983	126.25	2.875	1.49997	154.976	45.579	109.397
0.0503	1.0983	152.54	2.553	1.49884	150.715	44.241	106.474
0.0999	1.0991	185.89	2.261	1.49771	146.403	42.892	103.511
0.1703	1.1001	260.87	1.806	1.49585	140.306	40.976	99.330
0.2498	1.1009	388.81	1.458	1.49365	133.475	38.834	94.641
0.3280	1.1015	571.81	1.136	1.49099	126.791	36.720	90.071
0.4491	1.1020	1020.12	0.734	1.48604	116.500	33.450	83.050
				T = 303.15 K			
0	1.0952	93.62	3.736	1.49867	155.410	45.606	109.804
0.0503	1.0952	111.68	3.365	1.49750	151.142	44.265	106.877
0.0999	1.0960	134.68	2.995	1.49641	146.817	42.918	103.899
0.1703	1.0970	185.54	2.425	1.49458	140.707	41.003	99.703
0.2498	1.0977	270.91	1.988	1.49235	133.864	38.860	95.004
0.3280	1.0983	389.50	1.580	1.48971	127.168	36.748	90.420
0.4491	1.0989	672.61	1.056	1.48482	116.832	33.474	83.358
				T = 308.15 K			
0	1.0924	71.26	4.730	1.49732	155.818	45.620	110.197
0.0503	1.0921	83.95	4.309	1.49617	151.562	44.287	107.275
0.0999	1.0929	100.14	3.888	1.49505	147.234	42.940	104.293
0.1703	1.0939	135.50	3.188	1.49322	141.105	41.024	100.082
0.2498	1.0946	194.03	2.656	1.49097	134.251	38.880	95.371
0.3280	1.0951	273.26	2.151	1.48839	127.539	36.771	90.769
0.4491	1.0956	458.10	1.476	1.48350	117.184	33.496	83.687
				T = 313.15 K			
0	1.0894	55.52	5.869	1.49597	156.247	45.641	110.606
0.0503	1.0891	64.56	5.423	1.49483	151.989	44.310	107.678
0.0999	1.0898	76.17	4.936	1.49366	147.652	42.960	104.692
0.1703	1.0908	101.26	4.103	1.49182	141.506	41.041	100.465
0.2498	1.0915	142.31	3.486	1.48959	134.632	38.897	95.736
0.3280	1.0919	196.62	2.857	1.48700	127.909	36.788	91.122
0.4491	1.0924	320.87	2.009	1.48217	117.523	33.514	84.009
				T = 318.15 K			
0	1.0864	44.15	7.605	1.49465	156.678	45.663	111.015
0.0503	1.0860	50.66	6.710	1.49344	152.418	44.329	108.089
0.0999	1.0867	59.09	6.170	1.49228	148.074	42.980	105.094
0.1703	1.0876	77.20	5.186	1.49040	141.914	41.059	100.856
0.2498	1.0883	106.56	4.486	1.48822	135.024	38.917	96.107
0.3280	1.0888	144.61	3.706	1.48561	128.277	36.804	91.474
0.4491	1.0892	230.31	2.673	1.48081	117.869	33.532	84.336
				T = 323.15 K			
0	1.0834	35.74	9.180	1.49331	157.112	45.684	111.428
0.0503	1.0829	40.46	8.620	1.49205	152.854	44.349	108.505

0.0999	1.0835	46.65	7.965	1.49085	148.502	42.998	105.504
0.1703	1.0845	59.89	6.410	1.48902	142.320	41.077	101.243
0.2498	1.0852	81.25	5.616	1.48677	135.406	38.928	96.478
0.3280	1.0857	108.40	4.714	1.48419	128.644	36.817	91.827
0.4491	1.0862	168.88	3.469	1.47942	118.201	33.544	84.657

Table S2 | Density, ρ, dynamic viscosity, η, ionic conductivity, σ, refractive index, n_D, molar volume, V_m, molar refraction, R_m, and free molar volume, f_m, for the binary system $[C_2MIM][Ac]$ (1) + $[NH_4]Cl$ (2) at several temperatures.

x_2	ρ ($g \cdot cm^{-3}$)	η (mPa·s)	σ ($mS \cdot cm^{-1}$)	n_D	V_m ($cm^{-3} \cdot mol^{-1}$)	R_m ($cm^{-3} \cdot mol^{-1}$)	f_m ($cm^{-3} \cdot mol^{-1}$)
			T = 298.15 K				
0	1.0983	126.25	2.875	1.49997	154.976	45.579	109.397
0.0505	1.1012	171.74	2.343	1.50091	149.220	43.956	105.264
0.0999	1.1040	236.36	1.903	1.50176	143.614	42.366	101.248
0.1702	1.1083	405.44	1.385	1.50278	135.649	40.085	95.564
0.2500	1.1134	774.92	0.911	1.50385	126.663	37.496	89.166
0.3297	1.1184	1608.07	0.567	1.50474	117.782	34.920	82.863
			T = 303.15 K				
0	1.0952	93.62	3.736	1.49867	155.410	45.606	109.804
0.0505	1.0981	124.59	3.084	1.49958	149.636	43.979	105.657
0.0999	1.1008	167.80	2.548	1.50043	144.027	42.392	101.635
0.1702	1.1052	277.71	1.921	1.50150	136.038	40.112	95.925
0.2500	1.1102	510.76	1.295	1.50262	127.028	37.527	89.501
0.3297	1.1153	1040.75	0.843	1.50345	118.106	34.940	83.166
			T = 308.15 K				
0	1.0924	71.26	4.730	1.49732	155.818	45.620	110.197
0.0505	1.0951	92.92	3.977	1.49820	150.051	43.998	106.053
0.0999	1.0978	122.56	3.332	1.49904	144.425	42.409	102.016
0.1702	1.1020	196.41	2.587	1.50014	136.425	40.134	96.291
0.2500	1.1071	348.45	1.791	1.50129	127.391	37.550	89.841
0.3297	1.1122	693.30	1.214	1.50217	118.435	34.962	83.474
			T = 313.15 K				
0	1.0894	55.52	5.869	1.49597	156.247	45.641	110.606
0.0505	1.0920	70.98	5.013	1.49682	150.472	44.018	106.454
0.0999	1.0947	91.75	4.308	1.49765	144.830	42.427	102.402
0.1702	1.0989	142.76	3.408	1.49876	136.809	40.154	96.656
0.2500	1.1040	244.97	2.422	1.49992	127.749	37.568	90.181
0.3297	1.1090	477.83	1.693	1.50085	118.777	34.985	83.793
			T = 318.15 K				
0	1.0864	44.15	7.605	1.49465	156.678	45.663	111.015
0.0505	1.0891	55.36	6.218	1.49547	150.878	44.034	106.843
0.0999	1.0917	70.19	5.367	1.49627	145.228	42.443	102.784
0.1702	1.0958	106.20	4.386	1.49736	137.196	40.171	97.025
0.2500	1.1008	176.75	3.200	1.49854	128.116	37.588	90.528
0.3297	1.1059	339.15	2.299	1.49951	119.117	35.006	84.112
			T = 323.15 K				
0	1.0834	35.74	9.180	1.49331	157.112	45.684	111.428
0.0505	1.0860	43.98	7.555	1.49409	151.299	44.053	107.246
0.0999	1.0887	54.73	6.610	1.49489	145.632	42.461	103.171

0.1702	1.0927	80.62	5.524	1.49594	137.586	40.188	97.398
0.2500	1.0977	130.47	4.143	1.49715	128.474	37.604	90.870
0.3297	1.1028	246.40	3.055	1.49817	119.445	35.022	84.423

Table S3 | Density, ρ, dynamic viscosity, η, ionic conductivity, σ, refractive index, n_D, molar volume, V_m, molar refraction, R_m, and free molar volume, f_m, for the binary system $[C_2MIM][Ac]$ (1) + $[NH_4][C_2SO_3]$ (2) at several temperatures.

x_2	ρ ($g \cdot cm^{-3}$)	η (mPa·s)	σ ($mS \cdot cm^{-1}$)	n_D	V_m ($cm^{-3} \cdot mol^{-1}$)	R_m ($cm^{-3} \cdot mol^{-1}$)	f_m ($cm^{-3} \cdot mol^{-1}$)
				T = 298.15 K			
0	1.0983	126.25	2.875	1.49997	154.976	45.579	109.397
0.0500	1.1050	157.19	2.468	1.49869	152.088	44.633	107.456
0.0999	1.1137	210.28	1.996	1.49756	148.976	43.635	105.341
0.1701	1.1241	298.77	1.639	1.49488	144.905	42.249	102.656
				T = 303.15 K			
0	1.0952	93.62	3.736	1.49867	155.410	45.606	109.804
0.0500	1.1018	114.96	3.232	1.49735	152.526	44.659	107.867
0.0999	1.1105	150.90	2.659	1.49624	149.405	43.663	105.743
0.1701	1.1208	209.82	2.215	1.49359	145.327	42.278	103.050
				T = 308.15 K			
0	1.0924	71.26	4.730	1.49732	155.818	45.620	110.197
0.0500	1.0987	86.26	4.151	1.49599	152.956	44.681	108.275
0.0999	1.1073	111.20	3.464	1.49488	149.828	43.684	106.144
0.1701	1.1176	151.50	2.933	1.49223	145.743	42.299	103.444
				T = 313.15 K			
0	1.0894	55.52	5.869	1.49597	156.247	45.641	110.606
0.0500	1.0956	66.19	5.224	1.49464	153.389	44.704	108.685
0.0999	1.1042	83.89	4.423	1.49346	150.258	43.703	106.555
0.1701	1.1144	112.07	3.804	1.49081	146.166	42.319	103.848
				T = 318.15 K			
0	1.0864	44.15	7.605	1.49465	156.678	45.663	111.015
0.0500	1.0925	51.82	6.495	1.49325	153.824	44.724	109.100
0.0999	1.1010	64.60	5.529	1.49204	150.690	43.721	106.969
0.1701	1.1112	84.65	4.806	1.48940	146.587	42.336	104.251
				T = 323.15 K			
0	1.0834	35.74	9.180	1.49331	157.112	45.684	111.428
0.0500	1.0894	41.30	7.747	1.49184	154.271	44.745	109.526
0.0999	1.0978	50.65	6.688	1.49060	151.129	43.740	107.389
0.1701	1.1080	65.14	5.878	1.48797	147.006	42.352	104.654

Table S4 | Density, ρ, dynamic viscosity, η, ionic conductivity, σ, refractive index, n_D, molar volume, V_m, molar refraction, R_m, and free molar volume, f_m, for the binary system [C_2MIM][Ac] (1) + Na[Ac] (2) at several temperatures.

x_2	ρ (g·cm^{-3})	η (mPa·s)	σ (mS·cm^{-1})	n_D	V_m (cm^{-3}·mol^{-1})	R_m (cm^{-3}·mol^{-1})	f_m (cm^{-3}·mol^{-1})
				T = 298.15 K			
0	1.0983	126.25	2.875	1.49997	154.976	45.579	109.397
0.0501	1.1045	160.47	2.318	1.49832	150.106	44.023	106.083
0.1001	1.1112	204.64	1.885	1.49654	145.233	42.465	102.768
0.1496	1.1101	206.54	1.992	1.49682	141.445	41.377	100.068
				T = 303.15 K			
0	1.0952	93.62	3.736	1.49867	155.410	45.606	109.804
0.0501	1.1014	117.14	3.052	1.49700	150.524	44.046	106.478
0.1001	1.1081	147.40	2.519	1.49525	145.640	42.490	103.149
0.1496	1.1070	148.24	2.646	1.49554	141.841	41.402	100.439
				T = 308.15 K			
0	1.0924	71.26	4.730	1.49732	155.818	45.620	110.197
0.0501	1.0983	87.95	3.917	1.49567	150.949	44.070	106.879
0.1001	1.1050	109.28	3.273	1.49392	146.048	42.512	103.536
0.1496	1.1040	109.67	3.427	1.49420	142.233	41.421	100.812
				T = 313.15 K			
0	1.0894	55.52	5.869	1.49597	156.247	45.641	110.606
0.0501	1.0955	67.68	4.914	1.49432	151.344	44.084	107.260
0.1001	1.1021	83.11	4.158	1.49258	146.432	42.525	103.907
0.1496	1.1009	83.29	4.347	1.49285	142.634	41.441	101.193
				T = 318.15 K			
0	1.0864	44.15	7.605	1.49465	156.678	45.663	111.015
0.0501	1.0925	53.18	6.062	1.49298	151.760	44.103	107.657
0.1001	1.0991	64.68	5.177	1.49121	146.832	42.541	104.291
0.1496	1.0979	64.72	5.380	1.49148	143.023	41.457	101.567
				T = 323.15 K			
0	1.0834	35.74	9.180	1.49331	157.112	45.684	111.428
0.0501	1.0894	42.66	7.336	1.49163	152.182	44.123	108.059
0.1001	1.0961	51.35	6.320	1.48990	147.234	42.560	104.674
0.1496	1.0949	51.31	6.594	1.49016	143.409	41.473	101.936

Table S5 | Density, ρ, dynamic viscosity, η, ionic conductivity, σ, refractive index, n_D, molar volume, V_m, molar refraction, R_m, and free molar volume, f_m, for the binary system [C_2MIM][Ac] (1) + Na[SCN] (2) at several temperatures.

x_2	ρ (g·cm^{-3})	η (mPa·s)	σ (mS·cm^{-1})	n_D	V_m (cm^{-3}·mol^{-1})	R_m (cm^{-3}·mol^{-1})	f_m (cm^{-3}·mol^{-1})
				T = 298.15 K			
0	1.0983	126.25	2.875	1.49997	154.976	45.579	109.397
0.0502	1.1057	150.36	2.424	1.50133	149.896	44.186	105.710
				T = 303.15 K			
0	1.0952	93.62	3.736	1.49867	155.410	45.606	109.804
0.0502	1.1026	110.38	3.164	1.50000	150.313	44.210	106.103

T = 308.15 K							
0	1.0924	71.26	4.730	1.49732	155.818	45.620	110.197
0.0502	1.0995	83.31	4.035	1.49867	150.737	44.234	106.503
T = 313.15 K							
0	1.0894	55.52	5.869	1.49597	156.247	45.641	110.606
0.0502	1.0965	64.41	5.043	1.49732	151.149	44.253	106.896
T = 318.15 K							
0	1.0864	44.15	7.605	1.49465	156.678	45.663	111.015
0.0502	1.0935	50.86	6.178	1.49597	151.569	44.274	107.295
T = 323.15 K							
0	1.0834	35.74	9.180	1.49331	157.112	45.684	111.428
0.0502	1.0904	40.90	7.342	1.49465	151.990	44.297	107.694

Table S6 | Molar volume, V_m, molar refraction, R_m, and free molar volume, f_m, for the binary system $[C_2MIM][Ac]$ (1) + $[NH_4][SCN]$ (2) at several temperatures.

x_2	V_m ($cm^{-3}\cdot mol^{-1}$)	R_m ($cm^{-3}\cdot mol^{-1}$)	f_m ($cm^{-3}\cdot mol^{-1}$)
T = 298.15 K			
0.0200	152.817	44.934	107.883
0.1002	145.570	42.973	102.598
0.1998	136.768	40.533	96.235
0.2514	132.398	39.326	93.072
0.3001	128.216	38.148	90.068
0.3199	126.518	37.748	88.771
0.3413	124.640	37.229	87.412
T = 303.15 K			
0.0200	153.249	44.984	108.265
0.1002	145.980	42.996	102.984
0.1998	137.156	40.625	96.530
0.2514	132.778	39.373	93.405
0.3001	128.576	38.169	90.407
0.3199	126.877	37.770	89.107
0.3413	124.994	37.231	87.763
T = 308.15 K			
0.0200	153.668	44.979	108.690
0.1002	146.392	43.008	103.384
0.1998	137.542	40.626	96.916
0.2514	133.160	39.420	93.740
0.3001	128.950	38.152	90.798
0.3199	127.242	37.795	89.447
0.3413	125.353	37.296	88.057
T = 313.15 K			
0.0200	154.100	45.002	109.098
0.1002	146.802	43.067	103.735
0.1998	137.935	40.604	97.331
0.2514	133.548	39.446	94.102
0.3001	129.314	38.174	91.140
0.3199	127.609	37.798	89.812
0.3413	125.718	37.280	88.439

	T = 318.15 K		
0.0200	154.529	45.024	109.505
0.1002	147.223	43.068	104.155
0.1998	138.338	40.630	97.708
0.2514	133.935	39.426	94.508
0.3001	129.704	38.224	91.480
0.3199	127.990	37.826	90.164
0.3413	126.074	37.280	88.794
	T = 323.15 K		
0.0200	154.956	45.122	109.834
0.1002	147.642	43.067	104.575
0.1998	138.756	40.661	98.096
0.2514	134.332	39.431	94.901
0.3001	130.084	38.217	91.867
0.3199	128.369	37.809	90.560
0.3413	126.455	37.288	89.167

Table S7 | Activation energy, E_a, for the binary systems [C_2MIM][Ac] (1) + IS (2).

Salt	x_2	E_a (KJ·mol^{-1})	*Error*
	0	40.403	0.017
[NH_4][Ac]	0.0503	42.485	0.017
	0.0999	44.257	0.016
	0.1703	47.102	0.015
	0.2498	50.114	0.016
	0.3280	53.227	0.017
	0.4491	57.570	0.019
[NH_4]Cl	0.0505	43.605	0.017
	0.0999	46.831	0.018
	0.1702	51.690	0.019
	0.2500	57.027	0.021
	0.3297	60.103	0.022
[NH_4][C_2SO_3]	0.0500	42.792	0.016
	0.0999	45.572	0.016
	0.1701	48.759	0.016
[NH_4][SCN]	0.0200	41.138	0.017
	0.1002	42.517	0.015
	0.1998	43.908	0.013
	0.2514	44.617	0.012
	0.3001	44.223	0.012
	0.3199	44.065	0.012
	0.3413	43.938	0.014
Na[Ac]	0.0501	42.422	0.019
	0.1001	44.268	0.019
	0.1496	44.573	0.020
Na[SCN]	0.0502	41.672	0.018

Table S8 | Theoretical molar volumes and molecular ionic radius for the IL and ISs used in this work.

Compound	Cation V_m ($cm^3 \cdot mol^{-1}$)	Anion V_m ($cm^3 \cdot mol^{-1}$)	Cation radius (Å)	Anion radius (Å)
$[C_2MIM][Ac]$	87.401	38.767	3.26	2.49
$[NH_4][Ac]$	19.866	38.767	1.99	2.49
$[NH_4]Cl$	19.866	13.723	1.99	1.76
$[NH_4][C_2SO_3]$	19.866	63.824	1.99	2.94
$[NH_4][SCN]$	19.866	33.812	1.99	2.38
Na[Ac]	8.512	38.767	1.50	2.49
Na[SCN]	8.512	33.812	1.50	2.38

8. References

1. M. J. Earle, J. M. S. S. Esperança, M. A. Gilea, J. N. C. Lopes, L. P. N. Rebelo, J. W. Magee, K. R. Seddon and J. A. Widegren, The distillation and volatility of ionic liquids, *Nature*, 2006, **439**, 831-834.

2. L. P. N. Rebelo, J. N. C. Lopes, J. M. S. S. Esperança, H. J. R. Guedes, J. Lachwa, V. Najdanovic-Visak and Z. P. Visak, Accounting for the unique, doubly dual nature of ionic liquids from a molecular thermodynamic, and modeling standpoint, *Acc. Chem. Res.*, 2007, **40**, 1114-1121.

3. N. V. Plechkova and K. R. Seddon, Applications of ionic liquids in the chemical industry, *Chem. Soc. Rev.*, 2008, **37**, 123-150.

4. H. Niedermeyer, J. P. Hallett, I. J. Villar-Garcia, P. A. Hunt and T. Welton, Mixtures of ionic liquids, *Chem. Soc. Rev.*, 2012, **41**, 7780-7802.

5. A. Abebe, S. Admassie, I. J. Villar-Garcia and Y. Chebude, 4,4-Bipyridinium ionic liquids exhibiting excellent solubility for metal salts: Potential solvents for electrodeposition, *Inorg. Chem. Commun.*, 2013, **29**, 210-212.

6. I. M. AlNashef, in *Fundamental of Chemical Engineering, Pts 1-3*, eds. Z. Cao, L. Sun, X. Q. Cao and Y. H. He, 2011, vol. 233-235, pp. 2760-2764.

7. C. Chiappe, M. Malvaldi, B. Melai, S. Fantini, U. Bardi and S. Caporali, An unusual common ion effect promotes dissolution of metal salts in room-temperature ionic liquids: A strategy to obtain ionic liquids having organic-inorganic mixed cations, *Green Chem.*, 2010, **12**, 77-80.

8. J.-C. Lassègues, J. Grondin, C. Aupetit and P. Johansson, Spectroscopic identification of the lithium ion transporting species in LiTFSI-doped ionic liquids, *J. Phys. Chem. A*, 2009, **113**, 305-314.

9. Z. P. Rosol, N. J. German and S. M. Gross, Solubility, ionic conductivity and viscosity of lithium salts in room temperature ionic liquids, *Green Chem.*, 2009, **11**, 1453-1457.

10. A. B. Pereiro, J. M. M. Araújo, F. S. Oliveira, J. M. S. S. Esperança, J. N. C. Lopes, I. M. Marrucho and L. P. N. Rebelo, Solubility of inorganic salts in pure ionic liquids, *J. Chem. Thermodyn.*, 2012, 29-36.

11. T. V. Doherty, M. Mora-Pale, S. E. Foley, R. J. Linhardt and J. S. Dordick, Ionic liquid solvent properties as predictors of lignocellulose pretreatment efficacy, *Green Chem.*, 2010, **12**, 1967-1975.

12. Y. Qin, X. Lu, N. Sun and R. D. Rogers, Dissolution or extraction of crustacean shells using ionic liquids to obtain high molecular weight purified chitin and direct production of chitin films and fibers, *Green Chem.*, 2010, **12**, 968-971.

13. N. Sun, M. Rahman, Y. Qin, M. L. Maxim, H. Rodriguez and R. D. Rogers, Complete dissolution and partial delignification of wood in the ionic liquid 1-ethyl-3-methylimidazolium acetate, *Green Chem.*, 2009, **11**, 646-655.

14. J. Vitz, T. Erdmenger, C. Haensch and U. S. Schubert, Extended dissolution studies of cellulose in imidazolium based ionic liquids, *Green Chem.*, 2009, **11**, 417-424.

15. S. R. Tomlinson, C. W. Kehr, M. S. Lopez, J. R. Schlup and J. L. Anthony, Solubility of the corn protein zein in imidazolium-based ionic liquids, *Ind. Eng. Chem. Res.*, 2014, **53**, 2293-2298.

16. H. Zhao, L. Jackson, Z. Song and A. Olubajo, Using ionic liquid [emim][CH_3COO] as an enzyme-'friendly' co-solvent for resolution of amino acids, *Tetrahedron-Asymmetr.*, 2006, **17**, 2491-2498.

17. G. Gurau, H. Rodríguez, S. P. Kelley, P. Janiczek, R. S. Kalb and R. D. Rogers, Demonstration of chemisorption of carbon dioxide in 1,3-dialkylimidazolium acetate ionic liquids, *Angew. Chem. Int. Ed.*, 2011, **50**, 12024-12026.

18. W. Shi, C. R. Myers, D. R. Luebke, J. A. Steckel and D. C. Sorescu, Theoretical

and experimental studies of CO_2 and H_2 separation using the 1-ethyl-3-methylimidazolium acetate ([emim][CH_3COO]) ionic liquid, *J. Phys. Chem. B*, 2012, **116**, 283-295.

19. M. B. Shiflett and A. Yokozeki, Phase behavior of carbon dioxide in ionic liquids: [emim][acetate], [emim][trifluoroacetate] and [emim][acetate] + [emim][trifluoroacetate] mixtures, *J. Chem. Eng. Data*, 2009, **54**, 108-114.

20. A. B. Pereiro, J. M. M. Araújo, F. S. Oliveira, C. E. S. Bernardes, J. M. S. S. Esperança, J. N. C. Lopes, I. M. Marrucho and L. P. N. Rebelo, Inorganic salts in purely ionic liquid media: The development of high ionicity ionic liquids (HIILs), *Chem. Commun.*, 2012, **48**, 3656-3658.

21. H. Tokuda, S. Tsuzuki, M. Susan, K. Hayamizu and M. Watanabe, How ionic are room-temperature ionic liquids? An indicator of the physicochemical properties, *J. Phys. Chem. B*, 2006, **110**, 19593-19600.

22. K. Ueno, H. Tokuda and M. Watanabe, Ionicity in ionic liquids: Correlation with ionic structure and physicochemical properties, *Phys. Chem. Chem. Phys.*, 2010, **12**, 1649-1658.

23. D. R. MacFarlane, M. Forsyth, E. I. Izgorodina, A. P. Abbott, G. Annat and K. Fraser, On the concept of ionicity in ionic liquids, *Phys. Chem. Chem. Phys.*, 2009, **11**, 4962-4967.

24. W. Xu, E. I. Cooper and C. A. Angell, Ionic liquids: Ion mobilities, glass temperatures, and fragilities, *J. Phys. Chem. B*, 2003, **107**, 6170-6178.

25. H. Tokuda, K. Hayamizu, K. Ishii, M. Abu Bin Hasan Susan and M. Watanabe, Physicochemical properties and structures of room temperature ionic liquids. 1. Variation of anionic species, *J. Phys. Chem. B*, 2004, **108**, 16593-16600.

26. H. Tokuda, K. Hayamizu, K. Ishii, M. Susan and M. Watanabe, Physicochemical properties and structures of room temperature ionic liquids. 2. Variation of alkyl chain length in imidazolium cation, *J. Phys. Chem. B*, 2005, **109**, 6103-6110.

27. H. Tokuda, K. Ishii, M. Susan, S. Tsuzuki, K. Hayamizu and M. Watanabe, Physicochemical properties and structures of room-temperature ionic liquids. 3. Variation of cationic structures, *J. Phys. Chem. B*, 2006, **110**, 2833-2839.

28. K. Ueno, K. Yoshida, M. Tsuchiya, N. Tachikawa, K. Dokko and M. Watanabe,

Glyme–lithium salt equimolar molten mixtures: Concentrated solutions or solvate ionic liquids?, *J. Phys. Chem. B*, 2012, **116**, 11323-11331.

29. S. Bulut, P. Eiden, W. Beichel, J. M. Slattery, T. F. Beyersdorff, T. J. S. Schubert and I. Krossing, Temperature dependence of the viscosity and conductivity of mildly functionalized and non-functionalized $[Tf_2N]^-$ ionic liquids, *ChemPhysChem*, 2011, **12**, 2296-2310.

30. C. Chiappe, A. Sanzone, D. Mendola, F. Castiglione, A. Famulari, G. Raos and A. Mele, Pyrazolium- versus imidazolium-based ionic liquids: Structure, dynamics and physicochemical properties, *J. Phys. Chem. B*, 2013, **117**, 668-676.

31. T.-Y. Wu, L. Hao, P.-R. Chen and J.-W. Liao, Ionic conductivity and transporting properties in LiTFSI-doped bis(trifluoromethanesulfonyl)imide-based ionic liquid electrolyte, *Int. J. Electrochem. Sci.*, 2013, **8**, 2606-2624.

32. K. Hayamizu, Y. Aihara, H. Nakagawa, T. Nukuda and W. S. Price, Ionic conduction and ion diffusion in binary room-temperature ionic liquids composed of emim BF_4 and $LiBF_4$, *J. Phys. Chem. B*, 2004, **108**, 19527-19532.

33. F. S. Oliveira, A. B. Pereiro, J. M. M. Araújo, C. E. S. Bernardes, J. N. Canongia Lopes, S. Todorovic, G. Feio, P. L. Almeida, L. P. N. Rebelo and I. M. Marrucho, High ionicity ionic liquids (HIILs): Comparing the effect of -ethylsulfonate and -ethylsulfate anions, *Phys. Chem. Chem. Phys.*, 2013, **15**, 18138-18147.

34. M. Tariq, P. J. Carvalho, J. A. P. Coutinho, I. M. Marrucho, J. N. C. Lopes and L. P. N. Rebelo, Viscosity of (C_2-C_{14}) 1-alkyl-3-methylimidazolium bis(trifluoromethylsulfonyl)amide ionic liquids in an extended temperature range, *Fluid Phase Equilib.*, 2011, **301**, 22-32.

35. S. Tsuzuki, K. Hayamizu and S. Seki, Origin of the low-viscosity of emim $(FSO_2)_2N$ ionic liquid and its lithium salt mixture: Experimental and theoretical study of self-diffusion coefficients, conductivities, and intermolecular interactions, *J. Phys. Chem. B*, 2010, **114**, 16329-16336.

36. M. J. Monteiro, F. F. C. Bazito, L. J. A. Siqueira, M. C. C. Ribeiro and R. M. Torresi, Transport coefficients, Raman spectroscopy, and computer simulation of lithium salt solutions in an ionic liquid, *J. Phys. Chem. B*, 2008, **112**, 2102-2109.

37. M. Tariq, P. A. S. Forte, M. F. C. Gomes, J. N. C. Lopes and L. P. N. Rebelo, Densities and refractive indices of imidazolium- and phosphonium-based ionic liquids: Effect of temperature, alkyl chain length, and anion, *J. Chem. Thermodyn.*, 2009, **41**, 790-798.

38. M. G. Freire, A. R. R. Teles, M. A. A. Rocha, B. Schröder, C. M. S. S. Neves, P. J. Carvalho, D. V. Evtuguin, L. M. N. B. F. Santos and J. A. P. Coutinho, Thermophysical characterization of ionic liquids able to dissolve biomass, *J. Chem. Eng. Data*, 2011, **56**, 4813-4822.

39. C. Kolbeck, T. Cremer, K. R. J. Lovelock, N. Paape, P. S. Schulz, P. Wasserscheid, F. Maier and H. P. Steinrück, Influence of different anions on the surface composition of ionic liquids studied using ARXPS, *J. Phys. Chem. B*, 2009, **113**, 8682-8688.

40. Y. Gu and T. Yan, Thole model for ionic liquid polarizability, *J. Phys. Chem. A*, 2012, **117**, 219-227.

41. M. R. Moldover, in *Vol. VI: Measurement of the Thermodynamic Properties of Single Phases*, eds. A. R. H. Goodwin, K. N. Marsh and W. A. Wakeham, Elsevier, 2003, pp. 435–451.

42. C. M. S. S. Neves, K. A. Kurnia, J. A. P. Coutinho, I. M. Marrucho, J. N. C. Lopes, M. G. Freire and L. P. N. Rebelo, Systematic study of the thermophysical properties of imidazolium-based ionic liquids with cyano-functionalized anions, *J. Phys. Chem. B*, 2013, **117**, 10271-10283.

43. C. Schreiner, S. Zugmann, R. Hartl and H. J. Gores, Fractional walden rule for ionic liquids: Examples from recent measurements and a critique of the so-called ideal KCl line for the walden plot, *J. Chem. Eng. Data*, 2010, **55**, 1784-1788.

44. T. Yasuda, H. Kinoshita, M. S. Miran, S. Tsuzuki and M. Watanabe, Comparative study on physicochemical properties of protic ionic liquids based on allylammonium and propylammonium cations, *J. Chem. Eng. Data*, 2013, **58**, 2724-2732.

45. M. Yoshizawa, W. Xu and C. A. Angell, Ionic liquids by proton transfer: Vapor pressure, conductivity, and the relevance of Delta pK_a from aqueous solutions, *J. Am. Chem. Soc.*, 2003, **125**, 15411-15419.

Chapter 3

Part II: Interactions between the IL and the different ISs

Adapted from: **Filipe S. Oliveira**, Eurico J. Cabrita, Smilja Todorovic, Carlos E. S. Bernardes, José N. Canongia Lopes, Jennifer L. Hodgson, Douglas R. Macfarlane, Luís P. N. Rebelo and Isabel M. Marrucho, Mixtures of the 1-ethyl-3-methylimidazolium acetate ionic liquid with different inorganic salts: insights into their interactions, *manuscript in preparation*, 2015.

The author was involved in all the experiments, as well as on the discussion, interpretation and preparation of the manuscript, with the exception of the Molecular Dynamics section. The NMR studies and the *ab initio* calculations were performed in collaboration with Eurico J. Cabrita, and Jennifer L. Hodgson and Douglas R. Macfarlane, respectively. The Raman experiments were performed by Smilja Todorovic, while the Molecular Dynamics simulations were performed by Carlos E. S. Bernardes and José N. Canongia Lopes.

1. Abstract

In this work, we explore the interactions between the ionic liquid 1-ethyl-3-methylimidazolim acetate and different inorganic salts belonging to two cation families, those based on ammonium and others based on sodium. NMR and Raman spectroscopy are used to screen for changes in the molecular environment of the ions in the ionic liquid + inorganic salt mixtures as compared to pure ionic liquid. The ion self-diffusion coefficients are determined from NMR data, allowing the discussion of the ionicity values of the ionic liquid + inorganic salt mixtures calculated using different methods. Our data reveal that preferential interactions are established between the ionic liquid and ammonium-based salts, as opposed to sodium-based salts. Computational calculations show the formation of aggregates between the ionic liquid and the inorganic salt, which is consistent with the spectroscopic data, which indicate that the acetate anion of the ionic liquid establishes preferential interactions with the ammonium cation of the inorganic salts, leaving the imidazolium cation less engaged in the media.

2. Introduction

Ionic liquids (ILs) are low temperature melting salts which possess a wide range of unique properties, such as negligible vapour pressure, large liquid range, highly specific and tunable solvent ability, that are responsible for the increased interest in this class of compounds in last decades. Better known as "designer solvents", due to the multiple possible combinations between cations and anions that allow the tune of their thermophysical properties, ionic liquids offer high-potential solutions to a broad range of applications in many areas ranging from biology to chemistry, engineering and industry.[1, 2]

Although ILs are composed by discrete ions, these compounds form aggregates and clusters to some extent, as result of their complex nature that emerges from the interplay between their Coulombic, hydrogen-bonding and dispersive (van der Waals and π–π) interactions. Furthermore, studies have shown that ILs are nano-structured, i.e., composed

of micro-segregated polar and non-polar domains, where the polar domain is composed of the high charge-density parts of both the cations and anions, while the apolar domain is typically constituted by the alkane-type moieties of their organic ions.[3]

Lately, Molecular Dynamics (MD) and *ab initio* have become powerful tools for the understanding of thermophysical properties and phase equilibria, contributing with important insights in the proposal of structure-property relationships of ILs. Brüssel et al.[4, 5], used *ab initio* MD calculations to study the binary mixture of the ILs based on the 1-ethyl-3-methylimidazolium cation combined with thiocyanate and chloride anions. In their work, these authors showed that while in the neat ILs the main anion–cation interaction takes place through the most acidic proton of the imidazolium ring (H2), this observation does not hold for their mixture. In other works regarding mixtures of ILs and inorganic salts (ISs), Umebayashi et al.[6, 7] used Raman spectroscopy and *ab initio* calculations to study the solvation structure of the lithium ion (from lithium bis(trifluoromethylsulfonyl)amide salt, Li[NTf_2]) in three different ILs, two imidazolium-based (1-ethyl-3-methylimidazolium bis(trifluoromethylsulfonyl)amide and 1-butyl-3-methylimidazolium bis(trifluoromethylsulfonyl)amide) and one pyrrolidinium-based (*N*-butyl-*N*-methylpyrrolidinium bis(trifluoromethylsulfonyl)amide). The *ab initio* calculations showed that the lithium cation coordinated to the four oxygen atoms of the bidentate $[NTf_2]^-$ anion and that the IL cation played a key role in the stabilization of the complex formed by the lithium cation and the $[NTf_2]^-$ anions. Tsuzuki et al.[8] studied the transport properties of the 1-ethyl-3-methylimidazolium bis(fluorosulfonyl)amide IL and its lithium salt mixtures and used *ab initio* calculations to infer about the stabilization energies of the complexes formed between the different ions. The results obtained were then compared with those of the 1-ethyl-3-methylimidazolium bis(trifluoromethylsulfonyl)amide IL and also its lithium salt mixture. It was showed that the both the imidazolium and the lithium cations had weaker electrostatic and induction interactions with the bis(fluorosulfonyl)amide anion than with the bis(trifluoromethylsulfonyl)amide anion, corroborating the lower viscosity of the system containing the first anion.

NMR spectroscopy offers the ability to study the changes in the supramolecular IL's structure with solvation, enabling a closer look at the molecular interactions *in situ*. It was

already demonstrated that nuclear Overhauser effect (NOE) techniques can be used successfully with neat IL and IL mixtures to study solvation and preferential interactions.[9-12] The analysis of intermolecular NOEs in solution can reflect the mutual position of interacting species in terms of short range effects (d < 5Å) or, as proposed by Gabl et al.[13], be a consequence of long-range effects and interactions far beyond the first coordination shell. The combination of NOE data with MD simulations is therefore a powerful tool for the rationalization of the network of interactions occurring in ILs at the nano-level.

In our recent work,[14] we reported thermophysical properties of mixtures of 1-ethyl-3-methylimidazolium acetate IL with several ammonium/sodium-based ISs and determined their ionicity through the Walden plot approach. We observed different behaviours upon the addition of different ISs; for instance, when sodium-based ISs were added the ionicity of the system decreased, while with ammonium-based ISs the opposite behaviour was found. In addition, when [NH_4][SCN] was added to the IL, the mixtures showed distinct behaviours when comparing with the other ISs used. In this particular system, we observed that the conductivity increased and the viscosity was almost constant upon the addition of IS, leading to the highest ionicity of the IL-IS systems studied. As a follow up of this work, in the present study we explore the interactions that occur between the IL and IS in order to understand the increase in the ionicity caused by the addition of IS to the IL media. The IL used was the 1-ethyl-3-methylimidazolium acetate and the effect of the addition of six different ISs namely, ammonium acetate, ammonium chloride, ammonium thiocyanate, ammonium ethyl sulfonate, sodium acetate and sodium thiocyanate, was studied. Spectroscopic methods, NMR and Raman, were used for the screening of changes in the bulk IL as the IS concentration was increased, and MD and *ab initio* calculations complement and support the discussion of our spectroscopic findings. In addition, the ionicity calculated through different methods is finally discussed.

3. Experimental Section

3.1. Materials

The following six ISs were used in this work: ammonium acetate ([NH_4][Ac]), ammonium chloride ([NH_4]Cl), ammonium thiocyanate ([NH_4][SCN]), ammonium ethyl sulfonate ([NH_4][C_2SO_3]), sodium acetate (Na[Ac]) and sodium thiocyanate (Na[SCN]). Sodium acetate, ammonium acetate, chloride and thiocyanate were all provided by Sigma-Aldrich with a purity content superior to 99.0 %, 98.0 %, 99.5 % and 99.0 %, respectively. Sodium thiocyanate was provided by Fluka with a purity content superior to 98.0 %. Ammonium ethyl sulfonate was synthesized in the laboratory, the details are explained in our previous work.[14]

The ionic liquid 1-ethyl-3-methylimidazolium acetate ([C_2MIM][Ac]) was purchased from Iolitec with a mass fraction purity of ≥ 98 %. To reduce the water and other volatile substances contents, vacuum (10^{-1} Pa) and moderate temperature (no more than 318.15 K) were always applied to the ionic liquid for at least 2 days prior to their use. After drying, the ionic liquid purity was checked by ^{1}H NMR. Karl Fischer coulometric titration (Metrohm 831 KF Coulometer) was used to determine the final water mass fraction of the ionic liquid, which contained around 6000 ppm of water.

3.2. IL-IS mixtures

The binary mixtures of [C_2MIM][Ac] + IS were prepared in the range of 0 to 0.45 in IS molar fraction, taking into account the solubility limits of each IS, determined on our previous work.[15] The samples were prepared in an inert-atmosphere glove box, since the ionic liquid is moisture sensitive, using an analytical high-precision balance with an uncertainty of ± 10^{-5} g by weighing known masses of the each component into stoppered flasks. Good mixing was assured by magnetic stirring.

3.3. NMR spectroscopy

All NMR experiments were performed using a Bruker Avance III 400 operating at 400.15 MHz for protons, equipped with a 5 mm high-resolution BBFO probe and with a pulsed field gradient unit, capable of producing magnetic field pulsed gradients in the z-direction of 0.54 $T \cdot m^{-1}$. The samples were prepared by transferring approximately 2 mL of each IL-IS mixture to 5 mm NMR tubes. For the recording of all spectra, a capillary with deuterated dimethyl sulfoxide (DMSO-d_6) was inserted inside the tube for field-frequency lock and NMR internal reference. The structures and numbering of the IL and ISs are depicted in Figure 1.

Firstly, the changes in the ^1H chemical shifts of [C_2MIM][Ac] with increasing IS concentration, were analyzed. The ^1H spectra experiments were carried out at 298.15 K with 8 scans and 4 dummy scans. The ^1H NMR spectra of each one of the six IL-IS systems and their respective chemical shifts are depicted in Figures S1-S5 and in Table S1, respectively in the supporting information section (SI). Afterwards, NOESY data were acquired for the most concentrated samples of each system, in order to infer about the interaction of the IS with the IL. Yet, an initial screening of different mixing times was previously performed in order to assure the NOE effect was obtained. For the NOESY data obtained, a mixing time of 300 ms was selected and the spectra was obtained with 4 scans and 4 dummy scans at 298.15 K.

Lastly, the ion self-diffusion coefficients for the IL-IS systems were determined. The ^1H diffusion coefficients were measured using the pulsed gradient stimulated echo (PGSTE) pulse sequence at 323.15 K for viscosity purposes. Typically, in each experiment 32 spectra of 32 K data points were collected, with values for the duration of the magnetic field pulsed gradients (δ) of 6.0 ms, diffusion times (Δ) of 500 to 1000 ms, and an eddy current delay set to 5 ms. The gradient recovery time was 200 ms. The sine shaped pulsed gradient (*g*) was incremented from 5 to 95 % of the maximum gradient strength in a linear ramp. The ion self-diffusion coefficients for the cation and anions in the IL-IS systems were calculated using the integrals of the NMR signal and the Stejskal-Tanner equation. The standard relative deviation obtained for the ion- self-diffusion coefficients was of 0.37 % for the neat IL and

ranged between 0.58 % and 1.68 % for the mixtures.

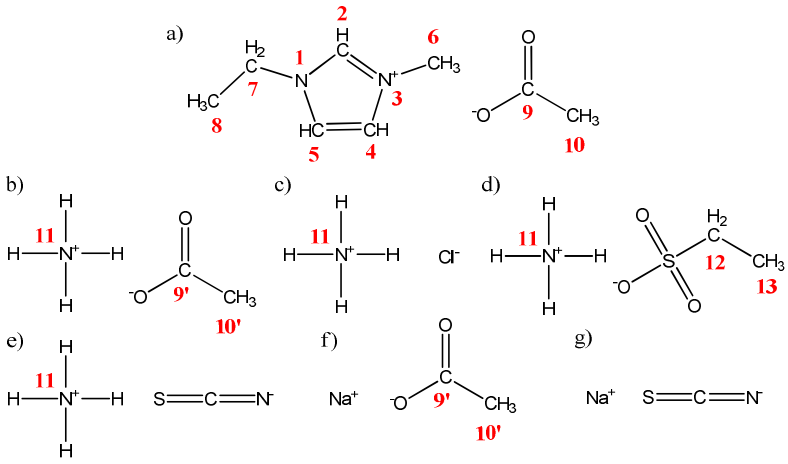

Figure 1 | Chemical structure and numbering of the ionic liquid and inorganic salts used in this work. a) 1-ethyl-3-methylimidazolium, b) ammonium acetate, c) ammonium chloride, d) ammonium ethyl sulfonate, e) ammonium thiocyanate, f) sodium acetate, g) sodium thiocyanate.

3.4. Raman spectroscopy

Raman spectra of all samples were measured with 1064 nm excitation (Nd-YAG cw laser) using an RFS 100/S (Bruker Optics, Ettlinger, Germany) Fourier-transform Raman spectrometer. Laser power was set to 400 mW and 100 scans were recorded for each sample at room-temperature.

3.5. Ab initio calculations

The geometries of the ion-pairs of the ISs $[NH_4][Ac]$, $[NH_4]Cl$, $[NH_4][SCN]$, $[NH_4][C_2SO_3]$, Na[SCN], and Na[Ac] were fully conformationally screened at the M06-2X/aug-cc-pVDZ level of theory. For the ionic liquid $[C_2MIM][Ac]$, the optimized geometry presented by Chen et al.[16] was used. The geometries of the 4 ion cluster structures (ionic liquid plus inorganic salt) were optimized at the same level of theory. The ethanol dielectric

constant was used in the optimization of all the structures (ion-pairs and clusters), in order to help mimic the IL media. Furthermore, the electronic energies were improved by calculation of the single point energies at a higher level of theory, the MP2/aug-cc-pVDZ, and also by adding the zero-point vibrational correction value, that was computed at the M06-2X/aug-cc-pVDZ level of theory. The obtained data for the IL, ISs and clusters as well as all the conformations screened, are depicted in Tables S3 and S4 and Figures S8-14 in the SI.

Table 1 presents the binding energy between the IL and IS molecules, Δ*E*, was calculated by the following expression: $\Delta E = E_{cluster} - (E_{IL} + E_{IS})$, where $E_{cluster}$, E_{IL} and E_{IS} are the sum of electronic energy and zero-point values of the cluster, the ionic liquid ion-pair and the inorganic salt ion-pair at their lower energy conformations, respectively.

For this study the GAUSSIAN 09 quantum chemical package[17] was used.

Table 1 | Binding energies for the IL-IS systems.

System	Δ*E* / KJ·mol^{-1}
[C_2MIM][Ac] + [NH_4][Ac]	-65.3054
[C_2MIM][Ac] + [NH_4]Cl	-72.5491
[C_2MIM][Ac] + [NH_4][SCN]	-84.1234
[C_2MIM][Ac] + [NH_4][C_2SO_3]	-79.5077
[C_2MIM][Ac] + Na[Ac]	-42.8886
[C_2MIM][Ac] + Na[SCN]	-49.2667

3.6. Molecular dynamics simulations

All molecular dynamic simulation where performed with DLPOLY 4.07.[18] The CL&P[19] and OPLS-AA force fields[20] were used to describe the [C_2MIM][Ac] ionic liquid, while a previously recommended parameterization[21] was used to model the $[NH_4]^+$ and $[SCN]^-$ ions. The MD runs were performed at 0.1MPa and 373.15 K, under the isotropic isothermal−isobaric ensemble (*N*-*p*-*T*). The temperature and pressure were controlled using Nosé−Hoover thermostats/barostats, with relaxation time constants of 1 and 4 ps, respectively. In all calculations a cutoff distance of 1.4 nm was applied, with the Ewald summation technique (*k*-values set to 16 and α = 0.27107 Å) used to account for

interactions beyond this limit. All simulation were prepared with the DLPGEN program,[22] by distributing the molecules in expanded boxes that were subsequently equilibrated to constant density. Besides the simulation of pure [C_2MIM][Ac], two mixtures of this IL with [NH_4][Ac] and [NH_4][SCN] at molar fractions 0.10 and 0.33 were investigated. All simulation boxes were composed by 900 ions (450 ion pairs). The production stages consisted of 10 ns runs, performed with a time step of 2 fs, where the simulation box configurations were recorded each 2 ps.

4. Results and discussion

4.1. Spectroscopic measurements

The changes on the chemical shifts of the IL + IS mixtures can be used in a quantitative way to evaluate the interactions occurring in the bulk system. Therefore, the ^{1}H NMR spectra of each one of the six IL + IS systems were acquired and the chemical shifts' deviations determined as depicted in Figure 2. Although the solubility range of the systems containing sodium-based ISs is smaller, it can be seen that the effect on the IL's chemical shifts in much less pronounced than for the ammonium-based IS. This finding shows that the interactions between the sodium-based ISs and the IL are weaker than those with ammonium-based ISs.

Moreover, in Figure 2a it can be observed that the protons H2, H4 and H5, belonging to the aromatic ring of the imidazolium, are the most affected by the presence of an IS. These three protons show strong negative deviations, meaning that they undergo an upfield shift, with the highest deviation for the H2 proton, the most acidic. The upfield shifts experienced by these aromatic protons indicate that their interactions become weaker as the IS concentration increases. Regarding the other two protons of the imidazolium cation, H6 and H7, they also present negative deviations, although the effect of the IS concentration is much less pronounced. On the other hand, protons H8 (from the terminal -CH_3 of the ethyl chain of the imidazolium cation) and H10 (from the acetate anion) present small positive deviations, i.e. downfield shifts, meaning that they establish stronger

interactions upon the addition of the IS to the IL medium.

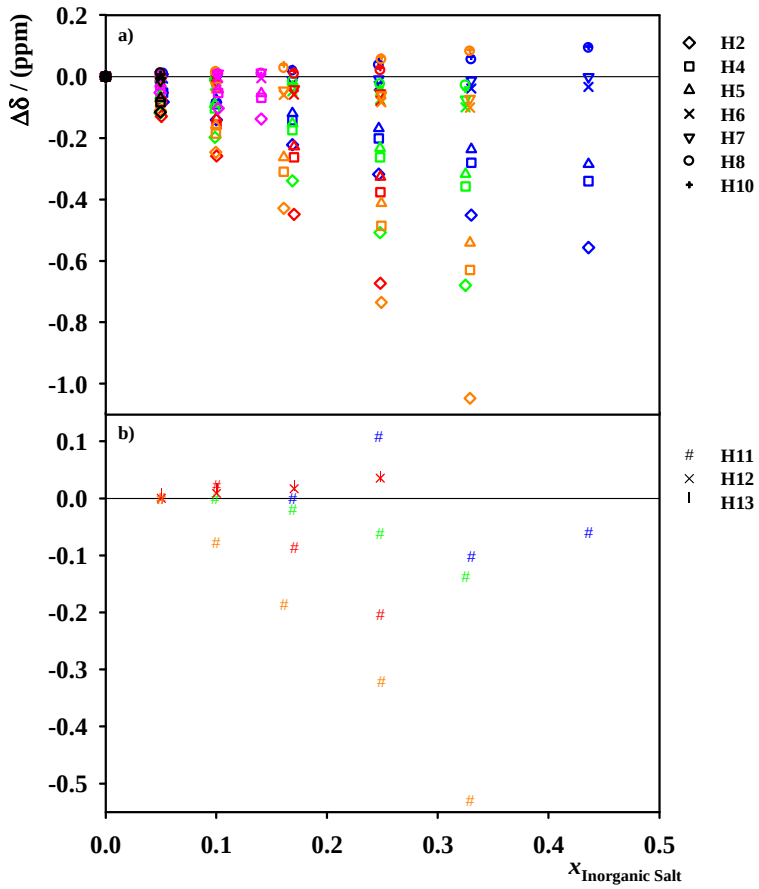

Figure 2 | ^{1}H NMR chemical shifts' deviations for the systems [C_2MIM][Ac] + IS determined at 298.15 K. Each symbol represents a different proton and each IS is represented by a different color: [NH_4][Ac] is blue, [NH_4]Cl is green, [NH_4][C_2SO_3] is red, [NH_4][SCN] is orange, Na[Ac] is pink, Na[SCN] is black. Panels a) and b) illustrate the chemical shift´s deviations in the IL and in the IS, respectively.

In general, all studied IL + IS systems with ammonium-based ISs show identical behaviour in terms of the up or downfield shifts of the protons. Nevertheless, few differences can be pointed out as the IS's anion is changed: i) for the chloride anion, protons H8 and H10 also display upfield shifts, which is in accordance with the large increase in the viscosity of the system;[14] ii) for the thiocyanate anion, the deviations on the chemical shifts of the protons are higher than those for any other anion, meaning that the [NH_4][SCN] is the

IS that affects most the IL bulk structure; iii) for the acetate anion, the deviations on the aromatic protons are smaller than for the other ammonium salts, as might be expected given that in this case there is no new anion present in the mixture.

In Figure 2b the same deviations trend observed for the IL protons can now be verified for the ISs. Regarding the protons of the $[NH_4]^+$ cation, they all present negative deviations, with $[NH_4][SCN]$ presenting the highest and $[NH_4][Ac]$ the lowest. The negative deviations of these protons were somewhat surprising, since we were expecting the ammonium cation to be engaged in interactions, especially with the IL anion. Nevertheless, these results could also mean that the ammonium cation is interacting less with its own counter-ion and thus getting looser in the network. In addition, the deviations of the protons of the ethane sulfonate anion (H12 and H13) are also depicted in Figure 2b, showing very small downfield shifts.

In addition, Raman spectroscopy was also employed to probe the molecular environment of the acetate (and thiocyanate) anions, by monitoring their frequencies (v) and bandwidths (Δv). Regarding the cations of the systems, it was not possible to extract any information due to the overlap of bands. For the cations of the systems, it was not possible to extract any information due to the overlap of bands. The shifts of the $(H_3)C\text{-}C(OO^-)$ stretching band of the acetate anion centered around 900 cm^{-1}, upon the addition of different amounts of IS, are shown in Figure 3. It can be seen that the addition of IS to the pure $[C_2MIM][Ac]$ causes the frequency upshift and band broadening. The upshifts indicate a stronger respective bond in the presence of IS, meaning that the acetate anion is becoming less engaged in the interaction with the imidazolium cation. At low concentrations of IS (x_{IS} = 0.10), both bandwidths and frequencies of the acetate band show minor alterations with respect to the neat IL in all IL + IS systems. As the concentration of IS increases (x_{IS} = 0.17), the $\nu_{C\text{-}COO}$ shifts of the systems with $[NH_4][Ac]$, $[NH_4]Cl$ and $[NH_4][C_2SO_3]$ are still comparable (when the intensity is normalized, the bands fully overlap), whereas in the system containing $[NH_4][SCN]$, the band is further broadened and upshifted. At the highest concentration of IS (x_{IS} = 0.33), the $\nu_{C\text{-}COO}$ band further upshifts and broadins. It can be seen that in the systems containing $[NH_4]Cl$ ($v_{C\text{-}COO}$ = 907 cm^{-1}, Δv = 31 cm^{-1}) and $[NH_4][Ac]$ ($v_{C\text{-}COO}$ = 904 cm^{-1}, Δv = 26 cm^{-1}) the bandwidths are much larger than in the neat IL ($v_{C\text{-}COO}$ =

900 cm^{-1}, $\Delta\nu$ = 16 cm^{-1}), suggesting a much more heterogeneous molecular environments of acetate anions. In the system containing $[NH_4][SCN]$ ($\nu_{C\text{-}COO}$ = 914 cm^{-1}, $\Delta\nu$ = 19 cm^{-1}), although the bandwidth is not as large as in the other cases, the upshift in the frequency indicates that $[NH_4][SCN]$ is the IS that affects the most the acetate anions in the system. Furthermore, for the system containing $[NH_4][SCN]$, the molecular environment of thiocyanate was also monitored via the S≡CN stretching mode at 2056 cm^{-1} (data not shown). However, no additional bands, band shifts or broadening were observed in the Raman spectra with the increase in the IS concentration, indicating uniform $[SCN]^-$ environment as previously reported for 1-ethyl-3-methylimidazolium ethyl sulfonate ($[C_2MIM][C_2SO_3]$) + $[NH_4][SCN]$.[23]

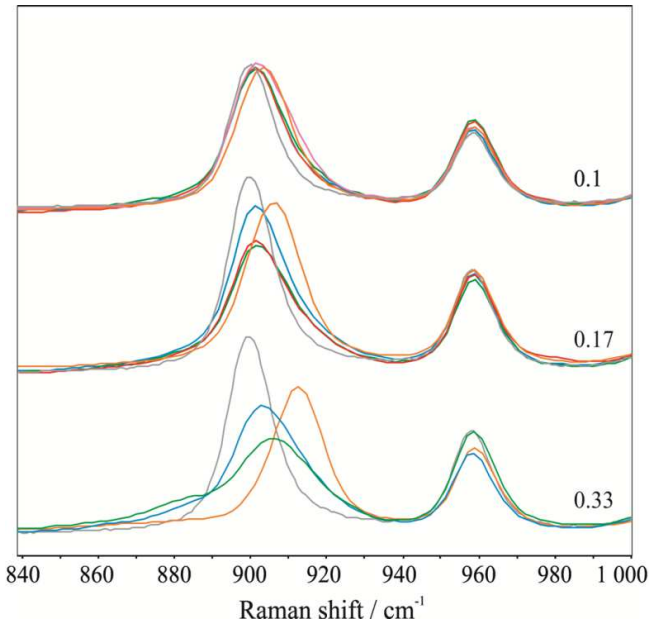

Figure 3 | Raman spectra of $[C_2MIM][Ac]$ + IS systems, acetate C-COO^- stretching regions. Each system is represented by a different colour: neat $[C_2MIM][Ac]$ is grey; $[NH_4][Ac]$ is blue, $[NH_4]Cl$ is green, $[NH_4][C_2SO_3]$ is red, $[NH_4][SCN]$ is orange and Na[Ac] is pink. The spectra were measured with 1064 mm excitation at 298.15 K.

In Figure 4, the mean orientations of the interacting ions are drawn from NOESY data from the evaluation of the relative strength of the cross peaks found between the four ions in the IL + IS cluster. The NOESY spectra could only obtained for the ammonium-based ISs

because the sodium-based ISs do not present protons in their ions (with the exception of acetate). The relative distance between ions was established using the areas of the cross peaks in the 2D NMR spectra. For all the studied IL + IS systems, the cross peak that showed the highest area and that was associated with the highest proximity between protons belonging to two different ions, was the one corresponding to the cross-relaxation between the protons from the terminal methyl group of the imidazolium (H6) and those in the acetate (H10). The area of this peak was set as reference point, and the areas of all the other peaks were divided by the area of the reference in order to obtain a relative scale of the NOE between the ions in the system.

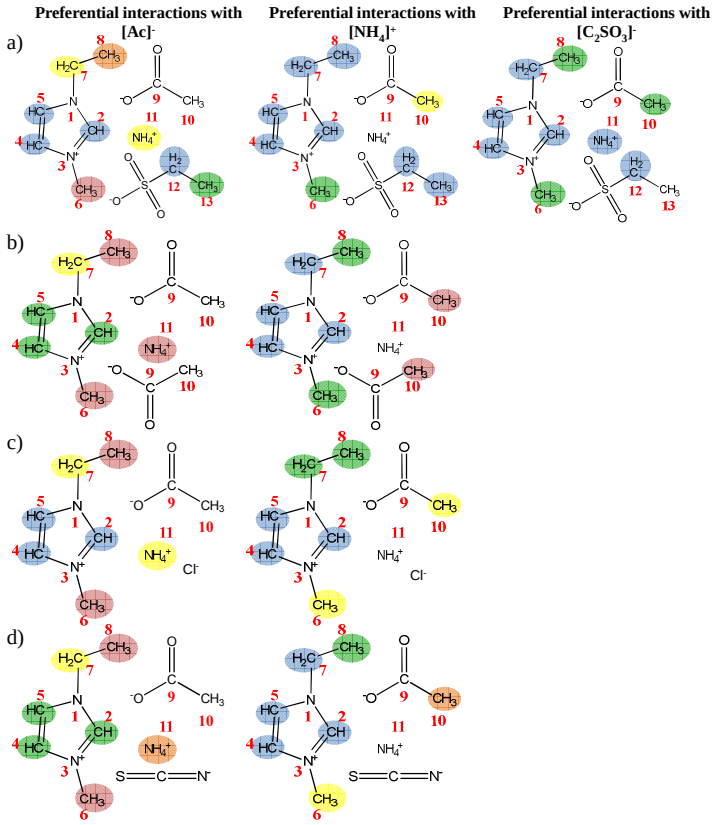

Figure 4 | Preferential interactions between the IL and IS ions for the systems [C_2MIM][Ac] + ammonium-based ISs as derived from NOESY spectra. a) [NH_4][C_2SO_3], b) [NH_4][Ac], c) [NH_4]Cl and d) [NH_4][SCN] determined at 298.15 K. The different colours represent the level of relative NOE: very low (0−0.20), low (0.21−0.40), medium (0.41−0.60), high (0.61−0.80) and very high (0.81−1).

As depicted in Figure 4, NOESY data suggest that in all systems the acetate anion detaches itself from the imidazolium cation. This is demonstrated by the low intensity of cross peaks between the acetate anion and the aromatic protons of the imidazolium cation, which is further corroborated by the large downfield shifts recorded in the imidazolium cation, presented in Figure 2a. These results are a direct consequence of the addition of IS to the IL, since it is recognized that in the neat [C_2MIM][Ac] the acetate anions establish in-plane interactions with the three imidazolium ring protons.[24] As the structure of ILs and ISs are both dominated by the Coulombic forces, it is expected that the introduction of ISs into the IL media will alter the whole set of interactions that are present, either by the disruption of interactions of the ion-pairs (IL-IL and IS-IS) and/or the establishment of new interactions (IL-IS).

Considering the ammonium cation of the ISs, it can be seen that in all systems there are stronger contacts between this cation and the acetate anion than with any other ion in the mixture. In the case of the [NH_4][Ac] IS, these results were expected since it is not possible to distinguish between the acetate anions from the IL and those belonging to the IS, and hence the high level of contact between the ammonium cation and the acetate anion was anticipated. Regarding the [NH_4][SCN] IS, where the second highest level of contacts was found, the results also support the idea of the establishment of a strong interaction between the $[Ac]^-$ of the IL and the $[NH_4]^+$ of the IS, that allow the other two ions to become more "free". This higher level of interaction of the $[Ac]^-$ anion with the $[NH_4]^+$ cation is consistent with the high downfield shifts of the aromatic protons obtained for this system and depicted in Figure 2a, showing that the imidazolium is interacting less with its own counter-ion (the acetate anion is less engaged, as seen in Figure 3) as the ammonium content in the mixture increases. For the other two ISs ([NH_4]Cl and [NH_4][C_2SO_3]), similar behaviour to that observed for the [NH_4][SCN] is found, with the low cross peak intensity between the IL's anion and the IS's cation being also consistent with their lower negative deviations in the aromatic protons shown in Figure 2a and the upshifted $\nu_{C\text{-}COO}$ frequencies (Figure 3). In addition, for [NH_4][C_2SO_3] it was also possible to obtain the proximity levels to the IS anion. In this case, $[C_2SO_3]^-$ anion becomes closer to the IL's ions than to its own counter-ion (the ammonium). Nevertheless these proximity levels are very low, which probably explain the

small, yet positive, chemical shift deviations.

The trends obtained from the deviations of the chemical shifts along with the relative contacts determined from the NOESYs are in agreement with the binding energies between the IL and IS molecules obtained from the *ab initio* calculations presented in Table 1. Here we can see that the formation of the four ion cluster is favoured in the case of the ammonium-based ISs compared to the sodium-based ISs, which is consistent with the large deviations observed in the chemical shifts of the former. It seems that for the latter, the ions of the IS prefer to remain associated instead of interacting with the ions of the IL.

Considering the values of the binding energy (ΔE) for the four ion cluster, it can be observed that the system containing the $[NH_4][SCN]$ is the one where the formation of the cluster is preferred, which is in agreement with the higher deviations of the chemical shifts obtained. In addition, if excluding the common ion system, we can also see in Figure 4 that the intensity of the relative NOE between $[NH_4]^+$ and the $[Ac]^-$ in the $[NH_4][SCN]$ containing system, is higher than for the systems with $[NH_4]Cl$ and $[NH_4][C_2SO_3]$, which present similar values in terms of their ΔE, chemical shift deviations and levels of proximity between the ions in the system. Regarding the system containing $[NH_4][Ac]$, due to the effect of the common ion, the chemical environment does not change as much as in the case of the other ammonium-based ISs, hence the ΔE and chemical shift deviations are lower.

In Figure 5, the ^1H NMR self-diffusion coefficients (D) for the individual ions of the IL + IS systems are depicted. These results are also presented in Table S2 in the ESI. Unfortunately, due to the lack of protons in some ions of the ISs (Cl^-, $[SCN]^-$ and Na^+), it was not possible to determine the ion self-diffusion coefficients of all species. Moreover, for some concentrations, the $[NH_4]^+$ cation peak overlapped with the H4 and H5 peaks of the imidazolium ring, making impossible the determination of $D_{[NH4]^+}$. Nevertheless, some general trends can be established from these experiments upon the addition of IS to the IL media.

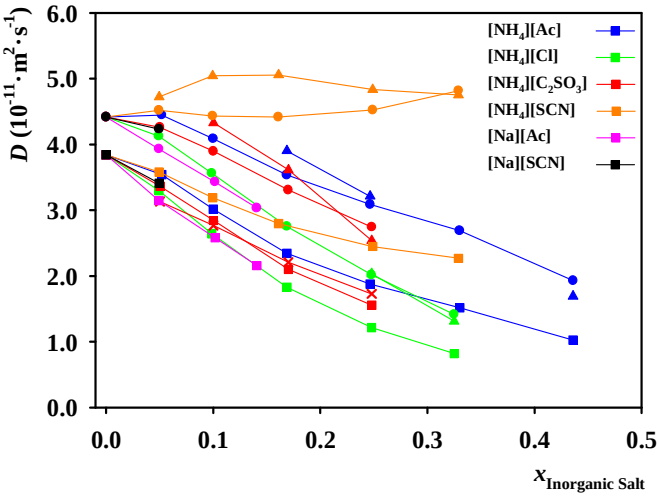

Figure 5 | ^{1}H NMR self-diffusion coefficients of the ions $[C_2MIM]^+$ (●), $[Ac]^-$ (■), $[NH_4]^+$ (▲) and $[C_2SO_3]^-$ (×) in the $[C_2MIM][Ac]$ + IS systems determined at 323.15 K.

First it can be seen that $[NH_4]^+$ has slightly higher diffusivity than $D_{[C2MIM]^+}$, except for the most concentrated mixtures. With the increase in the amount of IS in the mixture, the $D_{[NH4]^+}$ starts to decrease to the point it becomes lower than $D_{[C2MIM]^+}$. This behaviour can be correlated with the approximation between $[NH_4]^+$ and $[Ac]^-$ and the establishment of aggregates between the two (*vide infra*). Since $[NH_4]^+$ is a smaller and more mobile molecule than $[C_2MIM]^+$ or $[Ac]^-$ it would be expected to have a higher D, however with the increase in amount of IS, the formation of aggregates involving $[NH_4]^+$ increases, making the $[NH_4]^+$ less mobile than $[C_2MIM]^+$.

Regarding the IL's diffusion coefficients, Figure 5 shows that the D of the cation (D_{IL}^+) is always higher than of the anion (D_{IL}^-), either in the neat IL or in the mixtures. Previous studies on the diffusion of $[C_2MIM][Ac]$ [24, 25] also showed that the smaller acetate anion diffuses more slowly than the larger imidazolium cation. The results obtained in this work are comparable to those in literature, showing relative standard deviations of 1.6 % and 0.7 % for the D_{IL}^+ and of 0.8 % and 4.4 % for the D_{IL}^- regarding the data presented by Remsing et al.[25] and Bowron et al.[24], respectively.

Other general trend that can be withdrawn from the diffusion measurements is that,

with the exception of the system containing [NH_4][SCN], both the D_{IL}^+ and D_{IL}^- decrease with the IS concentration. Literature shows that this behaviour is common to other IL-IS systems, namely those involving bis(trifluoromethylsulfonyl)amide-based (NTf_2) or bis(fluorosulfonyl)amide-based (FSA) ILs + [Li][NTf_2] or [Li][FSA] respectively,[8, 26-29] systems of *N*,*N*-diethyl-*N*-methyl-*N*-(2-methoxyethyl)ammonium (DEME) based ILs with lithium ISs, [DEME][BF_4] + Li[BF_4] and [DEME][CF_3BF_3] or [NTf_2] + Li[NTf_2],[30] and also the system of [C_2MIM][BF_4] + Li[BF_4] [31] where the addition of IS leads to the decrease of both D_{IL}^+ and D_{IL}^-.

In this study, the decrease observed in both D_{IL}^+ and D_{IL}^- follows the trend Na[Ac] > [NH_4]Cl > Na[SCN] > [NH_4][C_2SO_3] > [NH_4][Ac] > [NH_4][SCN], where the next to the last one is the IS where a smallest decrease in the D_{IL} was obtained; for [NH_4][SCN] the D_{IL}^- decreases and the D_{IL}^+ increases upon the addition of IS. This decrease in ion mobility with the IS concentration is in agreement with our previous studies of the ionic conductivities of these systems,[14] where an increase in the concentration of the IS led to the decrease of the ionic conductivity (with the exception of [NH_4][SCN] where the conductivity increased with the addition of IS). Interestingly, both of these trends (diffusion and ionic conductivity) do not follow the behaviour of the viscosity,[14] where the systems containing the ISs [NH_4][C_2SO_3] and [NH_4]Cl present the highest increase in viscosity, which should result in lower *D* for these systems, according to the Stokes-Einstein equation, equation 1, where it is assumed that the diffusing species are rigid spheres in a continuum of a solvent.[32]

$$D = \frac{k_B T}{c \pi \eta r} \quad (1)$$

where k_B is the Boltzmann constant, T is the temperature, η is the viscosity, r is the Stokes radius and c is a constant dependent on the strength of the interactions between the diffusing species and the medium, that usually ranges between 4 and 6 for slip and stick boundary conditions, respectively. Nevertheless, several studies on ILs have shown that the c value for these fluids could be lower than 4.[28, 30, 33]

In order to further explore this divergence, the diffusion data obtained in this work was correlated with the viscosity data of our previous study.[14] Figure S6 in the SI, plots the *D* for

each ion in the system versus the $k_B T/\pi\eta_{mix}$, where linear relationships ($r^2 \geq 0.99$) were only obtained for the $[Ac]^-$ anion (in all system) and for the $[C_2MIM]^+$ cation in the system containing Na[Ac]. However, in the $[C_2MIM][Ac]$ + ammonium-based ISs systems, no linearity was obtained, with special mention to the case of $[NH_4][SCN]$ since in this system the D_{IL}^+ increases with the increase in viscosity and the D_{IS}^+ does not decrease in a linear way. These findings are different from the results reported by Hayamizu et al.[26], who obtained linear plots for all ions in the studied IL-IS mixtures, thus allowing the use of the SE equation to obtain physical insights between the diffusional motion of the species and the viscosity. In the present work, the application of the SE equation is not valid. In fact, the validity of the SE equation for neat ILs is being debated by other authors.[34, 35]

Concerning the ion self-diffusion coefficients of the IS, the same behaviour of the IL was found where the increase in the IS concentration also lead to the decrease of both D_{IS}^+ and D_{IS}^-, again with the exception of $[NH_4][SCN]$. This trend is better illustrated in Figure S7 in the SI, where the ratio between the self-diffusion coefficients of each ion and the D_{IL}^+ is plotted against the molar fraction of IS. In this plot, it can be observed that in all systems containing ammonium-based ISs, for small concentration of IS, the $D_{[NH4]}^+$ is consistently higher than $D_{[C2MIM]}^+$ and as the concentration of IS increases the $D_{[NH4]}^+$ decreases to the point it becomes smaller than $D_{[C2MIM]}^+$.

For the system with the IS $[NH_4][C_2SO_3]$, it was possible to determine the D_{IS}^- which has the opposite behaviour of $D_{[NH4]}^+$ − at lower IS concentrations the $D_{[C2SO3]}^-$ is smaller than $D_{[Ac]}^-$ and as the concentration of IS increases $D_{[C2SO3]}^-$ becomes higher than $D_{[Ac]}^-$. Moreover, it can also be seen that the addition of IS always affects more the D_{IL}^- than the D_{IL}^+ (D_{IL}^- / D_{IL}^+ always < 1).

4.2. Molecular dynamic simulations

To gain further insight into the structure of $[C_2MIM][Ac]$ + ISs mixtures, several molecular dynamic simulations were performed, namely IL mixtures with $[NH_4][Ac]$ and $[NH_4][SCN]$. The selection of these two ISs is related with the irregular behaviour observed

in the physical properties of IL + $[NH_4][SCN]$ mixtures relative to the other salts, that were presented above, while $[NH_4][Ac]$ was chosen to represent the most common trends observed when ISs are added to the IL.

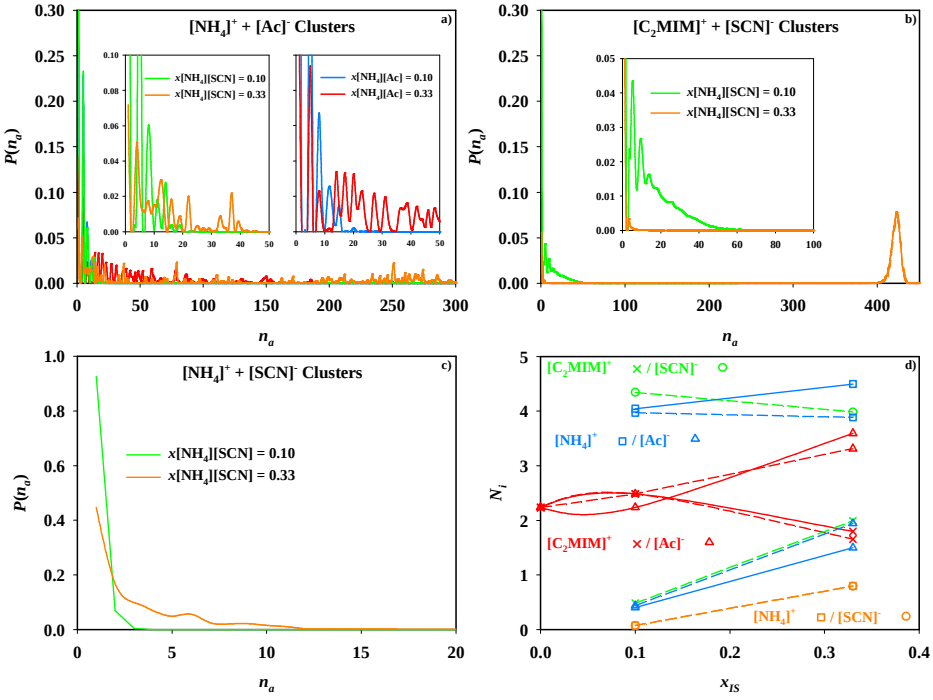

Figure 6 | Probability, $P(n_a)$, of finding an aggregate of size n_a, for mixtures with different molar fraction of $[NH_4][Ac]$ and $[NH_4][SCN]$ with $[C_2MIM][Ac]$, at 373.15 K. Each graphic represents the aggregates formed between a) $[NH_4]^+$ and $[Ac]^-$, b) $[C_2MIM]^+$ and $[SCN]^-$ and c) $[NH_4]^+$ and $[SCN]^-$. d) Average number of counter-ions, N_i, of (×) $[C_2MIM]^+$, (△) $[Ac]^-$, (○) $[SCN]^-$ and (□) $[NH_4]^+$ in different IL + ISs concentrations. The colour of each series denotes the interactions between $[C_2MIM]^+$ and $[Ac]^-$ (red), $[C_2MIM]^+$ and $[SCN]^-$ (green), $[NH_4]^+$ and $[Ac]^-$ (blue) and $[NH_4]^+$ and $[SCN]^-$ (orange). The solid and dashed lines correspond to mixtures with $[NH_4][Ac]$ and $[NH_4][SCN]$, respectively. In order to visualize all data points, a small offset along the *x* axis was applied. Thus all data correspond to IS molar fractions of 0, 0.10 or 0.33.

Figure 6 shows the probability, $P(n_a)$, of finding an aggregate of size n_a, computed from the MD simulation results with the methodology previously described.[36, 37] In Figure 6a it is observed that the size variation of the aggregates formed by $[NH_4]^+$ and $[Ac]^-$ does not change monotonically. Instead, several probability maxima are found for aggregates with a

particular size. This occurs because the ammonium cations tend to be surrounded by ~4 [Ac] anions (Figure 6d), while acetate, on average, are in contact with less than one $[NH_4]^+$ cation (considering the data for x_{IS} = 0.1). This suggests the formation of isolated clusters composed by ~5 ions, as illustrated in Figure 7. Thus, any time an anion produces a bridge between two $[NH_4]^+$ cations, the size of the aggregate changes in accordance to the number of acetate ions connected to the two cations, given rise to a high probability of finding aggregates with a specific size. This observation is in good agreement with the spectroscopic findings reported above, that preferential interaction exists between the ammonium and acetate ions. This interaction is sustained by the formation of hydrogen bonds (H-bonds), that according to Jeffrey's hydrogen bond distance criteria,[38] are relatively strong (strong and moderate H-bonds exhibit when H···O distances vary in the range 2.2 − 2.5 Å and 2.5 − 3.2 Å, respectively; see distances in Figure 7).

The analyses of Figures 6b and 6c shows a strong interaction between $[C_2MIM]^+$ and $[SCN]^-$ (these two ions are able to produce long polar networks, with the thiocyanate and imidazolium ions surrounded by ~4 and ~2 counterions, respectively; Figure 6d) and an almost absence of contact between the IS ions (with an average number of neighbours for each ion bellow 0.6, Figure 6d). This suggest a strong interaction between the IS ions and the IL polar network. Figure 6a also reveals that the aggregates formed between $[NH_4]^+$ and $[Ac]^-$ ions when $[NH_4][SCN]$ is added to the ionic liquid tend to be larger than in the case of $[NH_4][Ac]$. This observation suggest a bigger interaction between the former IS and the IL bulk structure, in accordance to the higher chemical shifts discussed above, observed when $[NH_4][SCN]$ is mixed with $[C_2MIM][Ac]$.

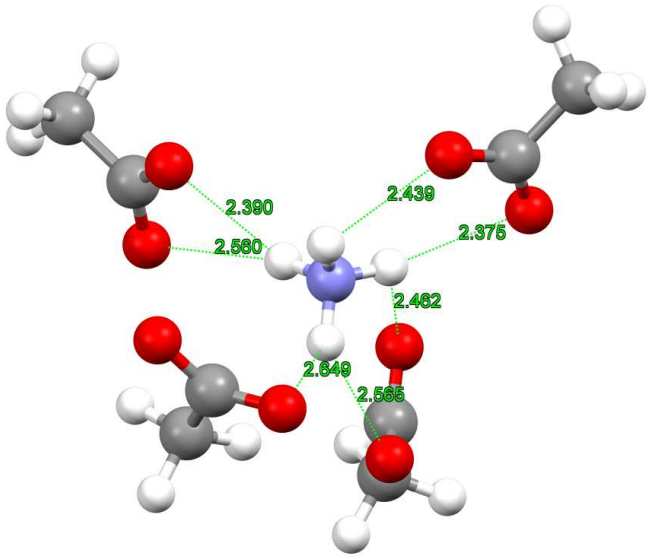

Figure 7 | Snapshot of an aggregate of $[NH_4]^+$ cation surrounded by acetate ions, found in a mixture of $[C_2MIM][Ac]$ with $[NH_4][SCN]$ at x_{IS} = 0.10 and T = 373.15 K.

4.3. Ionicity

The ionicity of ILs has been interpreted as a ratio between the effective concentration of charged species and the total concentration of the IL, measuring the dissociativity or degree of correlative motion of ions.[39, 40] There are two main methods to estimate the ionicity of ILs. The first is based on the Walden Plot approach, where plots made of the logarithm of the molar conductivity against the logarithm of the fluidity are drawn. In these plots, the ideal Walden line is given by a straight line with a unitary slope, drawn with data of an aqueous solution of KCl, which is usually taken to be representative of the ideal electrolyte, where the ions are known to be fully dissociated. The quantitative determination of the ionicity of the IL is given by the distance of the IL's data to the ideal Walden line. However, this method has been criticized due to the use of KCl solutions of arbitrary compositions as a reference, since Schreiner et al.[41] observed that the slopes of Walden plots for KCl solutions do not represent the unity. In addition, the use of the Walden plot as a quantitative method for the ionicity has also been questioned in the case of a weak electrolyte, where the degree of

dissociation is determined by the pK_a, which is a thermodynamic quantity.[42] Nevertheless, from a qualitative point the deviation from the ideal Walden line (ΔW) is still a versatile tool to access the ionicity of ILs.

In our recent study,[14] we used the ΔW to determine of the ionicity of the same IL + IS systems studied in this work and compared them to the ionicity calculated by other method proposed by Ueno et al.[43], also based on the Walden plot approach. In this last method the ionicity is defined as the ratio between the molar conductivity, calculated from the ionic conductivity measured by the electrochemical impedance method (Λ_{imp}), and the ideal molar conductivity (Λ_{ideal}), which is assumed to be equal to the fluidity (in Poise^{-1}) taken from the ideal Walden line. The results proved to be consistent from a qualitative point of view since they both produced the same conclusions − the addition of ammonium-based ISs increased the ionicity of the [C_2MIM][Ac] IL, while the sodium-based ISs decreased it.

The second and most consensual method used for the quantitative determination of the ionicity uses the ratio between the Λ_{imp}, that accounts for the migration of charged species in an electric field, and the molar conductivity calculated from the ion self-diffusion coefficients (Λ_{NMR}), that accounts for the migration of all species in the media (charged and neutral, ions and aggregates).[39] The value of Λ_{NMR} is determined by the Nernst-Einstein (NE) equation as follows:

$$\Lambda_{NMR} = \frac{F^2}{R \cdot T}\left(D^+ + D^-\right) \tag{2}$$

where R and F are the gas and Faraday constants, respectively, T is the temperature and $D^{+/-}$ are the ion self-diffusion coefficients of the IL obtained from the NMR. However, in a IL-IS binary systems, the mole fractions (x) of the IL and the IS have to be accounted for, as follows:

$$\Lambda_{NMR} = \frac{F^2}{R \cdot T}\left(x_{IL}D_{IL}^+ + x_{IL}D_{IL}^- + x_{IS}D_{IS}^+ + x_{IS}D_{IS}^-\right) \tag{3}$$

Since in the determination of the diffusion by NMR, *D* accounts for all species in solution, both free and associated forms, the value of Λ_{NMR} is always overestimated.[26] Thus, the ratio Λ_{imp} / Λ_{NMR} will always be smaller than the unity.[39] In this study, the determination of the *D* of all ions was only possible in the systems with the ISs $[NH_4][Ac]$ and $[NH_4][C_2SO_3]$, hence the calculation of the ionicity through the Λ_{imp} / Λ_{NMR} ratio was only accomplished for two IL-IS systems.

Figure 8 represents a comparison between the ionicity calculated using two different methods, the Λ_{imp} / Λ_{ideal} ratio and the Λ_{imp} / Λ_{NMR} ratio. The results obtained demonstrate opposite trends, showing that the addition of the IS to the IL makes the determination of these system's ionicity a challenge. It can be seen that the ionicities calculated trough the Λ_{imp} / Λ_{ideal} ratio increasing upon the addition of IS to the IL, while the ionicities calculated trough the Λ_{imp} / Λ_{NMR} ratio decrease and always presents values lower than the neat IL. However, the possible overestimation in the *D* can affect the determination of the ionicity since an increase in the Λ_{NMR} leads to a lower value of Λ_{imp} / Λ_{NMR} and thus not only the ionicity of the IL-IS mixture becomes lower than the neat IL, as also the difference between the determination of the ionicity by the two methods increases. Nevertheless, for the neat IL, $[C_2MIM][Ac]$, the rough consistency between the two methods is confirmed

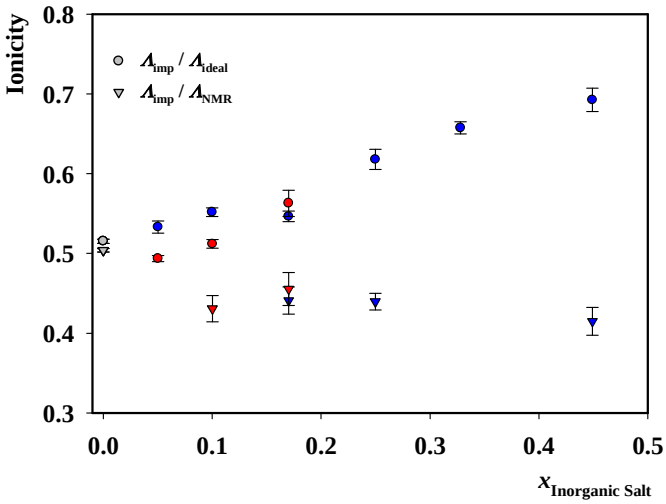

Figure 8 | Comparison between the Ionicity calculated using the Walden Plot approach[14] and using the ^1H

NMR self-diffusion coefficients, for the systems [C_2MIM][Ac] + [NH_4][Ac] (blue symbols) and [C_2MIM][Ac] + [NH_4][C_2SO_3] (red symbols) determined at 323.15 K.

The comparison between these two methods had already been made for neat aprotic ILs,[43, 44] protic ILs[45] and glyme-Li salt equimolar mixtures[43] and a rough consistency was observed. In addition, other studies on the ionicity of neat ILs[30, 33, 39] and aqueous solutions of ILs,[46] where Walden plots are drawn and the ionicity calculated from the Λ_{imp} / Λ_{NMR} ratio, have also corroborated the consistency of the results obtained from both methods. However, in another study concerning IL-IS systems, Hayamizu et al.[26] doped ILs *N*-methyl-*N*-propyl-pyrrolidinium (P_{13}) [NTf_2] and [FSA] with a fixed concentration of Li[NTf_2] and [FSA], respectively, and obtained different trends for the ionicity when the two methods described above are used. Using the Walden plot, the authors verified that the trend in the ΔW was [P_{13}][NTf_2] > [P_{13}][NTf_2] + Li[NTf_2] > [P_{13}][FSA] + Li[FSA] > [P_{13}][FSA], with the latter neat IL displaying the highest ionicity, whereas when the ionicity was calculated by the Λ_{imp} / Λ_{NMR} ratio, both IL-IS mixtures yielded higher ionicities than the neat ILs according to the following trend: [P_{13}][FSA] + Li[FSA] > [P_{13}][NTf_2] + Li[NTf_2] > [P_{13}][FSA] > [P_{13}][NTf_2]. In this study the authors do not explore any further these results. However, these different trends clearly indicate that the determination of the ionicity in IL-IS mixtures is not as simple as in neat ILs and additional studies are needed.

In addition, Holloczki et al.[47] recently showed that the charge transfer between the ions in neat ILs can also affect the determination of the ionicity, since the neutralization of the mobile species in the media occurs not only due to the formation of ion pairs but also as a result of the charge transfer. Indeed, their data suggested that both phenomena are significant factors that could explain the lower than expected conductivities (Λ_{NMR}). Moreover, these authors also performed MD simulations on a mixture of [Na][Cl] in the IL [C_4MIM][Br], and showed that by increasing the charge on the ions both the IS and the IL interactions become stronger and the association of the ion pair is favoured, while a decrease of the charge leads to the IL to behave more like a molecular liquid than a salt, showing higher fluidity.

5. Conclusions

In this work we present insights into the interactions between mixtures of the IL $[C_2MIM][Ac]$ with several ammonium and sodium-based ISs. Our studies reveal that the ammonium based ISs can establish more interactions with the IL than the sodium-based, which was verified by the higher deviations of the ^1H NMR chemical shifts and corroborated by the *ab initio* calculations. We found that these interactions were in part a result of the approximation of the IS's cation, the ammonium, to the IL's anion, the acetate, that lead to the establishment of aggregates and to a more detached imidazolium cation. These effects were more pronounced in the case were the IS was the $[NH_4][SCN]$.

The ion self-diffusion coefficients show that the introduction of IS had a deep effect on the diffusion of the IL's ions, specifically in the case of the imidazolium cation. Moreover, for the systems with $[NH_4][Ac]$ and $[NH_4][EtSO_3]$ ISs, the ionicity was calculated through the Λ_{imp} / Λ_{NMR} ratio and compared with the ionicity determined through the Walden plot approach. The two methods show divergent behaviours meaning that the interplay between the interactions of IL and IS is much more complex than in the case of neat ILs or molten salts.

6. Acknowledgements

Filipe S. Oliveira gratefully acknowledges the financial support of FCT/MCTES (Portugal) through the Ph.D. fellowship SFRH/BD/73761/2010 and Isabel M. Marrucho for a contract under FCT Investigator 2012 Program. The authors also acknowledge the Fundação para a Ciência e Tecnologia (FCT) for the financial support through the research units GREEN-it "Bioresources for Sustainability" (UID/Multi/04551/2013) and UCIBIO (UID/Multi/04378/2013). The NMR spectrometers are part of The National NMR Facility, supported by Fundação para a Ciência e a Tecnologia (RECI/BBB-BQB/0230/2012). Douglas R. MacFarlane is grateful to the Australian Research Council for funding of his Australian Laureate Fellowship.

7. Supplementary Information

7.1. NMR studies

Table S1 | ^{1}H NMR chemical shifts for the [C_2MIM][Ac]+ IS systems at 298.15 K.

Position	x[NH_4][Ac]						
	0	0.0520	0.1000	0.1688	0.2466	0.3302	0.4346
2	10.214	10.131	10.073	9.991	9.895	9.762	9.657
4	8.114	8.062	8.024	7.972	7.913	7.833	7.774
5	7.939	7.894	7.863	7.819	7.770	7.702	7.653
6	3.627	3.619	3.610	3.600	3.597	3.587	3.593
7	3.902	3.901	3.896	3.891	3.893	3.889	3.900
8	0.891	0.900	0.903	0.909	0.928	0.946	0.984
10/10'	1.128	1.143	1.147	1.155	1.176	1.193	1.225
11	-	-	-	8.140	8.248	8.039	8.080
Position	x[NH_4]Cl						
	0	0.0492	0.0988	0.1688	0.2479	0.3250	-
2	10.214	10.094	10.016	9.874	9.705	9.534	-
4	8.114	8.044	8.011	7.940	7.851	7.757	-
5	7.939	7.876	7.848	7.786	7.706	7.621	-
6	3.627	3.598	3.597	3.578	3.552	3.526	-
7	3.902	3.879	3.882	3.868	3.847	3.827	-
8	0.891	0.873	0.880	0.875	0.866	0.862	-
10	1.128	1.110	1.115	1.106	1.092	1.086	-
11	-	-	8.209	8.190	8.147	8.072	-
Position	x[NH_4][SCN]						
	0	0.0494	0.0995	0.1610	0.2490	0.3298	-
2	10.214	10.103	9.967	9.784	9.478	9.166	-
4	8.114	8.028	7.928	7.804	7.628	7.484	-
5	7.939	7.866	7.781	7.676	7.526	7.398	-
6	3.627	3.611	3.588	3.567	3.543	3.526	-
7	3.902	3.891	3.872	3.857	3.841	3.830	-
8	0.891	0.902	0.906	0.919	0.946	0.973	-
10	1.128	1.144	1.152	1.167	1.191	1.214	-
11	-	8.525	8.447	8.339	8.204	7.996	-
Position	x[NH_4][C_2SO_3]						
	0	0.0503	0.1002	0.1702	0.2481	-	-
2	10.214	10.084	9.955	9.765	9.541	-	-
4	8.114	8.033	7.957	7.851	7.738	-	-
5	7.939	7.868	7.802	7.711	7.612	-	-
6	3.627	3.608	3.592	3.567	3.547	-	-
7	3.902	3.890	3.880	3.861	3.847	-	-
8	0.891	0.894	0.898	0.899	0.911	-	-
10	1.128	1.137	1.145	1.147	1.156	-	-
11	-	8.284	8.306	8.197	8.080	-	-
12	-	2.000	2.008	2.016	2.035	-	-
13	-	0.526	0.534	0.540	0.555	-	-

Position	*x* Na[Ac]				*x* Na[SCN]		
	0	0.0493	0.1017	0.1406	0.0495	-	-
2	10.214	10.162	10.110	10.075	10.098	-	-
4	8.114	8.086	8.061	8.045	8.031	-	-
5	7.939	7.916	7.896	7.884	7.868	-	-
6	3.627	3.626	3.622	3.621	3.613	-	-
7	3.902	3.909	3.912	3.915	3.897	-	-
8	0.891	0.898	0.898	0.900	0.898	-	-
10/10'	1.128	1.136	1.133	1.132	1.138	-	-

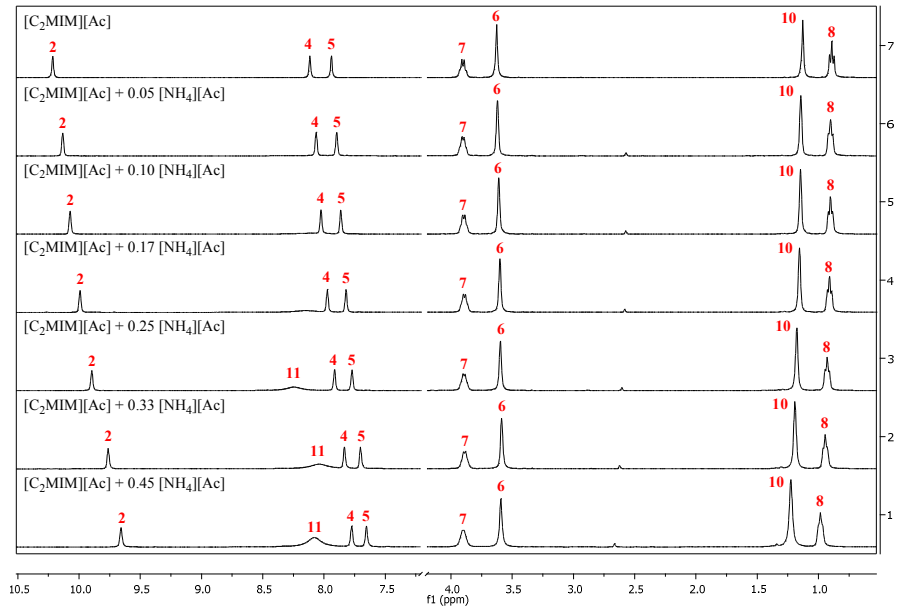

Figure S1 | Effect of $[NH_4][Ac]$ concentration on the ^1H NMR spectrum of $[C_2MIM][Ac]$ at 298.15 K.

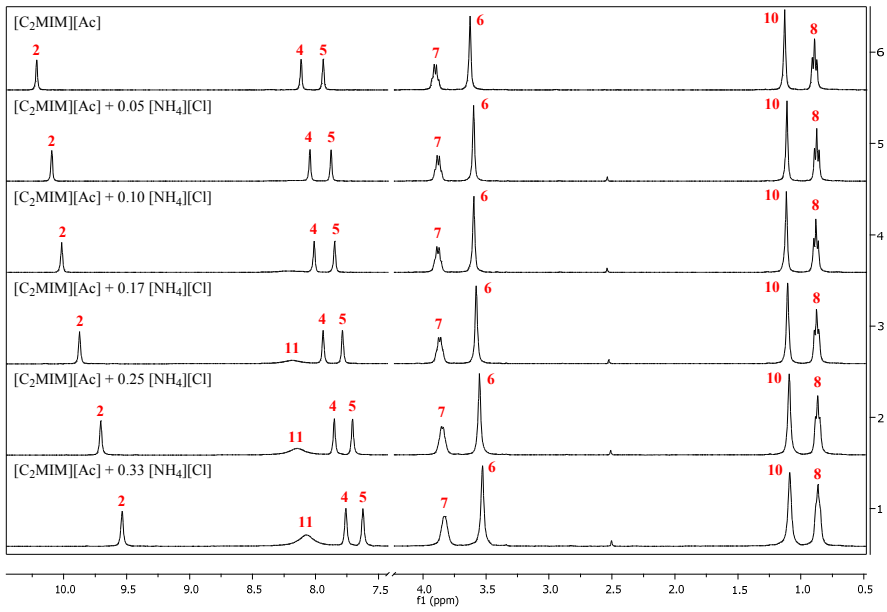

Figure S2 | Effect of $[NH_4]Cl$ concentration on the ^1H NMR spectrum of $[C_2MIM][Ac]$ at 298.15 K.

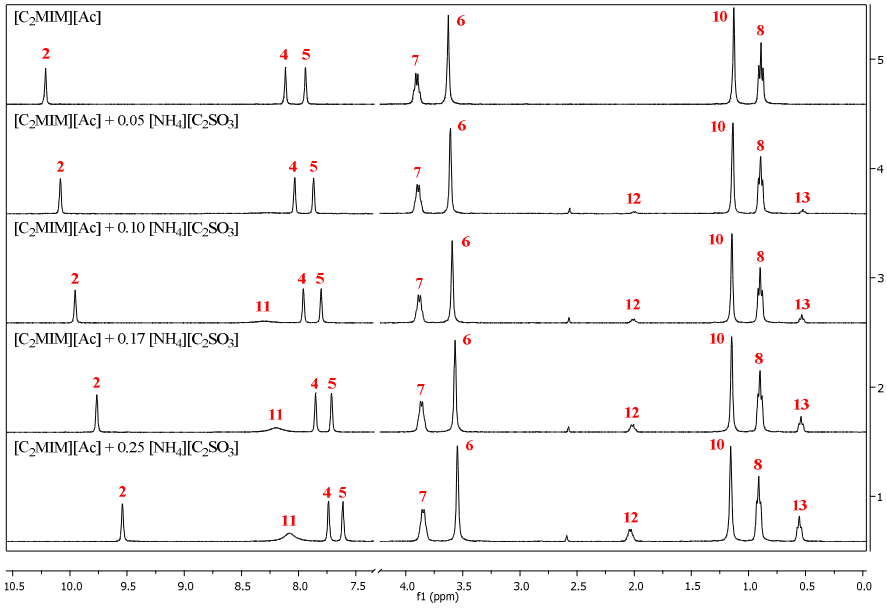

Figure S3 | Effect of $[NH_4][C_2SO_3]$ concentration on the ^1H NMR spectrum of $[C_2MIM][Ac]$ at 298.15 K.

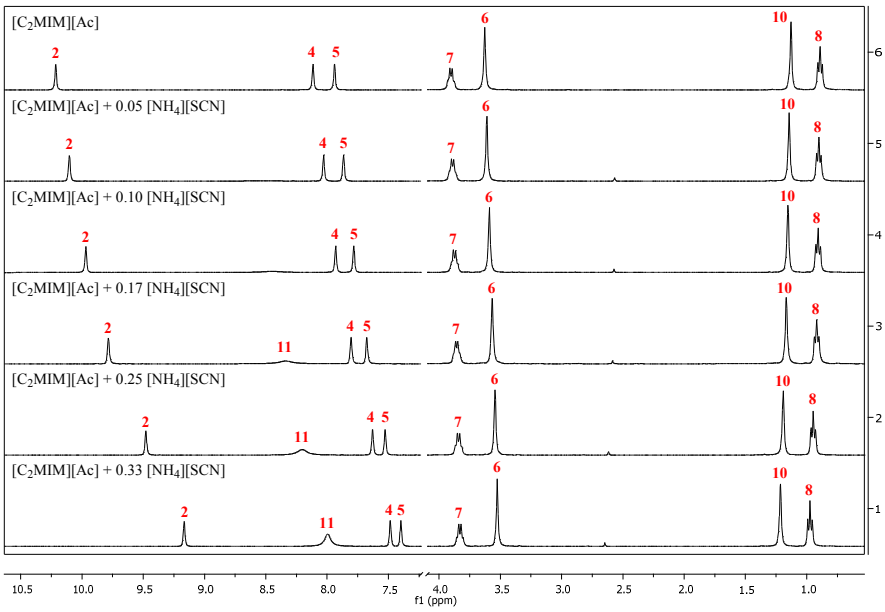

Figure S4 | Effect of [NH_4][SCN] concentration on the ^{1}H NMR spectrum of [C_2MIM][Ac] at 298.15 K.

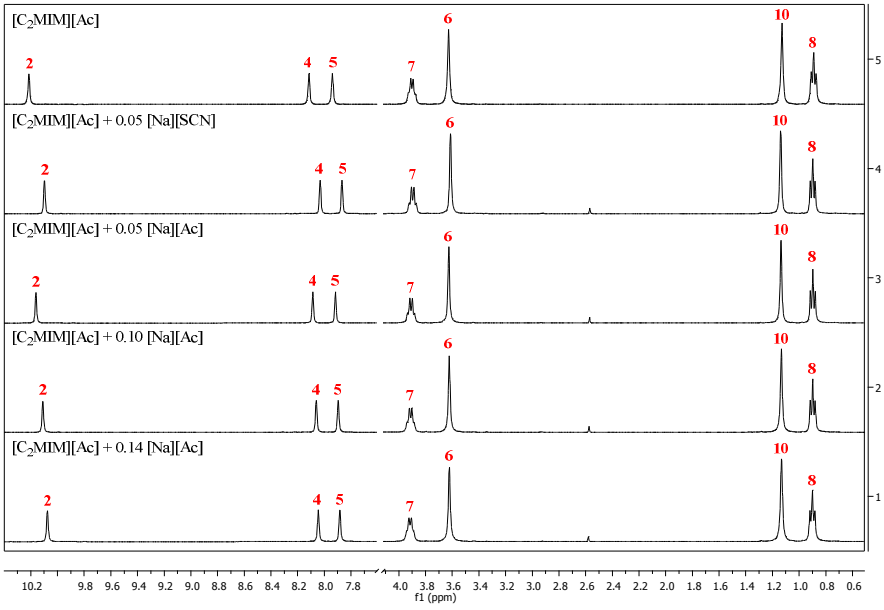

Figure S5 | Effect of Na[SCN] and Na[Ac] concentration on the ^{1}H NMR spectrum of [C_2MIM][Ac] at 298.15 K.

Table S2 | ^{1}H NMR self-diffusion coefficients of the different ions (D, in $10^{-11}\cdot m^2\cdot s^{-1}$) in the [$C_2$MIM][Ac]+ IS systems at 323.15 K.

x_{IS}	D_{IL}^{+}	D_{IL}^{-}	D_{IS}^{+}	D_{IS}^{-}
	[C_2MIM][Ac] + [NH_4][Ac]			
0	4.42	3.84	-	3.84
0.0520	4.45	3.54	-	3.54
0.1000	4.09	3.01	-	3.01
0.1688	3.54	2.35	3.90	2.35
0.2466	3.09	1.88	3.21	1.88
0.3302	2.69	1.52	-	1.52
0.4361	1.93	1.03	1.69	1.03
	[C_2MIM][Ac] + [NH_4]Cl			
0	4.42	3.84	-	-
0.0492	4.13	3.30	-	-
0.0988	3.56	2.64	-	-
0.1688	2.75	1.83	-	-
0.2479	2.02	1.22	2.03	-
0.3250	1.42	0.82	1.31	-
	[C_2MIM][Ac] + [NH_4][SCN]			
0	4.42	3.84	-	-
0.0494	4.52	3.58	4.72	-
0.0995	4.43	3.19	5.04	-
0.1610	4.42	2.80	5.05	-
0.2490	4.52	2.45	4.83	-
0.3290	4.81	2.27	4.75	-
	[C_2MIM][Ac] + [NH_4][C_2SO_3]			
0	4.42	3.84	-	-
0.0503	4.26	3.36	-	3.13
0.1002	3.89	2.84	4.33	2.77
0.1702	3.30	2.10	3.61	2.21
0.2481	2.74	1.56	2.54	1.73
	[C_2MIM][Ac] + Na[Ac]			
0	4.42	3.84	-	-
0.0493	3.93	3.14	-	3.14
0.1017	3.43	2.58	-	2.58
0.1406	3.03	2.16	-	2.16
	[C_2MIM][Ac] + Na[SCN]			
0	4.42	3.84	-	-
0.0495	4.23	3.41	-	-

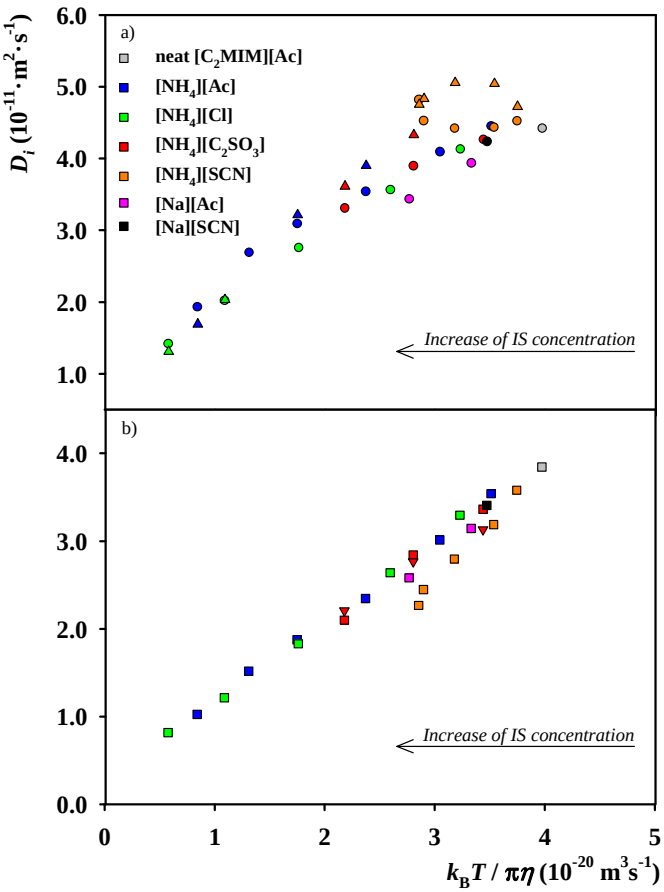

Figure S6 | Ion self-diffusion coefficients plotted against $k_BT/\pi\eta$ in the $[C_2MIM][Ac]$ + IS systems at 323.15 K. Panel a) represents the cations of the system $[C_2MIM]^+$ (●) and $[NH_4]^+$ (▲) whereas panel b) represents the anions $[Ac]^-$ (■) and $[C_2SO_3]^-$ (▼).

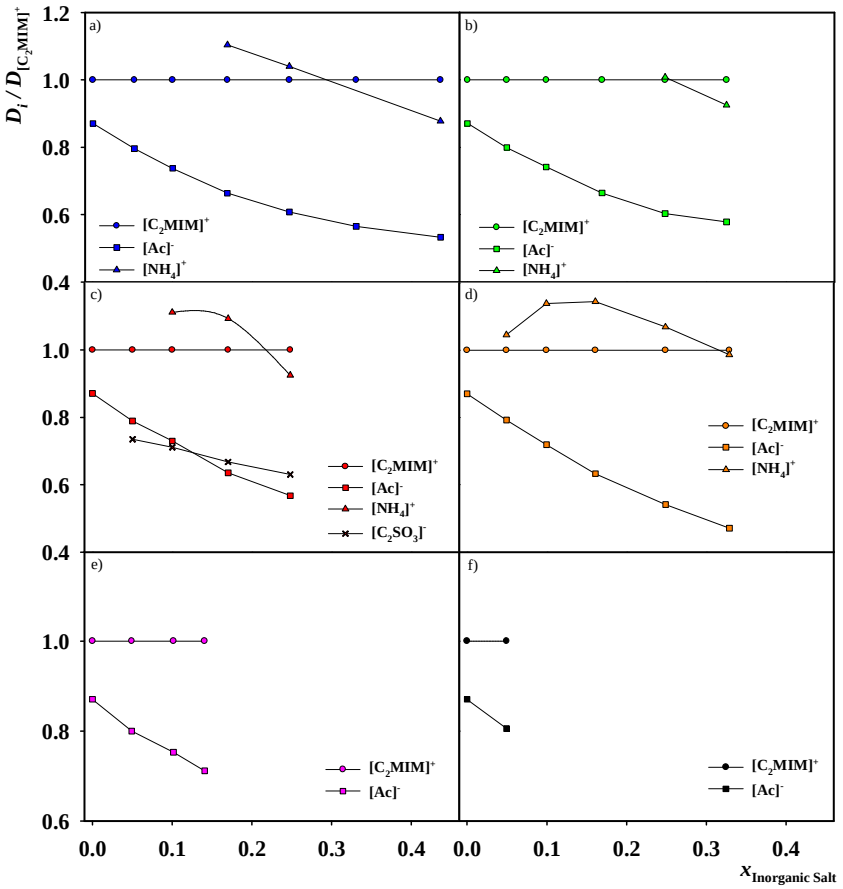

Figure S7 | ^{1}H NMR relative ion self-diffusion coefficients for the different ions in the $[C_2MIM][Ac]$ + IS systems at 323.15 K. Each panel represents a different IS: a) $[NH_4][Ac]$; b) $[NH_4]Cl$; c) $[NH_4][C_2SO_3]$; d) $[NH_4][SCN]$; e) Na[Ac] and f) Na[SCN];

7.2. Ab initio calculations

Table S3 | Electronic energies, SP and ZPVE, as well as the final energy (sum of SP and ZPVE), *E*, for the optimized structures of the pure IL and ISs.

Compound	SP / KJ·mol^{-1}	ZPVE / KJ·mol^{-1}	*E* / KJ·mol^{-1}
[C_2MIM][Ac]	-1500984	577	-1500406
[NH_4][Ac]	-748152	259	-747893
[NH_4]Cl	-1356605	130	-1356475
[NH_4][SCN]	-1436975	154	-1436821
[NH_4][C_2SO_3]	-1992313	339	-1991974
Na[Ac]	-1023702	131	-1023571
Na[SCN]	-1712557	25	-1712533

Table S4. Electronic energies, SP and ZPVE, as well as the final energy of the cluster (sum of SP and ZPVE), $E_{cluster}$, for the optimized structures of the IL + IS systems.

System	Conformation	SP / KJ·mol^{-1}	ZPVE / KJ·mol^{-1}	$E_{cluster}$ / KJ·mol^{-1}
[C_2MIM][Ac] + [NH_4][Ac]	1	-2249198	839	-2248359
	2	-2249183	840	-2248343
	3	-2249204	840	-2248364
	4	-2249196	843	-2248353
	5	-2249174	841	-2248334
	6	-2249174	839	-2248335
[C_2MIM][Ac] + [NH_4]Cl	1	-2857664	710	-2856954
	2	-2857648	708	-2856940
	3	-2857662	710	-2856952
	4	-2857659	712	-2856947
[C_2MIM][Ac] + [NH_4][SCN]	1	-2938041	734	-2937307
	2	-2938048	737	-2937311
	3	-2938043	734	-2937309
[C_2MIM][Ac] + [NH_4][C_2SO_3]	1	-3493379	918	-3492460
	2	-3493370	919	-3492451
	3	-3493381	921	-3492460
[C_2MIM][Ac] + Na[Ac]	1	-2524703	711	-2523993
	2	-2524719	712	-2524007
	3	-2524736	716	-2524020
[C_2MIM][Ac] + Na[SCN]	1	-3213595	608	-3212987
	2	-3213597	609	-3212988
	3	-3213587	606	-3212981

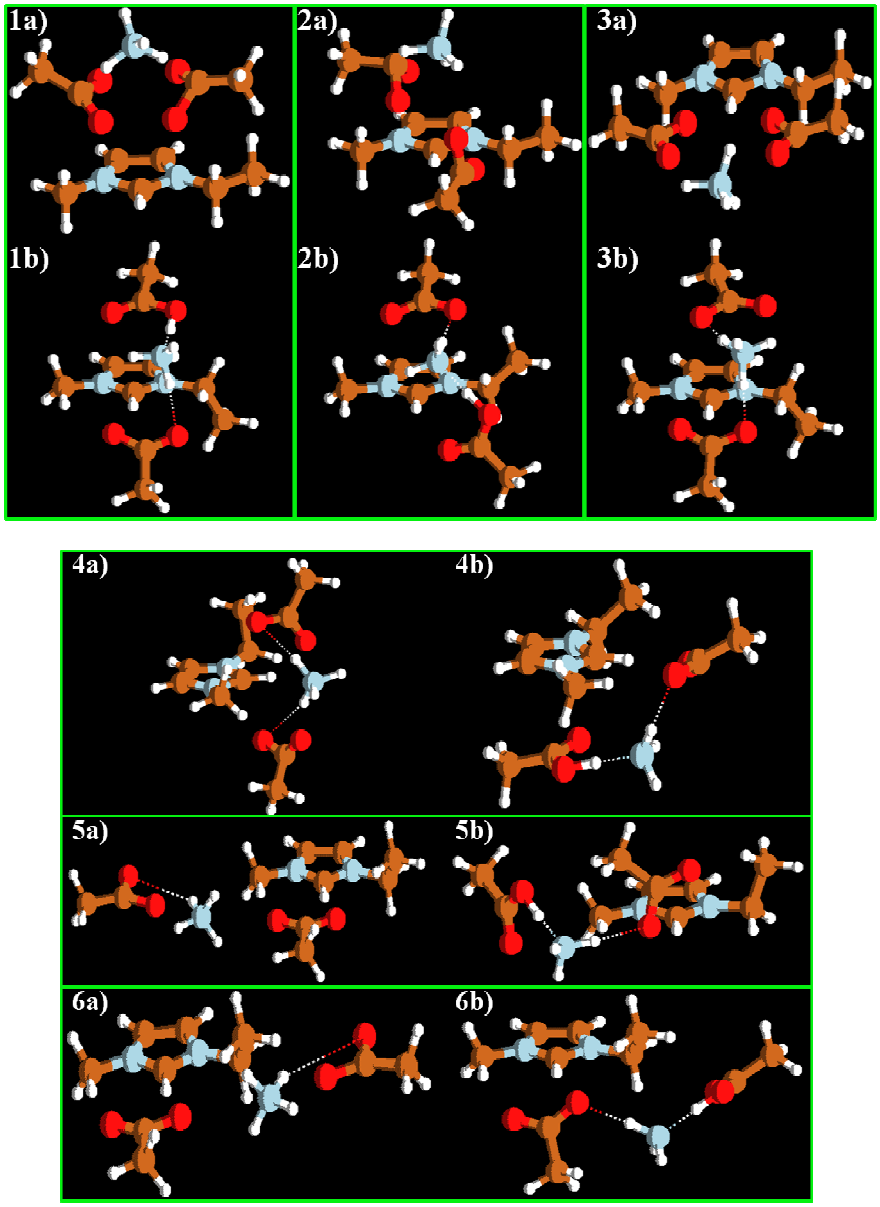

Figure S8 | Conformations drawn for the system $[C_2MIM][Ac]$ + $[NH_4][Ac]$. a) Initial conformation. b) Final conformation in ethanol.

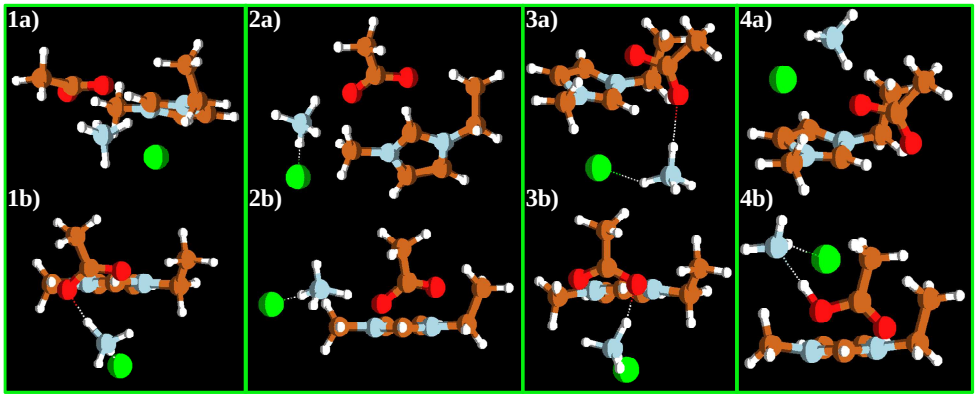

Figure S9 | Conformations drawn for the system $[C_2MIM][Ac] + [NH_4]Cl$. a) Initial conformation. b) Final conformation in ethanol.

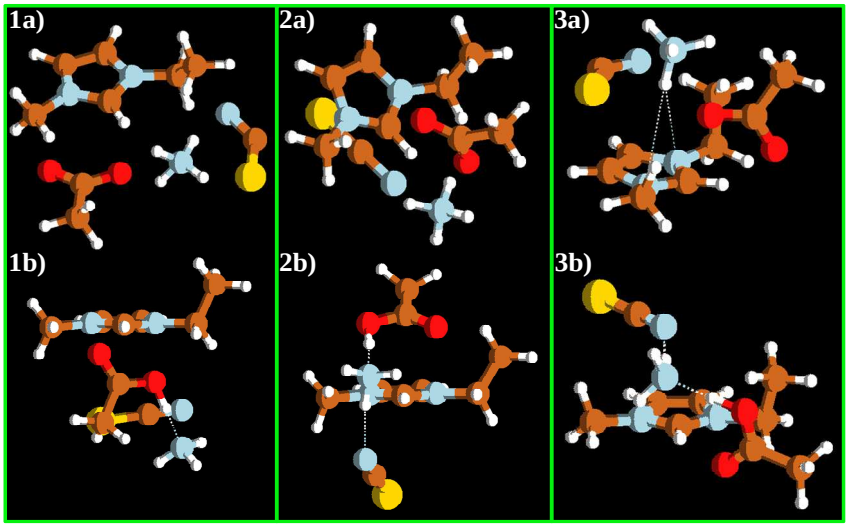

Figure S10 | Conformations drawn for the system $[C_2MIM][Ac] + [NH_4][SCN]$. a) Initial conformation. b) Final conformation in ethanol.

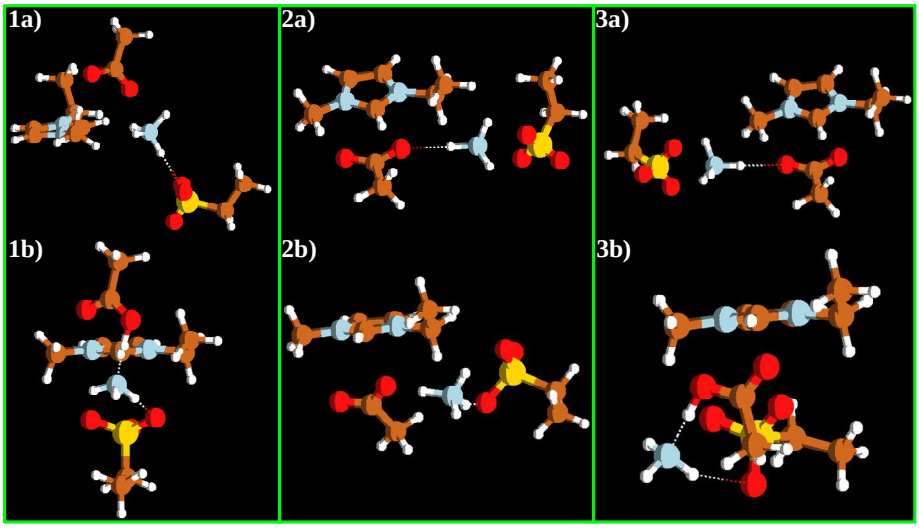

Figure S11 | Conformations drawn for the system $[C_2MIM][Ac]$ + $[NH_4][C_2SO_3]$. a) Initial conformation. b) Final conformation in ethanol.

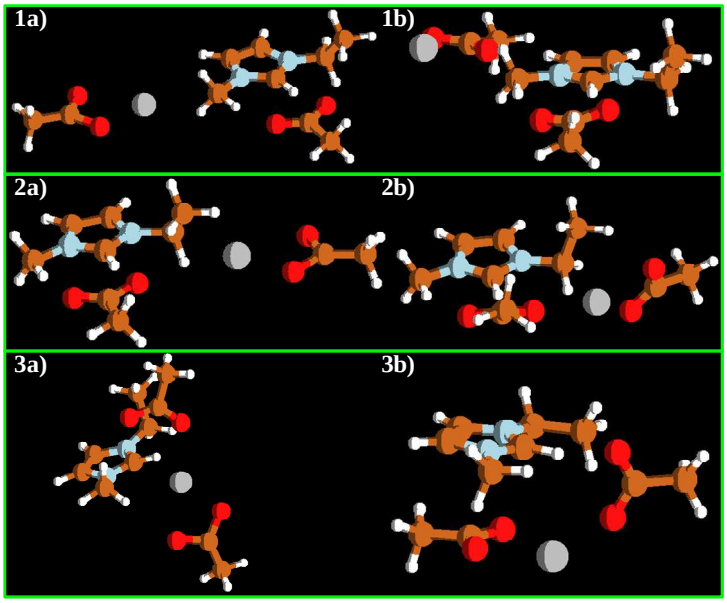

Figure S12 | Conformations drawn for the system $[C_2MIM][Ac]$ + Na[Ac]. a) Initial conformation. b) Final conformation in ethanol.

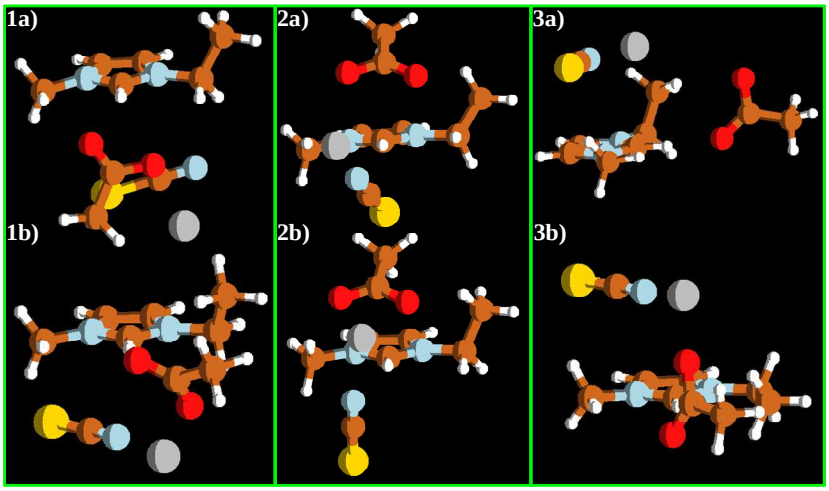

Figure S13 | Conformations drawn for the system [C_2MIM][Ac] + Na[SCN]. a) Initial conformation. b) Final conformation in ethanol.

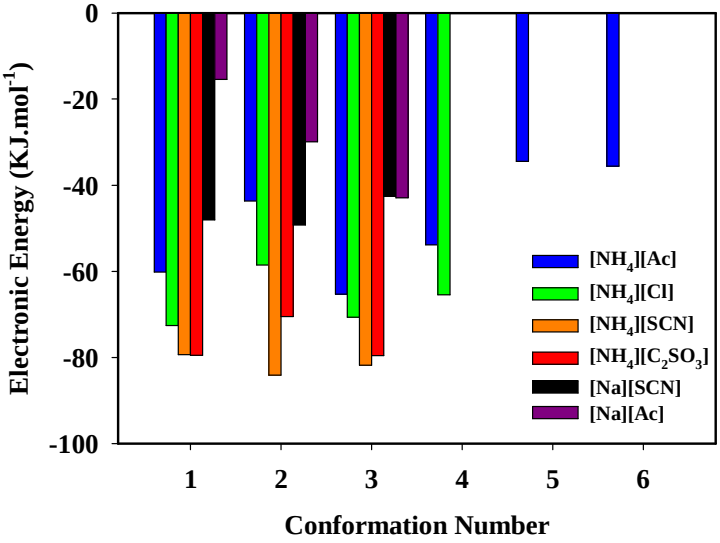

Figure S14 | Binding energies for the different conformations of all IL + IS systems studied.

8. References

1. D. R. MacFarlane and K. R. Seddon, Ionic liquids - Progress on the fundamental issues, *Aust. J. Chem.*, 2007, **60**, 3-5.

2. N. V. Plechkova and K. R. Seddon, Applications of ionic liquids in the chemical industry, *Chem. Soc. Rev.*, 2008, **37**, 123-150.

3. L. P. N. Rebelo, J. N. C. Lopes, J. M. S. S. Esperança, H. J. R. Guedes, J. Lachwa, V. Najdanovic-Visak and Z. P. Visak, Accounting for the unique, doubly dual nature of ionic liquids from a molecular thermodynamic, and modeling standpoint, *Acc. Chem. Res.*, 2007, **40**, 1114-1121.

4. M. Brüssel, M. Brehm, A. S. Pensado, F. Malberg, M. Ramzan, A. Stark and B. Kirchner, On the ideality of binary mixtures of ionic liquids, *Phys. Chem. Chem. Phys.*, 2012, **14**, 13204-13215.

5. M. Brüssel, M. Brehm, T. Voigt and B. Kirchner, Ab initio molecular dynamics simulations of a binary system of ionic liquids, *Phys. Chem. Chem. Phys.*, 2011, **13**, 13617-13620.

6. Y. Umebayashi, T. Mitsugi, S. Fukuda, T. Fujimori, K. Fujii, R. Kanzaki, M. Takeuchi and S.-I. Ishiguro, Lithium ion solvation in room-temperature ionic liquids involving bis(trifluoromethanesulfonyl)imide anion studied by Raman spectroscopy and DFT calculations, *J. Phys. Chem. B*, 2007, **111**, 13028-13032.

7. Y. Umebayashi, S. Mori, K. Fujii, S. Tsuzuki, S. Seki, K. Hayamizu and S.-i. Ishiguro, Raman spectroscopic studies and Ab Initio calculations on conformational isomerism of 1-butyl-3-methylimidazolium bis-(trifluoromethanesulfonyl)amide solvated to a lithium ion in ionic liquids: Effects of the second solvation sphere of the lithium ion, *J. Phys. Chem. B*, 2010, **114**, 6513-6521.

8. S. Tsuzuki, K. Hayamizu and S. Seki, Origin of the low-viscosity of emim $(FSO_2)_2N$ ionic liquid and its lithium salt mixture: Experimental and theoretical study of self-diffusion coefficients, conductivities, and intermolecular interactions, *J. Phys. Chem. B*, 2010, **114**, 16329-16336.

9. M. C. Corvo, J. Sardinha, S. C. Menezes, S. Einloft, M. Seferin, J. Dupont, T.

Casimiro and E. J. Cabrita, Solvation of carbon dioxide in [C_4mim][BF_4] and [C_4mim][PF_6] ionic liquids revealed by high-pressure NMR spectroscopy, *Angew. Chem. Int. Ed.*, 2013, **52**, 13024-13027.

10. A. Mele, G. Romanò, M. Giannone, E. Ragg, G. Fronza, G. Raos and V. Marcon, The local structure of ionic liquids: Cation-cation NOE interactions and internuclear distances in neat [BMIM][BF_4] and [BDMIM]-[BF_4], *Angew. Chem. Int. Ed.*, 2006, **45**, 1123-1126.

11. A. Mele, C. D. Tran and S. H. De Paoli Lacerda, The structure of a room-temperature ionic liquid with and without trace amounts of water: The role of C-H---O and C-H---F interactions in 1-n-butyl-3-methylimidazolium tetrafluoroborate, *Angew. Chem. Int. Ed.*, 2003, **42**, 4364-4366.

12. Y. Lingscheid, S. Arenz and R. Giernoth, Heteronuclear NOE spectroscopy of ionic liquids, *ChemPhysChem*, 2012, **13**, 261-266.

13. S. Gabl, O. Steinhauser and H. Weingärtner, From short-range to long-range intermolecular NOEs in ionic liquids: Frequency does matter, *Angew. Chem. Int. Ed.*, 2013, **52**, 9242-9246.

14. F. S. Oliveira, L. P. N. Rebelo and I. M. Marrucho, Influence of different inorganic salts on the ionicity and thermophysical properties of 1-ethyl-3-methylimidazolium acetate ionic liquid, *J. Chem. Eng. Data*, 2015, **60**, 781-789.

15. A. B. Pereiro, J. M. M. Araújo, F. S. Oliveira, J. M. S. S. Esperança, J. N. C. Lopes, I. M. Marrucho and L. P. N. Rebelo, Solubility of inorganic salts in pure ionic liquids, *J. Chem. Thermodyn.*, 2012, **55**, 29-36.

16. S. Chen, R. Vijayaraghavan, D. R. MacFarlane and E. I. Izgorodina, Ab Initio prediction of proton NMR chemical shifts in imidazolium ionic liquids, *J. Phys. Chem. B*, 2013, **117**, 3186-3197.

17. M. J. Frisch, G. W. Trucks, H. B. Schlegel, G. E. Scuseria, M. A. Robb, J. R. Cheeseman, G. Scalmani, V. Barone, B. Mennucci and G. A. Petersson, Gaussian 09, revision A.02, *Wallingford, CT*, 2009.

18. I. T. Todorov, W. Smith, K. Trachenko and M. T. Dove, DL_POLY_3: New dimensions in molecular dynamics simulations via massive parallelism, *J. Mater. Chem.*,

2006, **16**, 1911-1918.

19. J. N. C. Lopes, J. Deschamps and A. A. H. Pádua, Modeling ionic liquids using a systematic all-atom force field, *J. Phys. Chem. B*, 2004, **108**, 2038-2047.

20. W. L. Jorgensen, D. S. Maxwell and J. TiradoRives, Development and testing of the OPLS all-atom force field on conformational energetics and properties of organic liquids, *J. Am. Chem. Soc.*, 1996, **118**, 11225-11236.

21. A. B. Pereiro, J. M. M. Araújo, F. S. Oliveira, C. E. S. Bernardes, J. M. S. S. Esperança, J. N. C. Lopes, I. M. Marrucho and L. P. N. Rebelo, Inorganic salts in purely ionic liquid media: The development of high ionicity ionic liquids (HIILs), *Chem. Commun.*, 2012, **48**, 3656-3658.

22. C. E. S. Bernardes and A. Joseph, Evaluation of the OPLS-AA force field for the study of structural and energetic aspects of molecular organic crystals, *J. Phys. Chem. A*, 2015, **119**, 3023-3034.

23. F. S. Oliveira, A. B. Pereiro, J. M. M. Araújo, C. E. S. Bernardes, J. N. Canongia Lopes, S. Todorovic, G. Feio, P. L. Almeida, L. P. N. Rebelo and I. M. Marrucho, High ionicity ionic liquids (HIILs): Comparing the effect of -ethylsulfonate and -ethylsulfate anions, *Phys. Chem. Chem. Phys.*, 2013, **15**, 18138-18147.

24. D. T. Bowron, C. D'Agostino, L. F. Gladden, C. Hardacre, J. D. Holbrey, M. C. Lagunas, J. McGregor, M. D. Mantle, C. L. Mullan and T. G. A. Youngs, Structure and dynamics of 1-ethyl-3-methylimidazolium acetate via molecular dynamics and neutron diffraction, *J. Phys. Chem. B*, 2010, **114**, 7760-7768.

25. R. C. Remsing, G. Hernandez, R. P. Swatloski, W. W. Massefski, R. D. Rogers and G. Moyna, Solvation of carbohydrates in *N,N*-dialkylimidazolium ionic liquids: A multinuclear NMR spectroscopy study, *J. Phys. Chem. B*, 2008, **112**, 11071-11078.

26. K. Hayamizu, S. Tsuzuki, S. Seki, K. Fujii, M. Suenaga and Y. Umebayashi, Studies on the translational and rotational motions of ionic liquids composed of N-methyl-N-propyl-pyrrolidinium (P-13) cation and bis(trifluoromethanesulfonyl)amide and bis(fluorosulfonyl)amide anions and their binary systems including lithium salts, *J. Chem. Phys.*, 2010, **133**, 1945051-19450513.

27. K. Hayamizu, S. Tsuzuki, S. Seki, Y. Ohno, H. Miyashiro and Y. Kobayashi,

Quaternary ammonium room-temperature ionic liquid including an oxygen atom in side chain/lithium salt binary electrolytes: Ionic conductivity and H-1, Li-7, and F-19 NMR studies on diffusion coefficients and local motions, *J. Phys. Chem. B*, 2008, **112**, 1189-1197.

28. K. Hayamizu, S. Tsuzuki, S. Seki and Y. Umebayashi, Nuclear magnetic resonance studies on the rotational and translational motions of ionic liquids composed of 1-ethyl-3-methylimidazolium cation and bis(trifluoromethanesulfonyl)amide and bis(fluorosulfonyl)amide anions and their binary systems including lithium salts, *J. Chem. Phys.*, 2011, **135**, 0845051-08450511.

29. O. Borodin, G. D. Smith and W. Henderson, Li^+ cation environment, transport, and mechanical properties of the LiTFSI doped *N*-methyl-*N*-alkylpyrrolidinium$^+$TFSI$^-$ ionic liquids, *J. Phys. Chem. B*, 2006, **110**, 16879-16886.

30. K. Hayamizu, S. Tsuzuki and S. Seki, Transport and electrochemical properties of three quaternary ammonium ionic liquids and lithium salts doping effects studied by NMR spectroscopy, *J. Chem. Eng. Data*, 2014, **59**, 1944-1954.

31. K. Hayamizu, Y. Aihara, H. Nakagawa, T. Nukuda and W. S. Price, Ionic conduction and ion diffusion in binary room-temperature ionic liquids composed of emim BF_4 and $LiBF_4$, *J. Phys. Chem. B*, 2004, **108**, 19527-19532.

32. E. L. Cussler, *Diffusion mass transfer in fluid systems 2nd ed.*, Cambridge University Press, Cambridge, UK, 1997.

33. B. E. M. Tsamba, S. Sarraute, M. Traikia and P. Husson, Transport properties and ionic association in pure imidazolium-based ionic liquids as a function of temperature, *J. Chem. Eng. Data*, 2014, **59**, 1747-1754.

34. T. Koeddermann, R. Ludwig and D. Paschek, On the validity of Stokes-Einstein and Stokes-Einstein-Debye relations in ionic liquids and ionic-liquid mixtures, *ChemPhysChem*, 2008, **9**, 1851-1858.

35. A. W. Taylor, P. Licence and A. P. Abbott, Non-classical diffusion in ionic liquids, *Phys. Chem. Chem. Phys.*, 2011, **13**, 10147-10154.

36. C. E. S. Bernardes, M. E. Minas da Piedade and J. N. C. Lopes, The structure of aqueous solutions of a hydrophilic ionic liquid: The full concentration range of 1-ethyl-3-methylinnidazolium ethylsulfate and water, *J. Phys. Chem. B*, 2011, **115**, 2067-2074.

37. K. Shimizu, C. E. S. Bernardes and J. N. C. Lopes, Structure and aggregation in the 1-alkyl-3-methylimidazolium bis(trifluoromethylsulfonyl)imide ionic liquid homologous series, *J. Phys. Chem. B*, 2014, **118**, 567-576.

38. G. A. Jeffrey, *An introduction to hydrogen bonding*, Oxford University Press: New York, 1997.

39. K. Ueno, H. Tokuda and M. Watanabe, Ionicity in ionic liquids: Correlation with ionic structure and physicochemical properties, *Phys. Chem. Chem. Phys.*, 2010, **12**, 1649-1658.

40. C. Zhang, K. Ueno, A. Yamazaki, K. Yoshida, H. Moon, T. Mandai, Y. Umebayashi, K. Dokko and M. Watanabe, Chelate effects in glyme/lithium bis(trifluoromethanesulfonyl)amide solvate ionic liquids. I. Stability of solvate cations and correlation with electrolyte properties, *J. Phys. Chem. B*, 2014, **118**, 5144-5153.

41. C. Schreiner, S. Zugmann, R. Hartl and H. J. Gores, Fractional walden rule for ionic liquids: Examples from recent measurements and a critique of the so-called ideal KCl line for the walden plot, *J. Chem. Eng. Data*, 2010, **55**, 1784-1788.

42. K. R. Harris, Relations between the fractional Stokes-Einstein and Nernst-Einstein equations and velocity correlation coefficients in ionic liquids and molten salts, *J. Phys. Chem. B*, 2010, **114**, 9572-9577.

43. K. Ueno, K. Yoshida, M. Tsuchiya, N. Tachikawa, K. Dokko and M. Watanabe, Glyme–lithium salt equimolar molten mixtures: Concentrated solutions or solvate ionic liquids?, *J. Phys. Chem. B*, 2012, **116**, 11323-11331.

44. H. Tokuda, S. Tsuzuki, M. Susan, K. Hayamizu and M. Watanabe, How ionic are room-temperature ionic liquids? An indicator of the physicochemical properties, *J. Phys. Chem. B*, 2006, **110**, 19593-19600.

45. M. S. Miran, H. Kinoshita, T. Yasuda, M. A. B. H. Susan and M. Watanabe, Physicochemical properties determined by ΔpK_a for protic ionic liquids based on an organic super-strong base with various Bronsted acids, *Phys. Chem. Chem. Phys.*, 2012, **14**, 5178-5186.

46. J. M. Andanson, M. Traikia and P. Husson, Ionic association and interactions in aqueous methylsulfate alkyl-imidazolium-based ionic liquids, *J. Chem. Thermodyn.*, 2014,

77, 214-221.

47. O. Holloczki, F. Malberg, T. Welton and B. Kirchner, On the origin of ionicity in ionic liquids. Ion pairing versus charge transfer, *Phys. Chem. Chem. Phys.*, 2014, **16**, 16880-16890.

Chapter 4

Combining one IL with different amounts of one IS for the separation of ethanol from n-heptane

Adapted from: **Filipe S. Oliveira**, Ana B. Pereiro, João M. M. Araújo, Luís P. N. Rebelo and Isabel M. Marrucho, Designing high ionicity ionic liquids based on 1-ethyl-3-methylimidazolium ethyl sulfate for effective azeotrope breaking, *submitted to J. Chem. Thermodyn.,* 2015

The author was involved in all the experiments, as well as on the discussion, interpretation and preparation of the manuscript.

1. Abstract

In this work, the liquid-liquid extraction of ethanol from n-heptane + ethanol mixtures using combinations of one ionic liquid with different amounts of the same inorganic salt as extraction solvents, is studied. Three different mixtures of ionic liquid + inorganic salt, with different ionicities were prepared through the addition of different amounts of ammonium thiocyanate inorganic salt to 1-ethyl-3-methylimidazolium ethyl sulfate ionic liquid, and used. Liquid-liquid equilibria of ternary mixtures of n-heptane + ethanol + 3 different mixtures of ionic liquid + inorganic salt were experimentally measured at 298.15 K and 0.1 MPa. Both the selectivity and the distribution coefficient were used in the assessment of the extraction solvent feasibility and a correlation of these parameters with the ionicity of the ionic liquid + inorganic salt mixtures was established. A comparison between the different mixtures of ionic liquid + inorganic salt and the neat ionic liquid is also made.

2. Introduction

In many areas of industry, from the production of commodities to fine chemical processes, the accumulation of hazardous solvent mixtures, due to recycling difficulties, is a serious problem. In order to meet sustainability criteria, the separation of these mixtures into their pure components is mandatory so that they can be reused. For example, numerous problems related to the trade-off between efficiency and soot gases emissions are posed in the production and commercialization of fuels. In these processes, alkanols and alkanes are brought together to produce oxygenated additives for gasoline or diluted hydrocarbon fuels.[1] In this context, the azeotropes of either n-hexane or n-heptane with methanol or ethanol have been reported due to difficulties in separating these compounds.[2-19] The approach usually used to separate this type of azeotropes is to implement liquid–liquid separation.[20]

In order to break the azeotrope of a mixture a third component (i.e. separation agent) must be added, regardless of the technique used. The separation agent promotes the separation of the components in the azeotropic mixture. In the case of liquid-liquid extraction

processes, the separation agent is an extraction solvent that changes the solubility of the compounds, promoting the azeotrope breaking.

The choice of the separation agent is of utmost importance for the separation of azeotropic mixtures. Organic solvents are the most used separation agents in industry, nevertheless inorganic salts (ISs), the combination of both and more recently, ionic liquids (ILs) have also been tested.[21] Due to their remarkable properties, specifically almost null volatility at room temperature, recycling easiness and fine tunable properties, ILs have been emerging as an appealing alternative for the recycling of volatile organic solvent mixtures used in industry.[20] In addition, ILs have shown the ability to efficiently separate azeotropic mixtures including alcohols + alkanes mixtures,[2-8, 10-17, 19] aromatic + aliphatic mixtures,[22-32] ethyl acetate + alcohols or n-hexane,[33-35] ketones + alkanes or alcohols mixtures,[36, 37] and ethers + alcohols[38-41] through liquid-liquid extraction. The best separation results obtained in the previous examples were for the azeotropic mixtures of alkanes + alcohols.[20]

Lately, our group studied the solubility of common ISs in a wide range of different ILs[42] and showed that their solubilisation in the IL media can increase the Coulombic character of the latter, thus increasing the ionicity of ILs at very low cost, while the liquid state status is still preserved.[43-45] The ionicity of an IL is related to its ionic nature, which can be controlled by the magnitude and balance of the interactive forces of the IL. ILs present a complex nature where several interactions, such as Coulombic (the predominant), van der Waals, hydrogen-bonding and π-π interactions, are present. In addition, the formation of aggregates or clusters in ILs may also occur to some extent, affecting their structure and obviously their physicochemical properties such as viscosity, conductivity, and diffusion coefficients. Other IL's properties, namely vapour pressure and hydrogen acceptor or donor character, have also been linked to their ionicity.[46] Thus, the evaluation of the ionicity or the degree of dissociation/association of ILs and its correlation to their macroscopic properties has become an interesting and important parameter for the characterization of ILs.[47, 48]

In previous works,[43, 44] we studied the effects of the addition of ammonium thiocyanate on the thermophysical properties of three ILs based on the 1-ethyl-3-methylimidazolium cation combined with ethyl sulfate, ethyl sulfonate and acetate anions. NMR, Raman and MD calculations showed that by solubilising this salt into the IL media, modifications on the

IL's initial structure were promoted and the Coulombic character of the IL altered. Although an increase in the ionicity was observed in all the studied systems, this property did not change in a linear manner with composition indicating the formation of different complexes/aggregates depending on the IS concentration, in other words, different ion´s "availability" to participate in solvation schemes.

Recently, Lei et al.[49] just demonstrated that the combination of ISs and ILs shows promising results in the separation of ethanol and water azeotropic mixtures by extractive distillation. In the present work, our aim is to evaluate the performance of studied IL-ISs mixtures as extraction solvents for n-heptane + ethanol azeotropic mixtures in liquid-liquid extraction and, if possible, to link their ionicity to their extraction efficiency and capacity. For that purpose, liquid-liquid equilibria data for ternary systems of n-heptane + ethanol + (IL-IS) mixture were measured at 298.15 K and 0.1 MPa. Literature shows that alkyl sulfate-based ILs are some of the most promising ILs, presenting high efficiency in the separation of azeotropic mixtures, namely in the separation of mixtures of benzene + C_6-C_9 aliphatic compounds,[27, 32] ethyl acetate + ethanol[35] or 2-propanol,[33] ethyl *tert*-butyl ether + ethanol[39] and n-hexane or n-heptane + ethanol.[10, 11, 13-15] This family of ILs, specifically those with a cation derived from imidazolium, exhibit good chemical and thermal stability, low melting points and relatively low viscosities.[50] In particular, the 1-ethyl-3-methylimidazolium ethyl sulfate IL is highly efficient in the separation of the n-heptane + ethanol azeotropic mixture.[10]

Consequently, in this work, three different IL-IS mixtures, based on 1-ethyl-3-methylimidazolium ethyl sulfate IL with different amounts of ammonium thiocyanate, were used. Their separation capacity was evaluated through the calculation of the decisive parameters: distribution coefficient and selectivity. These IL-IS mixtures were selected for several reasons: i) the IL selected shows good efficiency in the separation of the targeted mixture,[10] ii) the IS chosen displays high solubility in the IL,[42] allowing the study of different concentrations of IS; and iii) the commercial availability and cheap price of the IL when comparing to other short chain alkyl sulfate-based imidazolium ILs.

3. Experimental Section

3.1. Materials

N-heptane and ethanol were supplied by Riedel-de-Haën with 99 % purity and by Scharlau with 99.9 % purity, respectively. Ammonium thiocyanate ([NH_4][SCN]) was provided by Sigma-Aldrich with a purity content superior to 99.0 %, while the IL 1-ethyl-3-methylimidazolium ethyl sulfate ([C_2MIM][C_2SO_4]) was purchased from Merck with a mass fraction purity of ≥ 99 %. To reduce the water and other volatile substances contents, vacuum (0.1 Pa) and moderate temperature (no more than 323.15 K) were always applied to the ionic liquid and inorganic salt for at least 3 days prior to their use. After drying, the ionic liquid purity was checked by ^{1}H NMR.

Three different concentrations of binary mixtures of [C_2MIM][C_2SO_4] + [NH_4][SCN] were prepared: x_{IL} = 0.83 + x_{IS} = 0.17 (SO4-SCN17), x_{IL} = 0.67 + x_{IS} = 0.33 (SO4-SCN33) and x_{IL} = 0.55 + x_{IS} = 0.45 (SO4-SCN45). These concentrations were chosen taking into account the solubility limits[42] and the ionicity of the system.[44] Table 1 presents the ionicity of the IL-IS mixtures used, calculated by the Walden Plot method.

Table 1 | Ionicity (ΔW) calculated from the Walden Plot deviations at 298.15 K for the neat IL and the IL-IS mixtures tested in this work.

Solvent	ΔW [a]
[C_2MIM][C_2SO_4]	0.164
SO4-SCN17	0.088
SO4-SCN33	0.061
SO4-SCN45	0.084

[a] The ionicity data was taken from the literature.[44]

In this method, the ionicity is determined by the deviation of the corresponding IL-IS mixture to the ideal Walden line (behaviour of ideal electrolyte). A higher deviation to the ideal line corresponds to a "less ionic" ionic liquid. The SO4-SCN33 mixture was chosen due to its highest ionicity (the lowest deviation to the ideal Walden line), while the other two (SO4-SCN17 and SO4-SCN45) present similar ionicity values, despite the fact that SO4-

SCN45 has a much higher viscosity and lower conductivity than SO4-SCN17.[44] The samples were prepared by weighing known masses of the each component into stoppered flasks using an analytical high-precision balance with an uncertainty of ± 10^{-5} g, under inert atmosphere. Afterwards, they were mixed with a magnetic stirring until a clear solution was obtained. In Figure 1, the chemical structures of the IL [C_2MIM][C_2SO_4] and of the IS [NH_4][SCN] are presented.

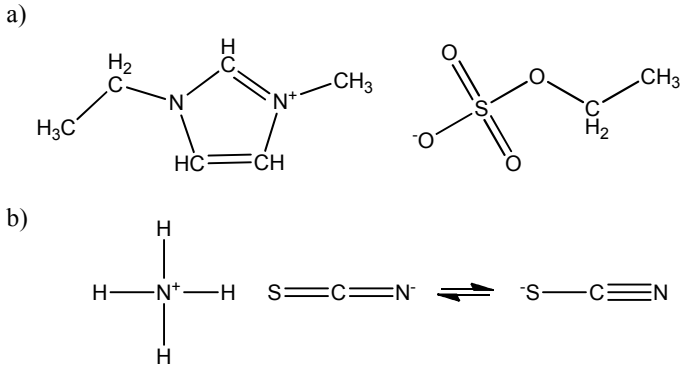

Figure 1 | Chemical structure of both ionic liquid and inorganic salt used in this work, a) [C_2MIM][C_2SO_4] and b) [NH_4][SCN].

3.2. Liquid-liquid equilibria measurements

The ternary LLE experiments were performed at 298.15 K and 0.1 MPa in a glass cell thermostatically regulated by a water jacket connected to an external water bath controlled to ± 0.01 K. The temperature in the cell was measured with a platinum resistance thermometer coupled to a Keithley 199 System DMM/Scanner that was calibrated with high–accuracy mercury thermometers (0.01 K). The mixing was assured by a magnetic stirrer.

The binodal curve of the ternary system was determined by preparing several binary mixtures of IL-IS + n-heptane in the immiscible region and then ethanol was added until the ternary mixture became miscible. Afterwards, the refractive index of those ternary mixtures was determined in triplicate. The measurements of refractive index were performed at

298.15 K and 0.1 MPa, using an automated Anton Paar Refractometer Abbemat 500 with an absolute uncertainty in the measurement of ± 0.00005.

The determination of the tie-lines, was carried out by preparing ternary mixtures of known composition that were vigorously stirred for at least 1 h and left to settle for at least 12 h at 298.15 K. Then, samples from both phases were taken with a syringe and their refractive indexes measured in triplicate. The composition of both phases in equilibrium was determined using the fitting of the refractive indexes at 298.15 K with the composition, along the binodal curve, using the following equations:

$$n_D = A \cdot w_1 + B \cdot w_1^2 + C \cdot w_1^3 + D \cdot w_1^4 + E \cdot w_2 + F \cdot w_2^2 + G \cdot w_2^3 + H \cdot w_2^4 + I \cdot w_3 + J \cdot w_3^2 + K \cdot w_3^3 + L \cdot w_3^4 \quad (1)$$

$$w_3 = M \cdot \exp\left[\left(N \cdot w_1^{0.5}\right) - \left(O \cdot w_1^3\right)\right] \quad (2)$$

$$w_3 = 1 - (w_1 + w_2) \quad (3)$$

where, w_1, w_2 and w_3 correspond to the mass fraction compositions of n-heptane, ethanol and IL-IS mixture, respectively, and the parameters *A* to *O* are adjustable parameters, which are given in Table S2 in the supporting information (SI) for the studied systems.

The method was validated using experimental data for the ternary system of n-heptane + ethanol + [C_2MIM][C_2SO_4] from the literature.[10] The measurements obtained were estimated to be accurate to ± 0.009 in mass fraction in comparison with the method used in literature[10] and the uncertainty in the composition is estimated to be ± 0.006 in mass fraction.

4. Results and discussion

The ternary diagrams for the system n-heptane + ethanol + (IL-IS) at 298.15 K and 0.1 MPa are presented in Figures 2-4. It can be observed that an increase in the molar ratio of IS in the IL-IS mixture leads to an increase in the immiscibility region of the ternary diagram. In addition, the tie-lines of the three studied systems present positive slopes meaning that the extraction of ethanol from n-heptane is always favourable. The composition of the phases in equilibrium, along with the distribution coefficient and the selectivity values are presented in Tables S1 in the SI.

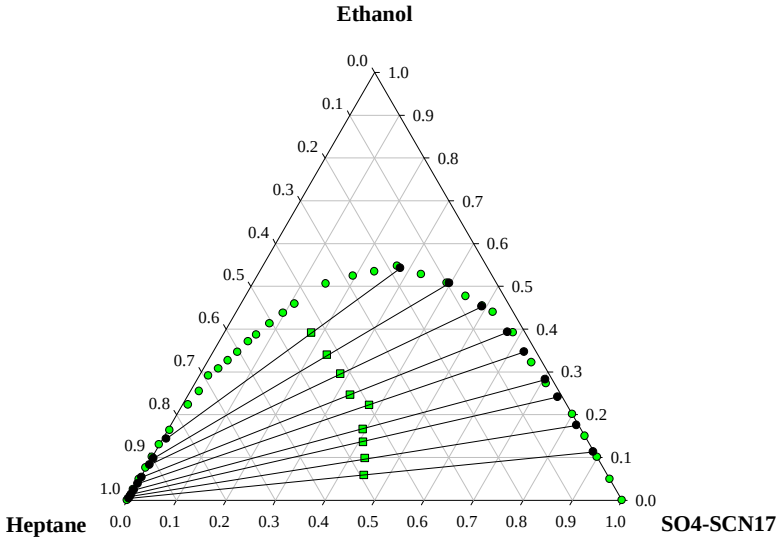

Figure 2 | Ternary diagram for the system n-heptane (1) + ethanol (2) + SO4-SCN17 (3) at 298.15 K and 0.1 MPa. The green dots represent the binodal curve and the green squares the composition of the initial mixture; the black dots and lines represent the composition of the co-exiting phases and the tie-lines, respectively.

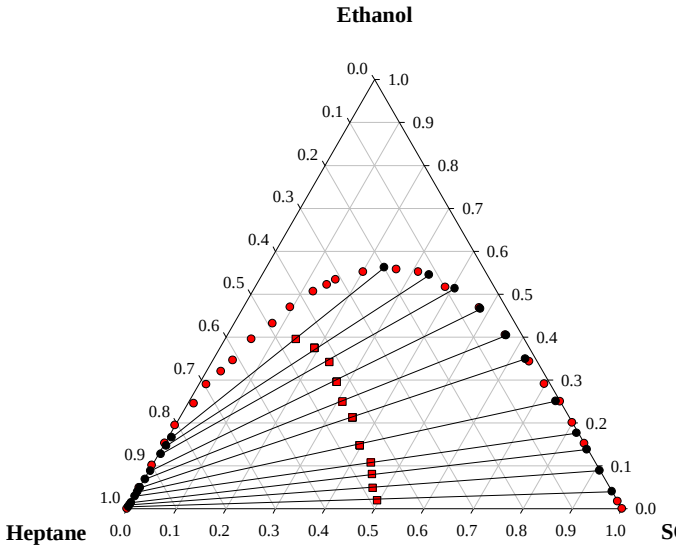

Figure 3 | Ternary diagram for the system n-heptane (1) + ethanol (2) + SO4-SCN33 (3) at 298.15 K and 0.1 MPa. The red dots represent the binodal curve and the red squares the composition of the initial mixture; the black dots and lines represent the composition of the co-exiting phases and the tie-lines, respectively.

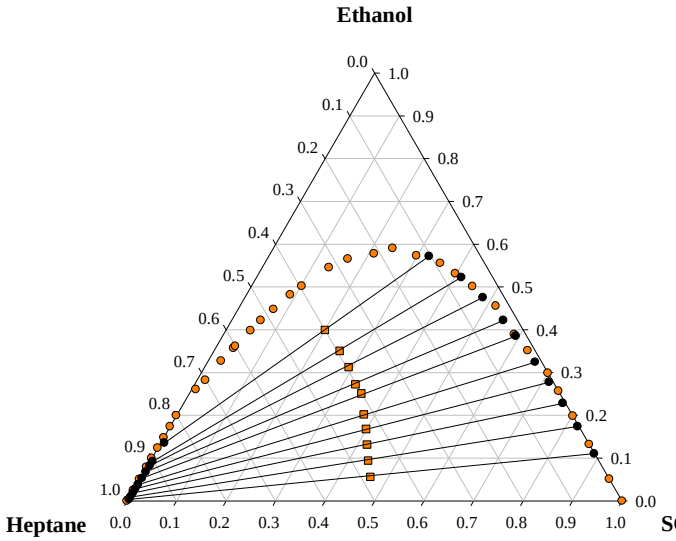

Figure 4 | Ternary diagram for the system n-heptane (1) + ethanol (2) + SO4-SCN45 (3) at 298.15 K and 0.1 MPa. The orange dots represent the binodal curve and the orange squares the composition of the initial mixture; the black dots and lines represent the composition of the co-exiting phases and the tie-lines, respectively.

The distribution coefficient and the selectivity are two required parameters to assess the performance of the extraction solvent in liquid-liquid extraction system. The first accounts for the solute-carrying capacity as well as the amount of extraction solvent (IL-IS mixture, in this case) required for the extraction process, while the latter evaluates the efficiency of the extraction solvent, indicating the ease of extraction of a solute (ethanol) from a diluent or inert (heptane). These two parameters can be determined by the following equations:

$$\beta_2 = \frac{w_2^{II}}{w_2^{I}} \tag{4}$$

$$S = \frac{w_1^{I}}{w_1^{II}} \times \beta_2 \tag{5}$$

where, β_2 is the distribution coefficient of ethanol, S is the selectivity, w_1 and w_2 the mass fractions of n-heptane and ethanol, respectively and superscripts I and II indicate the n-heptane-rich phase (upper phase) and IL-IS-rich phase (lower phase), respectively. A high selectivity allows fewer stages in the process of extraction and smaller amount of inert residual in the extract, while a high distribution coefficient value usually leads to a lower solvent flow rate, a smaller-diameter column and lower operating costs.[20]

Figure 5 depict the distribution coefficient values obtained for the IL-IS mixtures tested, while the data is listed in Table S1 (SI). In addition, the distribution coefficient values obtained for the neat IL, [C_2MIM][C_2SO_4], were also plotted for comparison. It can be observed that addition of IS did not promote any major effect on the distribution coefficient in comparison with the neat IL. In all systems, IL and IL-IS mixture, the β_2 values increase with the decrease of the ethanol mass fraction in the n-heptane-rich phase, showing similar values in the whole range with the exception of SO4-SCN33. For mass fraction values below 0.05, the β_2 values of SO4-SCN33 drop. This was not expected since SO4-SCN33 presents the highest ionicity. This fact indicates that the distribution coefficient is not related

with the extraction solvent ionicity. On the other hand, MD studies showed that, at this concentration (x_{IS} = 0.33), the original IL structure starts to break apart, and the ions are less ordered which might explain the less solute-carrying capacity of this IL-IS mixture.[44]

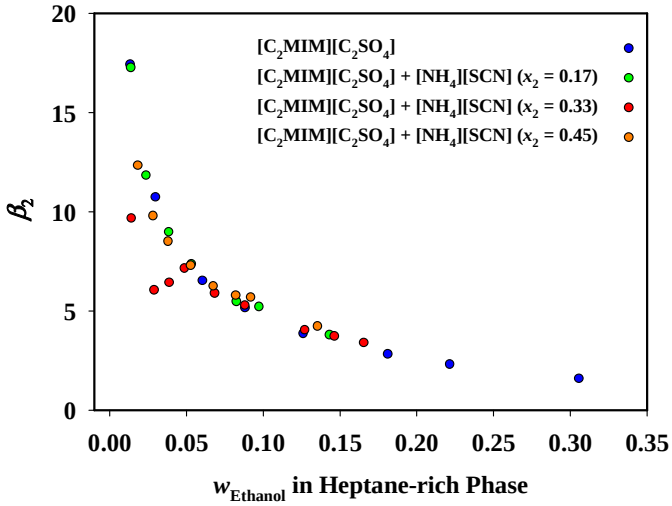

Figure 5 | Distribution coefficient values, β_2, for the ternary systems n-heptane (1) + ethanol (2) + IL-IS (3), as a function of ethanol mass fraction in n-heptane-rich phase at 298.15 K and 0.1 MPa. The data for the neat IL is taken from literature.[10]

The selectivity values obtained for the ternary systems containing IL-IS mixtures studied in this work are plotted in Figure 6 and the data presented in Table S1 in the SI. The selectivity values obtained for the neat [C_2MIM][C_2SO_4] were also plotted for comparison. It can be observed that the addition of IS to the IL increased the selectivity values in comparison to the pure IL. The results obtained also show that a correlation between the ionicity of the extraction solvent and its selectivity can be established. SO4-SCN33 is the extraction solvent that presented the highest selectivity values in accordance with its highest ionicity. When comparing SO4-SCN33 with the neat IL, the IL-IS mixture always presents higher selectivity values than the neat IL. Even at low ethanol concentrations, where the neat IL displays its highest selectivity, SO4-SCN33 has a selectivity of more than 3 times higher than that of the neat IL. Regarding the other two HIILs, the selectivity values obtained are also higher than those of the neat IL, with the SO4-SCN45 presenting higher selectivity

values than SO4-SCN17.

For mass fractions of ethanol lower than 0.05 it is possible to establish a trend, where the selectivity increases with the increase in the ionicity, following the order: SO4-SCN33 > SO4-SCN45 > SO4-SCN17 > neat IL.

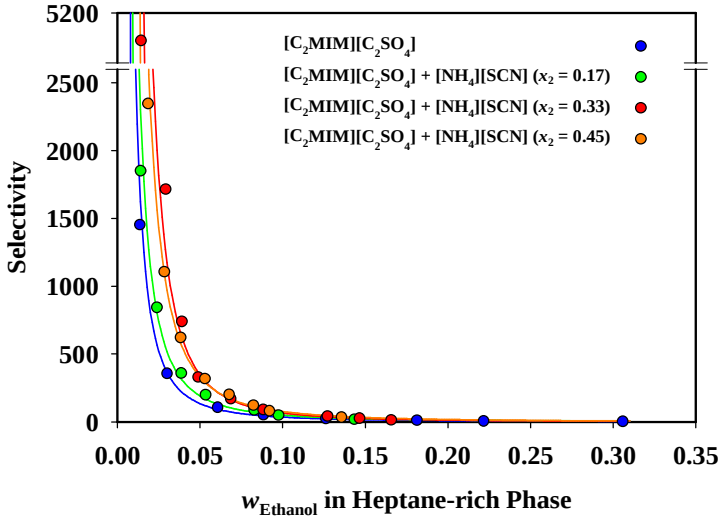

Figure 6 | Selectivity, *S*, of the three studied IL-IS mixtures for the ethanol in the n-heptane (1) + ethanol (2) + IL-IS (3) system, as a function of the ethanol mass fraction in the n-heptane-rich phase at 298.15 K and 0.1 MPa. The line are just for eyes' guidance and the data for the neat IL is taken from literature.[10]

In order to better evaluate the effect of the addition of IS to the IL in the efficiency of the IL-IS mixtures as extraction solvents, the ethanol mass fraction was fixed and the selectivity values were compared in Figure 7. Three different mass fractions of ethanol, 0.014, 0.030 and 0.090, were chosen to draw a direct comparison between the IL-IS mixtures containing systems and the system with the neat IL. As the mass fraction of ethanol increases in the n-heptane-rich phase, the effect of the ionicity becomes less pronounced, as shown in Figure 7 and Figure S2 in the SI. Nonetheless, the addition of $[NH_4][SCN]$ to the $[C_2MIM][C_2SO_4]$ always enhances the selectivity of the neat IL and SO4-SCN33 always displays the highest selectivity values at the 3 studied ethanol compositions, in accordance to its highest ionicity.

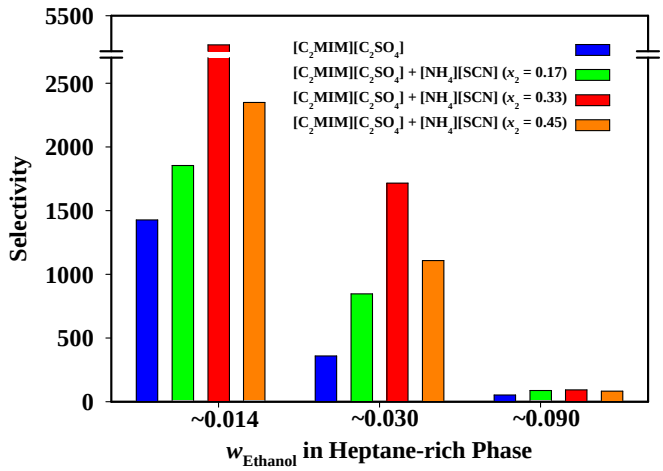

Figure 7 | Effect of the ionicity in the selectivity of the IL-IS mixture for the system n-heptane (1) + ethanol (2) + IL-IS (3), at a three fixed ethanol mass fractions in n-heptane-rich phase, at 298.15 K and 0.1 MPa. The data for the neat IL is taken from literature.[10]

In Figures 8 and 9, a comparison between the distribution coefficients and selectivity values of the IL-IS mixtures tested in this work and the ILs found in literature, for the n-heptane + ethanol azeotrope, at a fixed ethanol mass fraction in n-heptane-rich phase, is presented. The comparison in the full range of ethanol mass fraction is shown in Figures S1-S2 in the SI. Most of the literature data on the separation of n-heptane + ethanol azeotropic mixture using ILs as extraction solvents is based on ILs containing the bis(trifluoromethylsulfonyl)imide anion.

Seoane et al.[19] studied the effect of increasing the alkyl chain of the 1-ethyl-3-methylimidazolium bis(trifluoromethylsulfonyl)imide ([C_2MIM][NTf_2]) on the separation of n-heptane + ethanol mixtures and found that this increase lead to lower selectivity values, while the distribution coefficient values were not greatly affected. González et al.[8] tested two pyridinium-based ILs, 1-ethyl-3-methylpyridinium bis(trifluoromethylsulfonyl)imide ([C_2-3-C_1Py][NTf_2]) and 1-propyl-3-methylpyridinium bis(trifluoromethylsulfonyl)imide ([C_3-3-C_1Py][NTf_2]) and demonstrated the lower performance of these ILs when compared to their imidazolium counterparts. However, in another work the same authors[7] showed that pyrrolidinium-based ILs could provide better results than other ILs families. In this work

these authors combined the 1-butyl-1-methylpyrrolidinium cation ($[C_4\text{-}3\text{-}C_1pyr]^+$) with the dicyanamide ($[DCA]^-$) and the trifluoromethanesulfonate ($[OTf]^-$) anions. The results showed that the $[C_4\text{-}3\text{-}C_1pyr][DCA]$ was the more feasible extraction solvent for the separation of n-heptane + ethanol mixtures showing distribution coefficient values superior to 8 and selectivity values ranging from 80 to 1500. Aranda et al.[2] used two tetraalkyl ammoniums, butyltrimethylammonium bis(trifluoromethylsulfonyl)imide ($[BTMA][NTf_2]$) and tributylmethylammonium bis(trifluoromethylsulfonyl)imide ($[TBMA][NTf_2]$), for the separation of n-heptane or n-hexane + ethanol or methanol mixtures, where the best results were obtained for $[BTMA][NTf_2]$ in the n-hexane + methanol system, whereas for the n-heptane+ ethanol system the studied ILs tested performed more poorly than the pyridinium-based ILs studied by González et al.[8]

As mentioned before, some studies on the use of alkyl sulfate-based ILs to break this particular azeotrope were also found in the literature. Pereiro *et al.* studied the separation of n-heptane + ethanol, using the ILs 1-butyl-3-methylimidazolium methyl sulfate $[C_4MIM][C_1SO_4]$,[11] 1,3-dimethylimidazolium methyl sulfate ($[C_1MIM][C_1SO_4]$)[14] and also 1-ethyl-3-methylimidazolium ethyl sulfate ($[C_2MIM][C_2SO_4]$).[10] The results obtained showed that all these ILs used were suitable extraction solvents for the extraction of ethanol from its azeotropic mixture, especially in mixtures of n-heptane + ethanol, where particularly high efficiencies were obtained. In addition, it was observed that a shorter alkyl chain on the imidazolium cation led to better n-heptane/ethanol efficiencies.

Moreover, Pereiro et al.[12, 16] also tested hexafluorophosphate-based ILs, 1-hexyl-3-methylimidazolium ($[C_6MIM][PF_6]$) and 1-octyl-3-methylimidazolium hexaflurophosphate ($[C_8MIM][PF_6]$), for the separation of n-heptane + ethanol mixtures. Both the ILs proved to break the azeotropic point of the tested mixtures, with the $[C_6MIM][PF_6]$ IL showing very high selectivity values in the case of n-heptane + ethanol mixtures. However, the low distribution coefficients and its solutropic behaviour makes the use of this IL inadvisable.

Recently, Cai et al.[3] tested ILs based on di-alkyl phosphate anions for the extraction of ethanol from n-heptane + ethanol azeotropic mixtures. The extraction capabilities of the ILs tested showed to decrease with the increase in the alkyl chain of both cation and anion. The IL 1,3-dimethylimidazolium dimethylphosphate ($[C_1MIM][DMP]$) displayed both higher

distribution coefficient and selectivity values than the other two ILs tested, 1-ethyl-3-methylimidazolium diethylphosphate ([C_2MIM][DEP]) and 1-butyl-3-methylimidazolium dibutylphosphate ([C_4MIM][DBP]). However, in comparison with other neat ILs, [C_1MIM][DMP] still presents lower selectivity and distribution coefficient values than the alkyl sulfate-based ILs.

When comparing the performance of the IL-IS mixtures used in this work with the bis(trifluoromethylsulfonyl)imide-based ILs found in literature, it can be seen that IL-IS mixtures greatly outperform ILs both in terms of the distribution coefficient and the selectivity values in the hole range of ethanol composition. In the case of the di-alkyl phosphate-based ILs, the IL-IS mixtures tested presented slightly higher distribution coefficient values than the [C_1MIM][DMP] and higher than the other two ILs. However, IL-IS mixtures have much higher selectivity values than [C_1MIM][DMP]. The IL [C_4-3-C_1pyr][DCA] was, so far, the neat IL that yielded the highest distribution coefficient values. However, in terms of selectivity it still falls short in comparison with the alkyl sulfate-based ILs and IL-IS mixtures tested in this work.

Regarding the alkyl sulfate-based ILs, in terms of the distribution coefficient values, SO4-SCN17 and SO4-SCN45 displayed values in the same order of magnitude as the other alkyl sulfate-based ILs found in literature,[10, 11, 14] whereas for the selectivity, it can be seen that the addition of inorganic salt greatly enhances it in comparison with the neat IL, and in the case of SO4-SCN33 higher selectivity values than those of [C_1MIM][C_1SO_4] IL can be obtained.

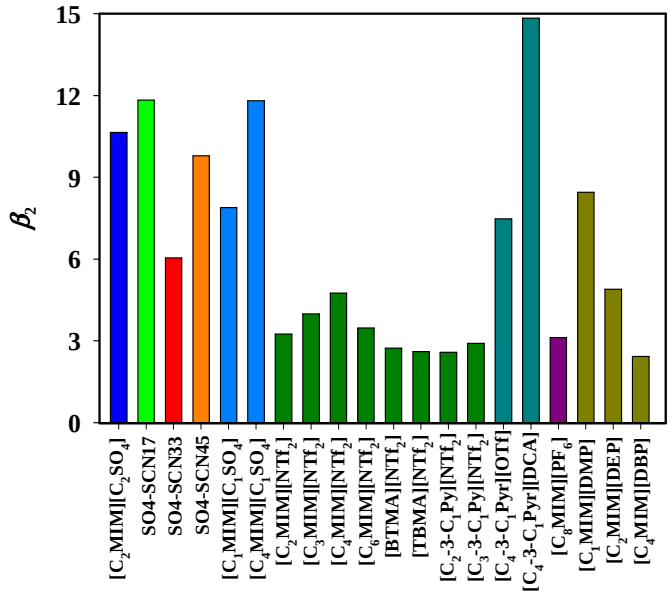

Figure 8 | Comparison of the distribution coefficient values, β_2, for the systems studied in this work and those from literature,[2, 3, 7, 8, 10-12, 14, 19] at an ethanol mass fraction between 0.02 - 0.03 wt% in n-heptane-rich phase at 298.15 K and 0.1 MPa.

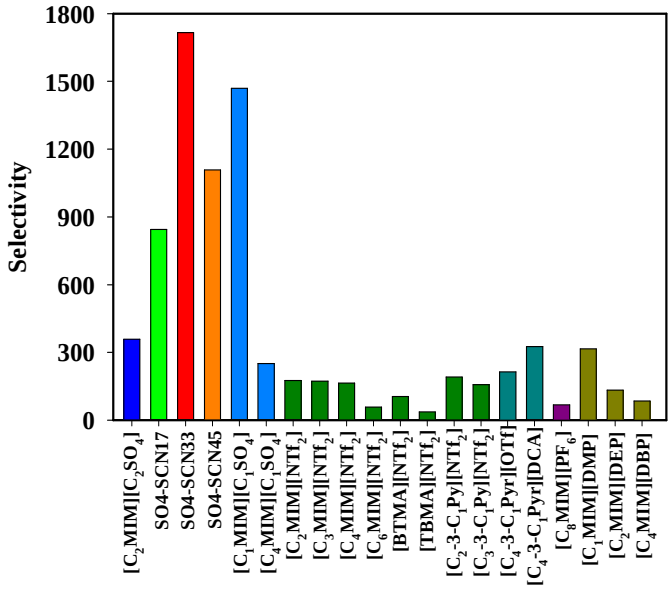

Figure 9 | Comparison of the selectivity, *S*, for the systems studied in this work and those found in literature,[2, 3, 7, 8, 10-12, 14, 19] at an ethanol mass fraction between 0.02 - 0.03 wt% in n-heptane-rich phase at 298.15 K and 0.1 MPa.

5. Conclusions

In this work, the effect of the ionicity of the ionic liquid on the separation of n-heptane + ethanol azeotropic mixtures was explored. To increase the ionicity of the IL 1-ethyl-3-methylimidazolium ethyl sulfate, the IS ammonium thiocyanate was added in three different concentrations, x_{IS} = 0.17, 0.33 and 0.45.

The LLE for the ternary systems n-heptane + ethanol + (IL-IS) was measured at 298.15 K and atmospheric pressure, and in order to analyze the IL-IS mixtures' extraction capacity, the distribution coefficients and selectivity values were determined. The results obtained show that the IL-IS mixtures tested are good candidates as extraction solvents for the n-heptane + ethanol azeotropic mixture breaking using liquid-liquid extraction process, since they proved to have higher selectivity values than the neat ILs found in literature, as well as distribution coefficient values of the same order of magnitude. Furthermore, by increasing the ionicity of a given IL, through the addition of an IS, the efficiency of the IL can be increase and a better separation for azeotropic mixtures can be obtained.

The knowledge gained in this study opens the door for the production of powerful tailor-made solvents, since a wide range of combinations of ionic liquids and inorganic salts is available at low cost.

6. Acknowledgements

Filipe S. Oliveira, Ana B. Pereiro and João M. M. Araújo gratefully acknowledge the financial support of FCT/MCTES (Portugal) through the PhD fellowship SFRH/BD/73761/2010 and the Post-Doc grants SFRH/BPD/84433/2012 and SFRH/BPD/65981/2009, respectively. Isabel M. Marrucho gratefully acknowledges Fundação para a Ciência e Tecnologia for a contract under the FCT Investigador 2012 Program.

The authors also acknowledge Fundação para a Ciência e Tecnologia for the financial support through the projects PTDC/EQU-FTT/116015/2009, PTDC/EQU-FTT/1686/2012 and PEST-OE/EQB/LA0004/2013.

7. Supplementary Information

7.1. Supporting tables

Table S1 | Composition of the experimental tie-lines, ethanol distribution coefficient (β_2) and selectivity (S) for the ternary system n-heptane + ethanol + IL-IS at 298.15 K.

n-heptane-rich phase			IL-IS-rich phase			β_2	S
w_1^I	w_2^I	w_3^I	w_1^{II}	w_2^{II}	w_3^{II}		
n-heptane (1) + ethanol (2) + SO4-SCN17 (3)							
0.994	0.004	0.002	0.002	0.113	0.885		
0.989	0.009	0.002	0.004	0.175	0.821	19.36	4512.16
0.984	0.014	0.002	0.009	0.242	0.749	17.26	1851.86
0.974	0.024	0.002	0.014	0.282	0.704	11.83	844.65
0.959	0.039	0.003	0.024	0.347	0.629	8.97	359.85
0.944	0.053	0.003	0.035	0.393	0.572	7.36	199.54
0.913	0.083	0.004	0.057	0.452	0.491	5.47	87.91
0.898	0.097	0.005	0.095	0.507	0.398	5.20	49.05
0.849	0.143	0.008	0.176	0.543	0.281	3.78	18.20
n-heptane (1) + ethanol (2) + SO4-SCN33 (3)							
0.995	0.004	0.001	0.000	0.040	0.960		
0.989	0.010	0.001	0.001	0.089	0.910	9.54	15195.70
0.984	0.014	0.002	0.002	0.138	0.860	9.66	5089.81
0.969	0.029	0.002	0.003	0.176	0.821	6.05	1715.34
0.959	0.039	0.002	0.008	0.251	0.741	6.43	740.32
0.949	0.049	0.002	0.021	0.349	0.630	7.14	330.05
0.929	0.068	0.003	0.032	0.404	0.564	5.89	170.84
0.908	0.088	0.004	0.053	0.466	0.481	5.28	90.71
0.868	0.127	0.005	0.081	0.513	0.406	4.04	43.29
0.847	0.147	0.006	0.117	0.545	0.338	3.72	26.97
0.827	0.166	0.007	0.199	0.562	0.239	3.39	14.08
n-heptane (1) + ethanol (2) + SO4-SCN45 (3)							
0.994	0.004	0.002	0.001	0.110	0.889		
0.989	0.009	0.002	0.003	0.174	0.823	20.10	7709.99
0.979	0.018	0.003	0.005	0.228	0.767	12.33	2347.45
0.969	0.028	0.003	0.008	0.278	0.714	9.79	1107.56
0.958	0.038	0.004	0.013	0.325	0.662	8.50	622.00
0.943	0.053	0.004	0.021	0.386	0.593	7.28	319.02
0.928	0.068	0.004	0.029	0.422	0.549	6.24	202.50
0.913	0.082	0.005	0.043	0.475	0.482	5.78	122.39
0.903	0.092	0.005	0.063	0.523	0.414	5.68	81.07
0.856	0.136	0.008	0.104	0.572	0.324	4.22	34.79

Table S2 | Adjustable parameters in equations 1 and 2, for the different IL-IS mixtures used.

Parameters	SO4-SCN17	SO4-SCN33	SO4-SCN45
A	1.4078	1.3829	1.3828
B	0.1753	0.2037	0.3348
C	-0.2155	-0.2111	-0.6311
D	0.0179	0.0099	0.2961

E	1.1459	1.1602	1.3118
F	0.3694	0.3726	-0.2236
G	-0.1072	-0.0724	0.6423
H	0.0091	-0.0674	-0.2901
I	1.4692	1.4593	1.3577
J	0.1954	0.1850	0.7056
K	-0.1585	-0.0916	-0.9637
L	-0.0209	-0.0612	0.3981
r^2	1.0000	1.0000	1.0000
M	99.5381	98.3916	97.9521
N	-0.2964	-0.3107	-0.3420
O	3.4670×10^{-6}	3.6275×10^{-6}	2.6354×10^{-6}
r^2	0.9988	0.9995	0.9990

7.2. Supporting figures

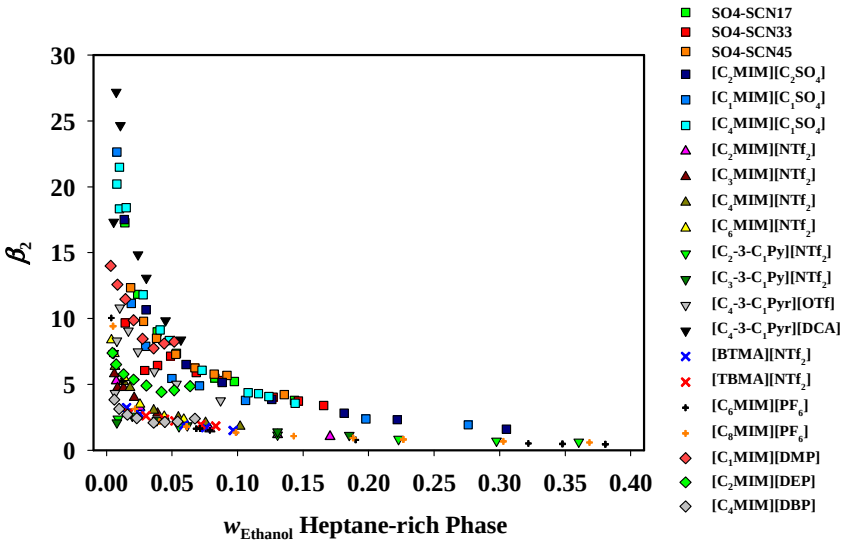

Figure S1 | Comparison of the distribution coefficient values, β_2, between the systems studied in this work and those found in literature,[2, 8, 10-12, 14, 19] as a function of the ethanol mass fraction in n-heptane-rich phase at 298.15 K and 0.1 MPa.

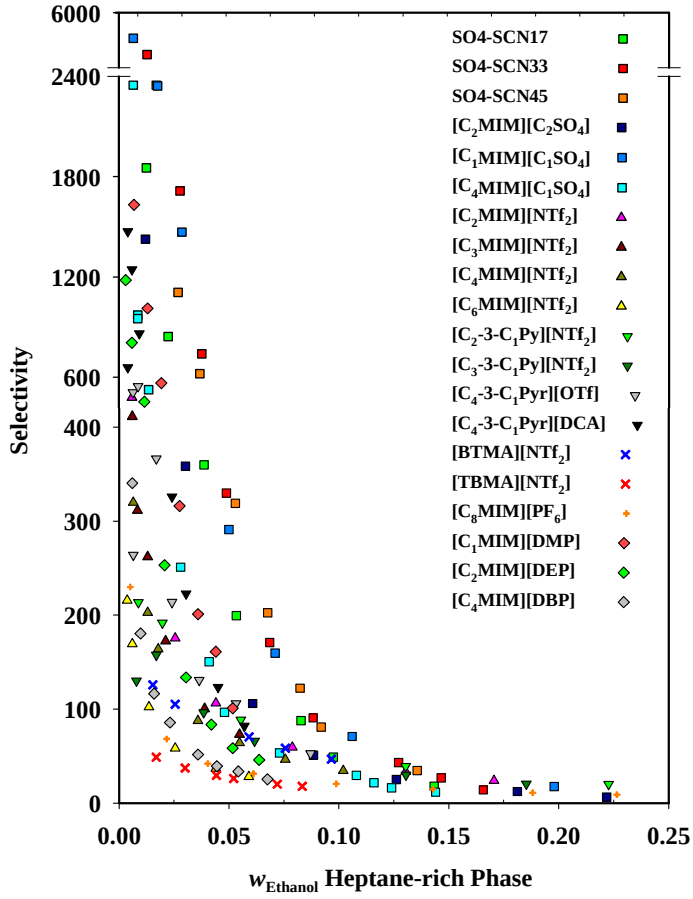

Figure S2 | Comparison of the selectivity, *S*, between the systems studied in this work and those found in literature,[2, 8, 10-12, 14, 19] as a function of the ethanol mass fraction in n-heptane-rich phase at 298.15 K and 0.1 MPa.

8. References

1. A. Pucci, Phase equilibria of alkanol/alkane mixtures in new oil and gas process development, *Pure Appl. Chem.*, 1989, **61**, 1363-1372.

2. N. M. Aranda and B. González, Cation effect of ammonium imide based ionic liquids in alcohols extraction from alcohol-alkane azeotropic mixtures, *J. Chem. Thermodyn.*, 2014, **68**, 32-39.

3. F. Cai and G. Xiao, Liquid-liquid equilibria for ternary systems ethanol + heptane + phosphoric-based ionic liquids, *Fluid Phase Equilib.*, 2015, **386**, 155-161.

4. F. Cai, M. Zhao, Y. Wang, F. Wang and G. Xiao, Phosphoric-based ionic liquids as solvents to separate the azeotropic mixture of ethanol and hexane, *J. Chem. Thermodyn.*, 2015, **81**, 177-183.

5. S. Corderí and B. González, Ethanol extraction from its azeotropic mixture with hexane employing different ionic liquids as solvents, *J. Chem. Thermodyn.*, 2012, **55**, 138-143.

6. S. Corderí, B. González, N. Calvar and E. Gómez, Ionic liquids as solvents to separate the azeotropic mixture hexane/ethanol, *Fluid Phase Equilib.*, 2013, **337**, 11-17.

7. B. González and S. Corderí, Capacity of two 1-butyl-1-methylpyrrolidinium-based ionic liquids for the extraction of ethanol from its mixtures with heptane and hexane, *Fluid Phase Equilib.*, 2013, **354**, 89-94.

8. B. González, S. Corderí and A. G. Santamaría, Application of 1-alkyl-3-methylpyridinium bis(trifluoromethylsulfonyl)imide ionic liquids for the ethanol removal from its mixtures with alkanes, *J. Chem. Thermodyn.*, 2013, **60**, 9-14.

9. F. S. Oliveira, A. B. Pereiro, L. P. N. Rebelo and I. M. Marrucho, Deep eutectic solvents as extraction media for azeotropic mixtures, *Green Chem.*, 2013, **15**, 1326-1330.

10. A. B. Pereiro, F. J. Deive, J. M. S. S. Esperança and A. Rodriguez, Alkylsulfate-based ionic liquids to separate azeotropic mixtures, *Fluid Phase Equilib.*, 2010, **294**, 49-53.

11. A. B. Pereiro and A. Rodriguez, Azeotrope-breaking using [bmim][meSO$_4$] ionic liquid in an extraction column, *Sep. Purif. Technol.*, 2008, **62**, 733-738.

12. A. B. Pereiro and A. Rodriguez, A study on the liquid-liquid equilibria of 1-alkyl-3-

methylimidazolium hexafluorophosphate with ethanol and alkanes, *Fluid Phase Equilib.*, 2008, **270**, 23-29.

13. A. B. Pereiro and A. Rodriguez, Purification of hexane with effective extraction using ionic liquid as solvent, *Green Chem.*, 2009, **11**, 346-350.

14. A. B. Pereiro and A. Rodriguez, Separation of ethanol-heptane azeotropic mixtures by solvent extraction with an ionic liquid, *Ind. Eng. Chem. Res.*, 2009, **48**, 1579-1585.

15. A. B. Pereiro and A. Rodríguez, Effective extraction in packed column of ethanol from the azeotropic mixture ethanol + hexane with an ionic liquid as solvent, *Chem. Eng. J.*, 2009, **153**, 80-85.

16. A. B. Pereiro, E. Tojo, A. Rodriguez, J. Canosa and J. Tojo, $HmimPF_6$ ionic liquid that separates the azeotropic mixture ethanol + heptane, *Green Chem.*, 2006, **8**, 307-310.

17. A.-L. Revelli, F. Mutelet and J.-N. Jaubert, Extraction of n-alcohols from n-heptane using ionic liquids, *J. Chem. Eng. Data*, 2011, **56**, 3873-3880.

18. N. R. Rodriguez, B. S. Molina and M. C. Kroon, Aliphatic + ethanol separation via liquid–liquid extraction using low transition temperature mixtures as extracting agents, *Fluid Phase Equilib.*, 2015, **394**, 71-82.

19. R. G. Seoane, E. J. González and B. González, 1-Alkyl-3-methylimidazolium bis(trifluoromethylsulfonyl)imide ionic liquids as solvents in the separation of azeotropic mixtures, *J. Chem. Thermodyn.*, 2012, **53**, 152-157.

20. A. B. Pereiro, J. M. M. Araújo, J. M. S. S. Esperança, I. M. Marrucho and L. P. N. Rebelo, Ionic liquids in separations of azeotropic systems - A review, *J. Chem. Thermodyn.*, 2012, **46**, 2-28.

21. Z. Lei, C. Li and B. Chen, Extractive distillation: A review, *Sep. Purif. Rev.*, 2003, **32**, 121-213.

22. A. Arce, M. J. Earle, H. Rodriguez and K. R. Seddon, Separation of benzene and hexane by solvent extraction with 1-alkyl-3-methylimidazolium bis{(trifluoromethyl)sulfonyl}amide ionic liquids: Effect of the alkyl-substituent length, *J. Phys. Chem. B*, 2007, **111**, 4732-4736.

23. A. Arce, M. J. Earle, H. Rodriguez and K. R. Seddon, Separation of aromatic hydrocarbons from alkanes using the ionic liquid 1-ethyl-3-methylimidazolium

bis{(trifluoromethyl) sulfonyl} amide, *Green Chem.*, 2007, **9**, 70-74.

24. A. Arce, M. J. Earle, H. Rodriguez, K. R. Seddon and A. Soto, 1-ethyl-3-methylimidazolium bis{(trifluoromethyl)sulfonyl}amide as solvent for the separation of aromatic and aliphatic hydrocarbons by liquid extraction - extension to C_7 and C_8 fractions, *Green Chem.*, 2008, **10**, 1294-1300.

25. A. Arce, M. J. Earle, H. Rodriguez, K. R. Seddon and A. Soto, Bis{(trifluoromethyl)sulfonyl}amide ionic liquids as solvents for the extraction of aromatic hydrocarbons from their mixtures with alkanes: Effect of the nature of the cation, *Green Chem.*, 2009, **11**, 365-372.

26. A. Arce, M. J. Earle, H. Rodriguez, K. R. Seddon and A. Soto, Isomer effect in the separation of octane and xylenes using the ionic liquid 1-ethyl-3-methylimidazolium bis{(trifluoromethyl)sulfonyl}amide, *Fluid Phase Equilib.*, 2010, **294**, 180-186.

27. J. García, A. Fernández, J. S. Torrecilla, M. Oliet and F. Rodríguez, Liquid–liquid equilibria for {hexane + benzene + 1-ethyl-3-methylimidazolium ethylsulfate} at (298.2, 313.2 and 328.2) K, *Fluid Phase Equilib.*, 2009, **282**, 117-120.

28. S. García, M. Larriba, J. García, J. S. Torrecilla and F. Rodríguez, 1-alkyl-2,3-dimethylimidazolium bis(trifluoromethylsulfonyl)imide ionic liquids for the liquid–liquid extraction of toluene from heptane, *J. Chem. Eng. Data*, 2011, **56**, 3468-3474.

29. S. García, M. Larriba, J. García, J. S. Torrecilla and F. Rodríguez, Liquid−liquid extraction of toluene from heptane using 1-alkyl-3-methylimidazolium bis(trifluoromethylsulfonyl)imide ionic liquids, *J. Chem. Eng. Data*, 2011, **56**, 113-118.

30. G. W. Meindersma and A. B. de Haan, Cyano-containing ionic liquids for the extraction of aromatic hydrocarbons from an aromatic/aliphatic mixture, *Sci. China Chem.*, 2012, **55**, 1488-1499.

31. G. W. Meindersma, A. R. Hansmeier and A. B. de Haan, Ionic liquids for aromatics extraction. Present status and future outlook, *Ind. Eng. Chem. Res.*, 2010, **49**, 7530-7540.

32. E. J. González, N. Calvar, E. Gómez and A. n. Domínguez, Separation of benzene from linear alkanes (C_6−C_9) using 1-ethyl-3-methylimidazolium ethyl sulfate at T = 298.15 K, *J. Chem. Eng. Data*, 2010, **55**, 3422-3427.

33. A. B. Pereiro and A. Rodriguez, Ternary (liquid + liquid) equilibria of the azeotrope

(ethyl acetate + 2-propanol) with different ionic liquids at T=298.15 K, *J. Chem. Thermodyn.*, 2007, **39**, 1608-1613.

34. A. B. Pereiro and A. Rodriguez, Phase equilibria of the azeotropic mixture hexane + ethyl acetate with ionic liquids at 298.15 K, *J. Chem. Eng. Data*, 2008, **53**, 1360-1366.

35. D. Naydenov and H.-J. Bart, Ternary liquid−liquid equilibria for six systems containing ethyl acetate + ethanol or acetic acid + an imidazolium-based ionic liquid with a hydrogen sulfate anion at 313.2 K, *J. Chem. Eng. Data*, 2007, **52**, 2375-2381.

36. A. B. Pereiro and A. Rodriguez, Ternary liquid-liquid equilibria ethanol + 2-butanone + 1-butyl-3-methylimidazolium hexafluorophosphate, 2-propanol + 2-butanone + 1-butyl-3-methylimidazolium hexafluorophosphate, and 2-butanone + 2-propanol + 1,3-dimethylimidazolium methyl sulfate at 298.15 K, *J. Chem. Eng. Data*, 2007, **52**, 2138-2142.

37. A. B. Pereiro and A. Rodriguez, Measurement and correlation of (liquid + liquid) equilibrium of the azeotrope (cyclohexane + 2-butanone) with different ionic liquids at T=298.15 K, *J. Chem. Thermodyn.*, 2008, **40**, 1282-1289.

38. A. Arce, H. Rodriguez and A. Soto, Purification of ethyl tert-butyl ether from its mixtures with ethanol by using an ionic liquid, *Chem. Eng. J.*, 2006, **115**, 219-223.

39. A. Arce, H. Rodriguez and A. Soto, Use of a green and cheap ionic liquid to purify gasoline octane boosters, *Green Chem.*, 2007, **9**, 247-253.

40. A. Arce, H. Rodriguez and A. Soto, Effect of anion fluorination in 1-ethyl-3-methylimidazolium as solvent for the liquid extraction of ethanol from ethyl tert-butyl ether, *Fluid Phase Equilib.*, 2006, **242**, 164-168.

41. I. C. Hwang, S. J. Park and R. H. Kwon, Liquid-liquid equilibria for ternary mixtures of methyl tert-amyl ether + methanol (or ethanol) + imidazolium-based ionic liquids at 298.15 K, *Fluid Phase Equilib.*, 2012, **316**, 11-16.

42. A. B. Pereiro, J. M. M. Araújo, F. S. Oliveira, J. M. S. S. Esperança, J. N. C. Lopes, I. M. Marrucho and L. P. N. Rebelo, Solubility of inorganic salts in pure ionic liquids, *J. Chem. Thermodyn.*, 2012, **55**, 29-36.

43. F. S. Oliveira, A. B. Pereiro, J. M. M. Araújo, C. E. S. Bernardes, J. N. Canongia Lopes, S. Todorovic, G. Feio, P. L. Almeida, L. P. N. Rebelo and I. M. Marrucho, High ionicity ionic liquids (HIILs): Comparing the effect of -ethylsulfonate and -ethylsulfate anions,

Phys. Chem. Chem. Phys., 2013, **15**, 18138-18147.

44. A. B. Pereiro, J. M. M. Araújo, F. S. Oliveira, C. E. S. Bernardes, J. M. S. S. Esperança, J. N. C. Lopes, I. M. Marrucho and L. P. N. Rebelo, Inorganic salts in purely ionic liquid media: The development of high ionicity ionic liquids (HIILs), *Chem. Commun.*, 2012, **48**, 3656-3658.

45. F. S. Oliveira, L. P. N. Rebelo and I. M. Marrucho, Influence of different inorganic salts on the ionicity and thermophysical properties of 1-ethyl-3-methylimidazolium acetate ionic liquid, *J. Chem. Eng. Data*, 2015, **60**, 781-789.

46. W. Xu, E. I. Cooper and C. A. Angell, Ionic liquids: Ion mobilities, glass temperatures, and fragilities, *J. Phys. Chem. B*, 2003, **107**, 6170-6178.

47. H. Tokuda, S. Tsuzuki, M. Susan, K. Hayamizu and M. Watanabe, How ionic are room-temperature ionic liquids? An indicator of the physicochemical properties, *J. Phys. Chem. B*, 2006, **110**, 19593-19600.

48. K. Ueno, H. Tokuda and M. Watanabe, Ionicity in ionic liquids: Correlation with ionic structure and physicochemical properties, *Phys. Chem. Chem. Phys.*, 2010, **12**, 1649-1658.

49. Z. Lei, X. Xi, C. Dai, J. Zhu and B. Chen, Extractive distillation with the mixture of ionic liquid and solid inorganic salt as entrainers, *AIChE J.*, 2014, **60**, 2994-3004.

50. J. D. Holbrey, W. M. Reichert, R. P. Swatloski, G. A. Broker, W. R. Pitner, K. R. Seddon and R. D. Rogers, Efficient, halide free synthesis of new, low cost ionic liquids: 1,3-dialkylimidazolium salts containing methyl- and ethyl-sulfate anions, *Green Chem.*, 2002, **4**, 407-413.

Chapter 5

Combining one IL with different ISs for the separation of ethanol from n-heptane

Adapted from: **Filipe S. Oliveira**, Ralf Dohrn, Luís P. N. Rebelo and Isabel M. Marrucho, Improving the separation of n-heptane + ethanol azeotropic mixtures combining the ionic liquid 1-ethyl-3-methylimidazolium acetate with different inorganic salts, *manuscript in preparation,* 2015.

The author was involved in all the experiments, as well as on the discussion, interpretation and preparation of the manuscript.

1. Abstract

In this work, the ionic liquid (IL) 1-ethyl-3-methylimidazolium acetate, [C_2MIM][Ac], was combined with three inorganic salts (ISs), namely ammonium acetate, [NH_4][Ac], ammonium chloride, [NH_4]Cl, and ammonium thiocyanate, [NH_4][SCN], and used as extraction solvent for the separation of the azeotropic mixture of n-heptane + ethanol. The liquid-liquid equilibria (LLE) of the ternary mixtures of n-heptane + ethanol + IL and (IL-IS) was experimentally measured at 298.15 K and 0.1 MPa. The feasibility of the used extraction solvents was assessed by calculation of the distribution coefficient and the selectivity. The results showed that the extraction solvents studied are suitable candidates for the separation of ethanol from n-heptane. Additionally, we show that the solubilisation of ISs in the IL can greatly increase the selectivity of the latter, while no significant impact on the distribution coefficient is verified. Moreover, the distribution coefficient values obtained for the [C_2MIM][Ac] and its mixtures with ISs are the highest among the neat ILs tested so far for the azeotropic mixture under study.

2. Introduction

In the last decades, the volume of oxygenated additives used in gasolines has been increasing from year to year. Lower alkyl chain alcohols, such as methanol, ethanol or butanol, and ethers such as, methyl-*tert*-butyl ether (MTBE), ethyl *tert*-butyl ether (ETBE) and *ter*-amyl ethyl ether (TAEE) are typical examples of oxygenated additives. These compounds are known for their higher octane number, which allows a boost in combustibility and the reduction of CO emissions, when added to gasolines. Due to the discontinuation of lead-based additives, the production of oxygenated compounds has gradually become higher, and along with it a growing number of processes in which alkanes and alcohols co-exist have emerged.[1-3]

The presence of an azeotropic point in mixtures of n-hexane or n-heptane + ethanol makes it impossible to separate these mixtures by a simple distillation, hence other techniques must be used. In literature, the separation of azeotropic mixtures of alkanes +

ethanol has already been studied by several groups, using liquid-liquid extraction and ionic liquids (ILs) as extraction solvents. Letcher et al.[4] were the first researchers to test an IL as extraction solvent for the separation of mixtures of alkanes + alcohols. Using 1-methyl-3-octylimidazolium chloride, Letcher and co-workers separated alkanes such as n-heptane, dodecane and hexadecane from alcohols such as methanol or ethanol. The highest selectivity values were obtained for mixtures of hexadecane + methanol.

Pereiro et al.[5, 6] started testing hexafluorophosphate-based ILs in the separation of n-hexane or n-heptane + ethanol mixtures. The ILs selected were 1-hexyl-3-methylimidazolium hexafluorophosphate ($[C_6MIM][PF_6]$) and 1-octyl-3-methylimidazolium hexafluorophosphate ($[C_8MIM][PF_6]$). Both proved to break the azeotropic point of the tested mixtures. In the case of n-heptane + ethanol mixtures, $[C_6MIM][PF_6]$ has shown to provide very high selectivity values. However, both the low distribution coefficients and its solutropic behaviour make the use of this IL inadvisable.

Afterwards, Pereiro et al. focused on alkyl sulfate-based ILs to break the azeotrope mixtures of n-hexane or n-heptane + ethanol. The ILs tested included the 1-butyl-3-methylimidazolium methyl sulfate $[C_4MIM][C_1SO_4]$,[7, 8] 1,3-dimethylimidazolium methyl sulfate ($[C_1MIM][C_1SO_4]$)[9, 10] and 1-ethyl-3-methylimidazolium ethyl sulfate ($[C_2MIM][C_2SO_4]$).[11] All of the ILs used proved to be suitable candidates for the extraction of ethanol, particularly in mixtures of n-heptane + ethanol, where high efficiencies were obtained. In addition, it was shown that a shorter alkyl chain on the imidazolium cation led to better n-heptane/ethanol efficiencies.

More recently, several ILs based on the bis(trifluoromethylsulfonyl)imide anion have been used in the separation of n-hexane or n-heptane + ethanol azeotropic mixtures.[12-16] Seoane et al.[14] studied the effect of increasing the alkyl chain of the imidazolium cation, using four different ILs, 1-ethyl-3-methylimidazolium bis(trifluoromethylsulfonyl)imide ($[C_2MIM][NTf_2]$), 1-propyl-3-methylimidazolium bis(trifluoromethylsulfonyl)imide ($[C_3MIM][NTf_2]$), 1-butyl-3-methylimidazolium bis(trifluoromethylsulfonyl)imide ($[C_4MIM][NTf_2]$) and 1-hexyl-3-methylimidazolium bis(trifluoromethylsulfonyl)imide ($[C_6MIM][NTf_2]$); González et al.[13] tested two pyridinium-based ILs, 1-ethyl-3-methylpyridinium bis(trifluoromethylsulfonyl)imide ($[C_2\text{-}3\text{-}C_1Py][NTf_2]$) and 1-propyl-3-

methylpyridinium bis(trifluoromethylsulfonyl)imide ([C_3-3-C_1Py][NTf_2]); and Aranda et al.[12] used two tetraalkyl ammoniums, butyltrimethylammonium bis(trifluoromethylsulfonyl)imide ([BTMA][NTf_2]) and tributylmethylammonium bis(trifluoromethylsulfonyl)imide ([TBMA][NTf_2]). The results obtained from these three studies, showed similar ranges of the distribution coefficient and selectivity values, with the imidazolium-based ILs showing slightly higher values and the ammonium-based ILs the lowest.

On another related work, Corderí and González showed that pyridinium-based ILs could yield better results than imidazolium-based ILs when combined with the trifluoromethanesulfonate anion ($[OTf]^-$) instead of the $[NTf_2]^-$ anion in the separation of n-hexane + ethanol azeotropic mixtures.[15] The same authors, used three different ILs all with the same cation, 1-hexyl-3-methylimidazolium, and observed that the extraction of ethanol in n-hexane + ethanol mixtures was more effective when the dicyanamide anion ($[DCA]^-$) was used, followed by the $[OTf]^-$ anion and lastly the $[NTf_2]^-$ anion.[16] In addition, these authors also observed high distribution coefficient and selectivity values in the separation of n-hexane or n-heptane + ethanol mixtures, using the 1-butyl-1-methylpyrrolidinium cation ($[C_4$-3-C_1pyr$]^+$) combined with $[DCA]^-$ or $[OTf]^-$ anions.[17]

Cai et al.[18, 19] used phosphate-based ILs in the separation of n-hexane or n-heptane + ethanol azeotropic mixtures. The results obtained showed that smaller alkyl chains in both the cation and / or the anion are preferential, with the IL 1,3-dimethylimidazolium dimethylphosphate ([C_1MIM][DMP]) showing higher efficiency in both n-hexane and n-heptane systems than the other two ILs tested, 1-ethyl-3-methylimidazolium diethylphosphate ([C_2MIM][DEP]) and 1-butyl-3-methylimidazolium dibutylphosphate ([C_4MIM][DBP]).

Moreover, the use of deep eutectic solvents, based on combinations of cholinium chloride with different organic acids or alcohols, has also been attempted by some of us[20] and Rodriguez et al.[21] These compounds proved to be highly efficient extraction solvents for the separation of n-heptane + ethanol mixtures, due to their ability to form H-bonds with ethanol. However, despite the higher selectivity values presented by these compounds, their distribution coefficients fall in the same range of those of neat ILs.

In this work, we explore the use of combinations of one IL and several ISs as

extraction solvents for azeotropic mixtures. It is our hope to combine the advantages of the ILs, easy operation / liquid state and non-volatility with the advantages of ISs, namely their high separation ability. The use of mixtures of IL-IS as separating agents for azeotropic mixtures has already been attempted by Lei et al.[22] in the separation of water + ethanol mixtures by extractive distillation, where it was shown that the addition of potassium acetate to the IL effectively increased the volatility of ethanol to water, allowing a better separation of the azeotropic mixture. Furthermore, in our previous work (described in the previous chapter of this thesis),[23] we also showed that by combination the IL 1-ethyl-3-methylimidazolium ethyl sulfate ($[C_2MIM][C_2SO_4]$) with different amounts of $[NH_4][SCN]$ (SO4-SCN17, SO4-SCN33 and SO4-SCN45), the selectivity values could be increased due to the higher ionicity of the mixtures, leading to a higher efficiency in the extraction of ethanol from n-heptane + ethanol azeotropic mixtures.

Therefore, and as a continuation of our previous work, in this study we used mixtures of the IL 1-ethyl-3-methylimidazolium acetate ($[C_2MIM][Ac]$) with the same concentration of three different inorganic salts (ISs), ammonium acetate ($[NH_4][Ac]$), ammonium chloride ($[NH_4]Cl$) and ammonium thiocyanate ($[NH_4][SCN]$) as extraction solvents for n-heptane + ethanol azeotropic mixtures. The liquid-liquid equilibria for the ternary systems n-heptane + ethanol + IL or IL-IS was measured at 298.15 K and 0.1 MPa and the distribution coefficient and selectivity parameters were determined in order to assess the feasibility of the IL and IL-IS mixtures as extraction solvents.

3. Experimental Section

3.1. Materials

N-heptane and ethanol were supplied by Riedel-de-Haën with 99 % purity and by Scharlau with 99.9 % purity, respectively. The inorganic salts, ammonium acetate ($[NH_4][Ac]$), ammonium chloride ($[NH_4]Cl$) and ammonium thiocyanate ($[NH_4][SCN]$), were all provided by Sigma-Aldrich with a purity content superior to 98.0 %, 99.5 % and 99.0 %, respectively and were used as received.

The ionic liquid 1-ethyl-3-methylimidazolium acetate ([C_2MIM][Ac]) was purchased from Iolitec with a mass fraction purity of ≥ 95 %. ^{1}H NMR was used for purity check and the water content was measured by Karl Fischer coulometric titration (Metrohm 831 KF Coulometer). The ionic liquid was used as received and the final water mass fraction ranged between 5000 − 8000 ppm of water.

3.2. Mixtures of ionic liquid with inorganic salts

Three different inorganic salts, [NH_4][Ac], [NH_4]Cl and [NH_4][SCN] were combined with the same ionic liquid [C_2MIM][Ac]. All of the IL-IS mixtures were prepared at the same IS concentration, 0.33 mole fraction, i.e., 1 mol of IS per 2 mol of IL. This concentration was chosen because it allows a direct comparison of the effects caused by the different ISs, but mainly due to the higher ionicity of the system at this mole fraction. Table 1, presents the ionicity of the IL-IS mixtures tested, calculated by the Walden Plot method. In this method, the determination of the ionicity is made by considering the deviation of the solution / compound from the ideal Walden line (ideal electrolyte), meaning that a smaller deviation leads to a higher ionicity.

Table 1 | Ionicity (ΔW) calculated from the Walden Plot deviations at 298.15 K for the neat IL and the mixtures of IL + IS tested in this work.

Solvent	ΔW [a]
[C_2MIM][Ac]	0.1238
0.67 [C_2MIM][Ac] + 0.33 [NH_4][Ac] (AC-33AC)	0.0881
0.67 [C_2MIM][Ac] + 0.33 [NH_4]Cl (AC-33CL)	0.0078
0.67 [C_2MIM][Ac] + 0.33 [NH_4][SCN] (AC-33SCN)	-0.0098

[a] Ionicity data were taken from literature.[24]

3.3. Liquid-liquid equilibria measurements

The ternary liquid-liquid equilibria (LLE) experiments were performed at 298.15 K in a glass cell thermostatically regulated by a water jacket connected to an external water bath

controlled to ± 0.01 K. The temperature in the cell was measured with a platinum resistance thermometer coupled to a Keithley 199 System DMM/Scanner that was calibrated with high–accuracy mercury thermometers (0.01 K). The mixing was assured by a magnetic stirrer.

The binodal curve of the ternary system was determined by preparing several binary mixtures of IL or (IL+IS) + n-heptane in the immiscible region and then ethanol was added until the ternary mixture became miscible. Afterwards, the density and the refractive index of those ternary mixtures were determined in duplicate. The measurements of density and refractive index were both performed at 303.15 K and atmospheric pressure, in order to assure that no phase splitting occurred during the measurements. The density measurements were performed using an automated Anton Paar Densimiter DMA 5000, while the refractive index measurements were performed using an automated Anton Paar Refractometer Abbemat 500, where the relative standard deviation of the measurements was 0.007 % and 0.002 % for the density and the refractive index, respectively.

The determination of the tie-lines was performed by preparing ternary mixtures of known composition that were vigorously stirred for at least 1 h and left to settle for at least 12 h in a thermostatic bath at 298.15 K. Then, samples from both phases were taken with a syringe and their densities and refractive indexes were determined in duplicate. The composition of both phases in equilibrium was calculated by MATLAB, using the fitting of the densities and of the refractive indexes versus composition along the binodal curve by the following equations:

$$\rho = A \cdot w_1 + B \cdot w_1^2 + C \cdot w_1^3 + D \cdot w_1^4 + E \cdot w_2 + F \cdot w_2^2 + G \cdot w_2^3 + H \cdot w_2^4 + I \cdot w_3 + J \cdot w_3^2 + K \cdot w_3^3 + L \cdot w_3^4 \quad (1)$$

$$n_D = M \cdot w_1 + N \cdot w_1^2 + O \cdot w_1^3 + P \cdot w_1^4 + Q \cdot w_2 + R \cdot w_2^2 + S \cdot w_2^3 + T \cdot w_2^4 + U \cdot w_3 + V \cdot w_3^2 + W \cdot w_3^3 + X \cdot w_3^4 \quad (2)$$

$$w_3 = 1 - (w_1 + w_2) \quad (3)$$

where, ρ and n_D correspond to the density and refractive index, respectively, w_1, w_2 and w_3 correspond to the mass fraction compositions of heptane, ethanol and IL or IL-IS, respectively, and *A* to *X* are adjustable parameters which are given in Table S2 in the supporting information (SI). The root-mean-square deviations obtained for the fittings were always lower than 0.02 % and 0.03 % for the refractive indexes and the density, respectively in all systems studied. In order to determine the uncertainty of the composition of the tie lines, duplicate samples with the same initial composition were prepared and their respective tie-lines were calculated, showing a standard deviation lower than 0.003 in the mass fraction.

4. Results and discussion

4.1. Ternary diagrams

The ternary diagrams for the systems n-heptane (1) + ethanol (2) + IL or IL-IS (3) obtained at 298.15 K and 0.1 MPa are presented in Figures 1-4 in mass fraction and Figures S1-S4 in the SI in mole fraction. From the inspection of these Figures, it can be seen that in all systems studied either using the neat IL or the IL-IS mixtures, large immiscibility regions were obtained independently of the extraction solvent used, where the n-heptane is always immiscible in the IL or IL-IS mixtures and the ethanol is always miscible in the whole composition range in both n-heptane and extraction solvent. In addition, Figure S5 in the SI depicts a comparison between the binodal curves of all studied extraction solvents in this work, where it is shown that the addition of IS to the IL increases the immiscibility region. This behaviour is consistent with that found in our previous work where different amounts of the same IS ([NH_4][SCN]) were added to the IL [C_2MIM][C_2SO_4], and it was observed that the immiscibility region increased as the [NH_4][SCN] content increased as well.[23] In this study, the IS [NH_4][Ac] showed the smallest increase of the immiscibility region, possibly due to the effect of the common ion, whereas the two other ISs, [NH_4]Cl and [NH_4][SCN], showed similar increments on the immiscibility region.

Moreover, Figures 1-4 also show the tie-lines calculated for each extraction solvent,

where it can be seen that positive slopes were obtained for all systems. This behaviour indicates that ethanol is more soluble than n-heptane in the extraction solvents studied, meaning that the extraction of ethanol from n-heptane is always favourable. Indeed, in Table S1 in the SI, the compositions for the tie-lines are presented and it is clear that in the n-heptane-rich phase of every system studied, the compositions of ethanol and IL or IL-IS are always very low, in some cases they fall below the error of our determination method and consequently the distribution coefficient and selectivity values cannot be calculated.

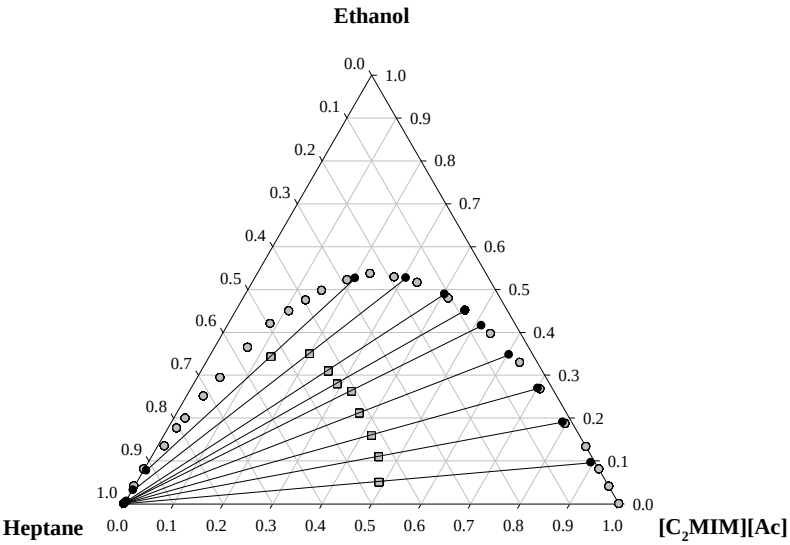

Figure 1 | Ternary diagram for the system n-heptane (1) + ethanol (2) + [C2MIM][Ac] (3) at 298.15 K and 0.1 MPa. The grey dots represent the binodal curve, the grey squares the composition of the initial mixture, the black dots the composition of the co-exiting phases and the lines represent the tie-lines. Compositions are given in mass fraction.

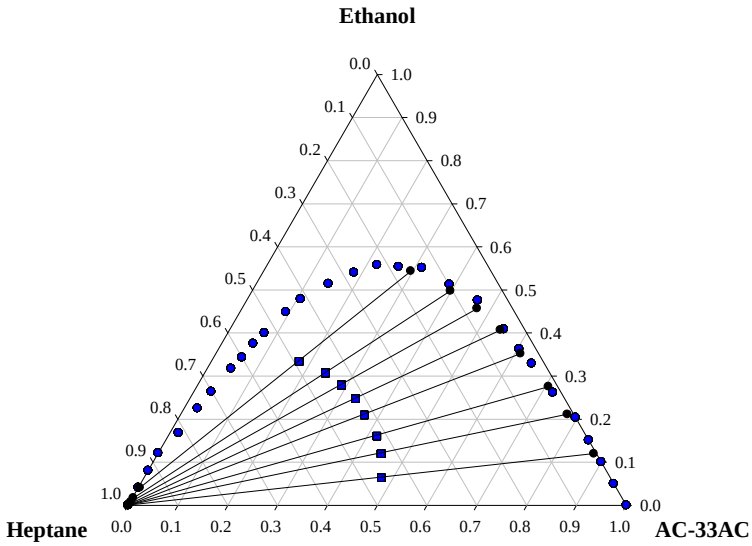

Figure 2 | Ternary diagram for the system n-heptane (1) + ethanol (2) + (0.67[C_2MIM][Ac] + 0.33[NH_4][Ac]) (3) at 298.15 K and 0.1 MPa. The blue dots represent the binodal curve, the blue squares the composition of the initial mixture, the black dots the composition of the co-exiting phases and the lines represent the tie-lines. Compositions are given in mass fraction.

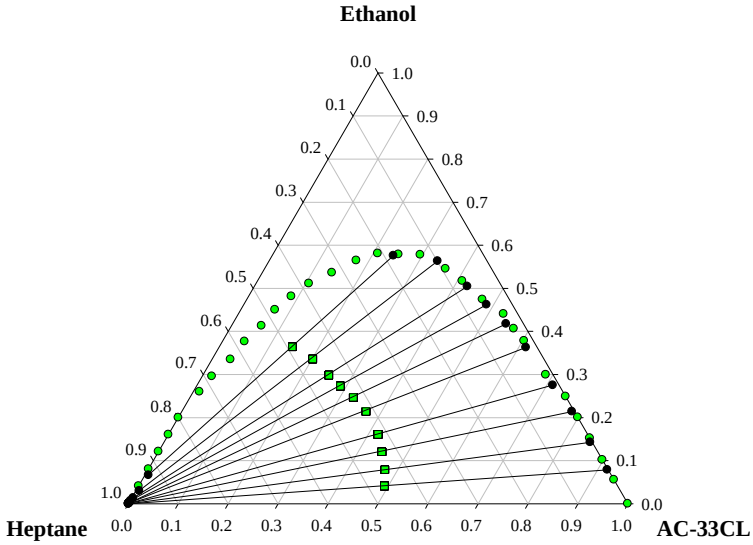

Figure 3 | Ternary diagram for the system n-heptane (1) + ethanol (2) + (0.67[C_2MIM][Ac] + 0.33[NH_4]Cl) (3) at 298.15 K and 0.1 MPa. The green dots represent the binodal curve, the green squares the composition of the initial mixture, the black dots the composition of the co-exiting phases and the lines represent the tie-lines. Compositions are given in mass fraction.

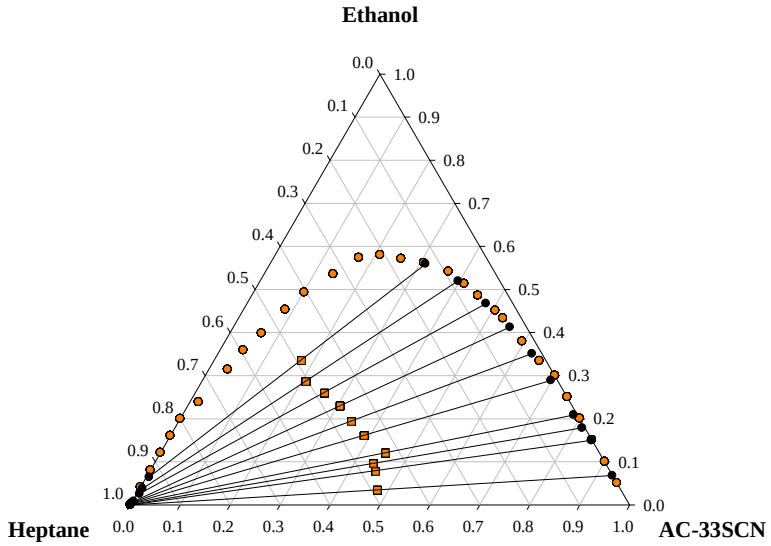

Figure 4 | Ternary diagram for the system n-heptane (1) + ethanol (2) + (0.67[C_2MIM][Ac] + 0.33[NH_4][SCN]) (3) at 298.15 K and 0.1 MPa. The orange dots represent the binodal curve, the orange squares the composition of the initial mixture, the black dots the composition of the co-exiting phases and the lines represent the tie-lines. Compositions are given in mass fraction.

4.2. Distribution coefficient and selectivity

In order to evaluate the feasibility of the neat IL and the mixtures of IL-IS in the separation of n-heptane + ethanol mixtures, two widely used parameters were calculated, the distribution coefficient and the selectivity. Since we are evaluating the ability of the extraction solvent (IL or IL-IS) to extract ethanol from n-heptane, the distribution coefficient, β, was calculated in respect to ethanol as shown in the following equation:

$$\beta_2 = \frac{w_2^{II}}{w_2^{I}} \tag{4}$$

where w_2^{I} and w_2^{II} represent the mass fraction of ethanol in the n-heptane rich phase

(upper phase) and in the IL or IL-IS rich phase (lower phase), respectively.

The distribution coefficient represents the ratio between the amount of ethanol that is extracted to the IL or IL-IS and the amount that remains in the n-heptane phase, thus accounting for the solute-carrying capacity of the extraction solvent. Figure 5 depicts the distribution coefficients obtained for all systems studied as a function of the mass fraction of ethanol in the n-heptane rich phase. These values are also presented in Table S1 in the SI. As expected, the distribution coefficient increases as the concentration of ethanol decreases in the n-heptane rich phase. In addition, the values obtained are very similar for all the systems, meaning that the addition of the IS or the increase in the ionicity did not promote a significant effect on this parameter. Nevertheless, the distribution coefficients presented are higher than those obtained using other neat ILs or other IL-IS mixtures as shown in Figure S6 in the SI, consistently showing values superior to 10 for $w_2^l < 0.05$. The high distribution coefficients obtained were somewhat expected due to the presence of the acetate anion on the IL, which will certainly establishes stronger H-bond interactions with the ethanol, owing to its carboxylate group -COO^-. A higher distribution coefficient allows the use of lower amounts of extraction solvent and usually leads to a lower solvent flow rate, a smaller-diameter column and lower operating costs.

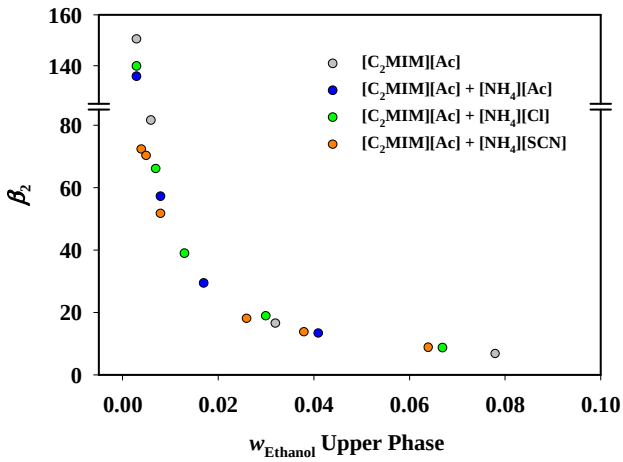

Figure 5 | Distribution coefficient values, β_2, for the ternary systems n-heptane (1) + ethanol (2) + IL or IL-IS (3), as a function of ethanol mass fraction in the n-heptane-rich phase at 298.15 K and 0.1 MPa.

The selectivity, *S*, is the parameter that evaluates the efficiency of the extraction solvent, indicating the ease of extraction of the solute, ethanol, from its diluent, n-heptane, and was determined by the following equation:

$$S = \frac{w_1^I}{w_1^{II}} \times \beta_2 \quad (5)$$

where, β_2 is the distribution coefficient of ethanol and w_1^I and w_1^{II} are the mass fractions of n-heptane in the n-heptane rich phase (upper phase) and IL or IL-IS rich phase (lower phase), respectively.

Figure 6 and Table S1 in the SI present the selectivity values obtained for all the systems studied. In agreement with the β_2 behaviour, the selectivity also increases as the concentration of ethanol decreases in the n-heptane rich phase. As shown in Figure 6, the addition of IS to the IL positively affects this parameter and a relation with the ionicity of the system is possible to establish. It can be seen that the selectivity increases according to the following trend, [C_2MIM][Ac] < AC-33AC < AC-33CL < AC-33SCN, which follows the same order as the ionicity of these extraction solvents, presented in Table 1. An increase in ionicity means that more ions become more mobile in the media. As a consequence, these ions create stronger interactions with ethanol, leading to an increase in selectivity. In our previous work,[23] we had already shown that by increasing the ionicity of the IL, the selectivity of the extraction could also be increased, thus indicating that the addition of an IS to an IL could improve the extraction of ethanol from n-heptane + ethanol azeotropic mixtures. A high selectivity means that we have a decrease of the amount of inert, n-heptane in the studied systems, in the extract which will be the IL-IS rich phase to where the ethanol is extracted. As shown in the ternary diagrams, the addition of an IS increases the immiscibility region of the system, making the n-heptane more insoluble in the IL-IS mixture than in the neat IL, consequently leading to a reduction of its amount in the IL-IS rich phase. In addition, a higher selectivity also allows for fewer stages in the process of extraction.

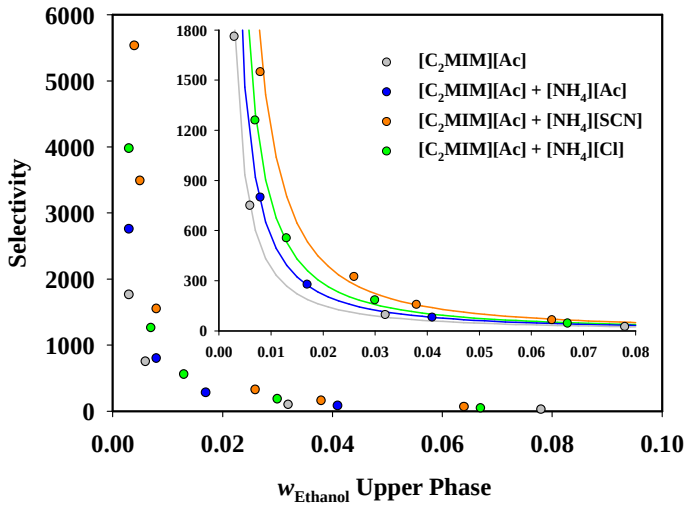

Figure 6 | Selectivity, *S*, for the ternary systems n-heptane (1) + ethanol (2) + IL or IL-IS (3), as a function of ethanol mass fraction in the n-heptane-rich phase at 298.15 K and 0.1 MPa. The inset figure represents an enlargement of the data plot, whereas the lines are just for eyes' guidance.

4.3. Comparison with literature

In this section, the β and the *S* values obtained in this work were compared with those of other neat ILs and IL-IS mixtures found in literature for the same azeotropic mixture.

The β values found in literature are expressed in mole fractions, hence they were converted to mass fraction because of the large differences in the molecular weights of the ILs, which resulted in lower values of β. In Figure 7 the comparison between the β values of this work and those found in literature is establish for approximately the same concentration of ethanol, while Figure S6 in the SI depicts the same comparison in the whole ethanol concentration range.

As mentioned in the previous section, the presence of ions that can establish H-bonds with ethanol is crucial to increase the β values. Since ethanol is a compound of small molecular weight and with an -OH group, IL or IL-IS mixtures with smaller ions and the capacity to establish H-bonds will be preferential to the extraction of ethanol. In this way, it can be seen from Figure 7 that either the neat [C_2MIM][Ac] or its mixtures with ISs are better

suited to extract ethanol than the other neat ILs found in literature. The increase in the distribution coefficient follows the trend acetated-based ILs > dicyanamide-based ILs > sulfate-based ILs > phosphate-based ILs > $[OTf]^-$ based ILs > $[NTf_2]^-$ based ILs. In addition, it can also be seen that the anion of the IL plays a much more important role in the β values than the cation. This behaviour was also observed by Corderí et al.[16] where several ILs with the same cation combined with different anions where tested; in the works where $[NTf_2]^-$ based ILs with different cations were tested [12-14] yielding similar β values (2-4); and in the works with phosphate-based ILs,[5, 18] where $[C_8MIM][PF_6]$, that presents a longer alkyl chain than $[C_1MIM][DMP]$, $[C_2MIM][DEP]$ and $[C_4MIM][DBP]$, has a higher distribution coefficient than $[C_4MIM][DBP]$ but smaller than the other two ILs.

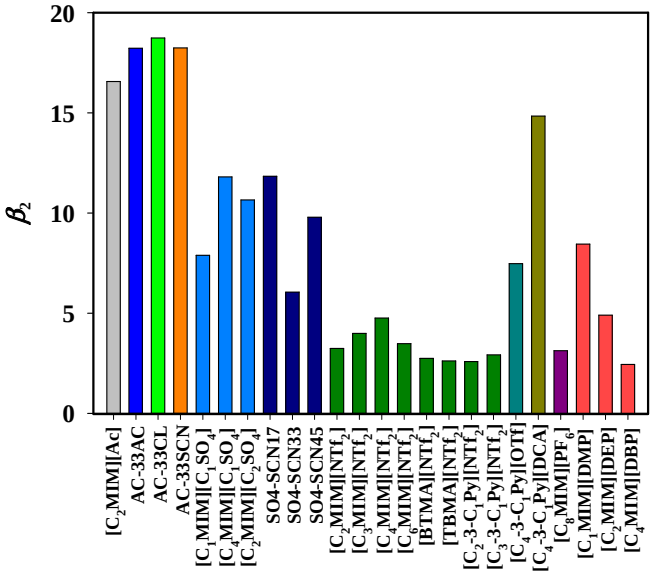

Figure 7 | Comparison between the distribution coefficient values, β_2, of the systems studied in this work, other IL-IS mixtures[23] and neat ILs found in literature.[5, 7, 9, 11-14, 17, 18] The comparison was done at an ethanol mass fraction between 0.02 - 0.03 wt% in the n-heptane-rich phase at 298.15 K and 0.1 MPa.

In Figures 8 and S7 (in the SI), the comparison between the *S* values of this work and those found in literature is established for approximately the same concentration of ethanol and in the whole ethanol concentration range, respectively. It can be seen from panel a) in Figure 8, that the ILs and IL-IS mixtures based on sulfate anions are the most efficient extraction solvents for ethanol in n-heptane + ethanol azeotropic mixtures. It was our expectation that the selectivity values found for the $[C_2MIM][Ac]$ and its mixtures with ISs would be higher than those obtained since we have an IL with a short alkyl chain in the cation and an anion capable of establishing strong H-bonds with ethanol. The reason for the lower selectivity values of the $[C_2MIM][Ac]$ and its mixtures might be due to its great solvent properties. As shown in other works, $[C_2MIM][Ac]$ as proven to be capable of dissolving a wide range of compounds, raging form different ISs,[25] to lignocellulosic materials,[26-29] proteins and enzymes[30, 31] and also of having a high performance in capturing CO_2.[32-34]

As mentioned in the previous section, the immiscibility of the IL in n-heptane may play a crucial role in the determination of the selectivity parameter. Hence, ILs that present small ability to dissolve n-heptane and that, at the same time, have low solubility in n-heptane can produce higher selectivity values. From panel b) in Figure 8, it is possible to see that as the alkyl chain of the IL increases (either in the cation or in the anion), the selectivity decreases.

Nevertheless, the results show that with the addition of an IS, the selectivity parameter can be greatly increased reaching a value of more than 3 times higher when $[NH_4][SCN]$ is added to the IL. Indeed, the AC-33SCN displayed selectivity values comparable to some of the better neat ILs, such as $[C_2MIM][C_2SO_4]$, $[C_4\text{-}3\text{-}C_1Pyr][DCA]$ and $[C_1MIM][DMP]$, and higher than the remaining neat ILs, including $[C_4MIM][C_1SO_4]$, $[C_4\text{-}3\text{-}C_1Pyr][OTf]$, some phosphate based ILs and all the $[NTf_2]^-$ based ILs.

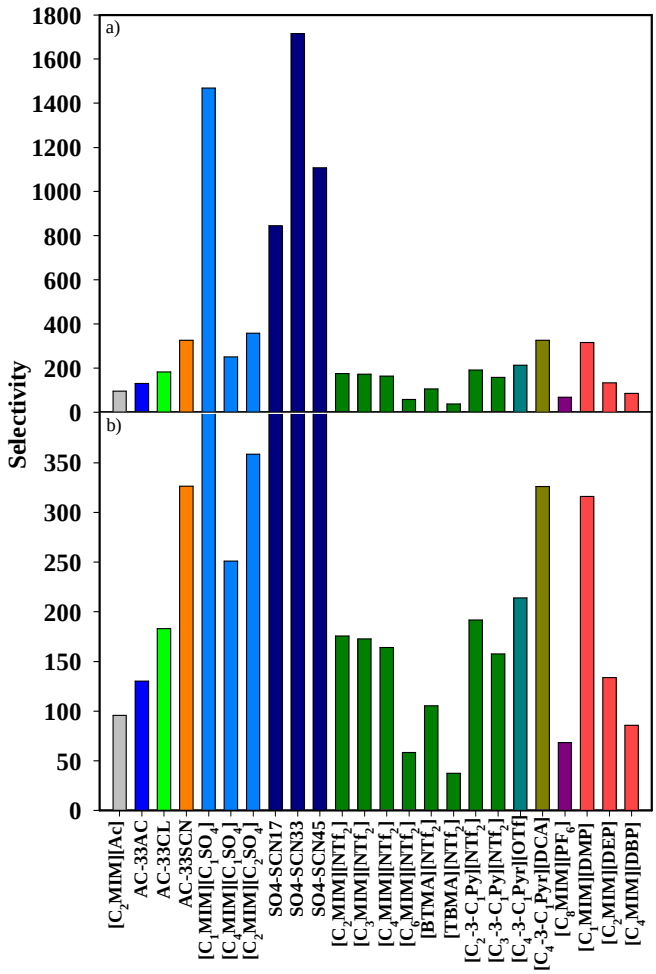

Figure 8 | Comparison between the selectivity, *S*, of the systems studied in this work, other IL-IS mixtures[23] and neat ILs found in literature.[5, 7, 9, 11-14, 17, 18] The comparison was done at an ethanol mass fraction between 0.02 - 0.03 wt% in the n-heptane-rich phase at 298.15 K and 0.1 MPa. Panel b) represents an enlargement in the scale of panel a).

5. Conclusions

In this work, the use of mixtures of an IL with different ISs was assessed for the separation of n-heptane + ethanol azeotropic mixtures. Three different ISs were tested at identical concentrations and the LLE for the ternary systems n-heptane + ethanol + IL or IL-IS was measured at 298.15 K and atmospheric pressure.

The feasibility of the IL and IL-IS mixtures was determined by the calculation of both the distribution coefficient and selectivity values. The results obtained show that the addition of the IS to the IL leads to an increase of the immiscibility region of the systems, which is translated as an increase in the selectivity of the extraction solvent. The increase in the selectivity observed followed the trend AC-33SCN > AC-33CL > AC-33AC > [C_2MIM][Ac], which could be correlated with the increase in the ionicity of the IL. The distribution coefficient values were not significantly affected by the addition of the IS; nevertheless, the data obtained showed that both ILs and IL-IS mixtures based on acetate anions lead to higher distribution coefficients than all the other neat ILs tested so far. However, the selectivity values obtained are lower than expected.

Thus, the addition of ISs to the ILs could provide a boost in the feasibility of the ILs as extraction solvents for the separation of azeotropic mixtures in LLE systems that can be obtained at a low cost. Therefore, the knowledge gained in this study may open doors for the production of more promising extraction solvents, due to the wide range of combinations that can be established between ILs and ISs.

6. Acknowledgements

Filipe S. Oliveira gratefully acknowledges the financial support of FCT/MCTES (Portugal) through the PhD fellowship SFRH/BD/73761/2010 and Isabel M. Marrucho for a contract under the FCT Investigador 2012 Program.

The authors also acknowledge Fundação para a Ciência e Tecnologia for the financial support through the research units GREEN-it "Bioresources for Sustainability" (UID/Multi/04551/2013) and UCIBIO (UID/Multi/04378/2013).

7. Supplementary Information

7.1. Supporting tables

Table S1 | Composition of the experimental tie-lines, ethanol distribution coefficient (β_2) and selectivity (S) for the ternary system n-heptane + ethanol + IL or IL-IS mixture at 298.15 K and 0.1 MPa.

n-heptane-rich phase			IL (or IL-IS)-rich phase			β_2	S
w_1^I	w_2^I	w_3^I	w_1^{II}	w_2^{II}	w_3^{II}		
n-heptane (1) + ethanol (2) + [C_2MIM][Ac] (3)							
0.999	0.001	0.000	0.009	0.096	0.895		
0.999	0.001	0.000	0.018	0.191	0.791		
0.999	0.001	0.000	0.030	0.269	0.701		
0.998	0.001	0.000	0.049	0.347	0.604		
0.997	0.002	0.001	0.070	0.416	0.514		
0.995	0.003	0.002	0.085	0.451	0.464	150.33	1759.78
0.992	0.006	0.002	0.108	0.489	0.403	81.50	748.59
0.966	0.032	0.003	0.167	0.527	0.306	16.47	95.26
0.916	0.078	0.007	0.270	0.526	0.204	6.74	22.88
n-heptane (1) + ethanol (2) + AC-33AC (3)							
1.000	0.000	0.000	0.005	0.120	0.875		
0.999	0.001	0.000	0.013	0.211	0.776		
0.999	0.001	0.000	0.018	0.276	0.706		
0.998	0.001	0.001	0.036	0.352	0.612		
0.995	0.003	0.002	0.049	0.407	0.544	135.67	2754.86
0.991	0.008	0.001	0.071	0.457	0.472	57.13	797.34
0.981	0.017	0.002	0.104	0.498	0.398	29.29	276.32
0.956	0.041	0.003	0.160	0.544	0.296	13.27	79.28
n-heptane (1) + ethanol (2) + AC-33CL (3)							
1.000	0.000	0.000	0.002	0.078	0.920		
0.999	0.000	0.001	0.004	0.143	0.853		
0.999	0.000	0.001	0.005	0.214	0.781		
0.999	0.001	0.000	0.012	0.276	0.712		
0.997	0.002	0.001	0.022	0.363	0.615		
0.996	0.003	0.001	0.035	0.419	0.546	139.67	3974.51
0.992	0.007	0.001	0.052	0.462	0.486	66.00	1259.08
0.984	0.013	0.003	0.069	0.504	0.426	38.85	553.98
0.963	0.030	0.007	0.099	0.564	0.337	18.80	182.87
0.926	0.067	0.007	0.181	0.576	0.243	8.60	43.98
n-heptane (1) + ethanol (2) + AC-33SCN (3)							
1.000	0.000	0.000	0.001	0.068	0.931		
0.999	0.000	0.001	0.002	0.150	0.848		
0.999	0.000	0.001	0.006	0.179	0.815		
0.997	0.002	0.001	0.008	0.209	0.783		
0.995	0.004	0.001	0.013	0.289	0.698	72.25	5529.90
0.993	0.005	0.002	0.020	0.351	0.629	70.20	3485.43
0.989	0.008	0.003	0.034	0.413	0.554	51.63	1547.19
0.968	0.026	0.006	0.054	0.467	0.478	18.00	322.67
0.957	0.038	0.005	0.084	0.520	0.396	13.68	155.90
0.930	0.064	0.006	0.129	0.559	0.312	8.73	62.97

Table S2 | Adjustable parameters in equations 1 and 2, for the different solvents used in this work.

Parameters	$[C_2MIM][Ac]$	AC-33AC	AC-33CL	AC-33SCN
A	0.67780	0.64858	0.65633	0.55005
B	-0.32095	0.28128	0.04087	0.55673
C	0.46530	-0.46467	0.01921	-0.94574
D	-0.14662	0.21040	-0.04101	0.51438
E	0.90884	0.72125	0.70271	0.94991
F	-0.09358	-0.07169	0.18452	-0.68974
G	-0.34012	0.30049	-0.08722	0.82553
H	0.20068	-0.08659	-0.01900	-0.18070
I	1.08803	0.95457	0.99417	0.95094
J	-0.42872	0.53033	0.26565	0.55177
K	0.61952	-0.70649	-0.17645	-0.86418
L	-0.20906	0.30020	0.03040	0.46365
r^2	1.0000	1.0000	1.0000	1.0000
M	1.37691	1.33752	1.38367	1.34106
N	0.21141	0.46716	-0.09056	0.27694
O	-0.33846	-0.94697	0.22399	-0.45943
P	0.13312	0.52517	-0.13428	0.22423
Q	1.27587	1.49145	1.30362	1.38040
R	-0.00837	-0.68609	0.23570	-0.23123
S	0.32745	0.87372	-0.26866	0.42643
T	-0.23097	-0.16862	0.04363	-0.18324
U	1.47420	1.36134	1.49779	1.45856
V	0.16394	0.65525	-0.13510	0.23751
W	-0.23724	-1.13090	0.29738	-0.37453
X	0.08233	0.59075	-0.15937	0.18470
r^2	1.0000	1.0000	1.0000	1.0000

7.2. Supporting figures

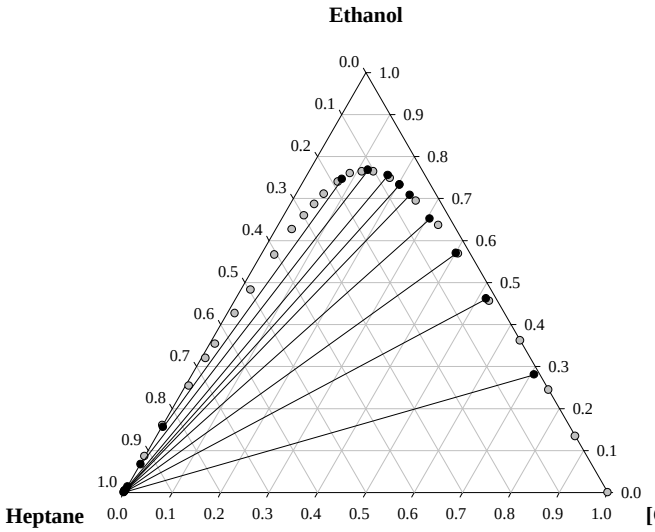

Figure S1 | Ternary diagram for the system n-heptane (1) + ethanol (2) + [C_2MIM][Ac] (3) at 298.15 K and 0.1 MPa. The gray dots represent the binodal curve, the black dots the composition of the co-exiting phases and lines the tie-lines, the compositions are given in mole fraction.

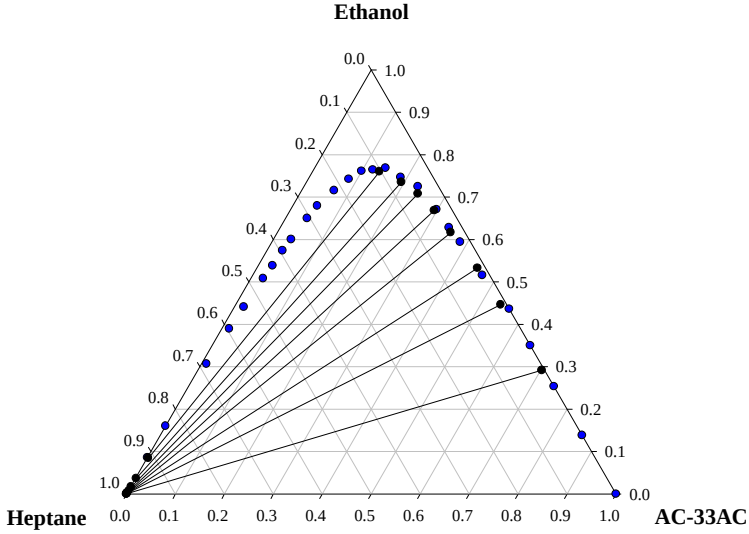

Figure S2 | Ternary diagram for the system n-heptane (1) + ethanol (2) + (0.67[C_2MIM][Ac] + 0.33[NH_4][Ac]) (3) at 298.15 K and 0.1 MPa. The blue dots represent the binodal curve, the black dots the composition of the co-exiting phases and lines the tie-lines, the compositions are given in mole fraction.

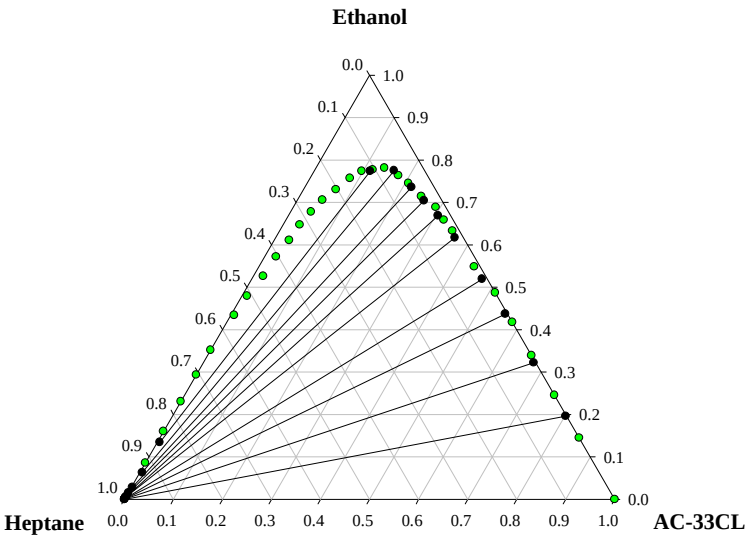

Figure S3 | Ternary diagram for the system n-heptane (1) + ethanol (2) + (0.67[C_2MIM][Ac] + 0.33[NH_4]Cl) (3) at 298.15 K and 0.1 MPa. The green dots represent the binodal curve, the black dots the composition of the co-exiting phases and lines the tie-lines, the compositions are given in mole fraction.

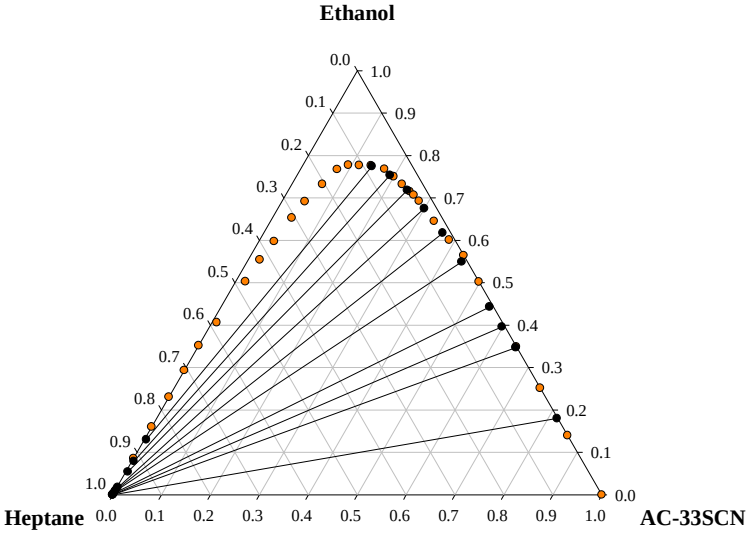

Figure S4 | Ternary diagram for the system n-heptane (1) + ethanol (2) + (0.67[C_2MIM][Ac] + 0.33[NH_4][SCN]) (3) at 298.15 K and 0.1 MPa. The orange dots represent the binodal curve, the black dots the composition of the co-exiting phases and lines the tie-lines, the compositions are given in mole fraction.

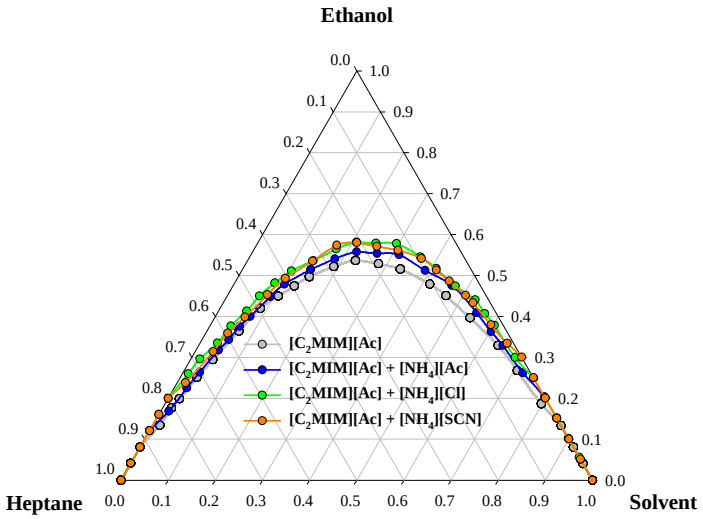

Figure S5 | Comparison between the binodal curve of the different systems studied in this work. The dots represent the experimental points obtained for each system while the line are just a guide to the eye.

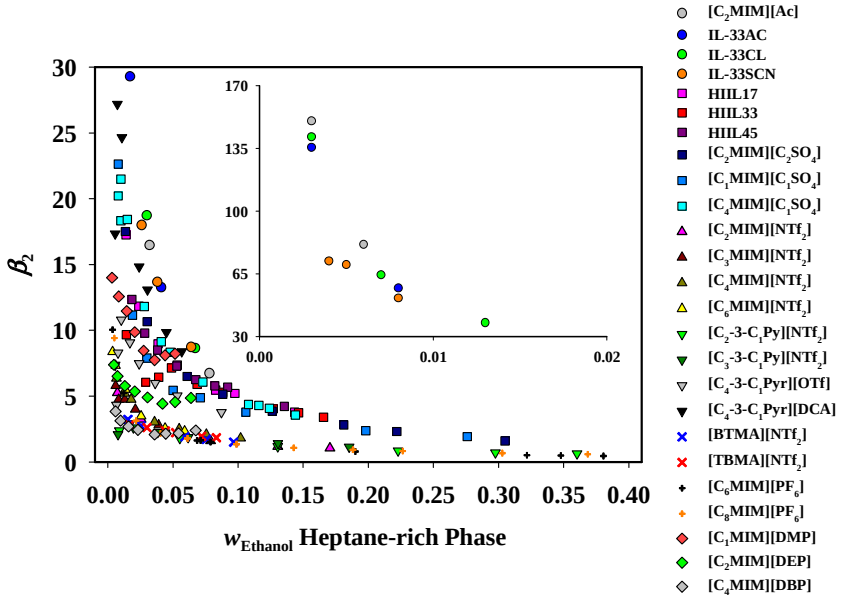

Figure S6 | Comparison between the distribution coefficient values, β_2, of the systems studied in this work, other IL-IS mixtures[23] and neat ILs found in literature.[5, 7, 9, 11-14, 17, 18] The comparison was done at 298.15 K and 0.1 MPa.

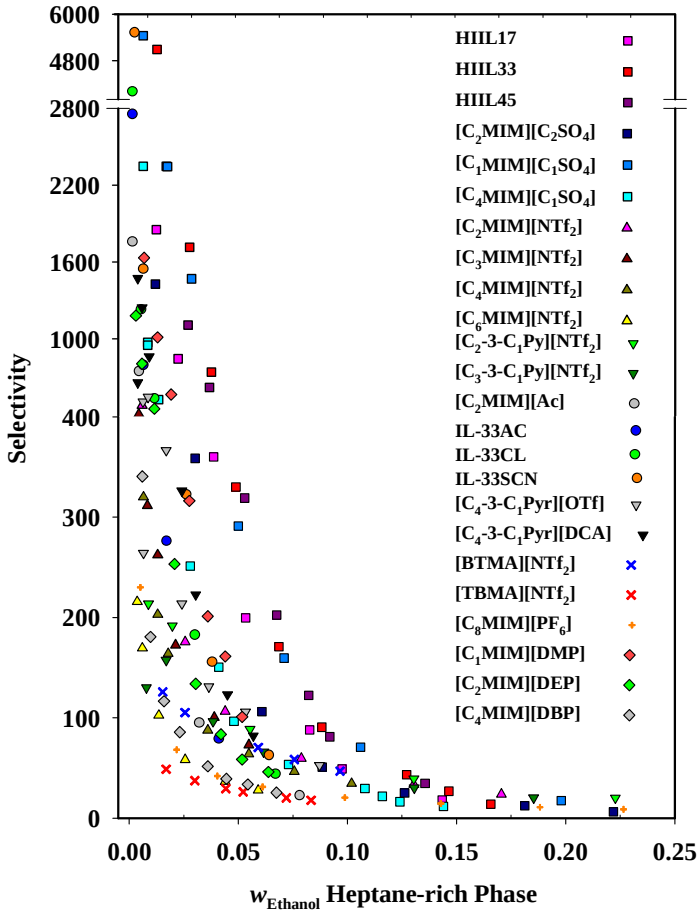

Figure S7 | Comparison between the selectivity values, *S*, of the systems studied in this work, other IL-IS mixtures[23] and neat ILs found in literature.[5, 7, 9, 11-14, 17, 18] The comparison was done at 298.15 K and 0.1 MPa.

8. References

1. A. M. Danilov, Fuel additives: Evolution and use in 1996-2000, *Chem. Technol. Fuels Oils*, 2001, **37**, 444-455.

2. S. Manzetti and O. Andersen, A review of emission products from bioethanol and its blends with gasoline. Background for new guidelines for emission control, *Fuel*, 2015, **140**, 293-301.

3. A. Pucci, Phase equilibria of alkanol/alkane mixtures in new oil and gas process development, *Pure Appl. Chem.*, 1989, **61**, 1363-1372.

4. T. M. Letcher, N. Deenadayalu, B. Soko, D. Ramjugernath and P. K. Naicker, Ternary liquid-liquid equilibria for mixtures of 1-methyl-3-octylimidazolium chloride plus an alkanol plus an alkane at 298.2 K and 1 bar, *J. Chem. Eng. Data*, 2003, **48**, 904-907.

5. A. B. Pereiro and A. Rodriguez, A study on the liquid-liquid equilibria of 1-alkyl-3-methylimidazolium hexafluorophosphate with ethanol and alkanes, *Fluid Phase Equilib.*, 2008, **270**, 23-29.

6. A. B. Pereiro, E. Tojo, A. Rodriguez, J. Canosa and J. Tojo, HmimPF$_6$ ionic liquid that separates the azeotropic mixture ethanol + heptane, *Green Chem.*, 2006, **8**, 307-310.

7. A. B. Pereiro and A. Rodriguez, Azeotrope-breaking using [bmim][meSO$_4$] ionic liquid in an extraction column, *Sep. Purif. Technol.*, 2008, **62**, 733-738.

8. A. B. Pereiro and A. Rodriguez, Purification of hexane with effective extraction using ionic liquid as solvent, *Green Chem.*, 2009, **11**, 346-350.

9. A. B. Pereiro and A. Rodriguez, Separation of ethanol-heptane azeotropic mixtures by solvent extraction with an ionic liquid, *Ind. Eng. Chem. Res.*, 2009, **48**, 1579-1585.

10. A. B. Pereiro and A. Rodríguez, Effective extraction in packed column of ethanol from the azeotropic mixture ethanol + hexane with an ionic liquid as solvent, *Chem. Eng. J.*, 2009, **153**, 80-85.

11. A. B. Pereiro, F. J. Deive, J. M. S. S. Esperança and A. Rodriguez, Alkylsulfate-based ionic liquids to separate azeotropic mixtures, *Fluid Phase Equilib.*, 2010, **294**, 49-53.

12. N. M. Aranda and B. González, Cation effect of ammonium imide based ionic liquids in alcohols extraction from alcohol-alkane azeotropic mixtures, *J. Chem. Thermodyn.*, 2014, **68**, 32-39.

13. B. González, S. Corderí and A. G. Santamaría, Application of 1-alkyl-3-methylpyridinium bis(trifluoromethylsulfonyl)imide ionic liquids for the ethanol removal from its mixtures with alkanes, *J. Chem. Thermodyn.*, 2013, **60**, 9-14.

14. R. G. Seoane, E. J. González and B. González, 1-Alkyl-3-methylimidazolium bis(trifluoromethylsulfonyl)imide ionic liquids as solvents in the separation of azeotropic mixtures, *J. Chem. Thermodyn.*, 2012, **53**, 152-157.

15. S. Corderí and B. González, Ethanol extraction from its azeotropic mixture with hexane employing different ionic liquids as solvents, *J. Chem. Thermodyn.*, 2012, **55**, 138-143.

16. S. Corderí, B. González, N. Calvar and E. Gómez, Ionic liquids as solvents to separate the azeotropic mixture hexane/ethanol, *Fluid Phase Equilib.*, 2013, **337**, 11-17.

17. B. González and S. Corderí, Capacity of two 1-butyl-1-methylpyrrolidinium-based ionic liquids for the extraction of ethanol from its mixtures with heptane and hexane, *Fluid Phase Equilib.*, 2013, **354**, 89-94.

18. F. Cai and G. Xiao, Liquid-liquid equilibria for ternary systems ethanol + heptane + phosphoric-based ionic liquids, *Fluid Phase Equilib.*, 2015, **386**, 155-161.

19. F. Cai, M. Zhao, Y. Wang, F. Wang and G. Xiao, Phosphoric-based ionic liquids as solvents to separate the azeotropic mixture of ethanol and hexane, *J. Chem. Thermodyn.*, 2015, **81**, 177-183.

20. F. S. Oliveira, A. B. Pereiro, L. P. N. Rebelo and I. M. Marrucho, Deep eutectic solvents as extraction media for azeotropic mixtures, *Green Chem.*, 2013, **15**, 1326-1330.

21. N. R. Rodriguez, B. S. Molina and M. C. Kroon, Aliphatic + ethanol separation via liquid–liquid extraction using low transition temperature mixtures as extracting agents, *Fluid Phase Equilib.*, 2015, **394**, 71-82.

22. Z. Lei, X. Xi, C. Dai, J. Zhu and B. Chen, Extractive distillation with the mixture of ionic liquid and solid inorganic salt as entrainers, *AIChE J.*, 2014, **60**, 2994-3004.

23. F. S. Oliveira, A. B. Pereiro, J. M. M. Araújo, L. P. N. Rebelo and I. M. Marrucho, Designing high ionicity ionic liquids based on 1-ethyl-3-methylimidazolium ethyl sulfate for effective azeotrope breaking, *J. Chem. Thermodyn.*, 2015, **submitted**.

24. F. S. Oliveira, L. P. N. Rebelo and I. M. Marrucho, Influence of different inorganic salts on the ionicity and thermophysical properties of 1-ethyl-3-methylimidazolium acetate ionic liquid, *J. Chem. Eng. Data*, 2015, **60**, 781-789.

25. A. B. Pereiro, J. M. M. Araújo, F. S. Oliveira, J. M. S. S. Esperança, J. N. C. Lopes, I. M. Marrucho and L. P. N. Rebelo, Solubility of inorganic salts in pure ionic liquids, *J. Chem. Thermodyn.*, 2012, **55**, 29-36.

26. T. V. Doherty, M. Mora-Pale, S. E. Foley, R. J. Linhardt and J. S. Dordick, Ionic

liquid solvent properties as predictors of lignocellulose pretreatment efficacy, *Green Chem.*, 2010, **12**, 1967-1975.

27. Y. Qin, X. Lu, N. Sun and R. D. Rogers, Dissolution or extraction of crustacean shells using ionic liquids to obtain high molecular weight purified chitin and direct production of chitin films and fibers, *Green Chem.*, 2010, **12**, 968-971.

28. N. Sun, M. Rahman, Y. Qin, M. L. Maxim, H. Rodriguez and R. D. Rogers, Complete dissolution and partial delignification of wood in the ionic liquid 1-ethyl-3-methylimidazolium acetate, *Green Chem.*, 2009, **11**, 646-655.

29. J. Vitz, T. Erdmenger, C. Haensch and U. S. Schubert, Extended dissolution studies of cellulose in imidazolium based ionic liquids, *Green Chem.*, 2009, **11**, 417-424.

30. S. R. Tomlinson, C. W. Kehr, M. S. Lopez, J. R. Schlup and J. L. Anthony, Solubility of the corn protein zein in imidazolium-based ionic liquids, *Ind. Eng. Chem. Res.*, 2014, **53**, 2293-2298.

31. H. Zhao, L. Jackson, Z. Song and A. Olubajo, Using ionic liquid [emim][CH_3COO] as an enzyme-'friendly' co-solvent for resolution of amino acids, *Tetrahedron-Asymmetr.*, 2006, **17**, 2491-2498.

32. G. Gurau, H. Rodríguez, S. P. Kelley, P. Janiczek, R. S. Kalb and R. D. Rogers, Demonstration of chemisorption of carbon dioxide in 1,3-dialkylimidazolium acetate ionic liquids, *Angew. Chem. Int. Ed.*, 2011, **50**, 12024-12026.

33. W. Shi, C. R. Myers, D. R. Luebke, J. A. Steckel and D. C. Sorescu, Theoretical and experimental studies of CO_2 and H_2 separation using the 1-ethyl-3-methylimidazolium acetate ([emim][CH_3COO]) ionic liquid, *J. Phys. Chem. B*, 2012, **116**, 283-295.

34. M. B. Shiflett and A. Yokozeki, Phase behavior of carbon dioxide in ionic liquids: [emim][acetate], [emim][trifluoroacetate] and [emim][acetate] + [emim][trifluoroacetate] mixtures, *J. Chem. Eng. Data*, 2009, **54**, 108-114.

Chapter 6

Using deep eutectic solvents for the separation of ethanol from n-heptane

Adapted from: **Filipe S. Oliveira**, Ana B. Pereiro, Luís P. N. Rebelo and Isabel M. Marrucho, Deep eutectic solvents as extraction media for azeotropic mixtures, *Green Chem.* (2013), **15**, 1326-1330.

The author was involved in all the experiments, as well as on the discussion, interpretation and preparation of the manuscript.

1. Abstract

In this work, deep eutectic solvents (DES) are tested as extraction solvents in the liquid-liquid separation of azeotropic mixtures. For this study three different DES, all based on choline chloride, were used as solvents for the liquid-liquid separation of the azeotropic mixture of n-heptane + ethanol at 298.15 K. The feasibility of DES as extraction solvents was assessed by the determination of the selectivities and distribution coefficients, and compared with literature data. The data obtained show that DES surpass the performance of the existing extraction solvents, leading to an increase in efficiency and a reduction in energy consumption of the overall process.

2. Introduction

In order to compensate for the continuous decrease of oil reserves, the search for alternative fuels and renewable energy sources has been the focus of many studies in recent years. Ethanol is viewed as an attractive alternative fuel since it is a renewable bio-based resource that can be used both as a fuel and as a gasoline oxygenated additive. In recent decades, oxygenated additives such as ethanol, methanol and methyl *tert*-butyl ether (MTBE) have been commonly used to replace lead in petrol. However, due to the growth in the production of oxygenated additives, several petrochemical industries face the presence of azeotropic or close-boiling mixtures in many processes, namely mixtures of alcohols and alkanes, which are impossible to separate by simple distillation processes.[1, 2]

The current solution for this problem resides in the highly effective use of extractive or azeotropic distillation processes. Nevertheless, these techniques require high pressures or high temperatures and, thus, high quantities of energy to obtain one fluid-phase system. Alternatively, liquid-liquid extraction has become more attractive since it provides greater energy efficiency as well as being more economic and environmentally friendly.[3-5]

In liquid-liquid extraction (LLE) processes, the separation is carried out by the introduction of a third component in the azeotropic mixture (extraction solvent) which

preferentially dissolves one of the components of the mixture and thus separates it from the initial liquid phase to a different one.[6] The most common extraction solvents used in industry are organic solvents, such as sulfolane, tetraethylene glycol and N-methylpyrrolidone, which, due to their general volatile, toxic and/or flammable natures, require additional investments and energy consumption for their recovery. To this end, ionic liquids (ILs) have emerged as an appealing alternative, since their use requires fewer separation steps and less energy.[7]

Ionic liquids are known for their negligible vapour pressures at room temperature which, in turn, facilitates their recovery and reusability in separation and purification processes.[8] Moreover, ILs have already been recognized for their remarkable azeotrope-breaking ability in ethanol or THF + water mixtures, alcohols + alkanes mixtures, aromatic + aliphatic mixtures, ethyl acetate + alcohols or hexane, ketones + alkanes or alcohols mixtures, and ethyl *tert*-butyl ether (ETBE) + ethanol mixtures.[6] The highest separation efficiency was obtained for azeotropic mixtures of alkanes + alcohols, in particular of n-hexane or n-heptane + ethanol. However, despite their clear advantages, most ILs are more difficult and more costly to prepare than organic solvents. Also, the environmental impact of ILs is largely dependent on the cation or anion in their structure, meaning that ILs are not universally green.[9-12]

Recently, deep eutectic solvents (DES) have been proposed as a versatile alternative to ionic liquids, since their physicochemical properties resemble those of ILs. DES are eutectic mixtures of halide salts with hydrogen bond donors (HBD) such as amines, amides, alcohols or carboxylic acids that have much lower melting points than the starting materials. The mixing of these two types of compounds leads to their self-association via hydrogen bonding, generating a new single compound, a new liquid phase. The main advantage of DES over ILs is related to the sustainable character of the former. These compounds can be produced from cheap, non-toxic, completely biodegradable and biocompatible materials and their preparation is very simple, requiring only heating and mechanical stirring to perform the synthesis in just one step. This fact makes the production of DES much cheaper than that of ILs, which require expensive starting materials and numerous purification steps. Furthermore, the synthesis of DES has 100% reaction mass efficiency, which means that

the purity of DES is only dependent on the purity of the starting materials.[13-15]

In this work, three different DES were tested for the separation of n-heptane + ethanol azeotropic mixtures. All the DES used were based on choline chloride and combined with HBD glycerol (DES1), levulinic acid (DES2) and ethylene glycol (DES3), in the molar ratio of 1 choline chloride : 2 HBD, which represent the respective eutectic composition.[16-18] Preliminary work showed that these DES have much lower viscosities than other common DES composed of choline chloride and urea or xylitol. Furthermore, all of the DES in this study are liquid at 298.15 K.

Deep Eutectic Solvents based on choline chloride have already been used successfully in the separation of glycerol from biodiesel,[16] alcohols from esters,[19] hydroxymethylfurfural (HMF) from HMF-esters[20] and phenol from oils (hexane, toluene and p-xylene).[21] Moreover, Kareem et al.[22] synthesized DES using phosphonium-based ILs and ethylene glycol as HBD, for the selective separation of aromatic/aliphatic mixtures (benzene/hexane) and superior results to those of the commonly used sulfolane were obtained. Concerning the azeotrope n-heptane + ethanol, the most studied extraction solvents have been the imidazolium-based ILs. Letcher et al.[23] studied the effectiveness of 1-methyl-3-octylimidazolium chloride as an extraction solvent for several alkanol-alkane mixtures. Seoane et al.[24] used different alkyl-imidazolium ILs all with the same anion, bis(trifluoromethylsulfonyl)imide (NTf_2), and obtained distribution coefficient values between 1.81 and 26.72 and values of selectivity between 18.84 and 474.16. Pereiro et al.[3-5, 25] studied the extraction of ethanol from n-hexane and n-heptane with several 1-alkyl-3-methylimidazolium ILs with different anions. The highest distribution coefficient and selectivity values were obtained with the 1,3-dimethylimidazolium methyl sulfate ($[C_1MIM][C_1SO_4]$) IL and a laboratory-scale packed column achieved a raffinate purity of over 98 wt%.

The main goal of this work is to evaluate the potential of DES as extraction solvents for azeotropic mixtures of n-heptane + ethanol in liquid-liquid extraction processes. For that purpose, the binodal curves and tie lines for each ternary system were obtained, and the selectivities and distribution coefficients were determined in order to establish which DES is the most suitable solvent for the extraction of ethanol by liquid-liquid extraction.

3. Experimental Section

3.1. Materials

The eutectic mixtures were prepared in a glove box within nitrogen atmosphere. The choline chloride was first dried at 323.15 K under vaccum for at least 2 days, whilst the HBD were used as received and without any further purification. The DES were synthesized by heating the two components at 373.15 K and stirring until a homogeneous liquid was formed. Figure 1, presents the chemical structures of the DES used in this work.

In order to prove the reusability of the DES, after their used in the extraction of ethanol from the n-heptane + ethanol mixtures, the DES were dried in a high vacuum pump at ambient temperature to evaporate the ethanol extracted and the n-heptane remains. The composition of the synthesized DES, as well as the recovered DES, was checked by ^{1}H NMR (see SI) and it could be seen that the reusability of the DES tested is possible.

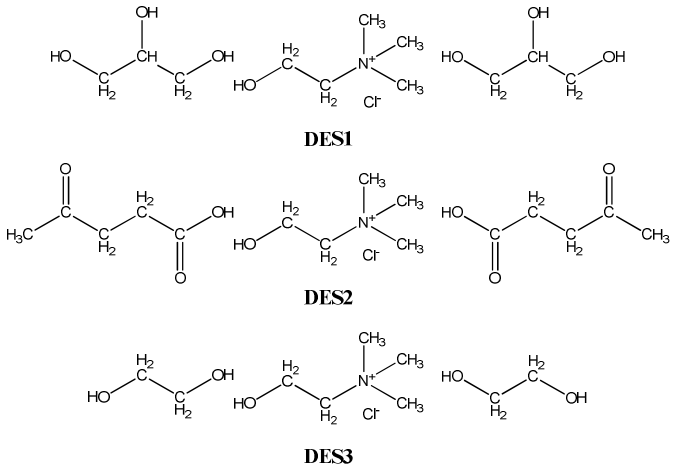

Figure 1 | Chemical structure of the DES studied in this work.

3.2. Liquid-liquid equilibria measurements

The ternary LLE experiments were performed at 298.15 K in a glass cell containing a magnetic stirrer and thermostat regulated by a water jacket connected to a bath controlled to ± 0.01 K. The temperature in the cell was measured by means of a platinum resistance thermometer coupled to a Keithley 199 System DMM/Scanner. The thermometer was calibrated against high-accuracy mercury thermometers (0.01 K). The binodal curve of the ternary system was determined by preparing several binary mixtures of n-heptane + DES in the immiscible region and then ethanol was added until the ternary mixture became miscible. The refractive index of those ternary mixtures was determined in triplicate. The measurements of refractive index were performed at 298.15 K and atmospheric pressure, using an automated Anton Paar Refractometer Abbemat 500 with an absolute uncertainty of the refractive indexes of ± 5 x 10^{-4}.

For the determination of the tie-lines, ternary mixtures of known composition were prepared in vials and were vigorously stirred for at least 1 h and left to settle for at least 12 h in a thermostatic bath at 298.15 K. Samples from both phases were taken with a syringe and their refractive indexes were determined in triplicate. Deviation between the triplicates of the refractive indexes was always lower than 8 x 10^{-4}. The composition of both phases in equilibrium was determined using the fitting refractive indexes with the composition along the binodal curve using the following equations:

$$n_D = A \cdot w_1 + B \cdot w_1^2 + C \cdot w_1^3 + D \cdot w_1^4 + E \cdot w_2 + F \cdot w_2^2 + G \cdot w_2^3 + H \cdot w_2^4 + I \cdot w_3 + J \cdot w_3^2 + K \cdot w_3^3 + L \cdot w_3^4 \quad (1)$$

$$w_3 = M \cdot \exp\left[\left(N \cdot w_1^{0.5}\right) - \left(O \cdot w_1^3\right)\right] \quad (2)$$

$$w_3 = 1 - (w_1 + w_2) \quad (3)$$

where, w_1, w_2 and w_3 correspond to the mass fraction compositions of n-heptane,

ethanol and DES, respectively, and the parameters A to O are adjustable parameters which are given in Table S1 in the SI.

The method was validated by using experimental data for the ternary system of n-heptane + ethanol + [C_2MIM][C_2SO_4] from the literature.[3] The measurements obtained were estimated to be precise to ± 0.009 in mass fraction in comparison with the method used in literature and the uncertainty in the composition is estimated to be ± 0.006 in mass fraction.

4. Results and discussion

The experimental results for the liquid-liquid extractions of ethanol from the n-heptane + ethanol azeotropic mixtures with the three DES are presented in Table 1. Figure 2 to 4, indicate the immiscibility region of the ternary diagram for the systems n-heptane + ethanol + DES as well as the binodal curve and the tie-lines. It can be seen that all DES and n-heptane are practically immiscible and that the ternary diagram presents a great immiscibility region between the three components in the mixture. Furthermore, the tie lines obtained present positive slopes which imply distribution coefficient values higher than the unity and also that the extraction of ethanol is favoured. In addition it can also be seen that the immiscibility region for the systems containing DES1 and DES3 in slightly larger than that of DES2.

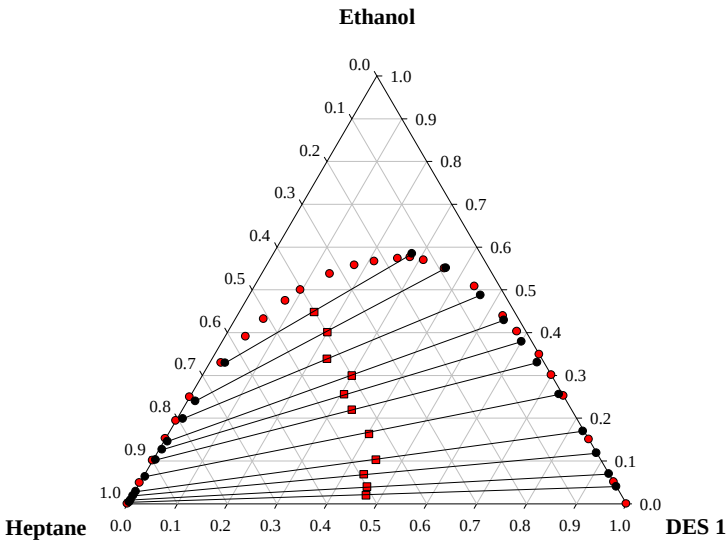

Figure 2 | Ternary diagram for the system n-heptane + ethanol + DES1 at 298.15 K. The red dots represent the binodal, the red squares the experimental starting point of the mixture and the black dots and lines the system tie-lines.

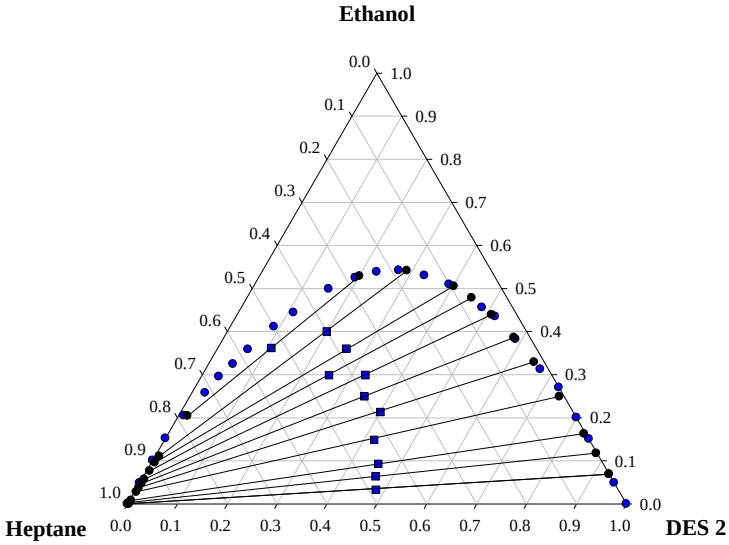

Figure 3 | Ternary diagram for the system n-heptane + ethanol + DES2 at 298.15 K. The blue dots represent the binodal, the blue squares the experimental starting point of the mixture and the black dots and lines the system tie-lines.

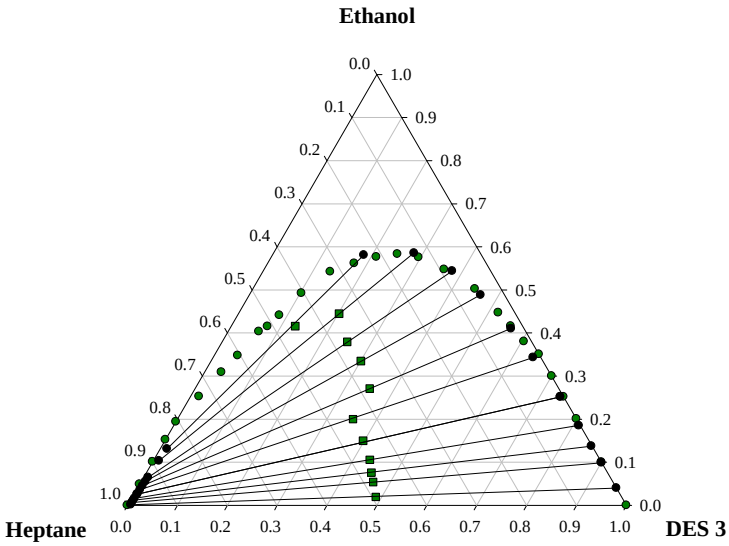

Figure 4 | Ternary diagram for the system n-heptane + ethanol + DES3 at 298.15 K. The green dots represent the binodal, the green squares the experimental starting point of the mixture and the black dots and lines the system tie-lines.

Two crucial parameters widely used in the assessment of an extraction solvent feasibility are the distribution coefficient, β and the selectivity, S, which are defined as follows:

$$\beta_2 = \frac{w_2^{II}}{w_2^{I}} \tag{4}$$

$$S = \frac{w_1^{I}}{w_1^{II}} \times \beta_2 \tag{5}$$

where w_1^{I} and w_2^{I} are the mass fractions of n-heptane and ethanol in the upper phase (n-heptane-rich phase), respectively, and w_1^{II} and w_2^{II} are the mass fractions of n-heptane and ethanol in the lower phase (DES-rich phase). These parameters are also listed in Table S2 in the SI.

The distribution coefficient is related to the solute-carrying capacity of the DES and it determines the amount of DES required for the extraction process. Selectivity is related to the efficiency of the DES, indicating the ease of extraction of a solute (ethanol) from a diluent (inert, n-heptane). The ideal extraction solvent should have both high values of distribution coefficient and selectivity, since high selectivity values usually lead to fewer stages in the process and lesser amounts of inert residual in the extract, while high distribution coefficient values correspond to a lower solvent flow rate, a smaller-diameter column and lower operating costs.[3]

Figures 4 and 5 compare the distribution coefficient and selectivity values of the different DES used in this work, respectively. It can be observed that DES1 had the lowest distribution coefficient values and the highest selectivity values, while DES2 presented the highest distribution coefficient values (along with DES3) and the lowest selectivity values. These results can be explained by the different HBD present in the DES. In DES1 and DES3, the HBD are glycerol and ethylene glycol, which have 3 and 2 hydroxyl groups (-OH), respectively, whilst in DES2 the HBD is levulinic acid, which is a carboxylic acid, presenting a carboxylic group (-COOH) and also a carbonyl group (-C=O).

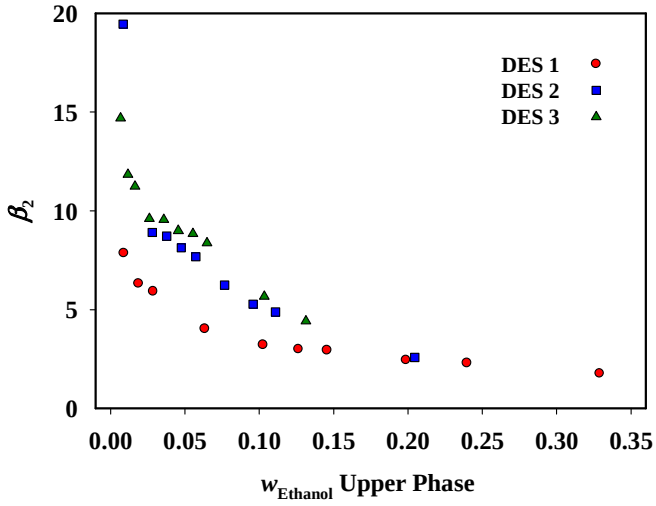

Figure 4 | Distribution coefficient values, β_2, for the systems n-heptane (1) + ethanol (2) + DES (3) studied in this work, as a function of the ethanol mass fraction in n-heptane-rich phase at 298.15 K.

In the case of DES2, the O-H bond in the carboxylic group is more strongly polarized than that of the alcohols, due to the presence of the adjacent carbonyl moiety. This structural feature enhances dipole magnitude and allows for the creation of a higher number and stronger dipoles, thus forming a larger number and stronger H-bonds with other substances capable of H-bonding interactions. The total energy of H-bonding interactions for carboxylic acids is greater than that observed for other organic compounds containing OH and/or C=O dipoles such as amines, alcohols, phenols, aldehydes, ketones, esters, amides and isosteric compounds.[26] This fact enables DES2 to form stronger H-bonding interactions with ethanol than DES1 or DES3, meaning that DES2 has higher solute-carrying capacity than the other DES used, which is explained by the higher distribution coefficients obtained.

On the other hand, DES2 presents lower selectivity values than the other two DES, which may be attributed to the number of O-H groups in DES1 and DES3. DES1 and DES3 present more groups capable of establishing H-bonding with the O-H group of ethanol, meaning that these two solvents can extract ethanol more easily than DES2, resulting in higher values of selectivity, which could also be related to the higher immiscibility regions observed. In addition, it can also be seen that DES3 presented high distribution coefficient values, in the same range as those of DES2. These results could be attributed to the smaller size of the ethylene glycol HBD, as well as the chemical similarity to the ethanol molecule, opposite to the glycerol molecule which is larger and could lead to steric effects.

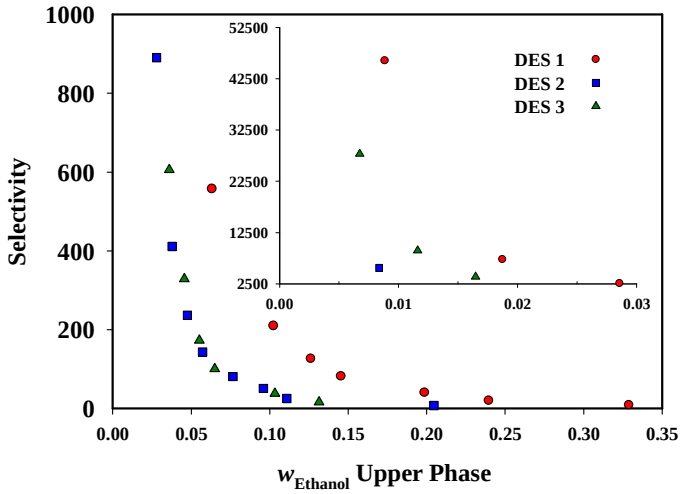

Figure 5 | Selectivity, *S*, for the systems n-heptane (1) + ethanol (2) + DES (3) studied in this work, as a function of the ethanol mass fraction in n-heptane-rich phase at 298.15 K.

Figures 6 and 7 compare the results obtained in this work with those found in literature for neat ILs at a specific ethanol mass fraction.[3-5, 24, 25] The comparison in the whole range of ethanol concentrations studied is depicted in Figures S1 and S2 in the SI. It can be seen that the DES used in this work surpass the performance of ILs with bis(trifluoromethylsulfonyl)imide (NTf_2) as anion, both in terms of distribution coefficient and selectivity values, since these ILs can only establish weak hydrogen bonds. Nevertheless, when comparing the distribution coefficient values, DES1 presented lower values than the alkylsulfate-based ILs. This is due to the stronger hydrogen bonds that can be formed by the oxygen atoms of the sulfate anion. Meanwhile, DES2 and DES3 presented some of the highest values of all the extraction solvents studied so far for this azeotrope. Regarding the selectivity values, all the DES tested presented better results than the ILs reported in the literature. So far, the best IL solvent identified to date for the extraction of this azeotropic mixture was the $[C_1MIM][C_1SO_4]$, due to its high distribution coefficient and selectivity values. Furthermore, Pereiro et al.[25] showed that not only could this IL be recovered, but the scaling up of the extraction process is feasible.

Comparing the performance of the DES used in this work with that of $[C_1MIM][C_1SO_4]$

IL, in the whole range of ethanol concentrations studied (Figures S1 and S2), all these compounds combine good distribution coefficient and high selectivity values. Moreover, the extraction solvent should meet the define criteria for the design of the operation. For instance, if DES1 or DES3 are used, fewer extraction stages will be required and the extract will present a high purity degree, due to their higher selectivity; if DES2 or DES3 are used, the extraction process will require less amounts of solvent since the distribution coefficients are higher for these solvents.

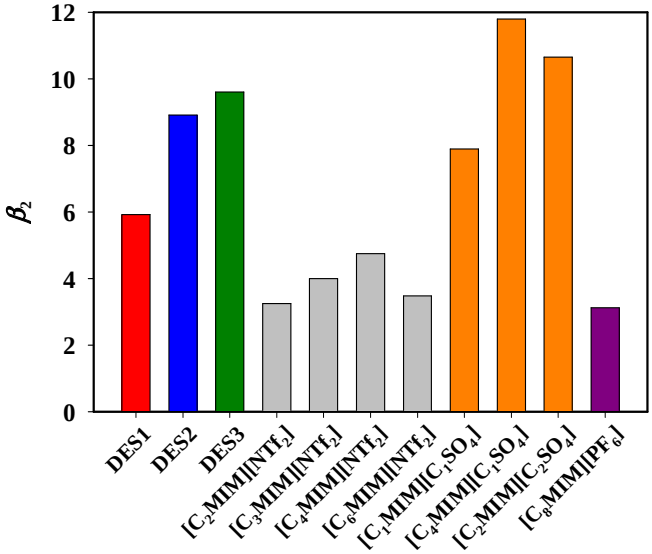

Figure 6 | Distribution coefficient values, β_2, of the system with the azeotrope n-heptane (1) + ethanol (2), at an ethanol mass fraction of approximately 3 wt% in n-heptane-rich phase at 298.15 K.[3-5, 24, 25]

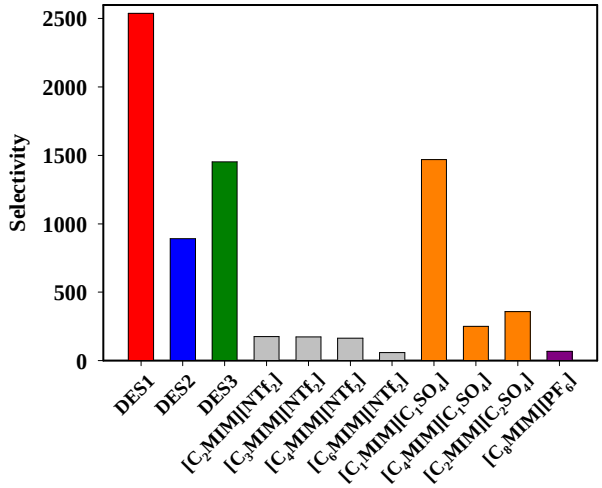

Figure 7 | Selectivity, *S*, of the system with the azeotrope n-heptane (1) + ethanol (2), at an ethanol mass fraction of approximately 3 wt% in n-heptane-rich phase at 298.15 K.[3-5, 24, 25]

5. Conclusions

The data obtained in this study show that DES are interesting alternatives to ILs as extraction solvents in the separation of ethanol-heptane mixtures. However, both the distribution coefficient and the selectivity values need to be considered in order to evaluate the real performance of an extraction solvent. It can be observed that the DES containing HBD with hydroxyl groups (1 and 3) exhibit greater selectivity, while the presence of the carboxylic group in the HBD (DES2) enhanced its distribution coefficient. In all studied DES the combination of the high selectivity and the high distribution coefficient values shows that DES are very promising for this application. Moreover, the recovery of the DES was also possible by evaporation of the ethanol and heptane after the extractions.

In conclusion, the data obtained in this work show that DES are an easier, cheaper and greener solution for the separation of azeotropic mixtures. The distribution coefficients and selectivity values obtained for the DES tested are high to justify a scaling up process by liquid-liquid extraction.

6. Acknowledgements

Filipe S. Oliveira and Ana B. Pereiro gratefully acknowledge the financial support of FCT/MCTES (Portugal) through the PhD fellowship SFRH/BD/73761/2010 and the Post-Doc grants SFRH/BPD/84433/2012, respectively. Isabel M. Marrucho gratefully acknowledges Fundação para a Ciência e Tecnologia for a contract under the Programa Ciência 2007.

The authors also acknowledge Fundação para a Ciência e Tecnologia for the financial support through the projects PTDC/EQU-EPR/104554/2008, PTDC/EQU-FTT/116015/2009 and PTDC/EQU-FTT/1686/2012.

The NMR spectrometers are part of the National NMR Network and were purchased within the framework of the National Program for the Renovation of Scientific Equipment, contract REDE / 1517 / RMN / 2005, with funds from POCI 2010 (FEDER) and FCT / MCTES.

7. Supplementary Information

7.1. Supporting tables

Table S1 | Adjustable parameters in equations 1 and 2, for the different DES used.

Parameters	DES1	DES2	DES3
A	1.3920	1.3935	1.3598
B	0.0854	0.1346	0.2360
C	-0.0785	-0.1393	-0.2328
D	-0.0136	-0.0033	0.0226
E	1.2388	1.1915	1.1795
F	0.2300	0.3373	0.3807
G	-0.0297	-0.0672	-0.1120
H	-0.0629	-0.0688	-0.0558
I	1.4359	1.4038	1.4204
J	0.1782	0.2623	0.2114
K	-0.0870	-0.1691	-0.0882
L	-0.0416	-0.0276	-0.0720
r^2	1.0000	1.0000	0.9999
M	97.1543	99.1621	97.2980
N	-0.3352	-0.2960	-0.3391
O	2.8571×10^{-6}	2.9399×10^{-6}	1.7864×10^{-6}
r^2	0.9960	0.9997	0.9976

Table S2 | Composition of the experimental tie-lines, ethanol distribution coefficient (β_2) and selectivity (S) for the ternary systems at 298.15 K.

n-heptane-rich phase		DES-rich phase		β_2	S
w_1^{I}	w_2^{I}	w_1^{II}	w_2^{II}		
n-heptane (1) + ethanol (2) + DES1 (3)					
0.989	0.009	0.000	0.070	7.87	46028.30
0.979	0.019	0.001	0.118	6.32	7214.35
0.969	0.029	0.002	0.169	5.92	2537.51
0.933	0.063	0.007	0.256	4.04	557.09
0.892	0.103	0.014	0.330	3.22	209.63
0.867	0.126	0.021	0.379	3.00	126.20
0.847	0.146	0.031	0.429	2.95	81.48
0.789	0.199	0.049	0.487	2.45	39.86
0.744	0.240	0.086	0.551	2.30	19.90
0.640	0.329	0.138	0.584	1.78	8.26
n-heptane (1) + ethanol (2) + DES2 (3)					
0.994	0.004	0.002	0.118		
0.989	0.008	0.003	0.163	19.45	5594.74
0.968	0.028	0.010	0.249	8.91	890.35
0.958	0.038	0.020	0.330	8.72	411.02
0.948	0.048	0.033	0.386	8.12	236.66
0.938	0.057	0.050	0.440	7.68	142.88
0.917	0.077	0.071	0.479	6.25	80.77
0.897	0.096	0.093	0.506	5.27	50.88
0.881	0.111	0.169	0.541	4.88	25.39
0.777	0.205	0.270	0.529	2.58	7.43
n-heptane (1) + ethanol (2) + DES3 (3)					
0.987	0.007	0.001	0.099	14.69	27838.66
0.982	0.012	0.001	0.138	11.84	8978.41
0.977	0.017	0.003	0.185	11.23	3855.75
0.967	0.026	0.006	0.252	9.60	1452.08
0.957	0.036	0.015	0.344	9.56	605.64
0.947	0.046	0.026	0.410	9.00	328.63
0.936	0.055	0.048	0.489	8.84	173.28
0.926	0.065	0.077	0.544	8.37	100.40
0.885	0.103	0.133	0.586	5.67	37.79
0.855	0.131	0.236	0.581	4.42	16.04

7.2. Supporting figures

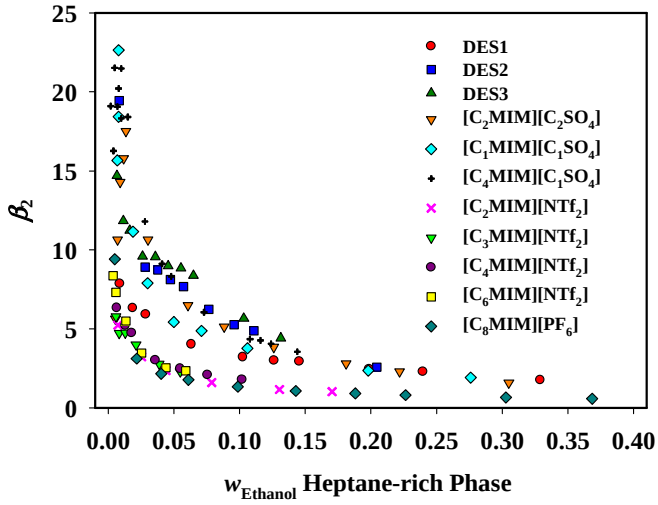

Figure S1 | Comparison of the distribution coefficient values, β_2, between the systems studied in this work and those found in literature,[3-5, 24, 25] as a function of the ethanol mass fraction in n-heptane-rich phase at 298.15 K and 0.1 MPa.

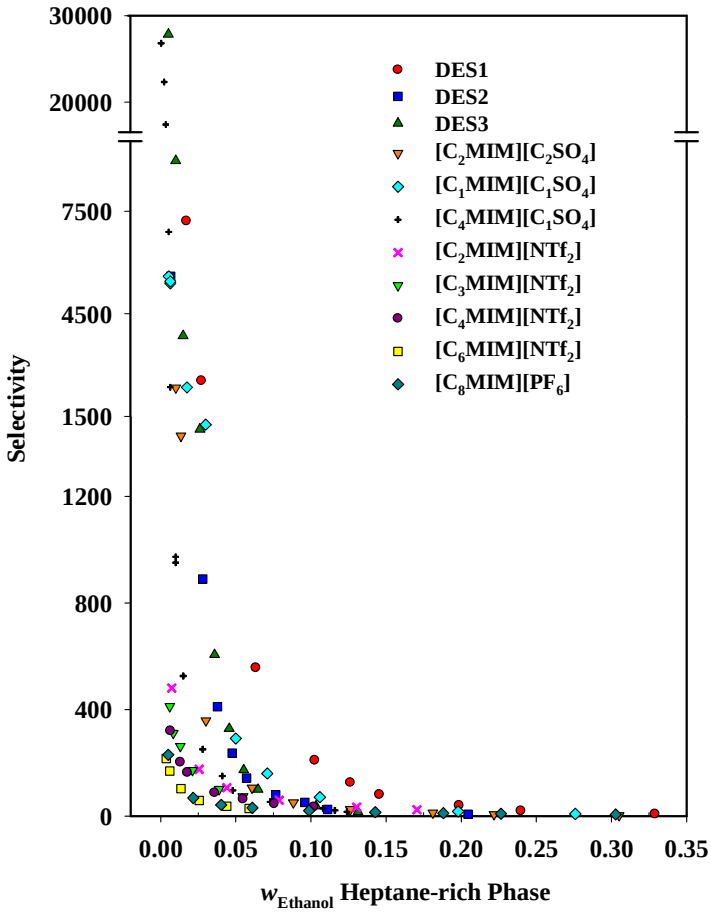

Figure S2 | Comparison of the selectivity, *S*, between the systems studied in this work and those found in literature,[3-5, 24, 25] a function of the ethanol mass fraction in n-heptane-rich phase at 298.15 K and 0.1 MPa.

7.3. NMR studies

The ^{1}H spectra of DES1, DES2 and DES3 are depicted in Figures S3, S4 and S5, respectively. The ^{1}H spectra of the recovered DES is depicted in Figure S6, DES3 was used as proof of concept. All the experiments were carried out on a Bruker AVANCE 400 spectrometer operated at room temperature with 16 scans for ^{1}H NMR, using oxide deuterium as solvent. The chemical shifts of the spectra are listed in Table S3.

Table S3 | ^{1}H NMR chemical shifts for the DES used in this work.

	DES1	DES2	DES3
1	3.98	3.98	3.98
2	3.44	3.44	3.45
3, 4, 5	3.12	3.12	3.13
6, 6’	3.55-3.59	–	3.58
7, 7’	3.70	2.79	3.58
8, 8’	3.44-3.49	2.52	–
10, 10’	–	2.15	–

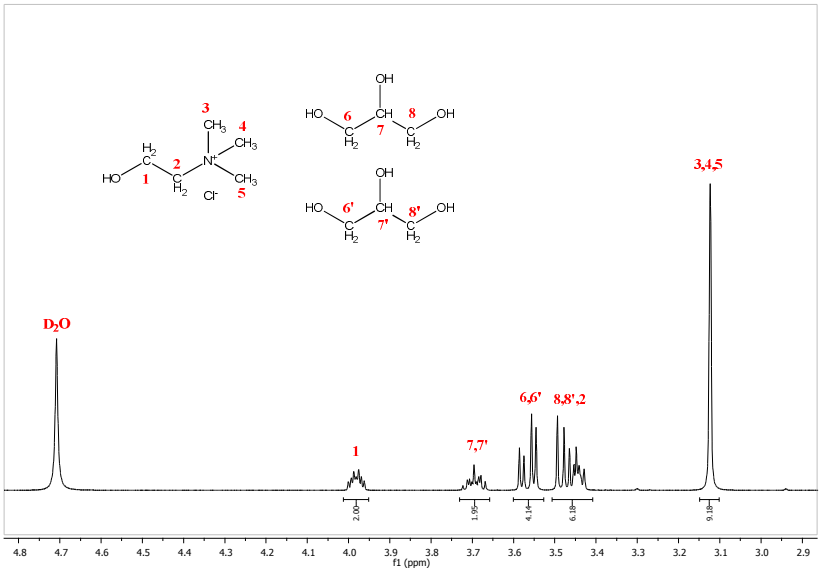

Figure S3 | ^{1}H NMR spectrum of DES1 in deuterium oxide at 298.15 K. The structure and numbering of the DES is also depicted.

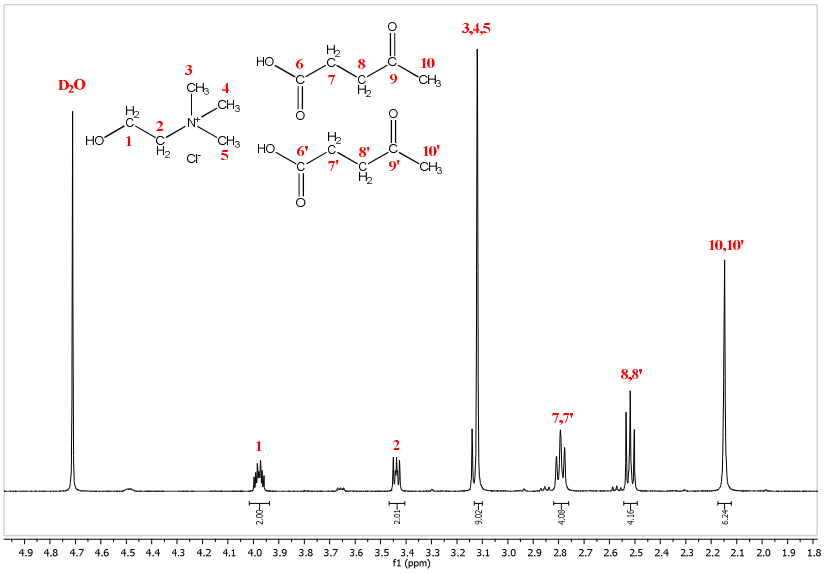

Figure S4 | ^{1}H NMR spectrum of DES2 in deuterium oxide at 298.15 K. The structure and numbering of the DES is also depicted.

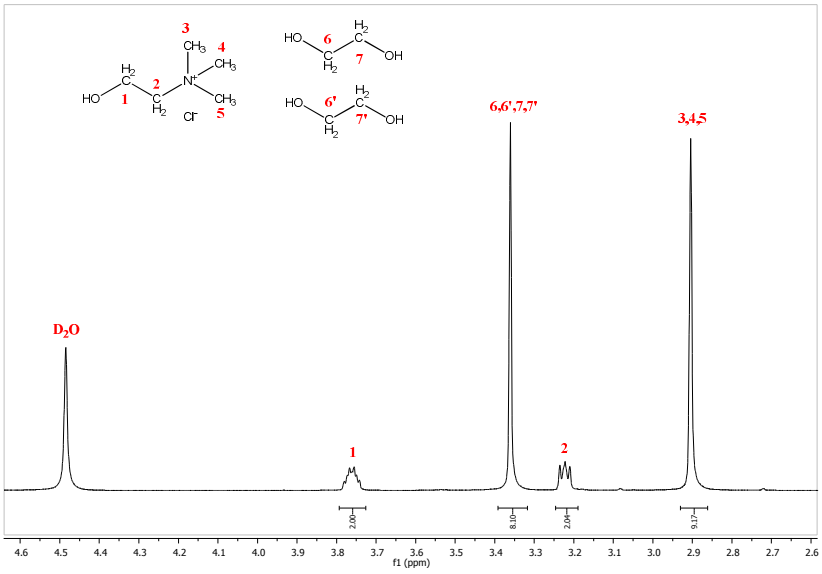

Figure S5 | ^{1}H NMR spectrum of DES3 in deuterium oxide at 298.15 K. The structure and numbering of the DES is also depicted.

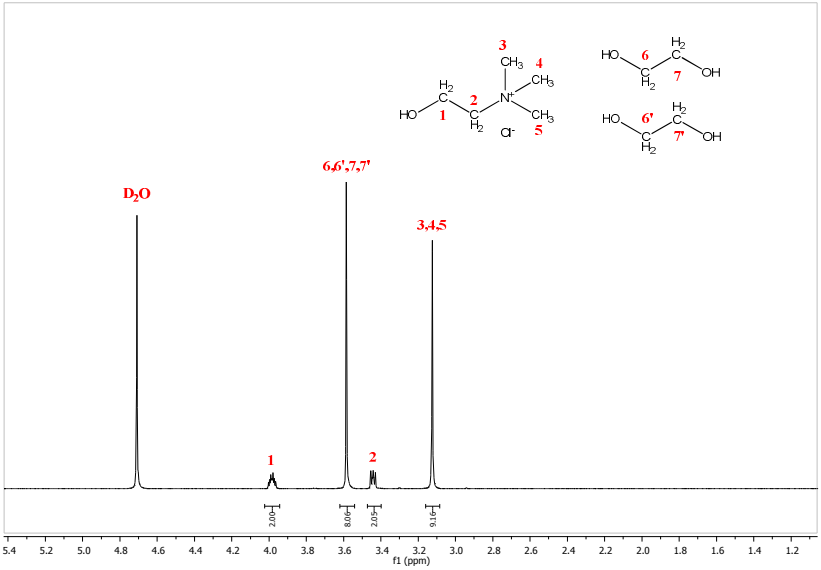

Figure S6 | ^{1}H NMR spectrum of recovered DES3 (after evaporation of n-heptane and ethanol) in deuterium oxide at 298.15 K. The structure and numbering of the DES is also depicted.

8. References

1. A. K. Agarwal, Biofuels (alcohols and biodiesel) applications as fuels for internal combustion engines, *Prog. Energy Combust. Sci.*, 2007, **33**, 233-271.

2. A. Pucci, Phase equilibria of alkanol/alkane mixtures in new oil and gas process development, *Pure Appl. Chem.*, 1989, **61**, 1363-1372.

3. A. B. Pereiro, F. J. Deive, J. M. S. S. Esperança and A. Rodriguez, Alkylsulfate-based ionic liquids to separate azeotropic mixtures, *Fluid Phase Equilib.*, 2010, **294**, 49-53.

4. A. B. Pereiro and A. Rodriguez, Azeotrope-breaking using [bmim][meSO$_4$] ionic liquid in an extraction column, *Sep. Purif. Technol.*, 2008, **62**, 733-738.

5. A. B. Pereiro and A. Rodriguez, A study on the liquid-liquid equilibria of 1-alkyl-3-methylimidazolium hexafluorophosphate with ethanol and alkanes, *Fluid Phase Equilib.*, 2008, **270**, 23-29.

6. A. B. Pereiro, J. M. M. Araújo, J. M. S. S. Esperança, I. M. Marrucho and L. P. N. Rebelo, Ionic liquids in separations of azeotropic systems - A review, *J. Chem. Thermodyn.*,

2012, **46**, 2-28.

7. G. W. Meindersma, A. R. Hansmeier and A. B. de Haan, Ionic Liquids for Aromatics Extraction. Present Status and Future Outlook, *Ind. Eng. Chem. Res.*, 2010, **49**, 7530-7540.

8. M. J. Earle, J. M. S. S. Esperança, M. A. Gilea, J. N. C. Lopes, L. P. N. Rebelo, J. W. Magee, K. R. Seddon and J. A. Widegren, The distillation and volatility of ionic liquids, *Nature*, 2006, **439**, 831-834.

9. R. F. M. Frade and C. A. M. Afonso, Corrigendum to impact of ionic liquids in environment and humans: An overview, *Hum. Exp. Toxicol.*, 2010, **29**, 1055-1057.

10. M. Petkovic, K. R. Seddon, L. P. N. Rebelo and C. S. Pereira, Ionic liquids: A pathway to environmental acceptability, *Chem. Soc. Rev.*, 2011, **40**, 1383-1403.

11. S. Steudte, P. Stepnowski, C.-W. Cho, J. Thoming and S. Stolte, (Eco)toxicity of fluoro-organic and cyano-based ionic liquid anions, *Chem. Commun.*, 2012, **48**, 9382-9384.

12. T. P. T. Pham, C.-W. Cho and Y.-S. Yun, Environmental fate and toxicity of ionic liquids: A review, *Water Res.*, 2010, **44**, 352-372.

13. A. P. Abbott, D. Boothby, G. Capper, D. L. Davies and R. K. Rasheed, Deep eutectic solvents formed between choline chloride and carboxylic acids: Versatile alternatives to ionic liquids, *J. Am. Chem. Soc.*, 2004, **126**, 9142-9147.

14. A. P. Abbott, G. Capper, D. L. Davies, R. K. Rasheed and V. Tambyrajah, Novel solvent properties of choline chloride/urea mixtures, *Chem. Commun.*, 2003, **1**, 70-71.

15. C. Ruß and B. König, Low melting mixtures in organic synthesis - an alternative to ionic liquids?, *Green Chem.*, 2012, **14**, 2969-2982.

16. A. P. Abbott, P. M. Cullis, M. J. Gibson, R. C. Harris and E. Raven, Extraction of glycerol from biodiesel into a eutectic based ionic liquid, *Green Chem.*, 2007, **9**, 868-872.

17. Z. Maugeri and P. Domínguez de María, Novel choline-chloride-based deep-eutectic-solvents with renewable hydrogen bond donors: Levulinic acid and sugar-based polyols, *RSC Adv.*, 2012, **2**, 421-425.

18. K. Shahbaz, F. S. Mjalli, M. A. Hashim and I. M. AlNashef, Using deep eutectic solvents for the removal of glycerol from palm oil-based biodiesel, *J. Appl. Sci.*, 2010, **10**, 3349-3354.

19. Z. Maugeri, W. Leitner and P. Domínguez de María, Practical separation of alcohol–ester mixtures using deep eutectic solvents, *Tetrahedron Lett.*, 2012, **53**, 6968-6971.

20. M. Krystof, M. Pérez-Sánchez and P. Domínguez de María, Lipase-catalyzed (trans)esterification of 5-hydroxy- methylfurfural and separation from HMF esters using deep eutectic solvents, *ChemSusChem*, 2013, **6**, 630-634.

21. K. Pang, Y. Hou, W. Wu, W. Guo, W. Peng and K. N. Marsh, Efficient separation of phenols from oils via forming deep eutectic solvents, *Green Chem.*, 2012, **14**, 2398-2401.

22. M. A. Kareem, F. S. Mjalli, M. A. Hashim and I. M. AlNashef, Liquid–liquid equilibria for the ternary system (phosphonium based deep eutectic solvent–benzene–hexane) at different temperatures: A new solvent introduced, *Fluid Phase Equilib.*, 2012, **314**, 52-59.

23. T. M. Letcher, N. Deenadayalu, B. Soko, D. Ramjugernath and P. K. Naicker, Ternary liquid-liquid equilibria for mixtures of 1-methyl-3-octylimidazolium chloride plus an alkanol plus an alkane at 298.2 K and 1 bar, *J. Chem. Eng. Data*, 2003, **48**, 904-907.

24. R. G. Seoane, E. J. González and B. González, 1-Alkyl-3-methylimidazolium bis(trifluoromethylsulfonyl)imide ionic liquids as solvents in the separation of azeotropic mixtures, *J. Chem. Thermodyn.*, 2012, **53**, 152-157.

25. A. B. Pereiro and A. Rodriguez, Separation of Ethanol-Heptane Azeotropic Mixtures by Solvent Extraction with an Ionic Liquid, *Ind. Eng. Chem. Res.*, 2009, **48**, 1579-1585.

26. J. D. Roberts and M. C. Caserio, *Basic principles of organic chemistry*, W. A. Benjamin, Inc., 2nd edn., 1977.

Chapter 7

Concluding Remarks and Outlook

The research described in this thesis aimed at separating azeotropic mixtures using combinations of IL and IS as separation agents. The most important results obtained during this PhD project are highlighted in this chapter. The following lines provide a critical evaluation of the work described before as well as an outlook for future research within this thesis subject.

1. Improving the ionicity of ILs

Up to date, besides the papers from this thesis, only one work found in literature reported the use of IL-IS mixtures as separation agents for azeotropic mixtures.[1] This study, dated from 2014, explored the combination of the IL $[C_2MIM][Ac]$ with 10 different ISs, fixing the concentration of IS at a mass fraction of 5 wt%. The results showed that indeed by mixing an IS with an IL, higher efficiencies in the separation of the chosen azeotropic mixture (water + ethanol) could be obtained. However, the reason why some ISs work better than others was not presented. Therefore, in order to design a suitable IL-IS mixture for the separation of a specific azeotropic mixture, it is paramount to study the IL-IS mixture, namely in terms of its physical / chemical properties and ionicity.

In an earlier work, Pereiro et al.[2] studied the solubility of different ISs, that cover a substantial part of the Hofmeister series, both in terms of the cation and the anion, in a wide variety of ILs. The results obtained showed that $[NH_4][SCN]$ was the most soluble IS in different ILs, particularly in the ILs $[C_2MIM][Ac]$, $[C_2MIM][C_2SO_3]$ and $[C_2MIM][C_2SO_4]$. Hence, the work developed in this thesis started by comparing the thermophysical properties of the binary IL-IS systems of $[C_2MIM][C_2SO_3]$ + $[NH_4][SCN]$ and $[C_2MIM][C_2SO_4]$ + $[NH_4][SCN]$ (Chapter 2). The data obtained, showed that the addition of $[NH_4][SCN]$ had a higher impact on the $[C_2MIM][C_2SO_4]$ system properties than on those of $[C_2MIM][C_2SO_3]$. Also, the ionicity of both systems, determined by the Walden plot approach, shown that the addition of $[NH_4][SCN]$ to the ionic liquid promoted an increase in both systems' ionicity. However, due to the fact that the neat IL $[C_2MIM][C_2SO_3]$ is much more viscous and also presents a smaller ionic conductivity than the $[C_2MIM][C_2SO_4]$, the increase in ionicity of the

former is lower.

Furthermore, spectroscopic techniques and Molecular Dynamic studies revealed that the sulfate-based IL is capable of establishing stronger interactions with the $[NH_4][SCN]$ than the sulfonate-based one, with the extra oxygen of the sulfate-based IL playing a key role in the structuring of complexes between the IL and the IS (namely between the $[C_2SO_4]^-$ anion and the $[NH_4]^+$ cation). The presence of the extra oxygen atom allows more flexibility in the sulfate anion, which allows the formation of more aggregates than in the sulfonate-based IL. This fact permits the other ions in the system to become less engaged, which resulted in the increase of the ionicity.

The other IL that also showed high solvation ability for $[NH_4][SCN]$ was $[C_2MIM][Ac]$. This IL is also known for its great solvent abilities, proving to be capable of solubilising a wide range of different compounds in high concentrations.[2-11] As shown by Pereiro et al.[12] the ionicity of this IL could also be increased with the addition of $[NH_4][SCN]$. These facts led to the study of the thermophysical properties, and consequently of the ionicity, of binary mixtures of $[C_2MIM][Ac]$ and six different ISs (Chapter 3). With the aim of covering different effects of the IS on the properties and ionicity of the IL, the ISs chosen were based on two different cations, the ammonium and the sodium, had different anions such as, acetate, chloride, thiocyanate and ethyl sulfonate, and also a common ion with the IL, the acetate.

The results described in Chapter 3 show that not all ISs can increase the ionicity of an IL, as observed for the sodium-based ISs. Also, the increase in ionicity can be well described by the ratio between the variation of viscosity and variation of ionic conductivity, meaning that even though the viscosity of the IL-IS system is increased by the addition of an IS, as long as the ionic conductivity does not decrease in an even way, the ionicity of the IL-IS binary system can be increased. Furthermore, it was shown by spectroscopic and simulation techniques that the presence of an $[NH_4]^+$ cation allowed the establishment of stronger interactions between the IL and the IS, which were in part a result of the approximation of the $[NH_4]^+$ cation to the IL's $[Ac]^-$ anion. This approximation leads to the establishment of aggregates and to a more unengaged imidazolium cation, consequently increasing the ionicity, as seen in the study described in Chapter 2. The ionicity was also determined by two different methods, with the results showing divergent behaviours on both.

However, these results might be impacted by the presence of residual water on the samples. Nevertheless, the interplay between the interactions of ILs and ISs is much more complex than in the case of neat ILs or molten salts making the determination of the ionicity in IL-IS mixtures much more challenging.

2. IL-IS mixtures as extraction solvents

The results obtained from the studies of the properties of different IL-IS mixtures allowed the selection of the most promising combinations of IL and IS, in terms of ionicity, to be used in the separation of azeotropic mixtures.

The azeotropic mixture of n-heptane + ethanol was selected because of the importance of ethanol as a biofuel and additive in gasoline. In addition, sulfate-based ILs were already shown to be the most effective in the separation of the aforementioned azeotropic mixture using liquid-liquid extraction, in particular the $[C_2MIM][C_2SO_4]$.[13-15]

Taking into account the high solubility of $[NH_4][SCN]$ in $[C_2MIM][C_2SO_4]$ and the higher ionicity of its binary system, the combination of the latter compounds was chosen over the binary system of $[C_2MIM][C_2SO_3]$ and $[NH_4][SCN]$. In order to check out the effect of the ionicity of the system in the separation of the n-heptane + ethanol azeotropic mixtures, three different concentration of IS were used (Chapter 4). The results, showed that the tested IL-IS mixtures can provide higher selectivity values than the neat ILs described in literature, as well as distribution coefficient values of the same order of magnitude. In addition, the increase in the ionicity promoted by the addition of $[NH_4][SCN]$, proved to increase the selectivity of the IL-IS mixture in comparison with the neat $[C_2MIM][C_2SO_4]$.

Afterwards, the effect of different ISs was also tested in the separation of n-heptane + ethanol azeotropic mixtures, by using combinations of $[C_2MIM][Ac]$ with the most soluble ISs, at concentrations were the ionicity of the system was higher (Chapter 5). The results obtained in this study confirmed the increase in selectivity with the addition of IS and also showed that the distribution coefficient values were not significantly affected by the introduction of the IS.

Figure 1 summarizes the work presented in this thesis, where the values of both selectivity and distribution coefficients are plotted against the ionicity of the IL-IS mixtures tested in the separation of n-heptane + ethanol azeotropic mixture. In addition, the values for the neat ILs are also plotted for comparison purposes.

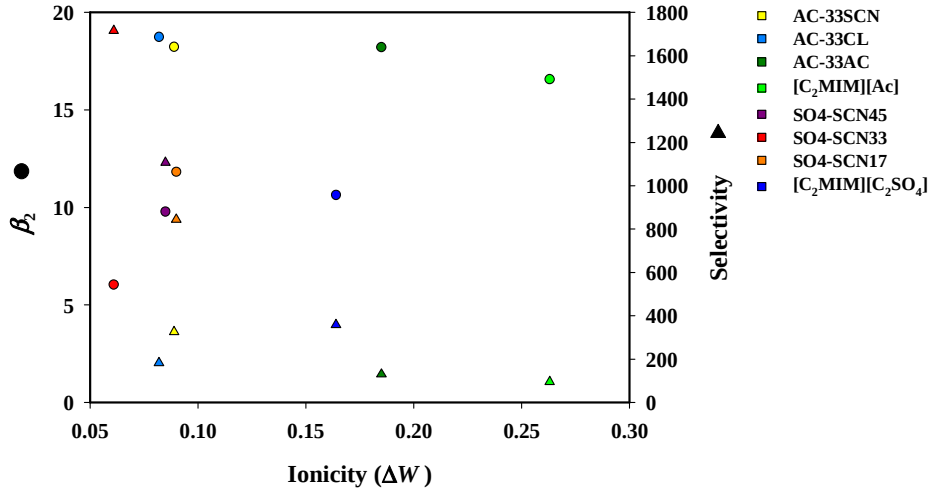

Figure 1 | Comparison between β_2 (●) and S (▲) as a function of ionicity for all the IL-IS mixtures and neat ILs tested as extraction solvents in n-heptane + ethanol mixtures. Each colour represents a different extraction solvent. The β_2 and S values are given for ethanol mass fractions between 0.02 - 0.03 wt% in the n-heptane-rich phase at 298.15 K.

From Figure 1, it can be seen that the addition of the IS in the IL increases the ionicity of the mixture and at the same time can increase both the selectivity and the distribution coefficient. However, the increase in the ionicity of the IL-IS mixture can only be related to the selectivity of the mixture, in a close to a linear way (Figure 2). In the case of the distribution coefficient, the increase in ionicity does not have the same effect. Indeed, the impact of the increase in ionicity on the distribution coefficients changes with the IL-IS mixture in question. For the sulfate-based IL-IS mixtures, the increase in ionicity leads to similar or lower distribution coefficients when compared to the neat $[C_2MIM][C_2SO_4]$, whereas in the acetate-based IL-IS mixtures the distribution coefficient suffers slight increases for the $[NH_4][Cl]$ and $[NH_4][SCN]$ and a large increase for $[NH_4][Ac]$.

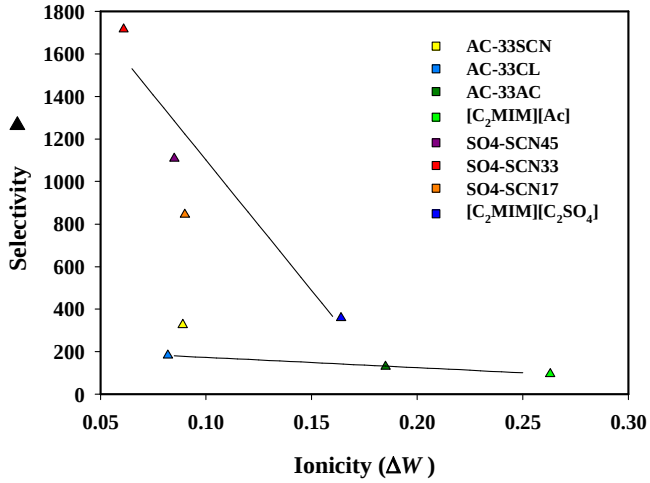

Figure 2 | Selectivity (▲) as a function of ionicity for all the IL-IS mixtures and neat ILs tested as extraction solvents in n-heptane + ethanol mixtures. Each colour represents a different extraction solvent. The Selectivity values are given for ethanol mass fractions between 0.02 - 0.03 wt% in the n-heptane-rich phase at 298.15 K. Black lines merely represent an eye's guide.

These results show that the addition of ISs, may provide a boost in the feasibility of the ILs as extraction solvents for the separation of azeotropic mixtures. Nevertheless, a careful selection of the IL-IS mixtures must be taken into account, as shown by the higher selectivity and lower distribution coefficient values of the sulfate-based IL-IS mixtures opposed to the higher distribution coefficients and lower selectivity values of the acetate-based IL-IS mixtures. Therefore, the knowledge gained by the work presented in this thesis may open the door for the production of more promising extraction solvents for azeotropic mixtures, due to the wide range of combinations that can be established between ILs and ISs. For that purpose, other azeotropic mixtures need to be studied within this context.

In addition, the possible application of DES as separation agents for the breaking of azeotropic mixtures was also considered in this thesis (Chapter 6). The results provided in this work showed that DES containing HBD with hydroxyl groups (DES1 and DES3) can exhibit greater selectivity, while the presence of the carboxylic group in the HBD (DES2) enhanced the distribution coefficient over the selectivity. The distribution coefficients and selectivity values obtained for the DES tested are sufficiently high in order to justify a scaling

up process by liquid-liquid extraction, proving that DES may become an easier, cheaper and greener solution for the separation of azeotropic mixtures.

3. Outlook

During the work of this thesis promising and innovative results were achieved for the separation of n-heptane + ethanol azeotropic mixtures. The work developed herein shows that the use of IL-IS mixtures as extraction solvents can significantly improve the efficiency of the separation. However, the study of more combinations of IL-IS mixtures as well as their application in different azeotropic mixtures is still required. The employment of simulation programs such as COSMO-RS among others may provide further insights into the feasibility of IL-IS mixtures for the separation of azeotropic mixtures. Moreover, other programs such as HYSYS can generate data concerning the scaling up of the separation process using IL-IS mixtures as separation agents, which can provide helpful information in order to achieve the application of these mixtures at an industrial level.

In addition, the corrosion capacity of the ISs is still a fact that has to be taken into consideration. Although, recent studies have shown that ILs can provide an inhibitory effect on the corrosion behaviour of metals in aggressive media,[16-19] studies of the corrosion of IL-IS mixtures in metals are vital to developing a feasible separation agent. Furthermore, the recovery of the separation agent, either the IL-IS mixture or the DES, must always be taken into account and further studies should be addressed, since in the case of IL-IS mixtures, depending on the IS chosen, the IS could decompose inside the IL while in the case of DES the use of high vacuum can disrupt the H-bonds of the compounds and thus destroy the DES.

In conclusion, the affinity of the separation agent for the solute has to be high enough in order to lead to high selectivity values and high distribution coefficients but not so high that irreversible interactions are established, hindering the recovery and subsequent re-use of the separation agent.

4. References

1. Z. Lei, X. Xi, C. Dai, J. Zhu and B. Chen, Extractive distillation with the mixture of ionic liquid and solid inorganic salt as entrainers, *AIChE J.*, 2014, **60**, 2994-3004.

2. A. B. Pereiro, J. M. M. Araújo, F. S. Oliveira, J. M. S. S. Esperança, J. N. C. Lopes, I. M. Marrucho and L. P. N. Rebelo, Solubility of inorganic salts in pure ionic liquids, *J. Chem. Thermodyn.*, 2012, **55**, 29-36.

3. T. V. Doherty, M. Mora-Pale, S. E. Foley, R. J. Linhardt and J. S. Dordick, Ionic liquid solvent properties as predictors of lignocellulose pretreatment efficacy, *Green Chem.*, 2010, **12**, 1967-1975.

4. G. Gurau, H. Rodríguez, S. P. Kelley, P. Janiczek, R. S. Kalb and R. D. Rogers, Demonstration of chemisorption of carbon dioxide in 1,3-dialkylimidazolium acetate ionic liquids, *Angew. Chem. Int. Ed.*, 2011, **50**, 12024-12026.

5. Y. Qin, X. Lu, N. Sun and R. D. Rogers, Dissolution or extraction of crustacean shells using ionic liquids to obtain high molecular weight purified chitin and direct production of chitin films and fibers, *Green Chem.*, 2010, **12**, 968-971.

6. W. Shi, C. R. Myers, D. R. Luebke, J. A. Steckel and D. C. Sorescu, Theoretical and experimental studies of CO_2 and H_2 separation using the 1-ethyl-3-methylimidazolium acetate ([emim][CH_3COO]) ionic liquid, *J. Phys. Chem. B*, 2012, **116**, 283-295.

7. M. B. Shiflett and A. Yokozeki, Phase behavior of carbon dioxide in ionic liquids: [emim][acetate], [emim][trifluoroacetate] and [emim][acetate] + [emim][trifluoroacetate] mixtures, *J. Chem. Eng. Data*, 2009, **54**, 108-114.

8. N. Sun, M. Rahman, Y. Qin, M. L. Maxim, H. Rodriguez and R. D. Rogers, Complete dissolution and partial delignification of wood in the ionic liquid 1-ethyl-3-methylimidazolium acetate, *Green Chem.*, 2009, **11**, 646-655.

9. S. R. Tomlinson, C. W. Kehr, M. S. Lopez, J. R. Schlup and J. L. Anthony, Solubility of the corn protein zein in imidazolium-based ionic liquids, *Ind. Eng. Chem. Res.*, 2014, **53**, 2293-2298.

10. J. Vitz, T. Erdmenger, C. Haensch and U. S. Schubert, Extended dissolution studies of cellulose in imidazolium based ionic liquids, *Green Chem.*, 2009, **11**, 417-424.

11. H. Zhao, L. Jackson, Z. Song and A. Olubajo, Using ionic liquid [emim][CH_3COO] as an enzyme-'friendly' co-solvent for resolution of amino acids, *Tetrahedron-Asymmetr.*, 2006, **17**, 2491-2498.

12. A. B. Pereiro, J. M. M. Araújo, F. S. Oliveira, C. E. S. Bernardes, J. M. S. S. Esperança, J. N. C. Lopes, I. M. Marrucho and L. P. N. Rebelo, Inorganic salts in purely ionic liquid media: The development of high ionicity ionic liquids (HIILs), *Chem. Commun.*, 2012, **48**, 3656-3658.

13. A. B. Pereiro and A. Rodriguez, Azeotrope-breaking using [bmim][$meSO_4$] ionic liquid in an extraction column, *Sep. Purif. Technol.*, 2008, **62**, 733-738.

14. A. B. Pereiro and A. Rodriguez, Separation of ethanol-heptane azeotropic mixtures by solvent extraction with an ionic liquid, *Ind. Eng. Chem. Res.*, 2009, **48**, 1579-1585.

15. A. B. Pereiro, F. J. Deive, J. M. S. S. Esperança and A. Rodriguez, Alkylsulfate-based ionic liquids to separate azeotropic mixtures, *Fluid Phase Equilib.*, 2010, **294**, 49-53.

16. X. Zhou, H. Yang and F. Wang, [BMIM][BF_4] ionic liquids as effective inhibitor for carbon steel in alkaline chloride solution, *Electrochim. Acta*, 2011, **56**, 4268-4275.

17. Q. B. Zhang and Y. X. Hua, Corrosion inhibition of mild steel by alkylimidazolium ionic liquids in hydrochloric acid, *Electrochim. Acta*, 2009, **54**, 1881-1887.

18. Q. B. Zhang and Y. X. Hua, Corrosion inhibition of aluminum in hydrochloric acid solution by alkylimidazolium ionic liquids, *Mater. Chem. Phys.*, 2010, **119**, 57-64.

19. L. C. Murulana, A. K. Singh, S. K. Shukla, M. M. Kabanda and E. E. Ebenso, Experimental and quantum chemical studies of some bis(trifluoromethylsulfonyl)imide imidazolium-based ionic liquids as corrosion inhibitors for mild steel in hydrochloric acid solution, *Ind. Eng. Chem. Res.*, 2012, **51**, 13282-13299.